



Sara Filipa Marques Nunes Aparício

Licenciatura em Ciências de Engenharia do Ambiente

**Impacts of Climate Change Scenarios on
Terrestrial Productivity and Biomass for
Energy in the Iberian Peninsula:
Assessment through the JSBACH model**

Dissertação para obtenção do Grau de Mestre em Engenharia
do Ambiente, Perfil de Gestão e Sistemas Ambientais

Orientador: Maria Júlia Fonseca de Seixas, Ph.D, FCT-UNL

Coorientador: Nuno Miguel Matias Carvalhais, Ph.D., FCT-UNL

Júri:

Presidente: Prof. Doutora Maria Teresa Calvão Rodrigues

Arguente: Prof. Doutor João Manuel Dias dos Santos Pereira

Vogal: Prof. Doutora Maria Júlia Fonseca de Seixas

Vogal: Nuno Miguel Matias Carvalhais



FACULDADE DE
CIÊNCIAS E TECNOLOGIA
UNIVERSIDADE NOVA DE LISBOA

Outubro, 2012

COPYRIGHT

The Faculty of Science and Technology and the New University of Lisbon entitled, perpetual and without geographic boundaries, archive and publish this dissertation through printed copies reproduced on paper or digital form, or by any other means known or to be invented, and through the promotion scientific repositories and admit your copying and distribution of educational objectives or research, not commercial, as long as credit is given to the author and publisher.

Calvin : "You can't just turn on creativity like a faucet. You have to be in the right mood".

Hobbes : "What mood is that?"

Calvin : "Last-minute panic".

In Calvin & Hobbes

ACKNOWLEDGMENTS

I would like in first place to address my deep gratitude to my coordinator Júlia Seixas. Thank you for guiding me throughout this thesis and for all your help in so many fields, from recommending helpful literature review; to providing of a working space and a computer (...with a blessing speed). Thank you as well for being so patient and kind in the beginning, during my ramblings on the thesis project I would choose.

I would like as well to thank with equal gratitude to my sub-coordinator, Nuno Carvalhais without whom this work wouldn't be possible. Thank you for your availability and for all the work that you have done in order to provide me the JSBACH data. Thank you for sharing your knowledge in fruitful and enthusiastic discussions.

My many thanks go to Christian Beer from the Max-Planck-Institut für Meteorologie, who processed and share the JSBACH data upon which all my practical work was based on.

I would like to express my gratitude to all my friends who supported me, and asked me countless times about my thesis progress (well...grateful is not *necessarily* the word for the last part), and I am sorry for not mention your names (this thesis is already big enough, ok?). Nevertheless, I would like to address my special thanks to those who had a particular and direct impact throughout the development of this thesis.

To Gonçalo and Favinha, for inviting me countless times to the catacombs of their department, where day is night, creating the ideal atmosphere distractions-avoidant.

To Lina and Miguel – to the first, because part of this thesis was written inside *Marineta* (beautiful specimen of camper) in Picos de Europa, and to the later because it had to be recorded somewhere my blessing to your marriage (80 years from now). Please, choose a shady place for the ceremony.

To Kathi, my sister-in-arms, despite the mere distance that separate us (2.750 km are nothing), it was a pleasure to share small victories and huge sighs during our thesis

construction. Hopefully we will celebrate everything with Justin and Joela somewhere in Europe?

To André, for being at this precise moment looking over my shoulder, helping me to make sure (within last-minute pressure on writing the Acknowledgements) that, I will not commit another horrible attack to English Grammar.

Thank you, my wonderful Grandparents and beautiful Mom (renewable and inexhaustible sources of love and affection), and Sofia (my Sister since the Beginning of Times). Thank you for supporting me with infinite patient.

I also want to thank my greatest life model... I have immense pride in being your daughter.

SARA
APARÍCIO 

ABSTRACT Greenhouse gas abatement policies (as a measure of preventing further contribution to global warming) are expected to increase the demand for renewable sources of energy driving a growing attention on Biomass as a valuable option as a renewable source of energy able to reduce CO₂ emissions, by displacing fossil fuel use. The vulnerability of the Iberian Peninsula (IP) to climate changes, along with the fact that it is a water-limited region, drive a great concern and interest in understand the potentials of biomass for energy production under projected climate changes, since water shortage is a projected consequence of it.

Henceforth the goals stated for this work include the understanding of the impact magnitude that climate changes and the sole effect of rising CO₂ (in accordance to the prescribed in A1B scenario from IPCC) have on biomass and productivity over the IP; the modeling of the interannual variability in terrestrial productivity and biomass across the region (having the period 1960-1990 as reference) and the energy potentials derived by biomass in future scenarios (2060-2090 and 2070-2100 periods). The carbon fluxes were modeled by JSBACH model and its results were handled using GIS and statistical analysis. A better understanding of the applicability (and reliability) of this model on achieving the latter stated goals was another goal purposed in this work.

IP has shown a broadly positive response to climate change, i.e. increased productivity under scenarios admitting elevation of atmospheric CO₂ concentration (increases in GPP by ~41%; in forest NPP by ~54% and herbaceous NPP by ~36%, for 2060-2090 period), and smaller and negative response under scenarios disregarding rising CO₂ levels (i.e. CO₂ constant at 296ppm). The productivity and biomass correlation with changing climate variables also differed between different CO₂ scenarios. The increase of water-use efficiency by 58% was as a result of CO₂ fertilization effect, could explain the increase of productivity, although many limitations of the model (such as disregard of nitrogen cycle and land-use dynamics) poses many considerations to the acceptability of results and the overestimating productivity comparatively to many projections for the IP. Notwithstanding the comparison of changes in climate variables, showed a great correlation of results with other authors.

A comprehensive analysis of biomass supply and its availability during scenarios with elevated CO₂, shown that by 2060-2090, residues from thinning and logging activities over forest biomass have a potential of 0,165 and 0,495 EJ, and residues from agricultural activities (herbaceous biomass) have a potential of 0,346 EJ under a *HIGH-YIELD* scenario (assuming 40% of residues removal rate), corresponding to a share of current energy consumption of 13, 42 and 30%, respectively. The reasonability of these results was assessed by comparing with similar studies during the reference period.

Key Words: Biomass, Vulnerability, Climate Change, A1B IPCC Scenario, Productivity, CO₂ Fertilization & Water-use efficiency,

RESUMO A Biomassa tem tido uma crescente atenção como opção relevante de fonte energia renovável e emissor neutro de CO₂ dadas as políticas de redução de gases de efeito estufa (visando a prevenção do aquecimento global). A vulnerabilidade da Península Ibérica (IP) face às mudanças climáticas, aliada ao facto de consistir numa região onde a água é um factor limitante, levam a um grande interesse em compreender as potencialidades da biomassa para produção energética em alterações climáticas previstas, visto que a escassez de água é uma das consequências esperadas.

Os objectivos deste trabalho incluem assim a compreensão da magnitude dos impactos que as mudanças climáticas e o efeito individual do aumento de CO₂ (de acordo com o prescrito no cenário A1B do IPCC) têm sobre a biomassa e produtividade sobre a IP; a modelação da variabilidade interanual da produtividade terrestre e da biomassa (tendo o período 1960-1990 como referência) e os potenciais energéticos de biomassa em cenários futuros (períodos de 2060-2090 e 2070-2100). Os fluxos de carbono foram modelados pelo modelo de JSBACH e os resultados foram tratados com SIG e análise estatística. Uma melhor compreensão da aplicabilidade (e confiabilidade) deste modelo na consecução das metas estabelecidas foi outro objectivo proposto neste trabalho.

A IP mostrou uma resposta amplamente positiva face a mudanças climáticas, ou seja, aumento de GPP em ~ 41%; NPP florestal em ~ 54% e NPP de herbáceas em ~ 36%, para período 2060-2090). Para cenários desconsiderando o aumento dos níveis de CO₂ a resposta foi menor e negativa. A produtividade de biomassa e correlação com variáveis climáticas mudança também diferiram entre os diferentes cenários de CO₂. O aumento da eficiência do uso da água em 58%, resultado de efeito de fertilização de CO₂, poderia explicar o aumento da produtividade, embora muitas limitações do modelo (tais como a desconsideração do ciclo de nitrogénio e dinâmica do coberto vegetal) coloca muitas considerações para quanto à aceitabilidade dos resultados, dados os valores obtidos serem sobrestimados comparativamente a muitas projecções. Não obstante a validação de mudanças em variáveis climáticas, mostrou uma grande correlação de resultados com outros autores.

Uma análise detalhada disponibilidade de biomassa durante a cenários com CO₂ elevado, mostraram, resíduos de desbaste e actividade madeireira (sobre biomassa florestal) tem um potencial de 0.165 e 0.495 EJ, e resíduos de actividades agrícolas têm um potencial de 0.346 EJ sob um cenário de alto rendimento (supondo uma taxa de 40% remoção de resíduos), correspondente a uma quota de consumo de energia actual, de 13, 42 e 30%, respectivamente. A razoabilidade destes resultados foi validada comparando com estudos semelhantes durante o período de referência.

Palavras-chave: Biomassa, Vulnerabilidade, Mudanças Climáticas, A1B Cenário IPCC, Fertilização Produtividade, CO₂ e do uso da água, eficiência

INDEX OF CONTENTS

Acknowledgments	VII
Abstract	XIX
Resumo	XI
Index of Contents	XIII
Index of Figures	XV
Index of Tables	XXI
tonnesAbbreviations	XXV
1. Introduction	1
2. Climate change and Biomass for Energy	7
2.1. Climate Change Scenarios	7
2.2. Climate Change Impact on Energy Systems	11
2.3. Biomass as Energy Resources	13
2.3.1. Biomass definition and properties	14
2.3.2. Biomass resources for energy	18
2.3.3. Biomass contribution for mitigation of CO ₂ emission	24
2.3.4. Potential of Biomass for Energy	27
2.3.5. Biomass for Energy Competition Factors	36
2.4. Terrestrial Productivity and its relationship with Biomass	42
2.4.1. Absorbed photosynthetically active radiation (APAR)	43
2.4.2. Gross and Net Primary productivity	47
2.4.3. Carbon cycle	49
2.5. Impacts of Climate Change on Biomass potential	51
2.5.1. Temperature increase	53
2.5.2. Changes in precipitation patterns	54
2.5.3. Global NPP perspectives under water limitations	56
2.5.4. Elevated CO ₂ concentration	59
2.6. Assessing Terrestrial Productivity and Biomass	59
2.6.1. Dynamic Global Vegetation Models (DGVMs)	63
2.6.2. Main pitfalls and differences between DGVMs	64
3. Methodology to Estimate Productivity and Biomass Potential under Climate Change	68
3.1. Study Area: the Iberian Peninsula	71
3.1.1. Bioclimatic patterns and zones	71
3.1.2. Climate Variability	73
3.1.3. Vegetation Cover	76
3.2. Modeling Tool: JSBACH	79
3.2.1. JSBACH overall description	79
3.2.2. BETHY module: Plant Functional Types (PFTs)	82
3.2.3. CBALANCE module	90
3.3. Model variables: inputs and outputs	90
3.4. Model datasets	92
3.4.1. WATCH data sets	92

3.4.2.ERA interim data sets	92
3.5. Simulation Condition and Scenarios	93
3.6. Data handling and treatment	95
3.6.1.Time aggregation	98
3.6.2.GIS Analysis	101
3.6.3.Statistical Analysis	103
3.7. Estimations of the potential of biomass for energy potentials	104
3.7.1.Biomass potentials	104
3.7.2.Biomass potential as resource	105
3.7.3.Biomass energy potential – Conversion into energy	107
4. Results and Discussion	111
4.1. Climate variables analysis – Reference Period	112
4.1.1.Land Surface Temperature (T)	112
4.1.2.Water Balance	113
4.1.3.Radiation Balance	120
4.1.4.Climate variables interaction	123
4.2. Carbon balance analysis – Reference Period	128
4.2.1.Gross Primary Production (GPP)	128
4.2.2.Net Primary Production (NPP)	134
4.2.3.Biomass	136
4.3. Climate changes analysis – Future Scenarios	145
4.3.1.Land Surface Temperature (T)	145
4.3.2.Water Balance	150
4.3.3.Radiation Balance	159
4.3.4.Climate variables interaction	163
4.4. Carbon balance analysis – Future Scenarios	164
4.4.1.Gross Primary Production (GPP)	179
4.4.2.Net Primary Production (NPP)	184
4.4.3.Biomass Potentials in Future Scenarios	192
4.5. Biomass Energy Potentials	197
5. Conclusions	203
5.1. Climate change and CO ₂ fertilization impact on productivity and biomass	203
5.2. Biomass energy potentials	206
5.3. Considerations about the model and future research	208
6. References	211
7. Appendix	233

INDEX OF FIGURES

Figure 1 - IPCCs' Representative concentrations pathways (RCPs) Source: adapted from Inman (2011)	8
Figure 2 - Schematic illustration of SRES scenarios. (Source: IPCC, 2000)	9
Figure 3 - CO ₂ emissions per year for the SRES scenarios (Source: IPCC, 2007)	10
Figure 4 - Atmospheric CO ₂ concentration projected under the 6 SRES marker and illustrative scenarios assessed by two carbon cycle models: BERN (solid lines) and ISAM (dashed). (Source: IPCC, 2001)	10
Figure 5 - Biomass model (Source: Gielen et al., 2001)	14
Figure 6 – The moisture percentage affects significantly the combustion quality and calorific power of Forest Biomass (Source: Adapted from Brand, 2007)	16
Figure 7 – The biomass components of a tree (Source: Redrawn from Juverics (2010))	20
Figure 8 - Dedicated cropping potential with perennials on released agricultural land in 2020 under reference and sustainability scenarios from Biomass Futures project (Source: Adapted from Elbersen <i>et al.</i> , 2012).....	35
Figure 9 - Relationship between above-ground net primary productivity (NPP) and above-ground biomass (AGB) (Source: O’Neill & Angelis, 1981)	43
Figure 10 - Photosynthesis, respiration and Net Primary Productivity along temperature and CO ₂ flux changes (Source: Whittaker & Likens, 1973)	45
Figure 11 – Relationships between NPP and temperature (a) and precipitation (b). (Source: Whittaker & Likens, 1973).....	46
Figure 12- The changes of carbon balance and stocks from present to future –condition (Source: Adapted from Ito & Oikawa, 2002)	51
Figure 13 - Stomata scheme (Source: Bonan, 2002)	55
Figure 15 – NPP under different scenarios: at the Present; assuming climate change; and assuming climate and CO ₂ levels change (Source: Adapted from Rost <i>et al.</i> , 2009).	60
Figure 16 – DGMV scheme (Source: Cramer <i>et al.</i> , 2001).....	66
Figure 17 – Map of the Iberian Peninsula – the darker brown is assigned to heights over 1000m; light brown is assigned to heights ranging between 500 and 1000m (i.e. high plateaus) and the greenish color are assigned to heights lower than 500m (Source: Solarnavigator.net)	72
Figure 18- Köppen-Geiger Climate Classification for the Iberian Peninsula and the Balearic Islands (Source: AEMET, 2000).....	73
Figure 19 -Iberian Peninsula Bioclimatic zones - In accordance with Rivas-Martinez <i>et al.</i> (2004)	75
Figure 20 - Monthly mean precipitation and temperature of temperate zone (left) and Mediterranean zone (right).....	75
Figure 21 - Interactions between JSBACH and ECHAM5.....	80
Figure 22 - JSBACH modules scheme	81
Figure 23 –BETHY scheme	83
Figure 24 - Grid cell example.....	84
Figure 25 - Examples of soft traits and associated functions (Source: Canadell <i>et al.</i> , 2007)	85
Figure 26 - The tilling approach (Source: Adapted from Brovnik <i>et al.</i> , 2009)	86
Figure 27- Cover Type per tile	89

Figure 28 - Scheme of different Carbon pools for different PFTs	90
Figure 29 - CBALCANCE Carbon Pool model	91
Figure 30 – Global carbon dioxide emissions (Gt(C)/year) for scenarios A1F1, A1R and A1B (IPCC, 2000)	95
Figure 31 - Reference Period and Future Scenarios considered for the results	96
Figure 32 - Atmospheric CO2 concentrations during the Reference Period and the Future Scenarios	96
Figure 33 - Assessments from possible comparisons between Scenarios C1, C2, E1, E2 and the Reference Period.....	97
Figure 34 - Overall Methodology Scheme.....	100
Figure 35 - Flowchart: creating an image with different units - example for temperature (degrees Kelvin to degrees Celsius conversion example)	101
Figure 36 – Procedure to evaluate percentage change of land surface temperature between <i>Temperature C1</i> (Scenario C1) and <i>Temperature C2</i> (Scenario C2).....	102
Figure 37 - Procedure to evaluate ratios GPP between reference period and scenario C1	103
Figure 38 - Methodology applied to assessment of residue and energy potentials for forest biomass sources (Tree) and Herbaceous biomass sources (Grasses)	109
Figure 39 – Mean Annual Land Surface Temperature during the Reference Period [1060-1990]	112
Figure 40 – Histogram and Statistical analysis of Mean Annual Land Surface Temperature over the Iberian Peninsula during the Reference Period [1960-1990]	113
Figure 41 – Mean Annual Precipitation during the Reference Period [1060-1990]	113
Figure 42 - Histogram and Statistical analysis of Mean Annual Precipitation over the Iberian Peninsula during the Reference Period [1960-1990].....	115
Figure 43 – Histogram of soil moisture content of layer I [m] of layers 1,2,3,4 and 5 during [1960-1990].....	116
Figure 44-Mean Annual Soil Moisture Content during the Reference Period [1060-1990] and comparison with the Iberian River Basins (Source:)	117
Figure 45 - Histogram and Statistical analysis of Mean Annual Water Soil Content over the Iberian Peninsula during the Reference Period [1960-1990].....	118
Figure 46 – Mean Annual Evapotranspiration during the Reference Period [1060-1990]	119
Figure 47 - Histogram and Statistical analysis of Mean Annual Evapotranspiration over the Iberian Peninsula during the Reference Period [1960-1990].....	120
Figure 48 - Mean Annual Photosynthetically Active Radiation map during the Reference Scenario.....	120
Figure 49 - - Mean Annual Absorbed Photosynthetically Active Radiation during the Reference Period	122
Figure 50 - Histogram and Statistical analysis of Mean Annual APAR over the Iberian Peninsula during the Reference Period [1960-1990]	122
Figure 51 - Ratio APAR/PAR during the Reference Period	123
Figure 52 - Correlation between climate variables during the Reference Period	127
Figure 53 – Mean Annual Gross Primary Production (GPP) during the Reference Period [1960-1990]	128
Figure 54 - Relationship between GPP and Precipitation and GPP and Evapotranspiration during the Reference Period [1960-1990]	130

Figure 55 - Comparison of spatial distribution between GPP, P and ET during [1960-1990] ...	130
Figure 56 –The relationship between GPP and APAR at the IP during the 1960-1990 period.	131
Figure 57 - Mean Annual WUE during reference period.....	132
Figure 58 - Mean Annual LUE during the Reference Period	133
Figure 59- Mean Annual Forest Net Primary Production (NPP) during the Reference Period [1960-1990].....	134
Figure 60 - Mean Annual Herbaceous Net Primary Production (NPP) during the Reference Period [1960-1990]	135
Figure 61 - Regression analysis between mean annual GPP and NPP (from all biomass) over the Iberian Peninsula during the Reference Period	136
Figure 62 - Mean Annual Forest Biomass Density during Reference Period [1960-1990].....	136
Figure 63 - Mean Annual Herbaceous Biomass Density during Reference Period [1960-1990]	137
Figure 64 - Statistical analysis of Mean Annual Forest Biomass during [1960-1990]	138
Figure 65 - Statistical analysis of Mean Annual Herbaceous Biomass during [1960-1990]	138
Figure 66 - Percentage and absolute values of Forest and Herbaceous Biomass during the Reference Period [1960-1990]	139
Figure 67 - Estimations of Biomass assigned to each PFT, during the Reference Period [1960-1990]	140
Figure 68 - Correlation between mean annual temperature and herbaceous/forest biomass during the Reference Period [1960-1990]	143
Figure 69 - Correlation between mean annual precipitation and herbaceous/forest biomass during the Reference Period [1960-1990]	143
Figure 70 - Correlation between mean annual ET and herbaceous/forest biomass during the Reference Period [1960-1990]	144
Figure 71 - Correlation between mean annual SWC and herbaceous/forest biomass during the Reference Period [1960-1990]	144
Figure 72 - Correlation between radiation variables and herbaceous/forest biomass during the Reference Period [1960-1990]	144
Figure 73 - Mean Annual Land Surface Temperature projected for scenario C1 [2060-2090].	146
Figure 74 – Histograms and Statistical analysis of Land Surface Temperature for Scenarios C1 and C2.....	147
Figure 75 – Multi-Model Averages and Assessed Ranges for Surface Warming (Source: Adapted from IPCC, 2007)	147
Figure 76 - Percentage Change of Mean Annual Land Surface Temperature between Reference Period [1960-1990] and Scenario C1 [2060-2090].....	148
Figure 77 - Percentage Change of Mean Annual Land Surface Temperature between Scenario C1 [2060-2090] and Scenario C2 [2070-2100]	149
Figure 78 - Annual Mean Precipitation during Scenario C1 [2060-2090]	150
Figure 79 - Histograms and Statistical analysis of Precipitation for Scenarios C1 and C2	150
Figure 80 - Percentage Change of Mean Annual Precipitation between Reference Period [1960-1990] and Scenarios C1 (upper image) and Scenario C2 (bottom). In this case, positive change refers to decrease in precipitation. Redish areas present higher decreases in precipitation and greenish areas present lower decreases in precipitation.	151
Figure 81 - min c1~5,2 mm/m ² /year min c24,8	152

Figure 82 – Number of models which simulate a precipitation increase between the time periods 2080-2099 and 1980-1999 for the scenario A1B (Source: Höschel <i>et al.</i> , n.d.).....	153
Figure 83 - Time series of globally averaged precipitation change (%) from various coupled models for Scenario A1B and E1, relative to the 1980-1999 annual average (Source: Adapted from Höschel <i>et al.</i> , n.d.).....	153
Figure 84 - Mean Annual Soil Moisture Content during Scenario C1 [2060-2090].....	154
Figure 85 - Histograms and Statistical Analysis of Mean Annual SWC during Scenarios C1, C2, E1 and E2.....	155
Figure 86 - Multi-model (10 models) mean change in soil moisture content (%). Changes are annual means for the SRES A1B scenario for the period 2080 to 2099 relative to 1980 to 1999. The stippled marks the locations where at least 80% of models agree on the sign of the mean change (Source: IPCC, 2007)	156
Figure 87 - Mean Annual Evapotranspiration during Scenario C1 [2060-2090]	156
Figure 88 - Histograms and Statistical Analysis of Mean Annual Evapotranspiration during Scenarios C1, C2, E1 and E2	157
Figure 89 - Differences between global mean ET during the period 1960-1990 and 2070-2100. Simulation results from ECHAM5 with IPCC climate scenario A1B (Source: Kim <i>et al.</i> , 2002) .	158
Figure 90 - Percentage Change of Mean Annual PAR between the Reference Period and Scenario C1 [2060-2090]	159
Figure 91 - Mean Annual APAR during Scenarios C1 and Scenario E1 [2060-2090]	160
Figure 92 -Histograms and Statistical Analysis of Mean Annual APAR during Scenarios C1, C2, E1 and E2.....	161
Figure 93 - Percentage Change of Mean Annual APAR between the Scenario E1 and E2 and the Reference Period.....	162
Figure 94 - Mean Annual GPP during the Scenario C1 [CO ₂] = 296 ppm (top) and during the Scenario E1 [CO ₂] = 556 pm (botom).....	164
Figure 97 - Histograms and Statistical Analysis of the differences of GPP between Scenarios E1 and C1 (top) and Scenarios E2 and C2	166
Figure 98 - Percentage Change of Mean Annual GPP between Scenario E1 and C1	166
Figure 99 - Histograms and Statistical analysis of percentage change of GPP in period 2060-2090 (left) and 2070-2100 (right).....	167
Figure 100 – Correlation between interannual variability of mean annual GPP and mean annual variables from water balance (i.e. precipitation (top); evapotranspiration (middle); soil moisture content (bottom) – between Scenarios E1 and C1 and Reference Period [1960-1990]	170
Figure 101 - Correlation between interannual variability of mean annual GPP and mean annual temperature (top) and variables from radiation balance (i.e. PAR (middle) and APAR (bottom) – between Scenarios E1 and C1 and Reference Period [1960-1990].....	171
Figure 102 - Mean Annual WUE during scenario C1 (top) and Scenario C2 (bottom).....	173
Figure 103 - Mean Annual WUE during scenario E1 (top) and Scenario E2 (bottom)	174
Figure 104 - Mean Annual LUE during Scenario C1 (top) and Scenario C2 (bottom)	177
Figure 105 - Mean Annual LUE during Scenario E1 (top) and Scenario E2 (bottom).....	178
Figure 106 - Mean Annual Forest NPP during Scenario C1 (top) and Scenario E1 (bottom)	179
Figure 107 - Figure 106 - Mean Annual Herbaceous NPP during Scenario C1 (top) and Scenario E1 (bottom)	180

Figure 108 - Percentage change of forest (top) and herbaceous (bottom) NPP between Scenario E1 and C1	181
Figure 109 - Histograms and statistical analysis of Percentage Change of Forest (left) and Herbaceous (right) NPP between Scenario E1 and C1	182
Figure 110 - Regression analysis and coefficients of determination between NPP and GPP during Future Scenarios	183
Figure 111 –Share of Herbaceous and Forest Biomass to the overall amount during Scenarios “C” (left) and Scenarios “E” (right)	185
Figure 112 – Comparison of Absolute Amounts of Forest Biomass between Reference Period and Scenarios “C” (left) and between Reference Period and Scenarios “E”(right) segregated by PFTs	186
Figure 113 – Comparison of Absolute Amounts of Herbaceous Biomass between Reference Period and Scenarios “C” (left) and between Reference Period and Scenarios “E”(right) segregated by PFTs.....	186
Figure 114 – Percentage of Change of Forest Biomass between Scenario E1 [CO2]=556ppm and Scenario C1 [CO2]=296ppm	189
Figure 115 – Histograms and Statistical Analysis of Percentage Change of Forest Biomass between Scenarios E1 and C1 (left) and between Scenarios E2 and C2 (right)	190
Figure 116 - Percentage of Change of Herbaceous Biomass between Scenario E1 [CO2]=556ppm and Scenario C1 [CO2]=296ppm.....	190
Figure 117 - Histograms and Statistical Analysis of Percentage Change of Herbaceous Biomass between Scenarios E1 and C1 (left) and between Scenarios E2 and C2 (right)	191
Figure 118 - Percentage of Change of Total Biomass between Scenario E1 [CO2]=556ppm and Scenario C1 [CO2]=296ppm	191
Figure 119 - Histograms and Statistical Analysis of Percentage Change of Total Biomass between Scenarios E1 and C1 (left) and between Scenarios E2 and C2 (right)	192
Figure 120- Correlation between interannual variability of Forest Biomass and climate variables – between Scenario C1 and Ref. Period (top six) and between Scenario E1 and Ref. Period (bottom six)	194
Figure 121 - Correlation between interannual variability of Herbaceous Biomass and climate variables – between Scenario C1 and Ref. Period (top six) and between Scenario E1 and Ref. Period (bottom six).....	195
Figure 122- Percentage Change of Biomass Energy Potential from Forest Biomass under a "Max Potential" approach	198
Figure 123 – Comparison of Forest and Herbaceous Biomass changes between futures scenarios and reference period (left) and between elevated atmospheric CO ₂ concentration scenarios (E1 & E2) and constant atmospheric CO ₂ concentration (C1 and C2) (right).....	204
Figure 124 - Potential biomass energy share in total electric consumption of Iberian Peninsula for the Scenario E1 through combustion (top) and gasification (bottom) as conversion pathway processes.....	207

INDEX OF TABLES

Table 1 - Extra electricity demand driven by climate change	11
Table 2 - Mechanisms of Climate Impacts on Energy Supplies (Source: Adapted from IEA, 2004)	13
Table 3 - Cellulose and Lignin contents (Source: McKendry, 2002EUBIA, 2007)	15
Table 4 - Proximate analysis of some biomass feedstock (dry weight basis) (Sources: McKendry, 2002)	17
Table 5 - Plant species for energy crops (Source: Hogan <i>et al.</i> , 2010; Hall, 2002; McKendry, 2002; Haber <i>et al.</i> , 2011).....	18
Table 6 - Residual forestry ratios by activity, type of residue and plant.....	21
Table 7 - Main agricultural and forestry by-products by categories and activities (Hall, 2002, BISIPLAN, 2012	22
Table 8 –Residue to Product Ratios (kg/kg) utilized for the selected crops	23
Table 9 - Technical potentials and biomass use (in EJ/year) compared to primary energy consumption (PEC) from fossil fuels & hydro (Source: Adapted from Kaltschmit, 2009)	27
Table 10 – Current global biomass use (Compilation after Haberl <i>et al.</i> , 2011).....	28
Table 11 - Current level of global energy use (Source: Compilation of estimates by Haberl <i>et al.</i> , 2011)	28
Table 12 –Compilation of projected future level of global biomass and energy use and global terrestrial NPP: a compilation of estimates	29
Table 13 - World Land Area and a Potential for Energy from Biomass (Source: Reilly & Paltsev, 2008)	30
Table 14 – Compilation of projected future level of biomass potentials for Europe	33
Table 15 – European Energy demand from biomass 20% scenario for 2020	34
Table 16 - EU-25 Energy statistics (in 2002) (Source: EUROSTAT, 2002)	34
Table 17 - Land available for biomass crop production in the EU-25 (Source: Wiegmann <i>et al.</i> 2005)	34
Table 18 - Share of agricultural land per biomass type in EU (Source: Elbersen <i>et al.</i> , 2008)....	34
Table 19 - Potentials (EJ) of rotational and perennial crops for Iberian Peninsula based on time period and scenario (Source: calculated after Elbersen <i>et al.</i> , 2012)	36
Table 20 - Food supply in 2000 and two assumptions for the year 2050: A “business-as-usual” forecast (BAU) as well as “fair and frugal” diet (“fair”) assuming a switch to equitable food distribution and less meat consumption. Absolute numbers are in MJ/cap/day (Source: adapted from Haberl <i>et al.</i> 2011).....	41
Table 21 - Global carbon budget, in GtC/year (IPCC 4th Assessment Report, 2007).....	49
Table 22 - Modeled climate impact on cropland yields in 2050 with and without CO2 fertilization (Source: Haberl <i>et al.</i> , 2011)	61
Table 23 - Iberian Peninsula Bioclimatic zones - In accordance with Rivas-Martínez <i>et al.</i> (2004)	74
Table 24 – Sensitivity of Bioclimatic zones: expected climate change and potential impacts (Source: Adapted from Lindner <i>et al.</i> (2008))	78
Table 25- BETHY processes	82
Table 26 - Plant Functional Types considered by JSBACH.....	87

Table 27- Major species existing in Iberian Peninsula assigned to forest type (Source: Alcaraz <i>et al.</i> , 2006).....	88
Table 28 – Climate input variables.....	92
Table 29 - Overview of main driving forces and CO ₂ emissions across the years for A1B Scenario (Source: IPCC, 2000).....	95
Table 30 - Work flow of the three main stages of data treatment.....	98
Table 31- Work flow of the three main stages of data treatment (cont.)	99
Table 32 – Product/residue ratio (wet basis) of main agriculture crop residues for Southern Europe	105
Table 33- Scenarios to assess the effect of selected environmental policy and resource management options on soil organic matter levels in the EU for the 2030 horizon.....	106
Table 34 –Electrical efficiencies of conversions biomass types (Source: Nikolau <i>et al.</i> , 2003)	108
Table 35 - Lower Heating Values (LHV) of selected biomass	108
Table 36 – Thicknesses and mid layer depth of the 5 layers of soil.....	116
Table 37 - Coefficient correlation between climate variables estimated by JSBACH model for the Reference period	124
Table 38- Correlation coefficients for GPP and climate variables during the Reference Period [1960-1990].....	129
Table 39 - Correlation coefficients between Biomass and Climate Variables during the Reference Period.....	141
Table 40 – Comparison of Correlation coefficients for GPP and Climate Variables during the Reference Period and the Future Scenarios	168
Table 41 - Correlation coefficients for variability of GPP in response to varying climate variables	169
Table 42 - Parson's coefficients between NPP and GPP over the IP, during Future Scenarios.	182
Table 45 –Absolute amounts of Forest and Herbaceous Biomass (tonnes) during the Future Scenarios C1, C2, E1 and E2	185
Table 46 Percentage of Change of Forest and Herbaceous Biomass between Scenarios “C” and Scenarios “E” – Effect of rising CO ₂ levels.....	187
Table 47 - Correlation coefficients between Changing Biomass and Changing Climate Variables	192
Table 49 –Biomass and Herbaceous Energy Potential from Clear Cutting activities (<i>Max Potential</i>) for all scenarios.....	197
Table 50- Plausible approach results for Forest and Herbaceous Biomass under scenarios assuming climate change and elevated CO ₂	199
Table 51 - Comparison between assessments on biomass resources (data in EJ/year) estimated by other authors and for the reference period.....	200
Table 53 - Energy consumption in 2010 in Portugal and Spain (Source.INE, 2010; Pordata, 2012)	206

ABBREVIATIONS

AGB	Above-ground biomass
APAR	Absorbed Photosynthetically Active Radiation
BEE	Biomass Energy Europe
CC	Climate change
CCS	Carbon capture and storage
CEEC	Central and Eastern Europe Countries
CO₂	Carbon dioxide
CV	Calorific value
dmt	Dry matter tones
DGVM	Dynamic Global Vegetation Model
EEA	Environmental Energy Agency
EC	European commission
ECHAM5	European Centre Hamburg Model 5
ECMWF	European Centre for Medium-Range Weather Forecasts
ET	Evapotranspiration
ETS	Emissions trading scheme
EU	European Union
iLUC	Indirect land use change
IPCC	Intergovernmental Panel on Climate Change
FF	Fossil fuels
GCM	Global climate model
GDP	Gross demand product
GHG	Greenhouse gas
GIS	Geographic Information System
GPP-	Gross Primary Production
HVV	Higher heating value
IP	Iberian Peninsula
JSBACH	Jena Scheme for Biosphere-Atmosphere Coupling in Hamburg
MPI	Max Plank Institute
MPIMET	Max Plank Institute for Meteorology
NPP	Net Primary Production
NREAP	National Renewable Energy Action Plans
P	Precipitation
PAR	Photosynthetically active radiation
PEC	Primary Energy Product
ppm	parts per million
LAI	Leaf area index
LHV	Lower heating values
LPJ	Lund-Postdam Jena
LUE	Light-Use Efficiency
RED	Renewable Energy Directive
RCP -	Representative carbon pathways
RPR	Residue to product ratio
SRES -	Special Report on Emission Scenarios
T	Temperature

toe	Tones Oil Equivalent
WATCH	Water and Atmosphere Change
WEC	World energy council
SWC	Soil water content
WUE	Water-Use Efficiency

1. Introduction

In order to push further in development and ultimately well-being, humankind has reached technological revolutions regardless the negative impacts that most of its actions have had on the quality of the ecosystems. This overall behavior played by humanity throughout times, overlooked the health of the ecosystems in many ways whether due to the lack of possibility of being less harmful (such as highly inefficient pollutant processes); due to a reckless conduct (motivated by the disrespect to the environment) or simply - just due to ignorance.

The world is continuously facing a growing demand for food, fiber and energy. This ever-increasing demand leads to a high pressure on the ecosystems which lead in turn to several forms of degradation. Hence, the generation of those three components above cited, result in land-use change affecting the local biodiversity, runoff patterns, and the buffering capacity of the ecosystems leading to soil and ecosystem degradation, as well as many other adverse effects (Haberl *et al.*, 2011). Moreover, worsening this scenario is the fact that, along with the pressures already mentioned, according to the United Nations (2007), the global population is estimated to grow up to 9 billion by the year of 2050 and if the current emissions path is kept, the amount of energy services that will be required to sustain the economic growth, are predicted to triple the annual greenhouse gas emissions (GHG). Thus, emissions are projected to rise (Ebinger & Vergara, 2011) contributing thus to the so-called *Climate Change* phenomenon.

According to the Third Assessment Report of the Intergovernmental Panel on Climate Change (IPCC, 2001), the term *climate* can be defined as a synthesis of meteorological conditions at a given point in time or location – and more specifically this term consists in a statistical description of the characteristics of weather conditions over a given period of time – which classically has a length of 30 years. On the other hand, climate change consists in a concept which has been addressed by multiple definitions. For instance, the United Nations Framework Convention on Climate Change (UNFCCC) defines it as “*a change of climate which is attributed directly or indirectly to human activity that alters the composition of the global atmosphere and which is in addition to natural climate variability observed over comparable time periods*”. On the other hand, according with the newest definition brought by the IPCC, climate change can be defined as “*A change in the state of the climate that can be identified (e.g., by using statistical tests) by changes in the mean and/or the variability of its properties and that persists for an extended period, typically decades or longer*” (IPCC, 2011). Even though both definitions are similar, the later assumes that climate change may be due to whether natural processes or to persistent anthropogenic changes in the atmospheric composition or land use.

Many international efforts have been made in order to prevent or mitigate climate change, throughout global treaties and other policy frameworks, including such agreements as the United Nations Framework Convention on Climate Change (UNFCCC) with the currently over passed Kyoto Protocol (KP); the Convention on Biological Diversity; the UN Framework on Forest and others (Zomer *et al.*, 2008).

Based in general circulation models of climate trends and several evidences collected by observations, it is predicted that all regions of the world will suffer an increase in temperature. Polar areas and mountain regions will be relatively marked and coastal lowland areas will experience the impact of sea level rise as a result of temperature increase. (Ebinger & Vergara, 2011). Hence, the concept of climate change includes changes in precipitation and temperature levels and patterns, which forces the urgent need of adaptation. Besides that, there are several aspects such as the effects of increased atmospheric carbon dioxide (CO₂) concentrations as well many other

changes on atmospheric composition which are not completely understood (Whitmarsh & Govindjee, 1995; Haberl *et al.*, 2011).

Fact Box A: Carbon Dioxide Concentrations and Trends

In accordance with Delmas *et al.* (1980) and Neftel *et al.* (1983) (as quoted by Mayeux *et al.*, (1997)), the information obtained from air bubbles trapped in ice cores, have shown that the atmospheric CO₂ concentration during the Last Glacial Era (i.e. ~18.000 years ago) ranged **between 160 and 200 parts per million (ppm)** and rose up to **275** at 10.000 years ago . However, since two hundred years ago, - around the Industrial Revolution the levels of atmospheric CO₂ have escalated much rapidly: they have increased from about **290 ppm** to its **current level of 360 ppm** (Whitmarsh & Govindjee, 1995). This increase of CO₂ emissions continues: direct measurements have shown that each year the atmospheric carbon content is increasing by about 3×10^{15} grams. In fact, **there are evidences that CO₂ level will reach 700 ppm within the next century** (Whitmarsh & Govindjee, 1995). The **consequences of this abrupt CO₂ atmospheric concentration levels are not fully known**. Some climate models have predicted that due to increased greenhouse effect driven by increased CO₂ emissions, the temperature of the atmosphere will increase by 2 – 8 °C. By 2100 it is expected an average global surface temperature rise ranging between **1, 8 and 4°C** (IPCC, 2007). This sudden rise of temperate could lead to significant **changes in rainfall patterns**. The impact of this as well as of many other climate change related issues are unknown in what concerns to **plant communities and crops** (Whitmarsh & Govindjee, 1995).

In fact, the increase of atmospheric CO₂ concentrations (as well as other GHG) has been one of the variables which have been drawing the major concern on anthropogenic change in the climate system (Smeets & Faaij, 2007), since it is widely stated that anthropogenic emissions of GHG are a direct cause for climate change (Ebinger & Vergara, 2011). The main source of GHG emissions – about 70 percent, is fossil fuel combustion for electricity generation for industries and buildings and for transportation (Ebinger & Vergara, 2011), whereas the rest of it is result of deforestation. Thus, several efforts on preventing further increases have been widely studied (e.g. EEA, 2006; Berndes & Hanson, 2007; Smeets & Faaij, 2007; Reilly & Paltsev, 2008; Bossetti *et al.*, 2012) in order to address the energy sector since it is closed linked to GHG emissions.

Due to what was previously explained, it is a major concern to take action in what comes to control GHG emissions – more specifically CO₂ emissions. In addition,

climate consequences such as weather variability and extreme weather events will imply the need of adaption. Hence, the understanding of potential vulnerabilities and stresses on energy services due climate consequences will help to support future plans and sustainable consumption patterns, allowing the avoidance of a carbon intensive based energy supply.

In order to fulfill the projected energy demand without compromising any further the environment, i.e. by contributing with CO₂ emissions, the hope relays on the conversion of the energy sector into a more renewable based and efficient energy system. An energy resource that has been drawing an increasing attention as an option to meet those conditions is the so-called *biomass*. Besides being a renewable source, biomass enables a pathway of energy generation which contributes to the mitigation of CO₂ emission – as it is able to replace the combustion of fuel fossils. Hence, this dissertation is aiming to assess the impact of expected climate changes on the biomass potentials over the Iberian Peninsula (IP) by the periods 2060-2090 and 2070-2100. The A1B scenario developed by the Intergovernmental Panel on Climate Change (IPCC, 2000) is assumed and a coupled biosphere-atmosphere model named JSBACH is used.

Several issues and their intrinsic complexity such as climate change and forecasted rise in CO₂ concentration (to which IP is said to be highly sensitive) hamper a direct assessment of biomass potentials. Therefore, this work has the following goals:

- i) To model the interannual variability in biomass and productivity fluxes of terrestrial ecosystems over the IP, following a bottom –up approach – having as reference, the period 1960-1990, and to assess the energy potentials derived from biomass.
- ii) To understand the magnitude of the impact on productivity and biomass that the solely effect of rising CO₂, will have on different plants response across the IP, since multiple studies (e.g. Tubiello *et al.*, 2007; Rost *et al.*, 2009) suggest that direct effects of elevated CO₂ lead to higher production rates.

- iii) To clarify the interaction between soil, water and vegetation preconditioning biomass production and to present an overview of water productivity (or water-use efficiency) tendency across the IP. This interest is driven by the fact that warming temperatures as a result of climate change may lead to water-scarce conditions driving hence a great concern regarding water availability.
- iv) To gain knowledge regarding the applicability of the JSBACH model on answering the former questions and to compare its climate changes outputs with other studies regarding the same A1B scenario and to recommend further improvements to the model.

The present dissertation is divided in five main chapters. Chapter 2 comprises the theory background concerning the climate changes and the use of biomass as a way of energy source with a CO₂ mitigation background. Chapter 3 presents the methodology used which translates the strategy followed to answer the goals set. In Chapter 4, the results from the JSBACH are present and discussed and finally, in Chapter 5 the overall conclusions are presented as well as recommendations for further research.

2. Climate Change and Biomass for Energy

In addition to the negative consequences triggered by climate changes briefly referred in section 1 (e.g. impacts on several key factors such as water availability; food production and physical safety (Bonan, 2002)), climate changes also plays a major impact on energy resources as well as on seasonal demand for energy services (Ebinger & Vergara, 2011). Due to its interest for the aiming of this study, both climate change impact on energy systems and on biomass as an energy source are addressed in this section. Hence, biomass properties, types and biggest constraints for energy production (posed by competition for food or land) are described too. In order to understand the dynamics of this natural resource, this section briefly addresses the biological processes related to biomass growth along with the climate factors that are responsible for affecting it. Some tools of assessment of biomass and productivity are also regarded.

2.1 Climate Change Scenarios

In order to allow a better understanding of what will mean the climate change in the future, i.e. how it will affect the future in terms of environmental and social factors some organizations such as the IPCC (2000) or Millennium Assessment (2001), have drawn different scenarios, each assigned to a projected future GHG emissions (Morita *et al.*, 2001). These scenarios are alternative images of how the future might unfold enabling thus to analyze how driving forces may influence future emission outcomes (IPCC, 2000). These scenarios are socioeconomic-based and hence they require several

estimations implicit to an admitted social background (e.g. future population levels, social values, technological change or economic activity) (Morita *et al.*, 2001).

The newest approach to scenarios by IPCC is based on a set of four emissions trajectories named as representative carbon pathways (RCPs) which consist in the new basis for running the latest climate models (Inman, 2011). Each RCP is labeled according to the amount of heat they would generate at the end of the century, i.e. 8,5, 6, 4,5 and 2,6 watts per square meter (W/m²) (Figure 1).

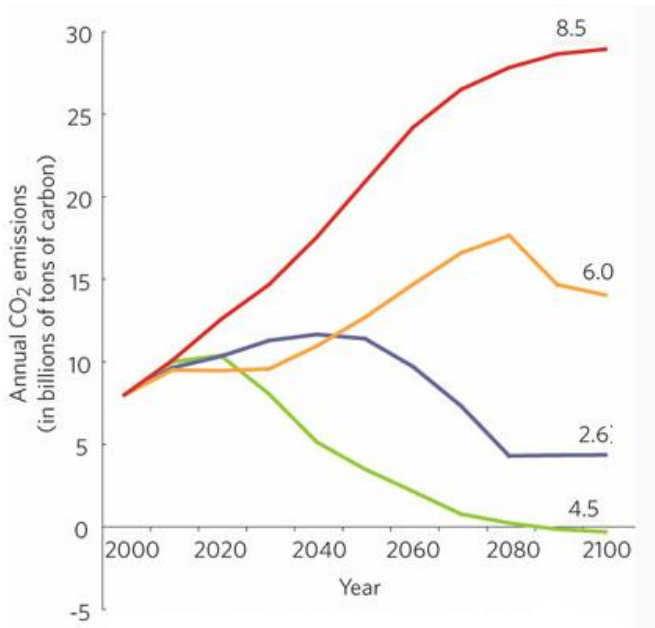


Figure 1 - IPCCs' Representative concentrations pathways (RCPs) Source: adapted from Inman (2011)

The range covered by the RCPs is wide and includes two considerable distant and unlikely to happen, future scenarios, namely the 8,5 the 4,5 W/m². The later is highly optimistic and it would be the result of a continuous decrease of GHG emissions (which would in fact reach 0 emissions by 2070). On the

other hand, the 8,5 W/m² would be the result of carbon dioxide

levels above 1300 parts per million (ppm) by 2100 – an unlikely result according to Jean Laherrère, cited by Inman (2011).

Prior to this new set of climate change scenarios, IPCC had other scenarios within the Special Report on Emission Scenarios (SRES), the so-called A1,A2, B1 and B2 scenarios (IPCC, 2001). The SRES developed into the RCP, thanks to the changes in the understanding of the driving forces of emissions (such as the carbon intensity of energy supply or income gap between developed and developing countries) as well as the methodologies to be addressed). Nonetheless, these previous scenarios were widely used in many studies which are mentioned later (e.g. Raddatz *et al.*, 2007) and in addition, this dissertation itself will be partly based in one of this scenarios.

Each scenario correspond to a qualitative storyline yielding the so-called scenarios named as “family” which in turn all together developed in six scenario groups as illustrated in Figure 2.

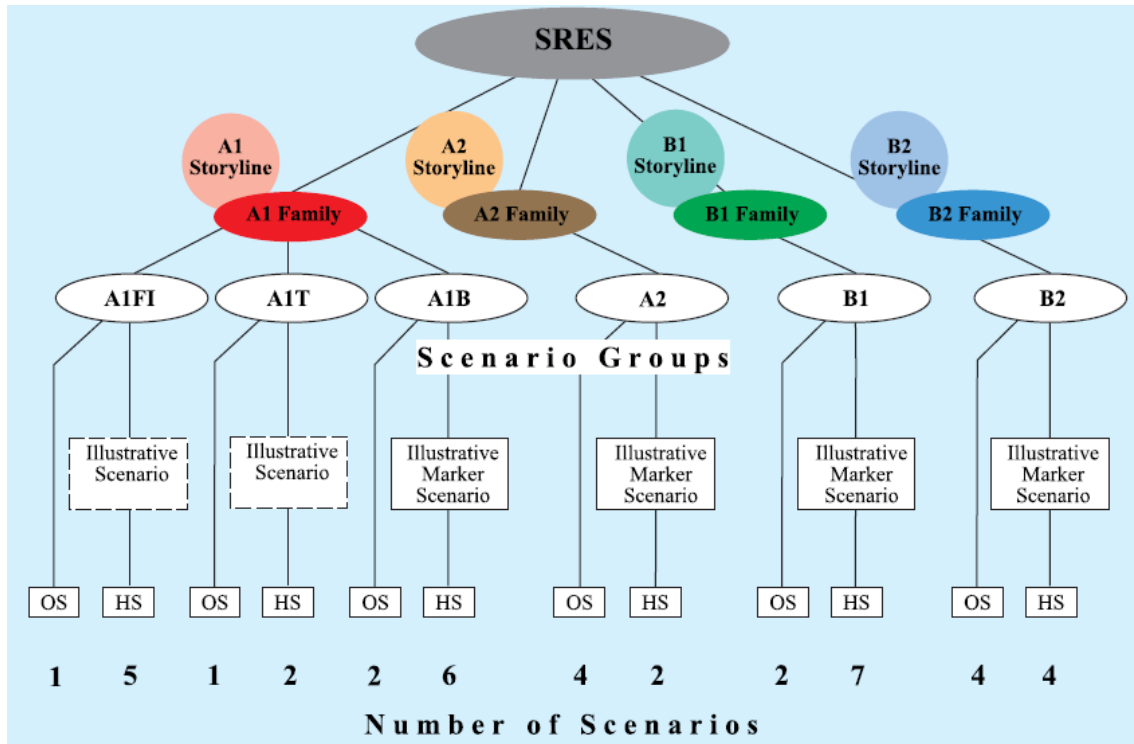


Figure 2 - Schematic illustration of SRES scenarios. (Source: IPCC, 2000)

The A1 storylines and scenario family regards a future world of very rapid economic growth with new and more efficient technologies. The growing global population is assumed to decline after the mid-century. Hence, each scenario distinguishes a certain type of technologic development: fossil intensive (A1F1), non-fossil energy sources (A1T) and a balance across all sources (A1B) (IPCC, 2000). The latter scenario will be afterwards more closely described, since it is of main of interest within the scope of the model used during this dissertation. The remaining scenarios, namely A2, B1 and B3, regard respectively, a very heterogeneous world with slower technological change and a continuously growing global population; a world with cleaner and resources-efficient technologies (but with the same behaviour in global population described in A1) and finally, a world with once again a ever growing global population and a intermediate level of economic development along with a less rapid and more diverse technological change than in the storylines B1 and A1. Figure 3 provides the emissions estimated for each one of these scenarios:

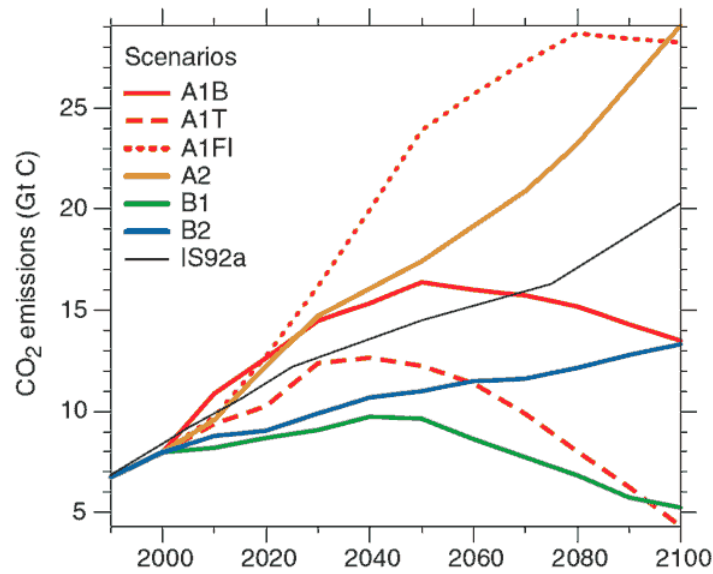


Figure 3 - CO2 emissions per year for the SRES scenarios (Source: IPCC, 2007)

The following graph (Figure 4) shows the CO₂ concentration projections underlying each SRES scenario. The worsened scenario, namely A1F1 accounts with CO₂ reaching up to nearly 1000 ppm by the end of the century. The A1B scenario was modeled to present an atmospheric CO₂ concentration around 500ppm by 2050 and nearly 700ppm by 2100. This is the least extreme scenario and its concentrations are in accordance with several CO₂ projections (e.g. Whitmarsh & Govindjee, 1995).

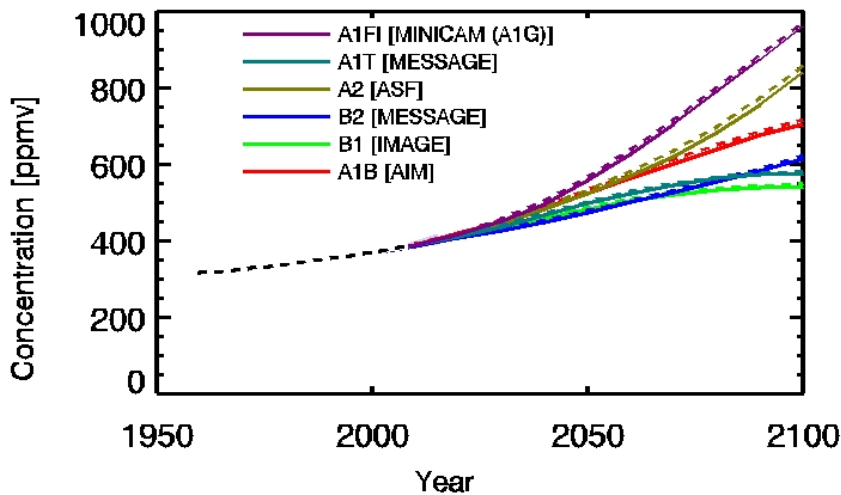


Figure 4 - Atmospheric CO₂ concentration projected under the 6 SRES marker and illustrative scenarios assessed by two carbon cycle models: BERN (solid lines) and ISAM (dashed). (Source: IPCC, 2001)

2.2 Climate Change Impacts on Energy Systems

The energy supply chain is highly vulnerable to climate variability, namely to several changes in climatic factors such as temperature, wind speed, precipitation pattern and cloud cover. Thus, the forecasted frequent extreme events can have a significant impact on energy systems, i.e. resources and supplies as well as seasonal demand for energy (EPA, 2010; Ebinger & Vergara, 2011).

Electricity demand is under a strong influence of climate variables (IPCC, 2007). In fact, already today, the energy sector is threatened by impacts of current and anticipated climate change trends which affect this sector by many ways starting with the fact that the energy demand changes as temperatures rise (EPA, 2010; IPCC, 2007; Ebinger & Vergara, 2011), as it can be perceived from the Table 1.

Table 1 - Extra electricity demand driven by climate change

COUNTRY	YEAR	EXTRA DEMAND (%)	AUTHOR
USA	2010-2055	14 – 23%	Linder <i>et al.</i> (1990)
USA	2025	24%	Ruth & Lin (2006)
GRECE	2080	3,6-5,6 %	Mirasgedis <i>et al.</i> (2007)
ISRAEL	n/a* (+ 4°C)	10% (peak summer)	Segal <i>et al.</i> (1992)
TAHILAND	2020	1,5-3,1	Parkpoom & Harrison (2008)
	2050	3,7-8,3	
	2080	6,6-15,3	

It is important to notice that there is a different shift on energy demand whereas it is being under consideration cooling or heating demand (Parkpoom & Harrison, 2008), i.e. cooling demand tends to increase while heating demands tend to decrease. However, the decreases in heating demand are unlikely to offset the increase in cooling demand as it was shown throughout many studies (Cartalis *et al.*, 2001; Hulme *et al.*, 2002; Venäläinen, *et al.*, 2004).

Fact box B: How temperature shift changes electricity demand

In developed countries, a warmer climate will likely change the amount and type of energy consumed. For instance, in North America an increase of **1,8°C** would **increase in about 5-20% the demand of energy** (i.e. electricity for air conditioned) used for cooling while the energy used for heating (e.g. natural gas, oil or wood) **would decrease by 3-15%** (USGCRP, 2009). Furthermore, a **6,3 to 9°C increase in temperature** would result in an increase of the **need for additional electricity** generating capacity by nearly 10-20% by 2050 (CCSP, 2006).

Besides changes in energy demand, climate changes also have considerable impacts on energy supply. In fact, in 2005 the energy productivity was affected by 13 % due to climate extremes alone, in developing countries (World Bank, 2009). The efficiency of power production of fossil fuel and many nuclear power plants can be compromised by warmer climate since, these plants require cooling water (because the efficiency of the generator decreases with higher water temperatures). Hence, the increase in temperature of both air and water can reduce the efficiency with which those plants convert fuel into electricity (CCSP, 2007; USGCRP, 2009).

Table 2 depicts some of the energy sectors, which are likely to be affected. Nevertheless, although many sectors may have a direct negative impact from changing climate patterns, in some cases renewable energy potential can also increase (e.g. solar and wind). Moreover, besides the extra pressure in energy supply caused by changing demand, it should be also take into account that other social factors – such as the fuel prices changes, drive an almost constant change in energy systems (Gielen *et al.*, 2003).

Table 2 - Mechanisms of Climate Impacts on Energy Supplies (Source: Adapted from IEA, 2004)

ENERGY IMPACT SUPPLIES		CLIMATE IMPACTS MECHANISMS	
FOSSIL FUELS	COAL	Cooling water quantity and quality (T), cooling efficiency (T,W,H), erosion in surface mining	
	NATURAL GAS	Cooling water quantity and quality (T), cooling efficiency (T,W,H), disruption of off-shore extractions (E)	
	PETROLEUM	Cooling water quantity and quality (T), cooling efficiency (T,W,H), disruption of off-shore extractions and transport(E)	
NUCLEAR		Cooling water quantity and quality (T), cooling efficiency (T,W,H),	
RENEWABLES	HYDROPOWER	Water availability and quality, temperature-related stresses, operation modification from extreme weather (floods/droughts), (T,E)	
	BIOMASS	Wood and forest products	Possible short-term impacts from timber kills or long-term impacts from timber kills and changes in tree growth rates (T,P,H,E,CO ₂ levels)
		Waste	n/a
		Agricultural resources	Changes in food crop residue and dedicated energy crop growth rates (T,P,H,E,CO ₂ levels)
	WIND	Wind resource changes (intensity and duration), damage from extreme weather	
	SOLAR	Insulation changes (clouds), damage from extreme weather	
GEOTHERMAL	Cooling efficiency for air-cooled geothermal (T)		

T= water/air temperature, W= wind, H= humidity, P= precipitation and E= extreme events

2.3 Biomass as Energy Resource

Biomass is a renewable source of energy and thus a valuable option for CO₂ emission reduction, due to its noticeable potential of displacing fossil fuels (Gielen *et al.*, 2001; Berndes & Hanson, 2007; Smeets & Faaij, 2007; Reilly & Paltsev, 2008). By substituting them, less combustion will take place diminishing the release of GHG emissions. The contribution for the mitigation of CO₂ emission will be closely addressed along with the potentials of biomass energy source at a Global, European and Iberian scale.

This section also depicts different types of biomass in what comes to properties and resources which define its suitability to energy purposes – as well as the competition triggered by the need of productive land for other purposes than energy production (such as food and fiber).

2.3.1 Biomass definition and properties

Quoting the Renewable Energy Directive (RED), biomass is by definition “the biodegradable fraction of products, waste and residues from biological origin from agriculture (including vegetal and animal substances), forestry and related industries including fisheries and aquaculture, as well as the biodegradable fraction of industrial and municipal waste”. Plant biomass is commonly referred in terms of the weight of biomass dry matter dried to constant moisture, and it can be measured whether on a plant or unit of land basis (O’Connor, 2003).

The organic matter that composes biomass can be converted into energy – or *bioenergy*. It can be made of algae, food crops, energy crops, crop residues; wood, wood waste and byproducts or even animal wastes (Riedy & Stone, 2010) (Figure 5), Researchers characterize the various types of biomass in different ways but one simple method defines four main types, namely: woody plants; herbaceous plants/grasses; aquatic plants and manures (McKendry, 2002). However, taking in consideration the scope of the present work, from now on, the term biomass will be addressed solely for terrestrial plants sources, i.e. henceforth; this term will be not including biomass from aquatic environments or animal sources.

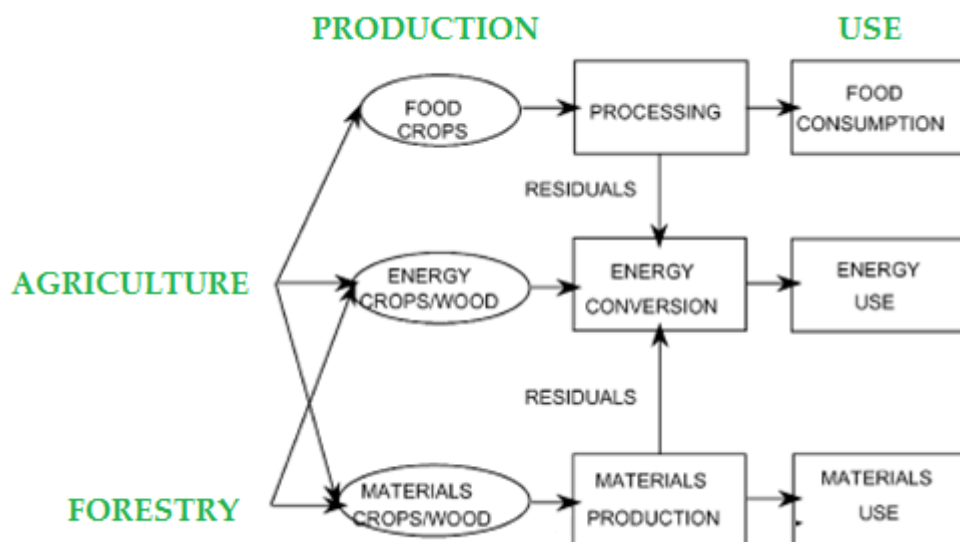


Figure 5 - Biomass model (Source: Gielen et al., 2001)

Each plant species has a different set of characteristics – or *properties*, which determines their suitability as an energy crop within a specific conversion process selected. The main material properties of interest include:

- i) Cellulose/lignin ratio
- ii) Moisture content;
- iii) Calorific value
- iv) Proportions of fixe carbon and volatiles;
- v) Ash/residue content
- vi) Alkali metal content

Each specie has a different amount of cellulose, hemicellulose and lignin. For instance, woody plants have far tightly bound fibers than herbaceous plants, due to a higher proportion of lignin (responsible for binding together cellulosic fibers), resulting thus in different energy potentials within the conversion process. The cellulose component generally accounts with 40-50% of the biomass weight (while hemi-cellulose portion represents 20-40% of the material by weight (McKendry, 2002) (Table 3).

Table 3 - Cellulose and Lignin contents (Source: McKendry, 2002EUBIA, 2007)

Biomass	Lignin (%)	Cellulose (%)	Hemi-cellulose (%)
Softwood	27-30	35-40	25-30
Hardwood	20-25	45-50	20-25
Wheat straw	15-20-	33-40	20-25
Switch grass	5-20	30-50	10-40

The intrinsic moisture content¹ and calorific value, two properties tightly correlated (Brito & Barrichelo, 1983; McKendry 2002), will be addressed, due to its interest for this study, conversely to other properties. Moisture content is inversely proportional to calorific value (Figure 6), since that per each kg of wood water content, it is needed around 600 kcal of energy (heat) in order to being evaporated which thereby must be deducted from their calorific value (Brito & Barrichelo, 1983).

¹ Intrinsic moisture: the moisture content of the material without the influence of weather effects (McKendry, 2002)

² Also known as net CV (GV)17,3

³ Also known as gross CV (GCV)18,5

⁴ NPP – Net primary production. This concept is addressed in following chapter 2.4

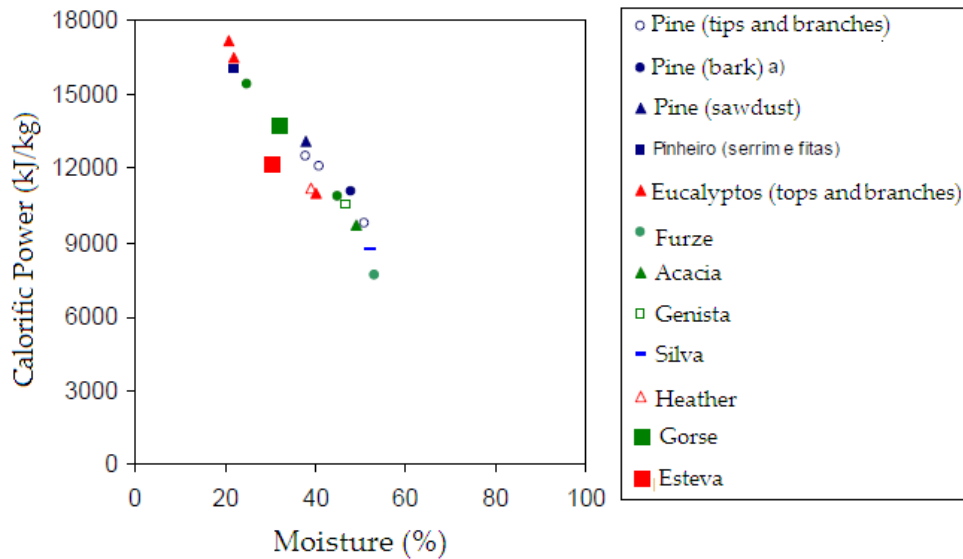


Figure 6 – The moisture percentage affects significantly the combustion quality and calorific power of Forest Biomass (Source: Adapted from Brand, 2007)

Calorific value (CV) is defined by the amount of heat (thermal energy) released during a complete combustion of a unit of mass or volume of a certain fuel (Nogueira & Lora, 2003), it hence consists in the expression of the energy content (or heat value) released when burnt in air (McKendry, 2002). Thus, within the scope of biomass energy production, it can be either measured in terms of energy content per volume (kJ/m^3) or per unit mass (MJ/kg) (McKendry, 2002; Nogueira & Lora, 2003).

CV can also be expressed as lower heating value (LHV)² or higher heating value (HHV)³. The latter regards the total energy released when the fuel is burnt (in air), i.e. it includes the latent heat contained in water vapor, representing the maximum amount of energy that is potentially recoverable from a certain biomass source). However, the latent heat contained in water vapor cannot be used effectively and hence, the LHV is the appropriate value to use for the energy available for subsequent use (since LHV does not account with that amount of energy) (McKendry, 2002).

Generally, when the CV of a set of biomass is presented, the moisture should be explicit, since it reduces the available energy from the biomass. Moreover, it is a common practice to quote both the CV and crop yield on the basis of dry matter tones (dmt), where moist content is assumed to be zero (McKendry, 2002) - hence, when

² Also known as net CV (GV) 17,3

³ Also known as gross CV (GCV) 18,5

moisture is present, this reduces the CV proportionally to the moisture content. Table 4 shows the analysis of the lower heating values of some biomass feedstock (on a dry weight basis), which is relevant for forward estimations of biomass energy potentials.

Table 4 - Proximate analysis of some biomass feedstock (dry weight basis) (Sources: McKendry, 2002)

SOURCE	TYPE/SPECIE	LOWER HEATING VALUE (dry weight basis)	AUTHOR*
ENERGY CROPS			
Herbaceous Crops	Miscanthus	17.8 - 18.1	(2)
	switchgrass	16.8 - 18.6	(2)
	Other grasses	16.9 - 17.3	(2)
	Black locust	18.5	(2)
	Eucalyptus	18.0	(1)
	Hybrid poplar	17.7	(2)
Woody Crops	Willow	16.7 - 18.4	(1,2)
AGRO-FORESTRY RESIDUES			
Forest Residues	Hardwood wood		(1)
	Softwood wood	17.5 - 20.8	(1,2,3,4)
	Corn stalks/stove	16.8 - 18.1	(1)
	Sugarcane bagasse	17.7 - 17.9	(1)
	Wheat straw	15.1 - 17.7	(1)
Agricultural Residues	Cereal straw	15,2	(5)

*Authors: 1- Jenkins, (1993); 2 – Jenkins *et al.*, (1998); 3 – Tilman, (1978); 4 – Bushnell (1989); 5 – Voivontas *et al.*, 2001

Biomass can be converted into three main types of products, namely electrical/heat energy; transport fuel and chemical feedstock (McKendry, 2002), however the generation of electricity is of particular interest in this study - notwithstanding the other products will also be briefly regarded. Biomass is converted into bioenergy through different pathways. The main conversion is oxidation (combustion) of biomass (mainly composed by carbon and hydrogen) resulting in a conversion of chemical energy into thermal energy (Sterner & Fritsche, 2011), which is currently the most used process (AEBIOM, 2011). The other key conversions routes are gasification and fermentation, where thermo-chemical and bio-chemical conversion occurs, respectively (Sterner & Fritsche, 2011).

Thus, besides LHV values it is important to take also into account the *efficiency* of conversion for biomass energy estimates. The overall efficiency of conversion of biomass to electricity is low, about 20%, although it can reach up to 35 – 40% of efficiency, when it is considered a combustion process using high efficiency, multi-pass, steam turbines to produce electricity (McKendry, 2002). Low efficiency conversion implies that it is required considerable land take in order to produce a relatively modest energy output as electricity, when compared with other sources.

2.3.2 Biomass resources for energy

Biomass resources for energy production can have two main types of origins: energy crops, which consist in dedicated production of biomass for energy purpose (comprising either short-rotation woody crops or herbaceous energy crops), or agroforestry residues (as a result from productive activity for food and forestry) (Hall, 2002; McKendry, 2002; Latzka, 2009).

The main advantage of energy crops is that they can be grown for energy in large quantities, just as food crops are (Latzka, 2009). However, due to the differences existing between the properties of different biomass types described in the previous section, there are resources more suitable for energy crops than others. Woody plants, herbaceous plants and grasses are the main types of interest for dedicated production of biomass for energy production. Some of these plant types are depicted in Table 5:

Table 5 - Plant species for energy crops (Source: Hogan *et al.*, 2010; Hall, 2002; McKendry, 2002; Haber *et al.*, 2011)

High dmt/ha (set aside)		Moderate dmt/ha (marginal/degraded land)
Woody species	Herbaceous	
<ul style="list-style-type: none"> ▪ Poplar (<i>Populus</i>); ▪ Willow (<i>Salix</i>); ▪ Eucalyptus(<i>Eucalyptus</i> spp) 	<ul style="list-style-type: none"> ▪ Sweet sorghum; ▪ Sugar cane; ▪ <i>Miscanthus</i>; ▪ Switchgrass (<i>Panicum virgatum</i>); ▪ Cord grasses 	<ul style="list-style-type: none"> ▪ Alder; ▪ Black locust; ▪ Birch; ▪ <i>Castanea saturia</i>; ▪ <i>Plantanus</i>; ▪ <i>Nicotania</i>

Typically, biomass has been made available for electricity production mostly as a waste of other product stream (Hughes, 2000; Yoshida & Suzuki, 2010), such as agricultural and forest field by-products (Latzka *et al.*, 2009; Esteban *et al.*, 2010; Esteban *et al.*, 2008). These agro-forestry by-products consist of those vegetal materials produced in croplands and forests which have experienced, up to the present date little or null commercial demand (Esteban *et al.*, 2010; Esteban *et al.*, 2008; Yoshida & Suzuki, 2010). Even though most of these residues are left in the field in order to avoid soil erosion, some can be used to produce energy without even harming the soil (Hall, 2002; Latzka, 2009).

Fact Box C: The contributions of residues to biomass energy potentials

The study conducted by Wit & Faiij (2010) regarding the estimations of feedstock supply of dedicated bioenergy crop for Europe (EU-27), ranges between 1,7 and 12,8 EJ/year. This **values increased** by 3,1 – 3,9 EJ/year and 1,4 – 5,4 EJ/year **if agricultural residues and forestry residues, respectively were added to the scheme**. According to Haber *et al.* (2011)'s study bioenergy potential on agricultural land might be in the order of magnitude of 100 EJ (when considering the current diet trajectories and a “food first” approach and taking into account agricultural residues). In fact, **this potential could rise up to 60%** if a poorer diet is chosen. Haberl *et al.* (2011) encourage further deeper studies on energy options that could combine both bioenergy production and soil fertility management.

Forest residues

Forest residues consist in by-products from the forest industry (Esteban *et al.*, 2010; Yoshida & Suzuki, 2010) which are collected after operations such as forest cleaning, logging and pruning – when used for energy purposes (Yoshida & Suzuki, 2010). These by-products consist mostly of branches, tops, bushes, understory vegetation, and, in general, wood which was not exploited for conventional uses such as timber sawing, pulp, and board production (Hall, 2002; Esteban *et al.*, 2010; Esteban *et al.*, 2008; Yoshida & Suzuki, 2010). As it is shown in Table 7, different processes generate

different forest by-products (Esteban *et al.*, 2010; Esteban *et al.*, 2008; Yoshida & Suzuki, 2010).

Only a percentage of biomass is merchantable (Figure 7) and because of that (and the properties of this type of resource) biomass of non-merchantable biomass trees consists in the main potential biomass source for energy (Yoshida & Suzuki, 2010).

Conventionally, forestry systems mainly yield biomass for energy solely as a by-product of timber production systems; which means

that only in certain circumstances biomass is produced for energy as a primary product (Hall, 2002). Forest residues usually constitute 25 to 45% of the harvested wood, so implementation of biomass production in such forestry systems represents a valuable decision since with would mean a considerable yield biomass by-product usable for energy generation(Hall, 2002). At present, in Europe only in Scandinavia these residues are captured to any significant extent, whereas in the remaining countries of EU these fractions are largely left in the forest (Hogan *et al.*,2010).

The estimation of potential available residues require to know the percentage of total harvested tree volume expected to be left on site, and the proportion of residues which is recoverable. The recovery rates can be dependent on available technology; costs; environmental constraints and other factors (such as tree form, stand quality and use limits) (Jurevics, 2010). Knowing the residue to production ratio (RPR) enables the assessment of biomass actually available for energy generation. Table 6 presents some of the amount of residues yielded from forestry industry and maintenance.

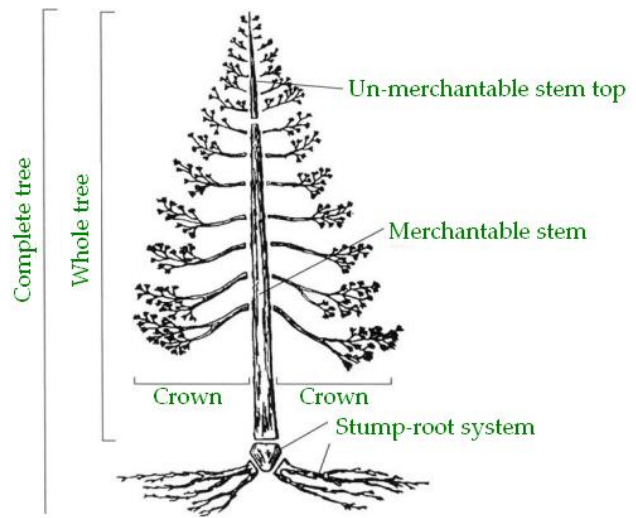


Figure 7 – The biomass components of a tree (Source: Redrawn from Jurevics (2010))

Table 6 - Residual forestry ratios by activity, type of residue and plant

Woody biomass use	Plant	Type of residues	RPR* (%)	Source
Logging Residues				
Logging residues	Rubber tree Plantation (PRT) (<i>Hevea brasiliensis</i>)	Top or branches	30	Yoshida & Suzuki (2010)
Clear cutting	Pine (<i>Pinus merkusii</i>)	Top and branches	10	Yoshida & Suzuki (2010)
Natural Wood production	n.d.	cracked and hollow logs	20-67	Yoshida & Suzuki (2010)
Industrial wood residues				
Sawmill	Teak (<i>Tectona grandis</i>)	n.d.	50-40	Yoshida & Suzuki (2010)
Plywood	Natural Teak	n.d.	45	Yoshida & Suzuki (2010)
	Planted Teak	n.d.	62	Yoshida & Suzuki (2010)
Plywood	Rosewood (<i>Dalbergia</i>) & Meranti (<i>Shorea</i>)	n.d.	40	Yoshida & Suzuki (2010)
Sawmill	Rubber tree Plantation (PRT) (<i>Hevea brasiliensis</i>)	n.d.	57	Yoshida & Suzuki (2010)

*RPR – Residue Production Ratio; n.d. – not disclosed, it can be empty fruit bunches (EFB), fronds, and trunks.

In some cases, final residues consist in residues from the so-called *primary residues* produced within some wood industry. Primary residues consist of sawdust, sander dust, log core, bark and edges, (which can be afterwards be laminated and used for packing material for instance) (Hogan *et al.*, 2010; Yoshida & Suzuki, 2010). Thereby, the remaining residues from this process became the secondary residues (which are the ones being addressed in the Table 6. In many developing countries, the secondary residues are actually directly used as household fuel (for the boiler, etc) and it is completely free of charge (Yoshida & Suzuki, 2010).

Agricultural residues

Agricultural land could provide residues from crops that are being grown for food purposes, for instance. Thus, in what concerns agricultural biomass residues, this term refers to waste generated by agricultural activities (Latzka, 2009). Residues from agricultural industry can be divided in two main categories: herbaceous by-products and woody by-products. Herbaceous by-products are considered to be those crop residues which are left in the field after the crop's harvesting process, so they nature is

quite diverse (i.e. it will depend on the type of crop; or the method applying during the harvesting process and so on). The woody by-products are those which were produced after pruning and regenerating orchards, vineyards and olives (Esteban *et al.*, 2010; Esteban *et al.*, 2008). Table 7 presents the main agricultural by-products from activities as well as the main type of plants.

Table 7 - Main agricultural and forestry by-products by categories and activities (Hall, 2002, BISIPLAN, 2012)

CATEGORY	ACTIVITY	BY PRODUCTS	LOCATION
FORESTRY	STAND ENHANCEMENT	<ul style="list-style-type: none"> ▪ Small trees ▪ Small branches ▪ Biomass from understory: shrubs and secondary tree species 	TIMBER FORESTS
	<ul style="list-style-type: none"> ▪ Pre-commercial thinning ▪ Brush cleanings ▪ Pruning 	<ul style="list-style-type: none"> ▪ Natural forests ▪ Plantations 	
	LOGGING	<ul style="list-style-type: none"> ▪ Logging slash: crowns, small bowls, decayed, etc ▪ Stumps ▪ Tops and limbs and unutilized cull trees ▪ Tops and branches 	
AGRICULTURE	HERBACEOUS CROPS HARVEST	<ul style="list-style-type: none"> ▪ Straw, bagasse, etc; ▪ Whole plant ▪ Husks ▪ Stover ▪ Stalks ▪ Cobs and leaves 	HERBACEOUS CROP LAND
			<ul style="list-style-type: none"> ▪ Cereals (corn, wheat, rice, barley, oats, etc; ▪ Cotton; ▪ Oilseed crop (sunflower, rape)
	TREE PRUNING	<ul style="list-style-type: none"> ▪ Small branches 	TREE FRUIT CROP LAND
			<ul style="list-style-type: none"> ▪ Olive, orange, apple, vineyard, nits, etc

Herbaceous crops such as, cereals, rape, maize, rice, and others, have in common the fact that the whole above ground biomass is cut every year. Usually the product harvested is the grain (or the fruit), while the rest of the plant is considered a residue or a by-product (Esteban *et al.*, 2010; Esteban *et al.*, 2008). Hence, similarly to what happens with forest residues, RPR is used to estimate the use of residual biomass (Esteban *et al.*, 2010; Esteban *et al.*, 2008). The crops selected as more interesting for biomass by-product production and the utilized RPR are shown in Table 8 for Spain and Portugal.

Table 8 –Residue to Product Ratios (kg/kg) utilized for the selected crops

Agro-residue	Spain	Portugal
Barley	0,94	1
Durum wheat	1,19	0,7
Soft wheat	1,19	0,7
Rye	1,3	1,3
Soya	2,12	2,12
Sunflower	1,33	1,5
Rape	3,8	3,8
Maize	1	1
Cotton	1,8	1,8
Rice	0,6	0,7
Vineyard	0,2	0,3
Orchard	0,28	0,27
Olive	0,5	0,5

It should be noticed that even though that RPRs are key numbers in every evaluation of this genre, these values should be addressed carefully, since they are typically applicable only at a regional or local level (Esteban et al., 2008; Esteban *et al.*, 2010). Frequently, under estimations of agricultural by-products, it is assumed a constant ratio of straw to grain. However, this assumption may not always be accurate since straw/grain ratios can vary greatly across environments and genotypes, two examples are provided in the following “Fact Box”.

Fact Box: D Changing RPR in changing conditions

Engel *et al* (2003) concluded that **straw/grain ratios were affected by many environmental conditions** such as water, nitrogen, and cultivar selection, having thus a **wide range**: from 0,91 to 2,37. The straw to product **ratios were higher** in Central and Northern EU than in Southern EU countries, as concluded Nikolau *et al.* (2003). In fact, this was corroborated by Di Blasi *et al.* (1997) who conducted a study which results showed that those ratios **were higher ratios in wet climates** than in dry ones.

2.3.3 Biomass contribution for mitigation of CO₂ emission

Since industrial revolution, the share of bioenergy has declined in favor of coal, oil and natural gas (i.e. fuel fossils). However, this decrease in bioenergy use is not trendy (Gielen *et al.* 2001; Elbersen *et al.*, 2012). Until few decades ago, biomass was usually perceived as a fuel from the past and it was commonly associated to poverty, and hence it tended to be left behind as the country developed (Hall & Scrase, 1998). Although, contrary to this perception, the World Energy Council (WEC); the United Nations Commission on Environment and Development (UNCED), the Intergovernmental Panel on Climate Change (IPCC), Greenpeace and Shell International as well as many other authors (Hall & Scrase, 1998; McKendry, 2002; Berndes & Hansson, 2007; Dornburg & Faaij, 2007; Smeets & Faaij, 2007; Reilly & Paltsev, 2008; Elbersen *et al.*, 2012), predict an expansion in global use of biomass for energy in the next century. Hall and Scrase (1998) expect biomass to remain an important source of energy and they predict that biomass use will be greatly expanded in future – in fact, during the last three decades the interest in bioenergy has increased steadily (Hall and Scrase, 1998; Gielen *et al.*, 2001; Dornburg & Faaij, 2007) (meaning that global demand for bioproductive land is also expected to increase) (Gielen *et al.*, 2001; Johansson & Azar, 2007; Dornburg & Faaij, 2007; Campbell *et al.*, 2008).

This changing path on biomass perception is, mainly due to its potential to reduce GHG emissions (Gielen *et al.*, 2001; McKendry, 2002; Gielen *et al.*, 2003; Smeets & Faaij, 2007) which is seen as the main benefit. Besides that, an expanded use of biomass for energetic purpose can inclusively be substantially encouraged as a result of policies to curb growing emissions of CO₂ (Gielen *et al.*, 2003; Johansson & Azar, 2007; Dornburg & Faaij, 2007; Elbersen *et al.*, 2012).

Fact Box E : Changing biomass perception

Nowadays biomass is stated as the largest renewable energy source, having a contribution around **10%** (46 EJ) of global primary energy demand of 489 EJ in 2005 (Dornburg & Faaij, 2007) (which bulk is dominated by fuel fossils sources accounting with 388 EJ/year). By 2008 this contribution rose up to **10,2 %** (50,3 EJ/yr) of the annual global primary energy supply (IPCC, 2011), while other forms of energy such as water or nuclear energy account only with 26 EJ (each). The major use of biomass (37 EJ) is non-commercial and is related to cooking and space heating, mainly by the poorer population from developing countries (Dornburg & Faaij, 2007). However, the **modern use of bioenergy (i.e. for electricity, industry and transport) has been increasing in the past years: 2005** it accounted with a significant **contribution of 9 EJ**.

Biomass energy is a useful option to avoid greenhouse gas emissions since it provides equivalent energy forms (electricity, transportation fuels and heat) as fuel fossils (Gielen *et al.*, 2001; Berndes & Hanson, 2007; Smeets & Faaij, 2007; Reilly & Paltsev, 2008, IPCC, 2011). According to IPCC (2011), bioenergy is able to deliver 80 to 90% emission reductions compared to the fossil energy baseline, in a scenario considering current systems (and future options such as perennial cropping systems) and considering the use of biomass residues and wastes as well as advanced conversion systems.

Plants play a notable role on achieving decreases (or avoiding further increases in atmospheric CO₂ atmospheric concentrations), since they have the potential to uptake CO₂ from the atmosphere and thus sequester the carbon in their biomass for long periods of time (Jansson *et al.*, 2010). In fact, 90% of biomass is resulting from the incorporation of carbon into organic compounds throughout the photosynthetic process (O'Connor, 2003). When produced by sustainable means, biomass emits roughly the same amount of carbon during conversion as taken up during plant growth (theoretically offsetting the combustible CO₂ (O'Connor, 2003), meaning that the use of biomass does contribute to a buildup of CO₂ in the atmosphere but with "recent" carbon – instead of fuel fossils which release on the atmosphere carbon which has been steady for million years (McKendry, 2002). Hence, the basis for all biomass strategies laid on the fact that carbon and energy are fixed during the biomass growth stage, leading to the reduction of CO₂ from emissions. Afterwards this biomass can be used as a renewable resource, accounting for zero CO₂ emissions according to some authors' perspective (e.g. Gielen *et al.*, 2001).

Around half of the total terrestrial carbon stock is stored in forests and forest soils – which consists in roughly 1146 Gt C (Dixon *et al.*, 1994; Smeets & Faaij, 2007). Due to this potential, carbon sequestration by forests has been receiving widespread attention in the past decades (Berndes & Hanson, 2007), and for that reason, the bioenergy sector has been proposed to have a central role in the future, where a more sustainable energy scenario is desired ((Riedy & Stone, 2010). The rising fuel prices, along with the environmental concerns, have been leading policymakers to adopt legislation aiming to encourage biomass conversion into electricity (and liquid fuels) (Riedy & Stone, 2010), motivated by the current undesirable dependence on fossil fuels and the possibility of curbing GHG emissions from fossil fuel use (Hall & Scrase, 1998; Haberl *et al.*, 2011).

Other major factors responsible for boosting a growing attention and acceptance of biomass, resulting in an improvement of biomass competitiveness in the energy market, are the rising prices of fossil fuels; the development of CO₂ markets (ETS) and the economic incentives for production, use and trade of biomass for energy, driven by the awareness of CO₂ emission and its impact on climate change (Hall & Scrase, 1998; McKendry, 2002, Dornburg & Faaij, 2007; Reilly & Paltsev, 2008; Haberl *et al.*, 2011).

A main goal of biomass use for energy purpose is the target net reduction of GHG gases compared to energy from fossil fuels. Furthermore, the current technological developments related to conversion, crop production and all the other processes involved promise the application of biomass at lower cost and with higher conversion efficiency than was possible before (McKendry, 2002) –contributing thus to the increase of competitiveness in energy markets. Moreover, at the local level if the economical scheme is favorable, biomass is very attractive because it is an indigenous energy source. And, in developing countries it generates labor-intensive activity (Yoshida & Suzuki, 2010). There is also the carbon capture and storage (CCS) technologies, which if applied on a large scale, might be an important option to achieve negative GHG emissions. Hence, this would be a good help on aiming to respect the limit global warming to 2°C until 2100 – which is the goal thought to be required to reduce the risk of catastrophic runaway events (Haberl *et al.*, 2011).

Fact Box F : Carbon Capture and Storage –Mitigation

According to the report *Energy Technology Perspectives* from IEA (IEA, 2010), CCS could account for approximately one-fifth of the emissions reduction required to cut GHG emissions from energy use in half by 2050. Moreover, Biomass Energy CCS (BECCS) is highlighted by IEA (2012) as being of special interest, since “it offers the potential **not only to reduce emissions, but also to actually remove CO₂ from the atmosphere**, thereby reducing atmospheric GHG concentrations and directly counteracting one of the main drivers of climate change”(p.7). Hence, theoretically, BECCS can achieve negative emissions. BECCS aims to reduce the rate of atmospheric CO₂ concentration by following the cycle: production of biomass which will sequester CO₂ from air as the plant grows and it will be stored as part of the biomass; combustion and finally placement of C underground. (IEA, 2012).

2.3.4 Potential of Biomass for Energy

According to CCSP (2006), global energy use is expected to increase from about 400 EJ/year in 2000 (McKendry, 2002; Ebinger & Vergara, 2011) to 700-1000 EJ/year in 2050 and to 1275-1500 EJ/year in 2100, highlighting the importance of understanding potential vulnerabilities and stresses on energy resources and demands due the climate change impacts (Ebinger & Vergara, 2011). Table 9 demonstrates both current potentials and uses of biomass from the world and Europe. This lower use percentage is justified by a lower exploitation due to poor matching between demand and resources, as well as many other constraints such as high costs (comparing to other energy exploitation)(EUBIA, 2007).

Table 9 - Technical potentials and biomass use (in EJ/year) compared to primary energy consumption (PEC) from fossil fuels & hydro (Source: Adapted from Kaltschmit, 2009)

	Fossil fuel (FF) & Hydro	Bioenergy use	Bioenergy potential	Use/potential	Use/FF	Potential/FF
Europe	74,8 EJ/year	2 EJ/year	8,9 EJ/year	22%	3%	12%
World	339,5 EJ/year	39,7 EJ/year	103,1 EJ/year	39%	12%	30%
			30 EJ/year*			

*According to McKendry (2002)

According to Haber *et al.* (2007) and Krausmann *et al.* (2008), the total amount of biomass harvested reached up to 310 EJ/year – from which 225 EJ/year were actually used. The total amount of biomass harvested consists hence in a considerable fraction of the current aboveground biomass (around 25%) since it accounts with 1241 EJ/year.

In accordance with EUBIA (2007), the estimations made by IPCC concluded that by 2050, bioenergy could actually supply around 250 – 450 EJ/year, which represents relatively a quarter of global energy demand. Similar results are presented in the table since potential of bioenergy reach 30% of global energy demand.

Furthermore, it can be concluded by the comparison between the Table 10 and Table 11, that some of the primary biomass potentials provided from many studies are considerable, taking in consideration the previously mentioned total amount of above ground NPP⁴ as well the current levels of human harvests and use of biomass.

Table 10 – Current global biomass use (Compilation after Haberl *et al.*, 2011)

Current global NPP and its human use (gross calorific value)	Energy flow (EJ/year)	Year	Sources
Total NPP of plant (land)	2191		Haberl <i>et al.</i> (2007)
Above ground NPP of plant (land)	1241		Haberl <i>et al.</i> (2007)
Human harvest of NPP including by-flows, total	346	2000	Haberl <i>et al.</i> (2007); Krausmann <i>et al.</i> (2008)
Human harvest of NPP including by-flows, aboveground	310		Haberl <i>et al.</i> (2007); Krausmann <i>et al.</i> (2008)
NPP harvested and actually used	225		Haberl <i>et al.</i> (2007); Krausmann <i>et al.</i> (2008)

Table 11 - Current level of global energy use (Source: Compilation of estimates by Haberl *et al.*, 2011)

Global energy use (physical energy content)	Energy flow (EJ/year)	Year	Sources
Fossil fuels (coal, oil, natural gas), gross calorific value	453	2008	BP (2006)
Nuclear heat (assumed efficiency of nuclear plants: 33%)	30	2008	BP (2006)
Hydropower (assumed efficiency: 100%)	11	2008	BP (2006)
Wind, solar and tidal energy (assumed efficiency: 100%)	1	2006	IEA (2008)
Geothermal (10% efficiency for electricity, 50% for heat)	2	2006	IEA (2008)
Biomass (plus biogenic wastes), gross calorific value	54	2006	IEA (2008)
Total (physical energy content, gross calorific value)	551	2006-2008	BP (2006); IEA (2008)

⁴ NPP – Net primary production. This concept is addressed in following chapter 2.4

World Potential

The range of estimations of biomass energy potential is considerable wide (Table 12).

Table 12 –Compilation of projected future level of global biomass and energy use and global terrestrial NPP: a compilation of estimates

Estimates of global bioenergy potentials or scenarios	Energy flow (EJ/year)	Year	Sources
Bioenergy crops and residues : excludes forestry	64 - 161	2050	Haber <i>et al.</i> (2011)
Mid-term potential biomass	94 - 280	2050	Turkenburg <i>et al.</i> 2000
Review of mid-term potentials biomass	35 - 450	2050	OECD (2008)
Mid-term potential biomass	370 - 450	2050	Fischer & Schratzenholzer (2001)
Potential biomass	33 - 1135	2050	Hoogwijk <i>et al.</i> (2003)
Potential biomass	200	2050	Price (1998)
IPCC-SRES scenarios mid-term	52 - 193	2050	Nakicenovic & Swart R (2000)
Bioenergy potential on abandoned farmland	27 - 41	2050	Field <i>et al.</i> (2008) CB
Bioenergy potential from forestry	32 - 52	2050	Smeets <i>et al.</i> (2004)
Bioenergy potentials in forests	0 - 71	2050	Smeets & Faaij (2007)
Surplus agricultural land (not needed for food and feed)	215 - 1272	2050	Smeets <i>et al.</i> (2007)
Bioenergy crops (second generation)	34 - 120	2050	WBGU (2009)
Bioenergy potential on surplus agricultural land	215 - 1272	2100	
Bioenergy production from agricultural and forestry residue & waste	76 - 96	2050	Hoogwik <i>et al.</i> (2005)
Total theoretical global bioenergy production potentials	71	2050	Smeets & Faaij (2006)
Bioenergy potential from wood produced for bioenergy	107	2050	Sørensen (1999)
Global increase in biomass production (ref. scenario)	30	2050	
Global increase in biomass production	180	2100	Reilly & Paltsev (2008)
Agricultural residues + bioenergy. in surplus agricultural lands	273 - 1471	2050	Smeets <i>et al.</i> (2004)

The considerable differences between the presented estimations can be due to a wide number of reasons – as a result of such a complex system, namely: the different methodologies used; the socio-economic scenarios assumed (e.g. land use patter for food production; agricultural management systems, wood demand evolution; production technologies used; natural forest growth), or even the type of biomass source (EUBIA, 2007; Haberl *et al.*, 2011; Smeets & Faaij, 2007). The studies presenting higher values (Hoogwijk *et al.*, 2003; Smeets *et al.*, 2007) did not considered for instance the links between food, feed and bioenergy.

Moreover, these comparisons should be addressed very carefully, since the definitions of potential also greatly differ among the studies, regarding the different potentials

types i.e. whether it is theoretical, technical, economic and ecological potential. The three last poses additional considerations to the theoretical potential and hence they actually tend to decrease within the order they were mentioned (EUBIA, 2007).

Fact Box G: Case study example: EUBIA’s projections of the “theoretical” biomass VS “technical” biomass use and demand

The European Biomass Industry Association (EUBIA) states that bioenergy could in fact provide the global energy needs. This estimate regards a theoretical approach. However within a technical and economic perspective, the potential would drop and become considerable lower. Currently and theoretically, the biomass potentials could reach the 2900 EJ/year, while a technical would drop to just 270 EJ/year.

Table 13 presents rough estimations of global potential for energy from biomass based on the total land area expected by 2050. In this projection (made by IPCC (2001), the average total energy yield was set to be 300 GJ/ha/year. The areas which were not suitable for cultivation (i.e. tropical savannas, deserts and semi-deserts, tundra and wetlands) represent about half of the total Earth land. The estimations predicted a global potential of around 2100 EJ/year from biomass, using the indicator of converting area in hectares into energy yield.

Table 13 - World Land Area and a Potential for Energy from Biomass (Source: Reilly & Paltsev, 2008)

	Area (Gha)	Bioenergy (dry)(EJ)	Bioenergy (Liquid)(EJ)
Tropical forest	1,76	528	211
Temperate forest	1,04	312	125
Boreal forest	1,37	411	164
Tropical Savannas	2,25	0	0
Temperate grassland	1,25	375	150
Deserts and Semi deserts	4,55	0	0
Tundra	0,95	0	0
Wetlands	0,35	0	0
Croplands	1,60	480	192
Total	15,12	2106	842

Despite the importance of the studies already made, such as providing useful benchmarks, they take market conditions as given, but prices and markets will

eventually change in the future and will depend on new policies such as GHG mitigation policies which could create additional incentives for biomass production for energy purposes (Reilly & Paltsev, 2008).

The Europe Challenge

The European Environmental Agency (EEA)(2006) estimated that, for 2020, biomass would be able to contribute with 13% (or 236 million tones oil equivalent (toe)⁵) of the energy demand (1,8 billion toe). This share is nearly 3,5 times the value provided back in 2003 (69 million toe⁶). The Impact Assessment of the Renewable Energy Roadmap (IARER) has also gotten similar conclusions, since the lower scenario presented a biomass potential of 195 million toe⁷, and the higher, of 230 million toe⁸.

However, both studies discriminate two stage patterns. One concerns a short or medium term, where biomass is partly from waste, forestry and residue while the other pattern is a longer run, and most of the genuine growth in biomass potential will have forcedly to come from agriculture or agricultural products. Hence, according to those predictions, the Agriculture and Rural Development department from European Commission has presently stated that in 2020, biomass will contribute with two-thirds of the renewable energy target, which means that the in order to reach this rate, biomass would have to double.

In order to decrease the dependency on energy supply, one of the main energy policy targets in EU is to double the RES in gross inland consumption, and the major contribution is expected to come from biomass. The Renewable Energy Directive 2009/28/EC (RED) adopted by the European Council in April 2009, states that by 2020 20% of the gross final consumption of energy should come from renewable sources as well as 10% of EU transport fuel (see Fact Box H). According to European Biomass

⁵ 236 Mtoe \approx 9,88 EJ;

⁶ 69 Mtoe \approx 2,89 EJ

⁷ 195 Mtoe \approx 8,16 EJ

⁸ 230 Mtoe \approx 9,63 EJ

Association (AEBIOM, 2011) biomass will remain the most important source for renewable energy in the EU (accounting for 57% of the total) – although this share is less than originally predicted by the European Commission, i.e. two-thirds of the renewable energy supply in 2020. The biggest increase is projected to come from agriculture (such as energy crops, biofuels crops and biomass). Actually the breakdown of EU-25 gross energy consumption by 2005, showed that biomass had a share of 66% from renewable energy, which represents 6% of the total energy consumed (EC, 2005).

Fact Box H: Member States' National Renewable Energy Action Plans (NREAP)	
Target year 2020	20% - of gross final consumption = renewable source 10% - of EU transport fuel= renewable source 37% . of electricity = renewable source

According to the Biomass Energy Europe (BEE) project, which compares over than 70 assessments regarding biomass potential, most of the studies converge in two main points: (1) biomass potentials from waste and forestry are relatively stable over time and (2) the biggest uncertainties rise upon the question addressing how much biomass for energy would EU agriculture be able to supply. Table 14 summarizes some of the projected biomass potentials for Europe.

Table 14 – Compilation of projected future level of biomass potentials for Europe

Estimates of bioenergy potentials for Europe (EU-25)	Energy flow (EJ/year)	Year	Sources
Potential bioenergy resource	16 - 17	2020	Elbersen <i>et al.</i> (2012)
Potential bioenergy resource	15 - 18	2030	
Agriculture, forestry, energy crops	100 - 400	n.d.	Panoutsou,(n.d)
Potential from energy crop from agriculture	5,96	2020	EEA (2006)
Potential from wood biomass	1,62	2030	
Potential from energy crop from agriculture	2,51	2020	LOT 5
Potential from wood biomass	2,15	2030	
Potential from energy crop from agriculture	2,09	2020	IIE (2006)
Potential from wood biomass	1,12	2030	
Total (wood from forest + waste and residues + energy crops from agriculture)	9,84	2020	EUROSTAT (2003)
	1,24	2030	
Biomass potential	8,4	2020	EUBIA (2008)
Biomass potential	16,7	2030	
Forest biomass, crop residues and energy crops	7,7 – 9,2	2030	Ericsson & Nilsson (2004)
Forest biomass, crop residues and energy crops	15,7 – 18,9	2050	
Agricultural residues + bioen. in surplus agric lands – West EU	8 – 25	2050	Smeets <i>et al.</i> (2004)
Agricultural residues + bioen. in surplus agric lands – East EU	4 - 29	2050	
Raw feedstock from dedicated bioenergy crops	3,3 – 12,2	2030	Wit & Faaij (2008)
Potential from energy crops+residues+surplus forest - CEEC	2 – 11,7	n.d.	Dam <i>et al.</i> (2007)

Between the WEC⁹ and CEEC¹⁰, the latter present the higher production potential (i.e. in countries such as Poland, Bulgaria, Romania and Ukraine). Moreover, in most CEEC, the production potentials of biomass are larger than the actual current energy use in the more favorable scenarios (Dam *et al.*, 2007). Nevertheless, France, Germany and Spain also present a considerable potential within the WEC (de Wit & Faaij, 2008).

According to energy projection, the use of biomass for energy generation in Europe should reach annually between 9 and 10 EJ/year in order to meet the European renewable energy targets (EC, 2006)(Table 15). Table 16 shows some of the energy statistics regarding the current energy panorama.

⁹ The Western European Countries (WEC) is an OECD term for the group of countries comprising the United Kingdom, France, Netherlands, Belgium, Luxembourg, Germany, Italy, Ireland, Denmark, Norway, Iceland, Sweden, Finland, Austria, Switzerland, Portugal, Spain, Greece, Vatican City, San Marino, Monaco, Andorra and Liechtenstein, and Malta

¹⁰ The Central and Eastern European Countries (CEECs) is an OECD term for the group of countries comprising Albania, Bulgaria, Croatia, the Czech Republic, Hungary, Poland, Romania, the Slovak Republic, Slovenia, and the three Baltic States: Estonia, Latvia and Lithuania.

Table 15 – European Energy demand from biomass 20% scenario for 2020

Maximum biomass contribution needed	9,63 EJ/year
With 15% of imports, maximum contribution from EU	8,16 EJ/year
Maximum contribution from agricultural crops:	2,64 EJ/year
Maximum contribution from other than agricultural biomass	5.53 EJ/year

Table 16 - EU-25 Energy statistics (in 2002) (Source: EUROSTAT, 2002)

Annual gross inland consumption (GIC)	70,3 EJ/year
Share of renewable energy sources in GIC	4,0 EJ/year
Share of bioenergy in GIC	2,6 EJ/year

European Commission – Agriculture and Rural Development - is confident that overall the EU has a great potential for increased production of biomass and moreover, that targets can be met without disrupting food and feed markets, although it is required a more efficient mobilization of forest resources though. In addition, according to Wiegmann *et al.* (2005), the land available for biomass crop production is expected to increase within the next two decades (Table 17).

Table 17 - Land available for biomass crop production in the EU-25 (Source: Wiegmann *et al.* 2005)

Land available (*1000 ha)	2010	2020	2030
EU-15	8 089,9	10 569	12 135
EU-8	5 846	7 392	8 029
Total	13 945	17 952	20 164

In fact, already in the period from 2004 to 2006, the European Commission estimated that the agricultural land use for energy in the EU increased drastically: from 0,3 to 1,3, of which the share per biomass type can be found in the Table 18. The energy crops accounted solely with 3-4% of the EU-25 arable area. The land use needed to meet the 10% biofuels production in 2020 where estimated to be around 17,5 Mil ha(15%) from the total arable land (i.e. 113,8 M ha) (Elbersen *et al.*, 2008).

Table 18 - Share of agricultural land per biomass type in EU (Source: Elbersen *et al.*, 2008)

Rapeseed	Wheat	Other Cereals	Sunflower	SRC	Grasses	Other
75 %	3%	5%	2%	1%	2%	12%
Total: 100%						

Elbersen *et al.* (2012) have mapped the potentials (in ktoe) within the Biomass Futures project for many classes of bioenergy which allow showing relative opportunities in the different Member States. For instance, Figure 8 presents the potential of dedicated perennial crops and agricultural residues under a reference scenario and a sustainability scenario (the reference scenario assumes that the current legislative requirements regarding the sourcing of biomass are met, while the sustainability scenario applies more stringent criteria in order to extend the requirement to deliver explicit GHG savings to all bioenergy consumed in the EU). The fact that these maps are broken down to at least the national level provides valuable information about the biomass opportunities, a crucial step for policy making.

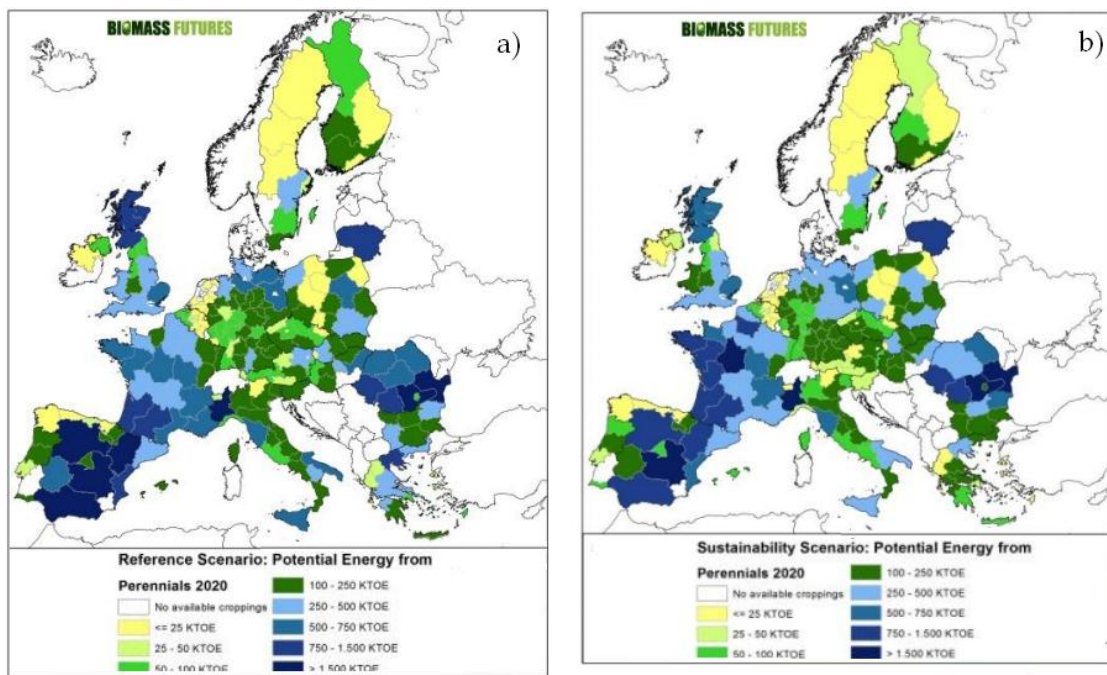


Figure 8 - Dedicated cropping potential with perennials on released agricultural land in 2020 under reference and sustainability scenarios from Biomass Futures project (Source: Adapted from Elbersen *et al.*, 2012)

Generally, the countries presenting larger potentials are the biggest and have the largest forest area; population as well as agricultural sector. However, most of the countries belonging to this group (such as Germany and Italy) are likely to decline their potential, conversely to other countries such as Spain.

The case of the Iberian Peninsula

Regarding solely the Iberian Peninsula, it presented a share of 8% of potentials in 2020 (Portugal accounted with 1% and Spain with 7%) (Elbersen *et al.*, 2012), that would result in the potentials shown in the Table 19.

Table 19 - Potentials (EJ) of rotational and perennial crops for Iberian Peninsula based on time period and scenario (Source: calculated after Elbersen *et al.*, 2012)

Class of bioenergy resource	Description of the class (examples of biomass sources included)	Current availability	2020 use (ref.)	2020 use (sus.)	2030 use (ref.)	2030 use (sus.)
Rotational crops	Crops grown meet bioenergy needs (e.g. maize for biogas) and crops used as biofuel feedstock (e.g. rape)	Spain	0	0,050	0	0,059
		Portugal	0,001	0,007	0	0,008
	Iberian Peninsula (total)	0,030	0,057	0	0,067	0
Perennial crops	Dedicated energy crops providing lingo cellulosic material	Spain	0	0,170	0,152	0,144
		Portugal	0	0,024	0,021	0,021
	Iberian Peninsula (total)	0	0,194	0,174	0,164	0,124

Smeets & Faaij (2007) have also made a study consisting in a bottom-up analysis of energy production potential for woody biomass (or wood fuel) from forestry in 2050, throughout an extensive review of key drivers which enabled to determine the potentials. The results showed that woody biomass (from plantations, forests, trees outside forests and wood logging) can theoretically provide a large source of bioenergy in 2050 up to 8,5 Gm³ (98 EJ) and 9,6 Gm³ (111 EJ) with and without deforestation, respectively.

2.3.5 Biomass for Energy Competition factors

As previously said in section 2.3.3, biomass use is expected to increase, so it is global demand for bioproductive land. However, besides biomass forecasted expansion, food and fiber are also expected to increase since global population will raise leading to a growing demand of food and animal products demand (Johansson & Azar, 1997; Gielen *et al.* 2003, Rost *et al.*, 2009). Hence, the increased use of biomass for energy production has been triggering a heated debate about sustainability since, the land

required for energy purposes generate *competition* with food and feed production (Dornburg & Faaij, 2007; Johansson & Azar, 2007; Campbell *et al.*, 2008; Reilly & Paltsev, 2008; Rost *et al.*, 2009; IPCC, 2001; Harbel, 2011). For instance, when it comes to land, we can say that there is a competition when there is the need of land to grow energy crops and land for food and wood production, and no surplus land is available (Reilly & Paltsev, 2008) – an explicit example is provided in the following Fact Box.

Fact Box I: Land competition between biomass for energy

Already in Europe, more specifically in Belgium, biofuels objective of 5,75% by 2012 (using local resources), imply that more than **20% of used agricultural land had to be dedicated to biofuel** (Pohl, n.d.)

Therefore, the rapid expansion of agricultural land dedicated to bioenergy, poses several consequences for global climate ecosystems as well food security. The use of food agriculture lands for bioenergy purposes can lead to the increase of food-insecure people worldwide and extra environmental pressures (Campbell *et al.*, 2008). These pressures can affect directly (such as economic affection of production, consumption and trade) or indirectly, through the creation of new markets. These markets are for products that can be used as biomass feedstock providing substitutes for the petroleum-based fuels (FAO, 2006).

Land Competition

Besides deforestation and land use changes, (which will ultimately result in an increase in the potential of positive feedback of CO₂ release) (Dornburg & Faaij, 2007), one of the most challenging aspect faced by biomass for energy production is its large-scale requirements for land, water and other production factors (IPCC, 2011). Moreover, energy crop and food production compete as well for water and many other factors (IPCC, 2011). A reckless land management can thus lead to overexploitation and resource degradation (IPCC, 2011). Hence, land availability (besides biomass yield) can be responsible for limiting the amount of biomass (Gielen *et al.*, 2001).

Due to the previous given reasons, the competition between land and resources destination requires an urgent need of a better understanding of the ecological processes involved, in order to enable a good planning and management – as well a correct policy deployment (Rost *et al.*, 2009). In fact, Haberl *et al.* (2011) predict that in the year 2050, the magnitude of global bioenergy potential is strongly affected by food production requirement for livestock and that biomass flows in the food system should be carefully addressed in order to derive realistic potentials for future bioenergy supply.

Fact Box J : Land competition assessed by Smeets & Faaij (2007)

Land competition can be seen in Smeets and Faaij (2007) study that has estimated a global theoretical potential of biomass from forestry in 2050 of **112 EJ/year**. However, this value got **reduced** to **71 EJ/year** **after taking into consideration the demand for other uses of biomass than bioenergy use** (e.g. wood production for furniture). Moreover, after considering economic considerations in their analysis, this number has decrease even more to 15 EJ/year. For Europe solely, in order to reach the EU targets for biofuel it would be required 11,2 Mha by 2010 corresponding to 13,6 % of total arable land (in the EU25).

The magnitude of the potential of biomass resource greatly depends on the priority given to bioenergy products against other products obtained from the land such as food, fodder, fiber and other products from forest. Another aspect on which the potential of biomass resource is dependent is the amount of total biomass that can be mobilized in agriculture and forestry. This last factor is affected by several conditions such as: natural conditions (like climate, soil and topography); by forest and agronomy practices; and by how nature conservation and protection is prioritized and thus how this priorities shape the production systems (IPCC, 2011). Hence, it is highly urgent to model and understand the magnitude as well as the spatial patterns of global bioenergy potentials (Haberl *et al.*, 2011). Also the interrelations between the supply of food, fiber and bioenergy have to be understood since these three products compete directly for land-use.

According to Tubiello, *et al.* (2007), developing countries are likely to have some agricultural land expansions, namely in sub-Saharan Africa and Latin America and crop yields are expected to continue to rise (from 2.7 t/ha today to 3.8 t/ha in 2050). Approximately 10 % of the ≈14 billion hectares of ice-free land on our planet are used for crop cultivation and 25 percent is used for pasture. According to Tubiello *et al.* (2007), every year food and feed production reaches over 2 billion tonnes of grains, which corresponds to two-thirds of the total direct and indirect protein intake. In regards to Europe, an IEA (2003) study estimated that a use of 38% of total acreage in the EU15 would be required in order to replace 10 % of fossil fuels by bioenergy by 2020 – whereas based on land requirements for food production and nature conservation, the availability of land for non-food production in Europe is large at 90 Mha (on a total of 158 Mha arable land and 77 Mha pasture, overall share 38% by 2030) (de Wit & Faaij, 2008).

Fact Box K:Overcoming land competition throughout the use of degraded land

Clearing forest land for new bioenergy crops can lead to CO₂ emissions from terrestrial carbon pools which are substantially greater than any GHG benefit provided by biofuels. Thus, raising new bioenergy crops on degraded land that once was agricultural land is **emerging as a sustainable approach to bioenergy** providing environmental benefits and contributing to climate change mitigation **without having to compete food production** (Johansson & Azar, 2007; Campbell *et al.*, 2008) or even leading to extra release of carbon stored in forests (Campbell *et al.*, 2008).

Food Competition

Questions regarding potential of world agriculture are increasingly pertinent, namely those related with food security and environmental implications (FAO, 2006). These prospects raise a great concern: for instance, could improvements in food consumption and nutrition be achieved in the foreseeable future? (FAO, 2006). The overall conclusion is that the scale of energy use in the world relative to biomass potential is so large, that land use and conventional agricultural markets are expect to be highly affected by bioenergy industry demand (Reilly & Paltsev, 2008).

FAO projections for 2050 (2006), help to establish how much food and related agricultural resources may be required by the world population, for each country. This data consists in fact in a very valuable perception when it comes to evaluate the driver of agricultural resource to other uses (and what can this imply for food security) (FAO, 2006). The United Nations *World Population Prospects-the 2002 Revision*, predicts a drastic slowdown in world demographic growth. In 2000, the world population was 6,071 billion, and it is projected to grow up to 8,920 by 2050. However, even though the growth rate is expected to suffer a considerable fall, the annual increments in population continue to be very large, mostly in developing countries (FAO, 2006). Once global demand for food is predicted to double within the next 40 years, it will lead to a competition between agricultural land use and biomass generation land use (Reilly & Paltsev, 2008). However, this competition is not likely affecting every country.

Fact Box L : Western Europe agricultural production is exceeding food and fodder demand

According to Gielen *et al.* (2001), fortunately for Western Europe has reached a condition where its **agricultural production potential exceeds the food and fodder demand** due the steadily increasing agricultural productivity. If the trend persists, a considerable amount (10 – 20 percent of the agricultural land) can be shifted towards other purposes instead of food production. Furthermore, if that land would receive a high-yield biomass crop, it could yield up to 500 Mt biomass per year – constituting thus an important option for GHG emission reduction (Gielen *et al.*, 2001).

One of the major consequences from food competition is the food commodities prices (Johansson & Azar, 2007) which are a consequence of cases similar to the one presented in Fact Box L. Since food and fiber are considered as the big constraint for bioenergy production, the creation of policies concerning bioenergy production will provide security regarding unintended food prices rising as well as environmental pressures (Haberl *et al.*, 2011).

Fact Box M: Shifting between food crop and energy crop

In Sweden, (unless agricultural commodity prices increase), farmers **shift toward energy crop cultivation as soon as profits from biomass plantations exceeds profits from food production**. This is one of the reasons justifying competition between biomass and food that will ultimately lead to increased food commodity prices (Johansson & Azar, 2007).

Even though the several studies regarding energy potentials (see Table 12 and Table 14) (Berndes *et al.*, 2003; ; Hoogwijk *et al.*, 2005; Smeets *et al.*,2007; Reilly & Paltsev, 2008), the interrelations between food and bioenergy (and their driven competition) have not been satisfactorily addressed. However, in order to overcome this lack observed on other approaches, Haber *et al.* (2011) has also included the interrelations between food and bioenergy through a socioeconomic approach, by developing a biomass balance model linking supply and demand of agricultural biomass.

For instance, estimating projections for bioenergy potentials for 2050, Haber *et al.* (2011) have assumed an approach where food demand is stated a priority. Hence, in order to calculate the area available for producing bioenergy on cropland, they subtracted the required for food, feed and fiber which were calculated within the biomass-balance model presented in the figure below.

Table 20 - Food supply in 2000 and two assumptions for the year 2050: A “business-as-usual” forecast (BAU) as well as “fair and frugal” diet (“fair”) assuming a switch to equitable food distribution and less meat consumption. Absolute numbers are in MJ/cap/day (Source: adapted from Haberl *et al.* 2011)

	Total food supply 2000	Share of animal products 2000	Total food BAU 2050	Change in total BAU 2050/2000 [MJ/cap/day] or %	Share animal products BAY	Total food “fair” 2050	Change in total “fair” 2050/2000	Share animal products “fair”
W. Europe	14,36	31%	14,75	3%	32%	11,72	-18%	7%
E & S.-E Europe	12,86	25%	13,62	6%	27%	11,72	-9%	9%
World	11,67	16%	12,53	7%	16%	11,72	0%	8%

Biomass availability for energy is thereby highly dependent on: (1) the future demand for food (which is driven by population growth and diet); (2) the type of food production system; (3) the productivity of forest and energy crops; (4) the change in the use of bio-materials and finally (5) the availability for degraded land and (6) competition among land use types (Hoogwik *et al.*, 2003). Hence, besides the already mentioned needs of a deeper understand of bioenergy potential and its sensitivity and affection under feedbacks it is of great interest and importance to assess as well the interrelations between bioenergy and food and fiber.(Whitmarsh & Govindjee, 1995; Harverl *et al.*, 2011; Schaphoff *et al.*, 2006).

2.4 Terrestrial Productivity and its relationship with Biomass

Productivity is the rate at which new biomass is generated, mainly due to photosynthesis. It is commonly expressed in units of mass per unit surface (or volume) per unit time, and the mass unit can refer to dry matter or mass of generated carbon (Allaby, 2006) (e.g. grams of Carbon per square meter per year (gC/m²/year).

Based in empirical observations, it is assumed a relationship between productivity and biomass and thus, biomass is said to be a direct function of productivity (O'Connor, 2003; Allaby, 2006; Keeling & Phillips, 2007). These observations consist of the fact that both productivity and biomass are limited by similar ecologic factors such as temperature, nutrient and moisture availability (Keeling & Phillips, 2007). However, contrarily to what would be expected (within an intuitive perspective) both productivity and biomass do not behave in a proportionally manner in space and time under comparisons or simulations of future high-productivity ecosystems (Keeling & Phillips, 2007). In other words, carbon storage does not evolve in a monotonically manner, i.e. it does not necessarily increases with increasing productivity. For instance, despite the highest rates of productivity in tropical areas, the most massive forests are found in temperate climates. Hence, besides growth rates (or productivity levels), there are other factors strongly related to biomass levels (Keeling & Phillips, 2007), such as the changing regimes which can affect the ability of accumulating carbon (Pregitzer & Euskirchen, 2004).

Despite its importance to the development of vegetation models, the empirical relationship between productivity and biomass has in fact been very poorly addressed in studies. However, few studies (Whittaker & Likens, 1973; O'Neill & Angelis, 1981), have shown a linear correlation between above-ground net primary productivity (ANPP) and above-ground biomass (AGB) (as illustrated in Figure 9), although, both studies were not regarding natural high-productivity sites.

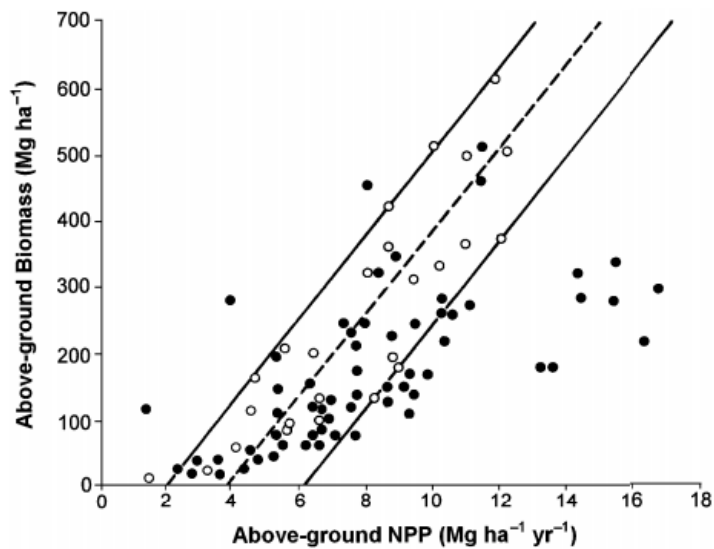


Figure 9 - Relationship between above-ground net primary productivity (NPP) and above-ground biomass (AGB) (Source: O'Neill & Angelis, 1981)

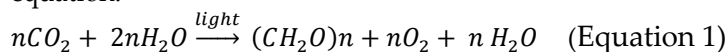
2.4.1 Gross and Net primary productivity

Within the scope of this study, biomass is only related to plants which are autotrophs beings (and hence primary producers) (Amthor & Baldocchi, 2001; Allaby, 2006), this productivity is called primary productivity - or production (Allaby, 2006). Primary production refers to the synthesis of new organic material from inorganic molecules (such as H₂O and CO₂), and this procedure is ruled by the so-called *photosynthesis* process (which is hereafter addressed more closely in Fact Box N) (Allaby, 2006).

Fact Box N: The photosynthesis process

Photosynthesis occurs in the leaves of plants and any other green tissue (such as stems) (O'Connor, 2003). Terrestrial vegetation responds to weather and climate through multiple processes which will determine where and how plant species grow; their composition, and structure of vegetation change over time. These processes are: (1) physiological (e.g. uptake and translocation of CO₂, nutrients and water); (2) demographic (e.g. growth, mortality and reproduction of plants) and (3) ecosystem nutrients (e.g. linking of the biotic and abiotic environments through the cycling of carbon, nutrients and water between soil and vegetation (Bonan, 2002).

In order to grow and survive plants produce carbohydrates (e.g. glucose, a six-carbon sugar) which provide energy, structural material and building blocks for other molecules. Its synthesis is possible through carbon dioxide (CO₂), water (H₂O) and light energy (i.e. radiation wavelengths ranging between 0.4 μm and 0.7 μm,) absorbed by plants. This consists in a complex chemical reaction, named as *oxygenic photosynthesis*, which can be simplified with the following equation:



where n stands for the number of CO₂ molecules that combine with water in order to form carbohydrates (CH₂O) n , leading to the release of n oxygen (O₂) molecules to the atmosphere (Whitmarsh & Govindjee, 1995; Bonan, 2002). The overall oxygenic photosynthesis occurs in the chloroplasts of leaves and during three main processes called *dark reactions*, *light reactions* and *diffusion* (Whitmarsh & Govindjee, 1995; Bonan, 2002).

During the light reactions plants produce chemical energy converted from light through electron and proton transfer reactions. After, while dark reactions occurs the chemical energy earlier produced during light reactions is used to reduce CO₂ to carbohydrates through enzymatic processes. The third process, i.e. diffusion consists in the opening of stomata to allow CO₂ to diffuse into leaves from the surrounding air (Whitmarsh & Govindjee, 1995; Bonan, 2002).

The Gross Primary Production (GPP) refers to the rate at which photosynthetic organisms capture and store a certain amount of chemical energy as biomass within a certain period of time (Amthor & Baldocchi, 2001). Some of the energy captured is afterwards used by primary producers for the respiration process, (as well as maintenance of tissues and reproduction of the primary producers). Thus the captured energy remaining is referred to as Net Primary Production (NPP) (Amthor & Baldocchi, 2001). Summing up, NPP is defined as GPP less autotrophic respiration (Amthor & Baldocchi, 2001; Running *et al.*, 2001; Sitch *et al.*, 2003; Knorr & Kattge, 2005; Rost *et al.*, 2009), and can be stated as follows:

$$NPP = GPP - R_a \quad (\text{Equation 2})$$

were R_a is autotrophic respiration. The figure below illustrates the relationship between NPP, GPP and temperature:

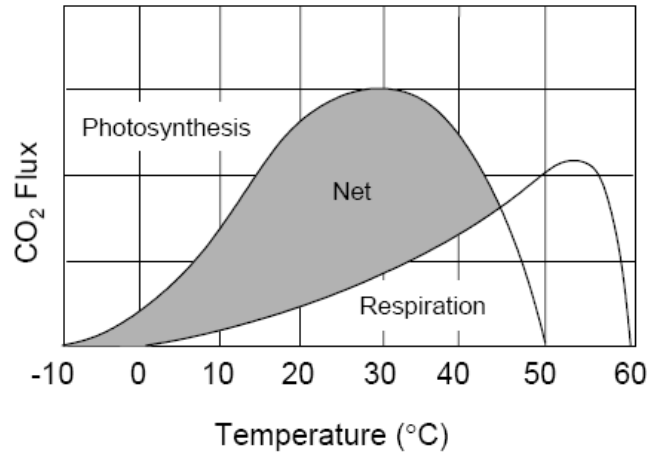


Figure 10 - Photosynthesis, respiration and Net Primary Productivity along temperature and CO₂ flux changes (Source: Whittaker & Likens, 1973)

NPP thus consists in the rate at which plants in a given ecosystem produces useful chemical energy (Amthor & Baldocchi, 2001), or in other words, the amount of energy trapped in organic matter during a specified interval (not accounting with the amount that is lost during respiration) (Rost *et al.*, 2009). Hence, both NPP and GPP units is the same, earlier present for productivity (Amthor & Baldocchi, 2001).

Net primary production (NPP) is widely used as a concept for meaning the amount of biomass produced by green plants through photosynthesis (as it was used in prior chapter 3.3- tables 5 and 6). The human appropriation of NPP (i.e. HANPP) concept, enables to record changes in biomass balance of terrestrial ecosystems resulting mainly by human-induced changes in NPP.

The change in terrestrial biological productivity may be one of the most fundamental measures of “global change” with the highest partial interest to humankind, since it is the source of all food, fiber and fuel (Running *et al.*, 2000). In fact the NPP varies considerably according to the ecosystem type, for instance, evergreen tropical rain forests present about 1000 gC/m², while this value drops to less than 30 gC/m² for deserts (Running *et al.*, 2000). NPP is also strongly constrained by climatic factors,

which are closely related to photosynthesis such as temperature and precipitation, as it is shown in Figure 11.

Temperature plays a major role in terrestrial productivity: at cold temperatures, both photosynthesis and respiration are very low which means a negligible CO₂ uptake. In warmer temperatures enzymes are more active and uptake exceeds loss for a net CO₂ gain. However, after reaching optimal temperature, photosynthesis declines and besides that, greater respiration at warm temperatures leads to net photosynthesis declination (Bonan, 2002).

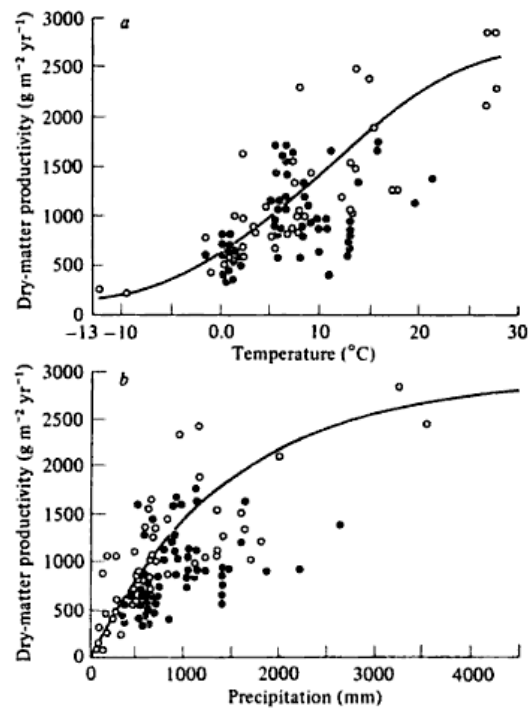


Figure 11 – Relationships between NPP and temperature (a) and precipitation (b). (Source: Whittaker & Likens, 1973)

NPP over large areas may change with increased atmospheric carbon dioxide (CO₂) and global climate change (Running *et al.*, 2000). Knowing the GPP and NPP changes in time, has a strong practical utility, since it is a measure of crop yield, as well as range forage and forest production. Economically and socially has a significant interest to assess and predict vegetation growth, for global policy and economic decision making (Running *et al.*, 2000). Due to photosynthesis process the amount of CO₂ removed from the atmosphere per year is considerable. It is estimated that photosynthetic organisms remove 100×10^{15} grams of carbon (C)/year which equates to 4×10^{18} kJ of free energy stored in reduce carbon (i.e. roughly 0,1 percent of the incident visible radiant energy incident on the earth per year. (Whitmarsh & Govindjee, 1995).

2.4.2 Absorbed Photosynthetically active radiation (APAR)

Another essential limiting factor affecting photosynthesis is light. Insufficient light incident on plants (i.e. when irradiance is below a certain level) leads to decrease of photosynthesis since, during the “light reactions” there is not enough chemical energy to fuel the “dark reactions” and thus, CO₂ uptake during photosynthesis is balanced by CO₂ respiration: net assimilation is zero. Hence, photosynthetic rates increase with greater irradiance until a certain light level (when increased light no longer enhances photosynthesis). After this “light saturation”, the rate of photosynthesis is then more affected – or limited by the amount of CO₂ and rubisco instead (available for the dark reactions) (Bonan, 2002).

When annual crop plants are well-watered and fertilized, the NPP is linearly related to the amount of solar energy absorbed by them (Running *et al.*, 2000). In fact, the growth rate is proportional to the amount of solar radiation received – when it is assumed that other environmental parameters are not limiting the growth rate (Kania & Giacomelli, 2002).

The fraction of the solar radiation called as visible light, which is a composite of wavelengths ranging between 400 and 700 nanometers (nm) can be defined as “absorbed photosynthetically active radiation” (APAR) is responsible for providing the light energy that the plants will use on their biochemical processes in photosynthesis in order to be converted into biomass (Kania & Giacomelli, 2002).

The APAR includes implicitly the amount of leaf area which is absorbing radiation, which is called the leaf area index (LAI) (Running *et al.*, 2000), and can be measured in radiometric units (W/m²) – to determine its total energy value or it may also be measured in quantum terms (μmol s⁻¹ m⁻²) to calculate the amount of the sunlight specifically available for plant growth during a specific growth period (mol/m²).

Light-Use Efficiency

Light-use efficiency (LUE) is the ability of canopy to use light for photosynthesis. Along with many other features LUE provides a physical basis for scaling carbon

uptake processes from the stand to the global scale. A better understanding of the factors that control LUE will hence result in enhanced estimates of carbon uptake from the terrestrial biosphere (Chasmer *et al.*, 2008).

LUE can be defined as the ratio of GPP to absorbed photosynthetically active radiation (Chasmer *et al.*, 2008; Polley *et al.*, 2011) (APAR), i.e.:

$$LUE = \frac{GPP}{APAR} \quad (\text{Equation 3})$$

LUE is typically estimated over averaging periods (like all the other variables, 30 years at the present case). Therefore, this ratio enables to describe the ability of vegetation to use light for photosynthesis. The LUE was in 1998 summarized by Dewar *et al.* in the following manner: “(1) LUE is constant during vegetation growth when water supply is non-limiting; (2) the use of carbon for gross photosynthesis (carbon-use efficiency; CUE) is constant across species; and (3) APAR is positively correlated with increased leaf nitrogen”. The previous generalization enable thus to aggregate LUE and vegetation productivity at many scales, throughout ecosystem models and land-cover types (Turner *et al.* 2002).

Effects of the environment on LUE may differ though among years, interannual dynamics of GPP and LUE are determined more by differences in weather patterns expressed over years, than by brief changes in the environment (Polley *et al.*, 2011). For this reason, LUE is affected by environmental “stresses” such as extreme temperatures or water shortages, since it is reduced lower than its potential value (Polley *et al.*, 2011). Multiple studies have also shown that LUE varies both linearly and nonlinearly with: changes in air temperature; vapor pressure deficit (VPD), soil fertility and soil water content (depending on vegetation type and so forth)(Chasmer *et al.*, 2008). Therefore, similarly to other ratios, LUE should not be addressed as a simple function of meteorological driving mechanisms. The efficiency with which vegetation uses light may change with increased air temperatures and drying, which is considered as to be one outcome of climate change in the IP. For instance, radiation can have a large but varying influence on LUE at two different sites, depending on canopy structural characteristics.

2.4.3 Carbon Cycle

Carbon can be stored in the atmosphere, oceans, biosphere and lithosphere and it exchange among these stores in the gas form (i.e. as carbon dioxide). This cycle of carbon exchange, can hence be characterized by *emissions* and *uptakes* (and pool storages). The net carbon uptake process represents the balance composed by two terms: the extra carbon emitted (due to fire emissions and ongoing land use change - (such as tropical deforestation) and carbon taken up by ecosystems through natural processes (Schaphoff *et al.*, 2006). The net uptake of carbon occurs essentially due to gains (resulting from increased growth or decreased decomposition outweigh losses), while net release of carbon (from biosphere may be resulted from soil decomposition rates in a warmer climate beginning to exceed the productivity of plants or where changes in vegetation composition implies a loss of woody biomass) (Schaphoff *et al.*, 2006).

Some studies of net carbon uptake by the land and ocean have estimated values of 2,6 and 2,2 GtC/year, respectively. On the other hand, according to Schaphoff *et al.* (2006), around the 1900s, fossil fuel burning accounted an average of 6,4 GtC/year of carbon emissions mainly by fossil fuel industries – whereas emissions by land use changes accounted with 1,6 GtC/year (Dixon *et al.*, 1994). The status of carbon in each store is controlled by forest management and climate changes, resulting in changes with time as can be accessed in Table 21. By convention, CO₂ “sinks”, i.e. CO₂ fluxes leaving the atmosphere reservoir have a negative sign

Table 21 - Global carbon budget, in GtC/year (IPCC 4th Assessment Report, 2007)

	1980s	1990s	2000-2005
ATMOSPHERIC INCREASE	3,3 ±0,1	3,2 ±0,1	4,1 ±0,1
EMISSIONS	5,4 ±0,3	6,4 ±0,3	7,0 ±0,2
OCEAN-ATMOSPHERE FLUXE	-1,8 ±0,8	2,2 ±0,4	-2,2 ±0,3
LAND USE CHANGE	1,3	1,6 ±	N.A ±
RESIDUAL LAND SINK	-1,6	-2,6 ±	N.A. ±

N.A.=No information available

In the previous century, the ocean and the land biosphere were both responsible for the uptake of the CO₂ released in the atmosphere by anthropogenic sources. However, this

continued uptake CO₂ remains highly uncertain due to the increase expected for CO₂ emissions for this century (Prentice *et al.*, 2001).

According to Whitmarsh & Govindjee (1995), more than 10 percent of the total atmospheric carbon dioxide is reduced to carbohydrate by photosynthetic organisms, each year. Major part of all the reduced carbon returns to the atmosphere as carbon dioxide by microbial, plant and animal metabolism and also through biomass combustion. Some estimations say that nearly 200 billion tonnes of CO₂ are converted to biomass annually, where 40% is by marine plankton while the remaining 60% from photosynthetic process (O'Connor, 2003). The amount of CO₂ released by the biota is about $1 - 2 \times 10^{15}$ grams of carbon/year while fire emissions contribute with 5×10^{15} grams of carbon/year. The oceans mitigate a considerable amount (which is estimated to be around 2×10^{15} grams of carbon /year)(Whitmarsh & Govindjee, 1995). In fact, in accordance with Cramer *et al.*, 2001, both oceanic and terrestrial uptake of CO₂ account each self to a quarter to a third of anthropogenic CO₂ emissions (although with uncertainty about the major location of the terrestrial sinks and with a strong interannual variability) (Cramer *et al.*, 2001).

The carbon cycle and climate have a great positive feedback since the expected effect of warming leads to a reduction in carbon sequestration in the biosphere, which may result in an amplified climate warming since net release of carbon to the atmosphere increases (Schaphoff *et al.*, 2006). This increase of CO₂ release is related to the effect that warming temperatures have on plant respiration: respiration increases in response to an increase in temperature (Atkin & Tjoelker, 2003) Thus, biosphere is strongly affected by climate change (Schaphoff *et al.*, 2006). Figure 12 presents the changes of carbon balances and stocks from present to future condition, after 70 years under twice time of CO₂ atmospheric concentration and an increase in temperature by 2,1°C estimated by the model Sim-CYCLE (Ito & Oikawa, 2002):

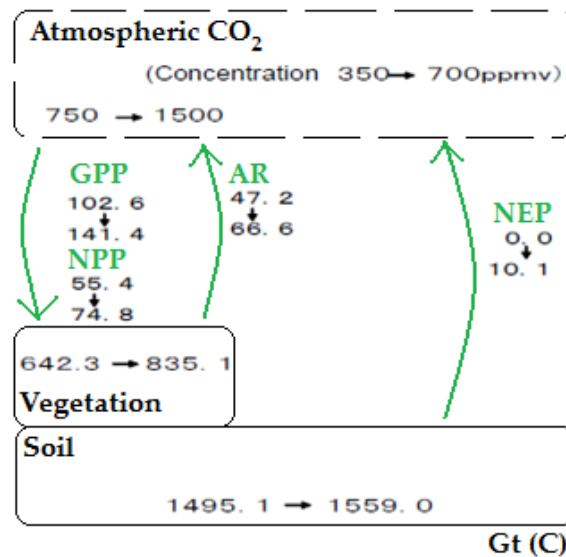


Figure 12- The changes of carbon balance and stocks from present to future –condition (Source: Adapted from Ito & Oikawa, 2002)

Terrestrial ecosystems are thus a fundamental component within the global carbon cycle and thus it is required a deeper understanding of the decadal to century-scale carbon balance dynamics in order to interpret observed variations in carbon exchanges between biosphere and atmosphere exchanges (Cramer *et al.*, 2001).

2.5 Impacts of Climate Change on Biomass

As previously described, the environmental factors directly affect and define the productivity of plants, as well as their carbon storage capacity. Productivity is influenced by both biotic and abiotic factors (Singh *et al.*, 2000). Plants, carry out all of their functions mainly through the availability of the so-called abiotic factors e.g. radiation, water and nutrients availability (Singh *et al.*, 2000). Hence, even though plants rarely reach their full biomass potential, the environmental limits to biomass accumulation come into effect rather before than genetic limits, by affecting the photosynthetic process (O'Connor, 2003). Therefore, the biomass resource potential can be influenced by impact of climate change.

As such, climate change (e.g. increases in atmospheric CO₂ concentration; higher temperatures; altered precipitation and transpiration regimes; increased frequency of

extreme temperature and precipitation events and weed; longer growing seasons ;floods and droughts as well as pest and pathogen pressure will affect plant development, growth, yield resulting in crop and pasture production impacts (IPCC, 2007; Haverl *et al.*, 2011; Whitmarsh & Govindjee, 1995; Bonan, 2002; Schaphoff *et al.*, 2006; IPCC, 2007; Tubiello *et al.*, 2007).

Global bioenergy potential on croplands (and forests) is therefore highly dependent on the (uncertain) effect of climate change on future global yields on agricultural areas. Moreover, Haberl *et al.* (2011) found the potential of primary bioenergy on cropland to be more sensitive to climate change than potential on grazing areas or residue potential, increasing thus the awareness of how climate change could affect energy crops potentials. Moreover, despite the high uncertainty related to the magnitude and spatial pattern of climate change, it is present a high confidence that climate change can influence technical potentials (Haber *et al.*, 2011).

Nitrogen is also another component with a relevant in photosynthetic rate, since is one of the constituent of chlorophyll and rubisco, and hence, greater amounts of nitrogen lead to higher rates of photosynthesis (Bonan, 2002). Even though these interactions still poorly understood it is predicted strong differences between different regions (IPCC, 2011). Moreover, the vegetation also interacts with biotic factors: in fact, their root system present is under the direct influence of a diverse group of micro-organisms which play an eminent role on the plant productivity. In fact, more than 90% of terrestrial plants are colonized by these organisms (in this case the mycorrhizal fungi).

Even though the impacts of climate change may negatively affect crop and pasture yields (and hence livestock) (Whitmarsh & Govindjee, 1995; Tubiello *et al.*, 2007), in some cases there are increases of yields and growth rates. In fact, the agro-ecosystems might be considerable affected by climate change but still, there is the idea that there can be both negative and positives effects on yields in different regions of the world (Haberl *et al.*, 2011). Hence, some of the known variables affecting the responses of crop and pasture: i.e. biogeographically changes in vegetation distribution and composition, are following described.

2.5.1 Temperature Increase

Temperature is one of the factor that affects net photosynthesis, since a certain range of temperature is required in order to allow biological activity Hence within this range, photosynthetic rate increases with temperature rise, until a certain temperature, beyond which afterwards will lead to lowers photosynthesis rates (Bonan, 2002) (as regarded in Figure 11). These ranges are very variable according to the natural environment of the plant and its specie. For instance, most of C₃ plants have an optimum temperature range from 15 up to 30 °C, while arctic and desert plants photosynthesize with below 0 or over 40°C, respectively (Bonan, 2002).

Moreover, one relevant consequence of rising temperatures is the declination of soil moisture which has strongly negative impact in crop production (Rost *et al.*, 2009), since it will decrease the water available to roots. Another relevant process driven by the warming of climate, is the fact that it leads to increase of transpiration water requirement which in turn leads to water use efficiency increase (through the increased stomatal closure) under a scenario of elevated atmospheric CO₂ concentrations (IPCC, 2011).

Fact Box O :The isolated effect of warming temperatures

According to the Intergovernmental Panel on Climate Change (IPCC) report (IPCC, 2007), at the plot level and without regarding changes in the frequency of extreme events, the moderate warming which occurred during the first half from the previous century might have increased crop and pasture yields in temperate regions and decreased yields in semiarid and tropical regions (Tubiello *et al.*, 2007). This increased yield in temperate regions occurred under temperature rising up to 1-3°C and associated CO₂ as well rainfall changes, on the other hand the negative yield impact in tropical regions occurred for the major cereals even though with moderate temperature increases – 1-2°C (Whitmarsh & Govindjee, 1995; IPCC, 2007 and Tubiello *et al.*, 2007).

Some high-resolution regional climate models (RCMs) have their ability to capture accurately certain observable climate conditions affected somehow. It may be mainly due to the fact that they share temperature-dependent biases (Bober & Christensen,

2012). Hence many present climate models may be overestimating regional amplification of global warming. For instance, Bober & Christensen (2012) have concluded that the Mediterranean summer temperature projections are reduced by nearly one degree. Moreover, some individual models may be overestimating increases in temperature by several degrees.

In those regions where NPP is mainly constrained by too low temperatures (such as in the northern high latitudes) Several predictions agree uniformly in that it is expected a positive climate-change effect on crop yields there by 2050 (Haberl *et al.*, 2011).

2.5.2 Changes in precipitation pattern

Decreased precipitation events predicted in many climate change scenarios, lead to replacement of some tropical forest areas by grasslands which will ultimately lead to a reduction of tropical NPP (Cramer *et al.*, 2001). However, precipitations patterns consist in one of the less consistent and reliable aspects of current climate models (Cramer *et al.*, 2001).

The lack of water – or water deficits, poses challenges to plant in what concerns productivity whether in dry season or growing season. During the first, lack of soil water leads to a nutritional stress since concentration of protein are low and also due to the lower dry matter digestibility of dead plant tissue (McCown & Williams, 1990). Although less common, the lack of water during the growing season results in feed shortages in the subsequent dry season (McCown & Williams, 1990).

The current world population consumes over than 8.000 km³/year of water – downscaling to a single person: an individual requires on average a 1.300 m³/cap/year to produce food (assuming a 3000 kcal/cap/day with a 20% share of meat) (Rost *et al.*, 2009). However, in accordance with IPCC's SRES A2r scenario, the global population is expected to rise up to 10 billion in 2050 (which would imply more 5000 km³/year of water to fulfill water needs) (Rost *et al.*, 2009).

Around 16% of the total cropland is equipped with irrigation. This water demand is expected to increase further, since during the last century, the “blue” water

withdrawals (e.g. from aquifers, lakes and rivers) has increased in order to provide irrigation systems as well for other purposes. Moreover, it is important to notice that the rate of increase of blue water withdrawal has been higher than the actual growth rate of the world population (Shiklomanov, 1993).

Photosynthesis decreases with the decrease of foliage water potential which could happen when transpiration is exceeding root uptake leading to the desiccated of the leaf (Bonan, 2002). Due to water essential role, photosynthesis decreases sharply when stomata close after the leaf water content falling below a minimal value. Stomata inclusively close under high vapor pressures deficits in order to reduce water loss during transpiration (Bonan, 2002).

Fact Box P :The role of stomata in photosynthesis

The plant feature which allows both CO₂ uptakes and water loss control during transpiration is the *stomata* which have evolved in order to maximize CO₂ uptake and minimize water loss as well (Bonan, 2002). Different irradiances; nutrient concentrations; ambient CO₂ concentrations; and leaf water potentials over different plants, leads to different and large variation in photosynthetic rate and stomatal conductance which vary proportionally i.e.: net photosynthesis increases with increases in stomatal conductance. In fact, there is a positive correlation between maximum stomatal conductance and maximum rate of photosynthesis.

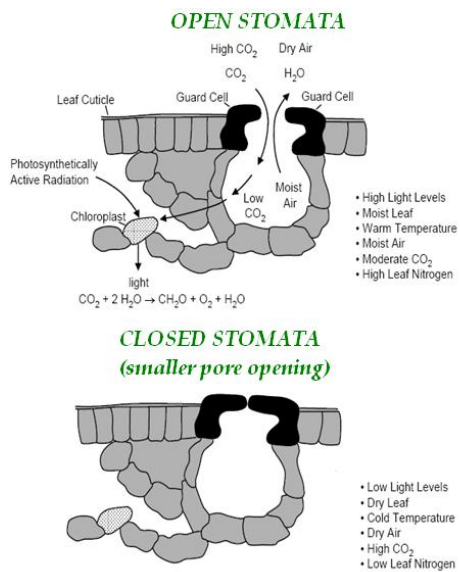


Figure 13 - Stomata scheme (Source: Bonan, 2002)

2.5.3 Global NPP perspectives under water limitations

The maximum achievable global crop NPP (admitting crop transpiration to be at its maximum value) was estimated to be 23,5 Gt in the absence of water limitation. Although 16% of global cropland has irrigation systems deployed and hence, this earlier theoretical potential drops around 50% (i.e. 11,4 Gt) when no irrigation is assumed (Rost *et al.*, 2009). Nevertheless, the existing irrigation allows reaching an increase in global crop NPP by 17% up to 13,3, Gt is currently achieved (Rost *et al.*, 2009).

The Rost *et al.* (2009)'s study, allow to understand that some regions of the world, namely those with lower ratio of NPP and NPP assuming that it is always under saturated soil, are strongly water limited and hence regions with this ratio closer to 0 are strongly water-limited whereas regions with regions showing values closer to 1 are the opposite. Both northern and central Europe presents a small water limitation, while Mediterranean countries present stronger water limitation. In fact, in Iberian Peninsula, roughly speaking, Spain present lower water limitations (ranging between 0,25 and 0.5) while Portugal exhibited the same rations in the South, and higher rations (ranging between 0,5 and 0,75) for the center and the North (Rost *et al.*, 2009).

Many studies present several results showing that such a decrease in crop production by 17% and on irrigated land by 54% in the absence of irrigation (Siebert & Döll, 2009).

Water scarcity poses great challenges for many countries placed in North Africa was well as Middle East and South Asia, since future food self-sufficiency is likely to remain unachievable (Rost *et al.*, 2009). In fact, the global population which lives in countries without enough blue and green water (on present cropland) for producing a healthy diet increases from 2,3 billion to roughly 6 billion by the 2050s. Hence, the associated additional water demand was estimated to be around 4500 km³/year (Rost *et al.*, 2009). Whereas there is a water-stressed situation, stomata are further closed until transpiration reaches a specific root supply rate which depends on soil moisture (Knorr & Kattge, 2005).

In accordance with Falkenmark *et al.* (1990), all forms of agriculture can be described as being water-dependent land use. Which means, that crop growth is conditioned by the availability of substantial volumes of root zone water for evapotranspiration. For that reason, water consists in the main limiting factor in biomass production (Falkenmark *et al.*, 1990). Therefore, an important issue driven within this context, is the need of developing a deeper understanding of water and soil interactions in biomass production. This knowledge can support the attempt of increase water productivity (or water-use efficiency), i.e. to produce more biomass per unit of water – which is necessary if agricultural productions is threaten by climate change, and more specifically, by a water-scarce condition (Rockström *et al.*, 2007).

The decreased biomass productivity is usually correlated to the declination in plant-available soil moisture and nutrients, along with fertility depletion, leading to a productivity crisis in the agriculture. Since that both water and soil are finite resources, the only way of increasing biomass production in agriculture is throughout the increase of water productivity, i.e. the water use efficiency (WUE) which means: more biomass per unit of water.

Water-Use Efficiency (WUE)

As previously found throughout the analysis of water balance, the climate change expected for the futures scenarios aggravate the problem of water shortages. When temperature rises and precipitation decreases, water requirements increase and being necessary to evaluate this increase. The changes suffered by herbaceous plants and forest as a consequence of the changing environmental patterns referring to yield are mainly caused by variations in water availability (when CO₂ elevation is disregarded). Therefore, one of the main concerns drawn by the variability in precipitation events pattern is the threat of desertification throughout the Iberian Peninsula (Puebla, 1998). One pathway to assess this concern is throughout the water use efficiency (WUE).

The WUE consists in the ratio of carbon gain during plant photosynthesis to water loss during evapotranspiration (ET). In other words, WUE can be defined as the gross

carbon uptake (i.e. the GPP) per amount of water lost from the ecosystem, coupling thus carbon and water cycles (Xiao & Chen, n.d.) ,i.e.:

$$WUE = \frac{GPP}{ET} \quad (\text{Equation 4})$$

where WUE stands for water-use efficiency, GPP stands for gross primary production and ET stands for evapotranspiration. Stewart (2001) also defines WUE as “*the units of a crop produced from each unit of available water*”. Hence, the more crop yield that is produced per unit of water, the greater is the WUE.

The WUE consists thus, in A valuable concept for studying the interactions between the two previously assessed carbon and water cycles (Xiao & Chen, n.d.), (although the definition of WUE made by Gregory (1989) was more complex since it took into account all the water flows which compose the hydrological cycle involved in biomass production). Therefore, similarly to the other variables, the spatial patterns, magnitude and interannual variability of the WUE (equation 4) over the IP will be hereafter addressed.

The physiological response to the increase of atmospheric CO₂ concentration that drives the hydrological cycle and ecosystem productivity is believed to be an increase in carbon uptake. This response is driven either by a stronger CO₂ gradient between stomata and the atmosphere or by an increase of Rubisco activity (Gelfand & Robertson, n.d.). The increase of WUE in plants might be a consequence of a stronger CO₂ gradient between stomata and the atmosphere (however the evidences of that increase have been, in accordance with Gelfand & Robertson, (n.d.) mostly based on modeling studies and FACE¹¹ experiments). Hence, these results agree with Gelfand & Robertson (n.d.), findings: that an increase in atmospheric CO₂ concentration will have positive effect on ecosystem productivity and WUE.

¹¹ FACE stands for Free-Air Carbon Dioxide Enrichment

2.5.4 Elevated CO₂ concentration

The CO₂ fertilization (along with water-use efficiency) are said to lead to increased vegetation growth (Amthor, 1998; DeLucia et al., 1999; Schaphoff *et al.*, 2006). Several studies regarding the direct effects of elevated CO₂ suggested that it leads to higher production rates (Tubiello *et al.*, 2007; Rost *et al.*, 2009) although, the magnitude of this effects is not yet well understood, which poses a great debate (Rost *et al.*, 2009).

Some studies encompassing the trends of vegetation growth across the globe, shown that in some places – in particular tropical croplands – yields are uniformly expected to experience decreases – when CO₂ effect is ignored. However, when CO₂ fertilization is assumed to occur, the overall studies do not uniformly reached the same conclusions in what concerns these decreasing tendency in crop yields (e.g. Haber *et al.*, 2011).

Rost *et al.* (2009) predicted a decrease in NPP under the effect of climate change (i.e. considering only the impact of climate change and disregarding CO₂ impact). Their results are due mainly to the decrease of regional precipitation and generally higher temperatures that will ultimately lead to higher crop water limitation, as well as more direct crop damage. Additionally, quoting Rost *et al.* (2009), similar results were obtained by Parry *et al.* (2004). However, Rost *et al.* (2009) has also concluded that the global joint effect of climate and CO₂ change will lead to increase in NPP. In fact, according to the same study, the isolated effect of rising CO₂ atmospheric concentration was enough to drive an increase in global crop by 28%, by 2050.

Moreover, in the same study, in simulations regarding both climate change and elevated CO₂, the addition of irrigation could be responsible for increasing NPP by 16% to 17 Gt (Rost *et al.*, 2009). After the latest bibliography review (in particular Gerten *et al.*, 2007; Rost *et al.*, 2009) it is thus noteworthy to highlight that the CO₂ effect more than offsets the global NPP decrease induced by climate change as it is shown in the picture below.

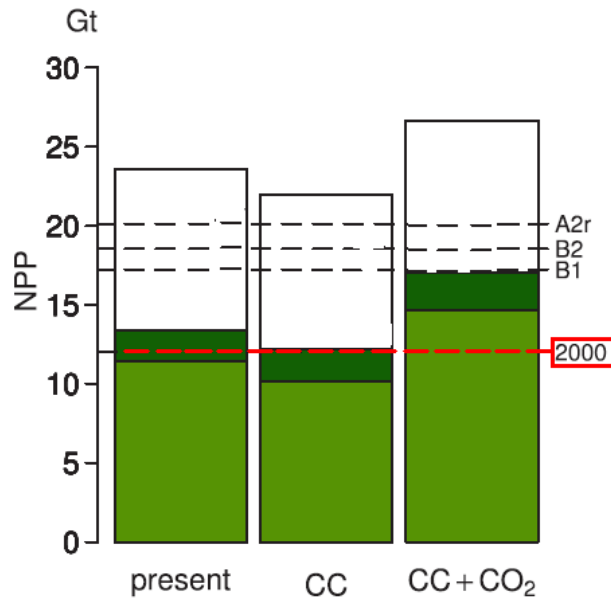


Figure 14 – NPP under different scenarios: at the Present; assuming climate change; and assuming climate and CO₂ levels change (Source: Adapted from Rost *et al.*, 2009).

Therefore, even though rising atmospheric [CO₂] consists in the driving force behind temperature rise and water stress – which are responsible for threatening crop yields (by reducing it), atmospheric [CO₂] has been proven to have a great potential to positively benefit crop physiology (Leakey, 2009). The studies that support this conclusion were done under several conditions such as greenhouses, controlled environment closed chambers, open and closed field top chambers and free-air carbon dioxide enrichment (FACE) experiments (Tubiello *et al.*, 2007).

The role of CO₂ as a source of carbon for vegetation has been proven 132 years ago by Justus von Liebig (Erbs & Fangmeier, 2006) and the atmospheric CO₂ beneficial effect on the growth of plants was discovered in the early eighteenth century (de Sussure 1804; cited in Erbs & Fangmeier, 2006). Hence, CO₂ enrichment has been used to promote the growth of vegetables for more than 50 years.

Taking into account the evolution of atmospheric CO₂ concentration levels, over the past two centuries it has become important and subject of great interest to evaluate or understand the response of vegetation (and ecosystems) to CO₂ enrichment, which had led to numerous studies regarding biosphere-atmosphere interactions with respect

CO₂ through experimentation and modeling. However, the growing awareness about atmospheric CO₂ concentrations at a global scale, started to draw an increase concerning and hence started to be monitored, only in the middle of the nineteenth century. The first study regarding specifically CO₂ enrichment effects on crops is attributed to Cure & Acock (1986) (cited in Erbs & Fangmeier, 2006), who reported an average increase in C3 crop yield after doubling CO₂ around 41 percent.

The increase in yield verified under elevated CO₂ experiments is due the fact that higher concentrations of CO₂ in the air enhance photosynthesis rate (Bonan, 2002). However, this behavior varies with the plant type. For instance, for C3 plants an increase in CO₂ concentrations lead to photorespiration reduction by increasing the ration of CO₂/O₂ reacting with rubisco (Bonan, 2002).

Fact Box Q: Crop yield response across the globe assuming/disregarding CO₂ fertilization

Crop yield are expected to increase in all 11 regions of the globe **if full CO₂ fertilization is assumed**. However, the range of growth varies widely between different regions (from 0,74% up to 28,22&)(Haberl *et al.*, 2011). Although, when the CO₂ was switched within the same study, **many losses were predicted** even though that there were still some regions that benefit some yield growth as stated in next table.

Table 22 - Modeled climate impact on cropland yields in 2050 with and without CO₂ fertilization (Source: Haberl *et al.*, 2011)

	Mean yield change under climate change 2050	
	with CO ₂ fertilization	without CO ₂ fertilization
Northern Africa and Western Asia	+ 4.44%	-8.65%
Sub-Saharan Africa	+8.46%	-6.17%
Central Asia and Russian Federation	+24.91%	+5.12%
Eastern Asia	+11.96%	-3.90%
Southern Asia	+18.45%	-15.61%
South-Eastern Asia	+28.22%	-15.83%
Northern America	+12.45%	-6.25%
Latin America & the Carribean	+12.39%	-7.02%
Western Europe	+16.42%	+ 2.04%
Eastern & South-Eastern Europe	+19.08%	-0.66%
Oceania and Australia	+0.74%	-16.02%

Furthermore, growth stimulations were as expected larger under well-watered conditions. Even under conditions of low soil nitrogen elevated CO₂ has stimulated growth stimulations. Woody perennials present larger growth responses to elevated CO₂ (and their reductions in stomatal conductance were smaller) (Kimball *et al.*, 2002). In what concerns to tissue compounds concentrations, tissue nitrogen and both carbohydrate and carbon-based compound react differently: while the latter went up due the increase CO₂, the tissue nitrogen concentrations went down (foliage and leaves were the most affected organs) (Kimball *et al.*, 2002).

More than a hundred FACE studies have been carried out allowing study the effects of high concentrations of CO₂ (475-600 ppm) on plants under natural conditions (i.e. without enclosure). The results have shown light saturated carbon uptake resulting in growth and above-ground production increase. On the other hand, with the same concentrations of CO₂, specific leaf area and stomatal conductance has decreased (Ainsworth & Long, 2005).

Similarly to what occurs with photosynthetic rate response to light, there is also a certain point or “saturation point” in CO₂ concentrations beyond which photosynthetic rate no longer increases and remains constant (Bonan, 2002). After this CO₂ saturation point, photosynthesis is now limited by the supply of NADPH and ATP (the previously called chemical energy in the chapter regarding photosynthesis) from the “Light reactions” (Bonan, 2002). This saturation point varies among species. For instance, FACE experiments concluded that trees were more sensitive to elevated CO₂ concentrations, than herbaceous species (C₄ showed little response for instance) and grain crop yield had a considerable low increase. The following *Fact Box* discloses further examples.

Fact Box R :FACE experiments on different crops

Free-air CO₂ enrichment (FACE) experiments have been conducted on several agricultural crops: on C₃ and C₄ grasses, C₃ legume and woody perennials. These FACE experiments have shown **different magnitude of responses** according to the functional type of plant (among other conditions such as soil nitrogen and water status). Like many previous studies and hence, as expected, the elevated CO₂ present lead to a high increase of photosynthesis and biomass production and yield. Although, **this increase** was far more **substantial in C₃ species than in C₄ species**. (However, both C₃ and C₄ presented a decreasing on stomatal conductance as well in transpiration. Both species have also shown improved water-use efficiency (Kimball *et al.*, 2002)).

The different photosynthetic yield behavior under the same environmental conditions relies on the different photosynthetic response to environmental factors. For example, **C₃ plants light and CO₂ have a strong photosynthetic interaction** (e.g. under high irradiance net photosynthetic increases more at high rather than low CO₂ concentrations). However, **C₄ plants reach much earlier** the so-called “**CO₂ saturation point**” – which occurs in these plants at 400ppm regardless of light (Bonan, 2002). Despite some differences in overall results, the FACE and chamber results have been consistent, giving a considerably high confidence those conclusions drawn from either FACE or chamber experiments are accurate (Kimball *et al.*, 2002; Ainsworth & Long, 2005).

Nevertheless, as corroborated by Rost *et al.* (2009), regardless the rate or approach taken when simulating the positive CO₂ impact on productivity levels, it should always be interpreted as the top effect i.e. the maximum effect possible. This interpretation represents a great challenge since there are several and complex interaction between yields, photosynthesis as well as limitations to crop growth through nutrient and water availability - in addition to soil degradation, diseases, weeds and pests (as mentioned earlier from Ainsworth *et al.* (2008)). One valuable example is the nitrogen feedbacks which are expected to strongly constraint the positive response of productivity to increased atmospheric CO₂ concentration (Zaehle *et al.*, 2010).

2.6 Assessing Terrestrial Productivity and Biomass

The impetus for conducting assessments of terrestrial productivity is the need for better understanding of terrestrial biosphere since it provides key services to humanity (e.g. food, water, shelter), and plays a great affection over the global carbon cycle

(within a timescale relevant to human activities). These assessments usually aim to test predictions and hypotheses concerning the responses of ecosystem structure and functioning to both past and future environmental changes (Pavlick *et al.*, 2012). Moreover, the predictions of biomass within a certain plausible future scenario enable a better support for policies definition and management of several sectors – especially energy and agriculture, since biomass for energy tightly links these two industries.

Determining net productivity can be done through several ways. In situ, it works by collecting and weighing the plant material produced on 1 m² of land during a certain time period. It can also be done throughout remote sensing. This technique allows determining the Normalized Difference Vegetation Index (NDVI) – consisting in an index based in spectrums of PAR derived by satellite data.

Vegetation phenology, as used and studied with remote sensing related research, refers to the relationship between climate and periodic development of photosynthetic biomass. Accurate estimates of canopy phenology are critical to quantifying carbon and water exchange between forests and the atmosphere and its response to climate change. Satellite monitoring of vegetation phenology has often made use of a vegetation index such as NDVI because it is related to the amount of green leaf biomass (Lillesand & Keifer, 2000). Annual time series NDVI data, for example, have been used to estimate the onset of leaf development and senescence in relation to interannual variations in average global air temperature for the past twenty years (Ahl *et al.*, 2006).

Another widely used way of assessing this two features are the so-called Dynamic Global Models (DGMVs) – which allow to estimate NPP as well as biomass and additionally it enables to estimate future NPP and biomass under different changes in climate and other variables, such as CO₂.

2.6.1 Dynamic Global Vegetation Models (DGVMs)

The dynamic global vegetation models (DGVMs) have been primarily developed (since late 1980) in order to quantify the global behavior of terrestrial ecosystem (Stich *et al.*, 2003), by projecting transient terrestrial ecosystems responses under rapid climate

change (Cramer *et al.*, 2001; Pavlick *et al.*, 2012). These models allow the combination of both biogeochemical processes and vegetation dynamic structures and composition (and hence changes in ecosystem geography) (Cramer *et al.*, 2001; Stich *et al.* 2003) and they have been widely applied to problems regarding global carbon cycle and climate change.

The DVGM consist of mechanistic, process-based, numerical models, which enable the simulation at the large-scale dynamics of terrestrial ecosystems (Pavlick *et al.*, 2012). They simulate the vegetation structure (i.e. distribution, physiognomy) and linked changes in ecosystem function such as water, energy and carbon exchange, in response to a scenario of changes in CO₂ concentration and climate obtained with the coupled atmosphere-ocean general circulation models(Cramer *et al.*, 2001).

Soil texture as well as vegetation biophysical processes will affect soil hydrology that influences the behavior of plant (e.g. its physiology and phenology) and soil (e.g. its respiration as well as nitrogen mineralization (Cramer *et al.*, 2001). For that reason, the DGVM include physiological, biophysical and biogeochemical processes, through mechanistic representations of photosynthesis, respiration and canopy energy balance, the controls of stomatal conductance and canopy boundary-layer conductance, as well as the allocation of carbon and nitrogen within the plant (Cramer *et al.*, 2001). Hence, DGVMs are inclusively embedded within comprehensive Earth System Models (ESMs) allowing capturing biogeochemical and biogeophysical feedbacks between the terrestrial biosphere and the physical climate system (Pavlick *et al.*, 2012).

However, each model gives a specific attention to certain processes, i.e. emphasis a particular detailed description of a process (e.g. plant physiological process including coupled atmosphere-biosphere model (Cramer *et al.*, 2001). The several existing models present different complexities as well as different suitability for certain functionalities (Cramer *et al.*, 2001). In fact, Cramer *et al.* (2001), have made a parallel evaluation on six different models (HYBRID, IBIS, SDGVM, TRIFFID, VECODE and LPJ), in order to point out significant variations between each one in order to represent potential sources of uncertainty. Moreover, according to Stich *et al.* (2008), the comparison

between several studies results based on DGVMs usually present a wide divergence between the results regarding the terrestrial biosphere and its function as a driver of the global carbon cycle under different assumed climate change scenario. The main uncertainty is mainly the response of the terrestrial carbon balance. Hence, it is fair to say that each DGVM, has a different degree of complexity and suitability for specific tasks. It should be taking into account that one of the possible reasons for the considerable existing divergences may be due to the course of each model or even to a different plant functional diversity (Stich *et al.*, 2008; Pavlick *et al.*, 2012). The following sections provide general information about three widely used DGVMs

The figure below (Figure 15) shows the development of a DGVM for a visual (a clearer) interpretation of it. As it is shown, the DGVMs integrate four main groups of processes: (1) plant geography, (2) biogeochemistry, (3) biophysics and (4) vegetation dynamics.

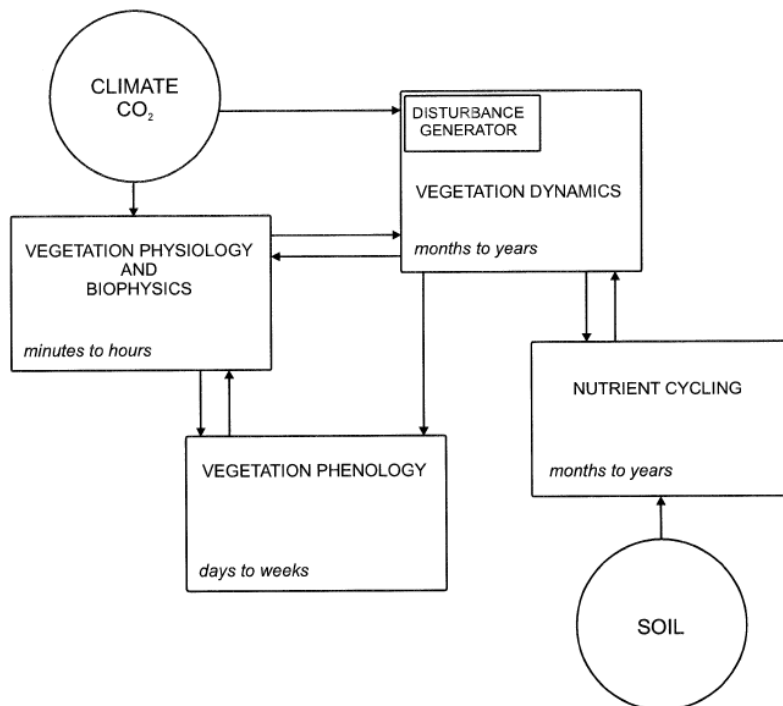


Figure 15 – DGMV scheme (Source: Cramer *et al.*, 2001)

Lund-Postdam-Jena (LPJ) Model

The Lund-Postdam-Jena (LPJ) Model, is considered of intermediate complexity and it is suitable for addressing several global issues. A feature that differs LPJ from other models is an explicit representation of vegetation structure, dynamics and competition between PFT population as well as soil biogeochemistry (Sitch *et al.*, 2003).

LPJ model provides a vegetation dynamic response to specific scenario of climate change. It has an individual-level scale process to the grid cell, where it is employed biophysical and physiological process parameterizations (as in equilibrium model BIOME3)(Cramer *et al.*, 2001). Vegetation dynamics are based both on annual net primary production (ANPP) and biomass growth and include: competition among PFT; probabilities of natural disturbance (e.g. fire) and succession following disturbance i.e. replacement of PFT. These processes are simulated explicitly by LPJ (Cramer *et al.*, 2001).

LPJmL was developed in order to simulate two main features: (1) the composition and distribution of vegetation and (2) stocks and land-atmosphere exchange flows of carbon and water atmosphere. This model computes processes such as photosynthesis, plant growth, maintenance and regeneration losses, fire disturbance, soil moisture, runoff, evapotranspiration, irrigation and vegetation structure through the combination of ecophysiological relations, generalized empirically established functions and plant trait parameters (PIK, 2012).

Physiological Principles Predicting Growth (3PG)

The Physiological Principles Predicting Growth (3PG) Model, models the general forest carbon allocation, published by Landsberg & Waring (1997). The model runs within simple and readily available input data (e.g. weather records; edaphic variables and others) and derives monthly estimates of GPP, carbon allocation as well as stand growth.

The 3PG has also been coupled to satellite imagery of canopy photosynthetic capacity to model forest growth across landscapes. Similar to other models, 3PG is under

constant revision in order to incorporate new research data. In what concerns to its weaknesses, the allocation and belowground processes are the least developed features of 3PG. 3PG's belowground processes.

Jena Scheme for Biosphere –Atmosphere Coupling in Hamburg (JSBACH)

Jena Scheme for Biosphere-Atmosphere Coupling in Hamburg (JSBACH) consists in a modular land surface scheme which is based on the biosphere model BETHY (Knorr, 2000). It is usually combined with the European Center Hamburg Model 5 (ECHAM5) soil scheme (Knorr, 2000; Knorr & Kattge, 2005; Thum *et al.*, 2011) enabling the study of the response of soil organic carbon to climate change, for instance (Thum *et al.*, 2011).

JSBACH enables a better understanding over the feedbacks between the physical climate system and land surface processes, since it provides a better understanding of processes that lead to major changes of wither regional or global climates. It bases in present (or recent past) climate system, allowing thus to comprehend the coupled climate system.

2.6.2 Main pitfalls and differences between DGVMs

The degree of processes' complexity also varies among each model Cramer *et al.*, 2001). One of the several pitfalls of DGVMs, could be pointed out as to be the inexistence of spatially treatment of seeds dispersal since in accordance with Cramer *et al.* (2001) the migration of dominant plants species involves the development of mature individuals producing seeds besides merely dispersal. Hence, this development would imply additional delays due to growth and competition processes, since the lack of these factors on vegetation dynamics, may cause lags of a century or more in the response of vegetation to climate change, since the results presented are considering stand development without dispersal.

Another considerable pitfall is the no inclusion of increased nitrogen deposition (resulting from industrial and agricultural activity) in the DGVM. This lack is considerable important, since the impacts caused by nitrogen are potentially important

to the carbon cycle through changes in plant nutrient availability. Furthermore, it will also contribute with negative impacts for parallel changes in tropospheric ozone (Cramer *et al.*, 2001).

Despite the uncertainties as well as different complexities and functionalities that characterizes each model, all of them treat vegetation cover as a fractional representation consisting of different types (Cramer *et al.*, 2001) the so-called Plant Functional Types (PFT).

3. Methodology to Estimate Productivity and Biomass Potential under Climate Change

The present goals were addressed by the carbon cycle model JSBACH (Jena Scheme for Biosphere-Atmosphere Coupling in Hamburg) which ran upon the input data provided by the climate model ECHAM5 (European Center-Hamburg-Model 5). JSBACH was expected to provide valuable results regarding the response of terrestrial productivity and carbon uptake to climate variables change. This carbon model enabled thus to model how a range of climatic conditions would affect the bioclimatic areas present in the study area, and therefore, to estimate how their productivity rates could change in response to a changing climate and atmospheric CO₂ concentration - as well as to understand how significant is the difference of response onto given different levels of CO₂ concentration. Ultimately the results treatment is expected to drive an understanding of the reliability and value of that model when downscaling the results at the scale of the Iberian Peninsula, and to comprehend its major limitations.

3.1. Study Area: the Iberian Peninsula

The study area covers the Iberian Peninsula (hereafter IP), the Balearic Islands and a small portion of North Africa, although a big emphasis was made upon the IP. The Iberian Peninsula is located in the western-most mainland Europe and it comprises three nations: Portugal, Andorra and Gibraltar with an area of ~580.000 km². The biggest of them, Spain, borders Portugal to the west and to the south of the region of Galicia. To the south it borders Gibraltar and to the northeast, along the Pyrenees

mountain range it borders France and the small principality of Andorra. The south and eastern continental shelves are bathed by the Mediterranean Sea, whereas the northern and western continental region it is bordered by the Atlantic Ocean. Figure 16, illustrates the main regions in which the IP territory is divided as well as the topographic scheme.



Figure 16 – Map of the Iberian Peninsula – the darker brown is assigned to heights over 1000m; light brown is assigned to heights ranging between 500 and 1000m (i.e. high plateaus) and the greenish color are assigned to heights lower than 500m (Source: Solarnavigator.net)

The most common orographic feature prevailing in the IP is high plateaus, which are divided by the Central Mountain System, into Northern and Southern Plateaus. These plateaus are isolated from the sea by the so-called Cantabria Mountains in the north and by the Baetic Mountains at the south. The Iberian Mountain System covers the north-eastern area and it is parallel to the Ebro River which flowing to Mediterranean Sea (whereas the remaining rivers flow to the Atlantic Ocean).

In what concerns the flora pattern, the Iberian Peninsula presents a mosaic of forests except in the most extreme habitats (e.g. alpine environments and arid zones in the

Southeast of the Peninsula where conditions struggle a proper tree growth and survival). Furthermore, human disturbance greatly contributes to unforested areas since the Neolithic (Blanco *et al.*, 1998).

3.1.1. Bioclimatic patterns and zones

The bioclimatic zones enable to depict the distribution of species across the area (Guisan & Zimmermann, 2000). Hence, the Iberian territory could be distributed in several “zones” – which can vary depending on author. For example, the Köpen classification accounts with five main zones (subdivided in turn in other divisions), and it is based as well on five vegetation groups (as it is shown in Figure 17) (Kottek *et al.*, 2006). In order to identify different climates, this climate classification system define them using average monthly values for precipitation and air temperature, based on their influence on the distribution of vegetation and human activity (Essenwanger, 2001).

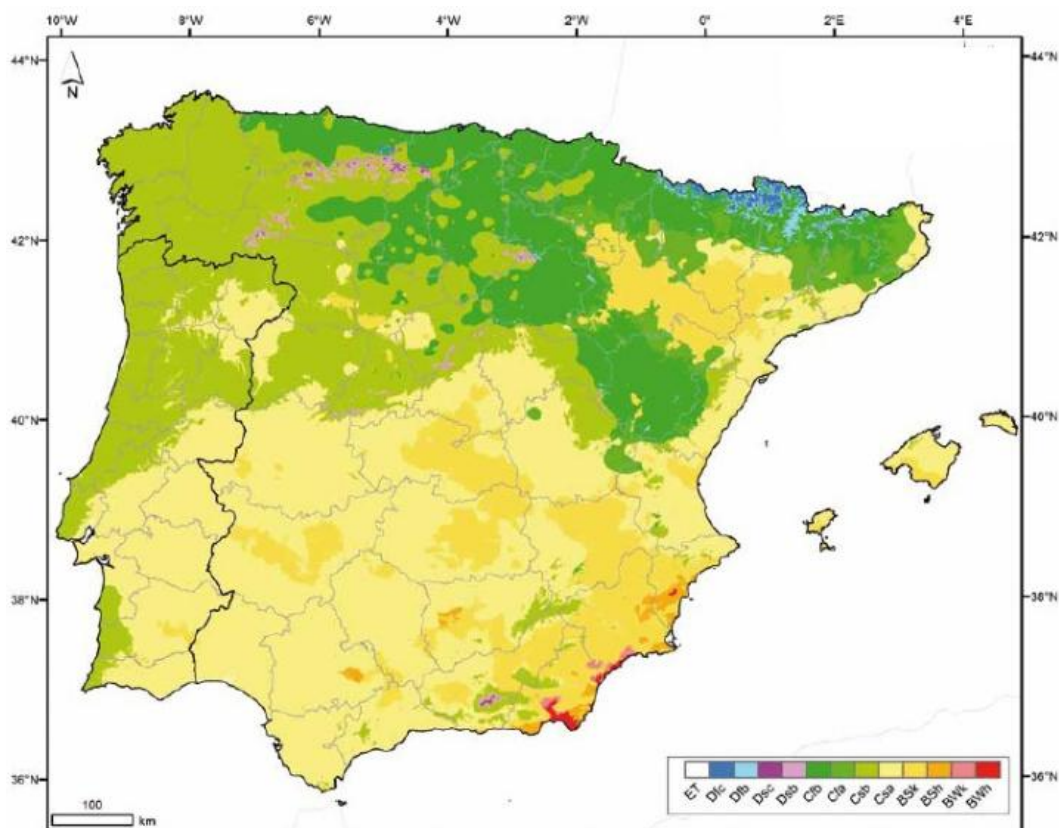


Figure 17- Köppen-Geiger Climate Classification for the Iberian Peninsula and the Balearic Islands (Source: AEMET, 2000)

Hence, the Iberian Peninsula, due to its geographical and orographic conditions, crosses three main types of climates: the “Mediterranean climate” which is the dominant and comprises two varieties (*Csa* and *Csb*); the “Oceanic climate” (named as *Cfb*); and the “Semiarid climate” (comprising the varieties *Bsh* and *Bsk*)(Kottek *et al.*, 2006; AEMET, 2011).

Even though that this Köppen-Geiger Climate Classification was created roughly 100 years ago (Kottek *et al.*, 2006), it continues to be one of the most widely used for climate studies purposes (AEMET, 2011). Table 23 provides a wider description of the varieties of climate present in the IP.

Table 23 - Iberian Peninsula Bioclimatic zones - In accordance with Rivas-Martínez *et al.* (2004)

Type	Sub-type	Main characteristics and locations
B Arid and Semi-arid (Dry) Climates P=20(T+7): P=20 T P=20(T+14):	BWk* - Hot desert climate	Or “Hot Desert” and “Cold Desert”. Small areas in the SW of IP. Spanish provinces of Almeria, Murica and Alicate, coinciding with minimum rainfall values for the IP.
	BWh* - Cold desert climate	
	Bsh* - Warm semi-arid climate.	Or “Hot steppe” and “Cold steppe”. Southeast of IP and Ebro Valley, less in the southern central plateau region, Extremadura and the Balearic Islands. In Portugal they cover only a small region of Baixo Alentejo, in the district of Beja
	Bsk* - Cold semi-arid climate	
C Temperate Climates 0°C <AT _c <18°C	Csa* - Warm Mediterranean climate.	Temperate with dry or hot summer. Occupies ~40% of IP area, southern central coastal region
	Csb* - Temperate Mediterranean climate.	Temperate with dry or temperature summer. NE of the IP ad west cost of Mainland Portugal and mountainous regions within the IP
	Cfa - Warm oceanic climate.	Or “humid subtropical climate”. Temperate with dry season and hot summer. NE of the IP, area of medium altitude surrounding the Pyrenees
	Cfb* - Temperate oceanic climate.	Temperate with a dry season and temperate summer Cantabrian Mountain, in Iberian M.R. Pyrenees
D Cold Climates AT _c <0°C AT _H >10°C	Dsb - Temperate continental climate.	Or “Mediterranean continental climate”. Cold with temperature and dry summer Small areas of the mountains regions at higher altitudes in the Cantabrian, Iberian and Central M.R. and Sierra Nevada.
	Dsc - Cold continental climate	Cold with dry and fresh summer. Cold with temperature and dry summer Small areas of the mountains regions at higher altitudes in the Cantabrian, Iberian and Central Mountain Ranges and Sierra Nevada.
E Polar Climates AT _H <0°C	ET - Tundra	Small areas at high altitudes in mountainous regions (Central Pyrenees and Cantabrian M.R.

AT_c – average temperature in coldest month; AT_H – average temperature in hottest month; * - Main climates

Although, one of the most common and simplest bioclimatic divisions is made in two macro bioclimatic areas: the Mediterranean zone which occupies a large area of the centre and south of the peninsula and the Temperate zone, occupying mainly the northern area (Rivas-Martínez *et al.*, 2004)(Figure 18). The latter has colder temperatures and higher precipitation than the Mediterranean zone.

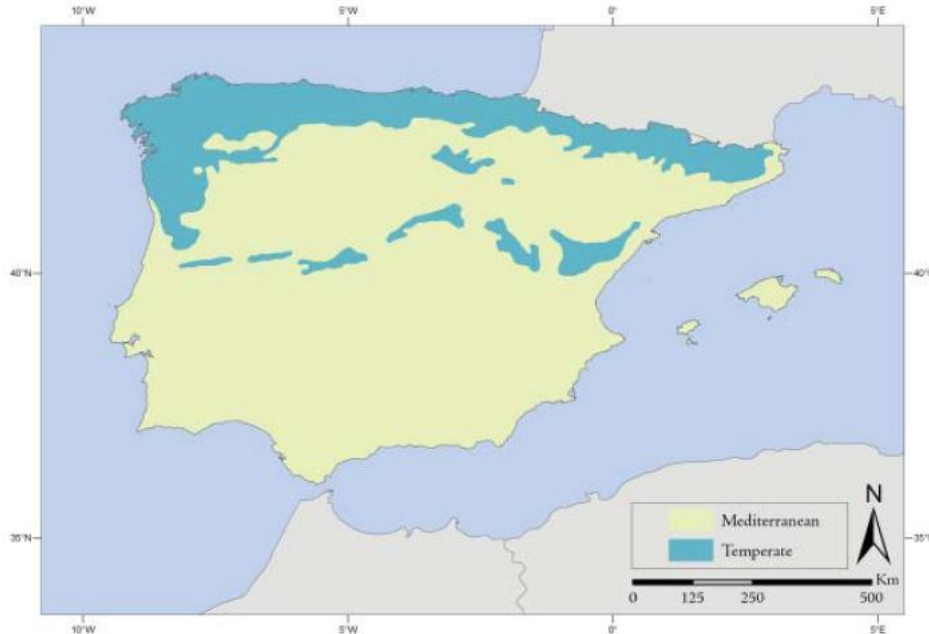
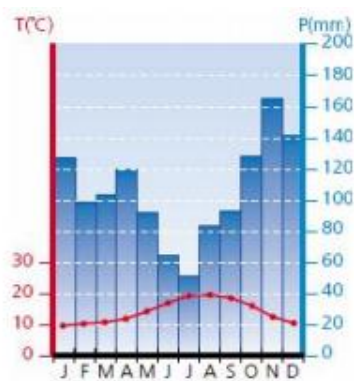
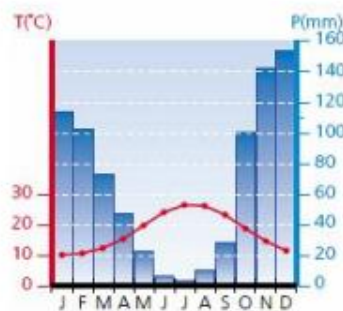


Figure 18 -Iberian Peninsula Bioclimatic zones - In accordance with Rivas-Martínez *et al.* (2004)

Conversely to the Atlantic region, the climate existing in the Mediterranean region is greatly characterized by a long period of summer drought (commonly lasting between two to four months). Rainfall can range from 1500 mm to less than 350mm, and temperatures are widely varying from regions where there is no frost to regions where winter temperatures drop further than -20°C. Figure 19 illustrates the mean



Temperate Zone



Mediterranean zone

precipitation and temperature of both zones along the year:

Figure 19 - Monthly mean precipitation and temperature of temperate zone (left) and Mediterranean zone (right)

3.1.2. Vegetation Cover

In the Atlantic zone, the forests are composed mainly by deciduous trees, more specifically by oak forests (followed by beech, birch and fir) (Lindner *et al.*, 2008). The main species account with the *Quercus petraea* (Sessile oaks), *Quercus robur* (English oaks), *Fraxinus excelsior* (European Ash), hazels, birches (more specifically *Betula* species) and *Abies alba* (Silver Firs) in the Pyrenees, although for higher altitudes, the fir forests are replaced by *Pinus uncinata* (the Black Pine). Due to a bit of Mediterranean influence throughout the area, the presence of *Quercus ilex* (Holm Oaks) with laurel is very common. The north Castilla inland sand dunes of the Iberian plateaus host dominantly stone pine and maritime pine (*Pinus pinea* and *Pinus pinaster*, respectively) (Bacaria *et al.*, 1999; Bohn & Hettwer, 2000) and consist in a very valuable source in what concerns within a socio-economic perspective as well as a conservation point of view (Regato-Pajares, 2004)..

The region that occupies the rest of the Iberian territory, i.e. Mediterranean region is mainly characterized by broadleaf evergreen trees, (as well as thermophilous deciduous forest; xerophytes coniferous forest; plantations and self shown exotic forest)(Lindner *et al.*, 2008). Within the shift from the Mediterranean vegetation to the Atlantic vegetation, the *Quercus pyrenaica* (also known as Pyrenean Oak) stands as a great importance in what concerns the wider area covered in the Iberian Peninsula. The resistance of this oak enables it to prosper along the mountain ranges in the centre of the Peninsula, as well as along the interior of Galicia to the south of the Cantabrian Cordillera and throughout the Central System reaching inclusively the south – Sierra Nevada and Cádiz. The main forests in Mediterranean forests are oak forests (where *Quercus ilex* is common), cork oaks, wild olives or juniper (to name few). The *Pinus halepensis* (or Aleppo Pine) is responsible for replace these trees in the warmer regions. For the areas characterized by sandy ground, forest of Stone Pine and juniper enable the sand dunes fixing.

The Central plateaus, valleys and low plains of the interior portion of the IP are mainly covered by sclerophyllous and semi-deciduous forests. Due to their more continental climate, the northern plateau was primarily evergreen broadleaf and conifer canopy

species, but to several degradation factors, it has currently turned into secondary, dense shrub land, or into agro-forestry landscapes mainly constituted by scattered trees on grasslands or crops. In the western part of the region, mixed cork oak (*Quercus suber*) and holm oak sylvopastoral woodlands are frequent.

The southeastern part of the IP, along with the Ebro valley, is covered by woodlands of juniper (*Juniperus thurifera*, *J. phoenicea*), Aleppo pine (*Pinus halepensis*) and holly oak (*Quercus coccifera*) mixed forests. These forests and woodlands alternate though with extensive steppe grasslands (such as *Stipa tenacissima*, *Lygeum spartium* and shrub communities (*Artemisia herba-alba*, *Thymelaea hirsuta*, *Ononistridentata*, *Helianthemum squamatum*, *Thymus mastigophorus*) resulting thus in a complex mosaic-like landscape (Bacaria *et al.*, 1999; Bohn & Hettwer, 2000). The southern part of the region and the river canyons of the Douro and Tejo river have a wide distribution of wild olive (*Olea europaea*) and carob (*Ceratonia siliqua*) woodlands as well as maquis – this plants have been strongly domesticated in order to produce food crops and olive oil.

In what concerns the herbaceous species (such as *Arisarum vulgare*, *Vinca difformis*, *Allium triquetrum*, and *Ballota hispanica*), those also frequently appear within the dense and shady tree layer. A wide range of the vegetated regions have been widely and intensively transformed into agricultural land of extensive wheat crops, vineyards, almond and olive groves, fruit tree orchards and other irrigated crops (Bacaria *et al.*, 1999; Bohn & Hettwer, 2000). Hence, the southwestern part of the region is highly characterized by manmade, semi-natural sylvopastoral woodlands known as “montados” in Portugal or “dehesas” in Spain (Regato-Pajares, 2004).

3.1.3. Climate Vulnerability

The IP presents high climate *vulnerability* caused by its peculiar complex environment and location in the transition area between subtropical and temperate climates (IPCC, 2007; Jerez *et al.*, 2012). In this context, vulnerability is defined as the degree to which the IP is susceptible to be affected by adverse effects of climate change. Under a climate change scenario, the climate fragility of the IP is altered and there are evidences of observed and predicted increases of temperature and decreases in projected

precipitation (IPCC, 2007). For the Temperate zone, annual mean temperature increases are projected to drive extreme and more frequent events are (such as floods, and higher volumes and intensities of precipitation in winter), whereas The Mediterranean zone is projected suffer droughts as result from forecasted decrease in annual precipitation (Lindner *et al.*, 2008). The table below shows some an overall assessment of the IP bioclimatic regions under a bio-geographical perspective (Table 24):

Table 24 – Sensitivity of Bioclimatic zones: expected climate change and potential impacts (Source: Adapted from Lindner *et al.* (2008))

TEMPERATE OCEANIC ZONE	
Expected climate change	Temperature increase +2.5 - +3.5°C (by the end of the century); Hotter and dryer summers; More frequent extreme events; Higher volumes and intensities of precipitation in winter
Potential impacts and key treats	Tree growth rates may increase but also decrease in water limited areas Extreme events such as storms, droughts, flooding, and heat waves Risk and frequency of wind damage increase Shifting natural species distribution ranges may negatively impact especially rare species living in isolated habitats Biotic pests are expected to have increased damage potential
MEDITERRANEAN ZONE	
Expected climate change	Temperature increases +3 - +4 °C, larger increases during the summer (+4 - +5 °C) and smaller increase in winter Annual rainfall is expected to decline up to 20% with even stronger reduction in summer Precipitation increase in winter Extreme events such as heat waves and heavy precipitation events more frequent
Potential impacts and key treats	The extreme forest fire risk Tree growth is expected to decline in large areas due to more severe drought limitations Increasing drought limitations are threatening the survival of many species

One of the most concerning consequences is the fact that these changes can be responsible for worsening the drought conditions c leading to aggravated water-scarcity conditions(IPCC, 2007). Making it necessary to estimate and predict the temporal variability of meteorological drought events over the IP, in order to project the severity of dry and wet conditions over 30 years-mean period.

Some major signs which support the latter concerns were found in summer season which in accordance with some studies (e.g. Jerez *et al.*, 2012) have been showing a strengthening in the increase projected for both mean temperature and temperature

variability as a consequence of soil moisture-temperature feedback. Thus, such influence of the land-surface processes – such as the soil moisture, draws a growing attention and need of wider assessments, when projecting the future changes for temperature, precipitation and wind over a complex are as the IP.

Parallel to this phenomenon of warming temperatures, the decrease in precipitation, soil moisture and evapotranspiration draw great concerns about vegetation productivity over the IP, since that in most of the IP territory (mainly the Mediterranean zone) the vegetation is water-limited (Rios-Enteza & Miguez-Macho, 2010, Jung *et al.* (2011)). Most of the tree species under climate change vulnerability are mainly affected by drought (such as the *Eucalyptus spp*, *Pinus spp* and oaks).

3.2. Modeling Tool: JSBACH

The goals stated for this work, were achieved by handling data results yielded by the JSBACH model which were processed by Christian Beer (Max-Planck-Institut für Meteorologie Hamburg (MPIBGC)) and post processed by Nuno Carvalhais (MPIBGC and Faculty of Sciences and Technology of New University of Lisbon (FCT-UNL)). This section addresses a more detailed description of the model along with the variables analyzed and data input sources.

3.2.1. JSBACH overall description

JSBACH consists in a modular land surface scheme. It enables to understand the interaction between the assimilation rate and stomatal conductance, which are explicitly modeled and dependent on temperature, soil moisture, water vapor, absorption of solar visible radiation as well as ambient CO₂ concentration (Raddatz *et al.*, 2007). The vegetation phenology is driven by temperature, soil moisture and NPP.

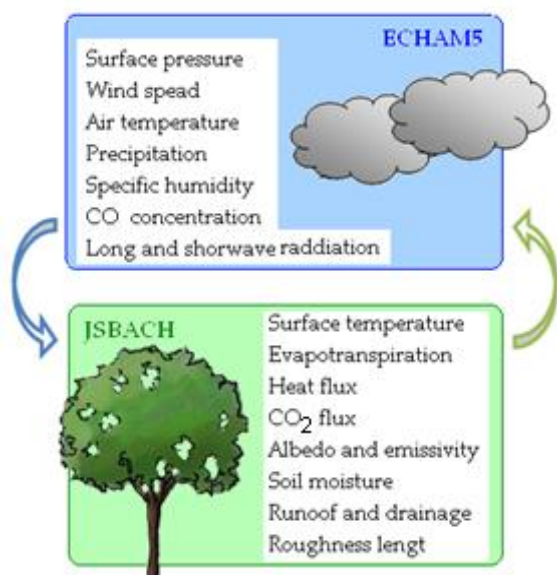
JSBACH aims to model land carbon fluxes throughout biologically control and therefore, other natural processes such as fires, leaching or weathering (Thum *et al.*, 2011) nutrient limitations (Raddatz *et al.*, 2007) and competition among plants derived

by climate change are not encompassed by the model. The carbon balance regards hence the cycle of carbon storage along the growth and death of the plant, and the model also accounts with anthropogenic impact on the land carbon cycle through land cover maps (Thum *et al.*, 2011).

JSBACH runs having as input data basis a global climate model (GCM), named as ECAHM developed by the Max Plank Institute (MPI) for Meteorology. More specifically, the ECHAM5 consists in an atmosphere/ocean general circulation model (AOGCM) and was created upon the modification of a previously developed global forecast model by the European Centre for Medium-Range Weather Forecasts (ECMWF) (Raddatz *et al.*, 2007). The interaction between JSBACH and ECHAM is multilateral and encompasses many parameters. For a clear interpretation of the coupled models setup, an illustrative overview is presented below (

).

The JSBACH climate components include atmosphere-biosphere interactions as well as



soil-biosphere and land-atmosphere interactions (Brovkin *et al.*, 2009; Reick, 2009). The boundary land-atmosphere poses on many features which are directly affected by the presence of vegetation: such as CO₂ exchange; surface roughness, albedo and surface temperature, as well as evapotranspiration and heat latent flux (Reick, 2009). As a technically modular framework, JSBACH model contains the

Figure 20 - Interactions between JSBACH and ECHAM5

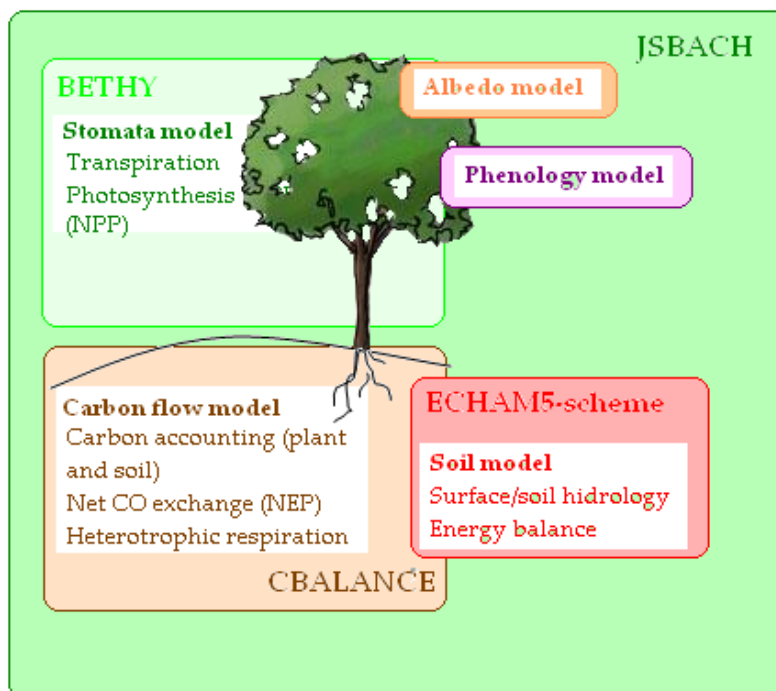
following components:

- Land surface scheme – in order to describe soil heat and moisture interactions;

- Fast vegetation processes – which derive carbon fluxes from photosynthesis in diurnal cycle embedded in the full land surface energy balance, accounting for plant phenological changes and respiration;
- Slow vegetation processes – which provide the description of long-term interaction between climate and vegetation.

JSBACH Modules

The estimations and modeled processes that JSBACH perform are possible since they are based on many other models – or modules (Figure 21). I.e., in what concerns to the vegetation processes, for the fast processes JSBACH is based on the BETHY scheme (or “stomata model”), which holds a description of photosynthesis embedded in the full land surface energy ecosystem balance as well as plant respiration and phenology scheme (Knorr, 2003; Thum *et al.*, 2011). Moreover, the actual soil carbon module used



is called CBALANCE (or “carbon flow model”), which in fact consists in the original soil carbon ever used for JSBACH (Thum *et al.*, 2011).

Figure 21 - JSBACH modules scheme

Besides the stomata and the carbon flow models (which will be addressed more closely afterwards), JSBACH also encompasses the phenology model (related to the Leaf Index Area (LAI)); the dynamic land cover; and the soil model: ECHAM5. The later regards surface and soil hydrology; energy balance and mosaic approach for surface properties. The dynamic land cover concerns the determination of the type of vegetation cover.

3.2.2. BETHY module: Plant Functional Types (PFTs)

Generally speaking, the BETHY model is responsible for simulating the water cycle throughout transpiration (i.e. assessing the stomatal conductance sensitivity to CO₂ in ambient air) and for the carbon cycle throughout the photosynthesis process, i.e. NPP or carbon assimilation (Knorr & Kattge, 2005; Raddatz *et al.*, 2007; Reick, 2009).

BETHY scheme simulates coupled photosynthesis and energy balance processes throughout simulations of the CO₂, water and energy exchanges between the atmosphere and plant canopy and it also computes absorption of PAR as well as the response of canopy conductance to PAR (Knorr & Kattge, 2005; Raddatz *et al.*, 2007). Moreover, the BETHY model enables the calculation of evapotranspiration and heat fluxes (Monteith, 1965). Some of the processes are computed upon many other authors, listed in the Table 25.

Table 25- BETHY processes

Parameters	Source
Transpiration	Penman-Monteith equation by Monteith, 1965
Sensible heat fluxes	
Carbon uptake for C3 plants	Model by Farquhar <i>et al.</i> (1980) GPP
Carbon uptake for C4 plants	Model by Collatz <i>et al.</i> , (1992)
Stomata and canopy model	Canopy simulation in response to PAR by Knorr (2000)

The model parameters are: photosynthesis, carbon balance, stomatal control as well as energy and radiation balance. The GPP estimations are provided throughout C3 and C4 photosynthesis and stomatal conductance processes; plant respiration is throughout growth respiration (~NPP) and maintenance respiration; soil respiration is throughout fast/slow pool response, temperature and moisture balance and finally, carbon balance, is simulated throughout average NPP at each grid point (Knorr, 2000).

Hence, the BETHY scheme (Figure 22) confers one of the main features that actually characterize JSBACH approach to production estimations: the fact that these are made, following an up scaling approach, i.e. from leaf to canopy. The Fact Box S below shows the processes. These processes and fluxes occurred at the level of each specific *Plant Functional Types* existing in the 0,5° x 0,5° grid cell deployed over the European region.

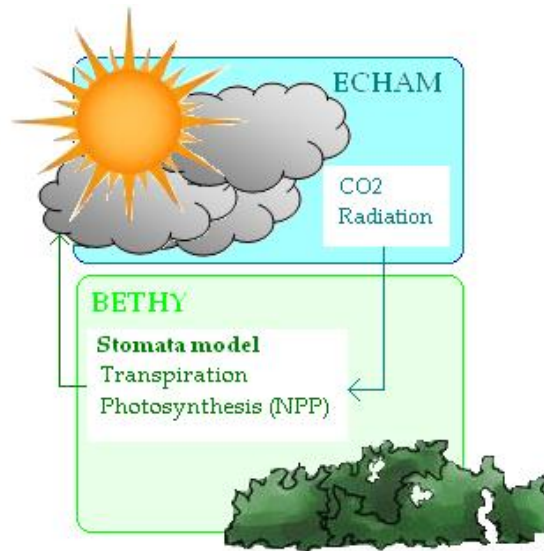


Figure 22 –BETHY scheme

BOX: S Scaling production from leaf to canopy (Source: Reick, 2009)

Having A as assimilation; R_d as dark respiration; R_g as growth respiration; R_m as maintenance respiration; R_h as heterotrophic (soil) respiration and LAI as leaf area index, hence:

From photosynthesis: A, R_d $(mol(C)/m^2(leaf))$

Gross primary

productivity: $GPP = A * LAI$ $(mol(C)/m^2(ground))$

Net primary productivity: $NPP = GPP - R_g - R_m$

Maintenance respiration: $R_m = \int_{leaf}^{-1} R_d * LAI$

Construction costs: $CC = \frac{NPP + R_g}{NPP} = 1,25$

(5 C are needed to allocate 4C)

$$\rightarrow NPP = (GPP - R_m) \quad \{CC^{-1} \text{ for } GPP > R_m ; 1 \text{ otherwise } \}$$

and

Net Ecosystem Exchange (NEE): $NEE = NPP - R_h$

Plant Functional Types (PFT) in JSBACH

In JSBACH, the vegetation (which allocated in a grid cell) is described in terms of different Plant Functional Types (PFTs) (Sitch *et al.*, 2003). PFTs symbolize broad phonological, biogeographically and morphological aggregations within every parameter value is held temporally and spatially constant and responses to physical and biotic factors are assumed to be similar (Prentice *et al.*, 2007). They enable thus, to account generally the variety of structure and function among plants (e.g. woody such as tropical, temperate and boreal; herbaceous) (Sitch *et al.*, 2003), by aggregating the biogeochemical fluxes and vegetation properties within each grid cell (Pavlick *et al.*, 2012). For that reason the average of a PFT consists in the fundamental entity simulated in JSBACH since this concept enables to deploy the processes run at the level of the plants individually within their PFT which will ultimately scaled up to the “population” over the grid-cell (Figure 23).

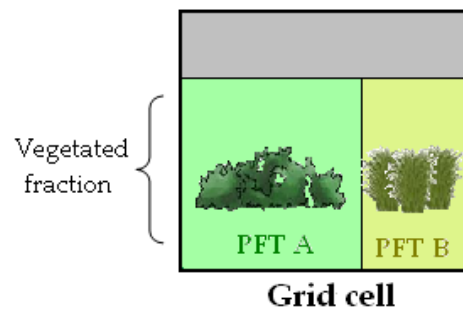


Figure 23 - Grid cell example

PFT are a main feature in a DGVM mainly due to two reasons. Firstly, to each PFT a set of parameterizations is assigned, concerning the ecosystem processes (such as (1) phenology; (2) leaf thickness; (3) minimum stomatal conductance; (4) photosynthetic pathway; (5) carboxylation rate; (6) maximum electron transport rate; (7) specific leaf area carbon content, and (8) phenotype, to name few) (Cramer *et al.*, 2001; Raddatz *et al.*, 2007), and thus the segregation of vegetation in groups assigned to range of similar behavior regarding responses to environmental conditions enables a simplification of the existing plant complexity. Moreover, it is also very useful for modeling in a mapping context such as when applying the DVGM (Lavorel *et al.*, 2007). Secondly, the structural characteristics of the vegetation can be defined by the representation of different PFTs at a certain point in time and space (Cramer *et al.*, 2001; Lavorel *et al.*, 2007) which will ultimately enable the monitoring effects of global change or management on vegetation distribution and ecosystem processes (Lavorell *et al.*, 2007).

It is important to notice that the classification applied to each PFT, depends on the ability of association between vegetation traits and function on model (see Figure 24 for examples) and ultimately it depends on the objectives of the modeling purpose.

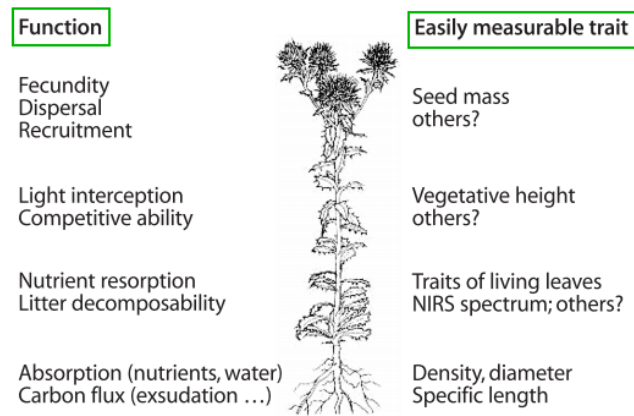


Figure 24 - Examples of soft traits and associated functions (Source: Canadell *et al.*, 2007)

In fact, some authors have categorized agriculture according to crop functional type based on management practices (besides phenology and physiological parameters); while others have performed a hierarchical classification based on response of vegetation to fire disturbances. Nevertheless, PFT schemes used by DGVMs use to be criticized for ignoring much of the knowledge about comparative plant ecology (Harrison *et al.*, 2010). Furthermore, several plant features present a considerable variation within PFTs and in fact, for many important features that variation can even become greater within PFT rather than between different PFT (Pavlick, *et al.*, 2012).

The grid cell simulation runs after the insertion of input data which includes seasonal (e.g. daily time scales) climatology; soil type and atmospheric CO₂ concentration which driven daily potential evapotranspiration and monthly soil temperatures. Thus, seasonal course of leaf phenology is calculated for each PFTs (Sitch *et al.*, 2003). The obtained results allow illustrating (within one particular scenario of atmospheric composition and climate change), the range of responses of state-of-the-art terrestrial biosphere models (Cramer *et al.*, 2001).

Each model grid cell is divided into tiles, and then, the surface condition and fluxes are calculated separately for each tile – which holds a single PFT. Afterwards, the grid cell average is given to the atmosphere (Figure 25).

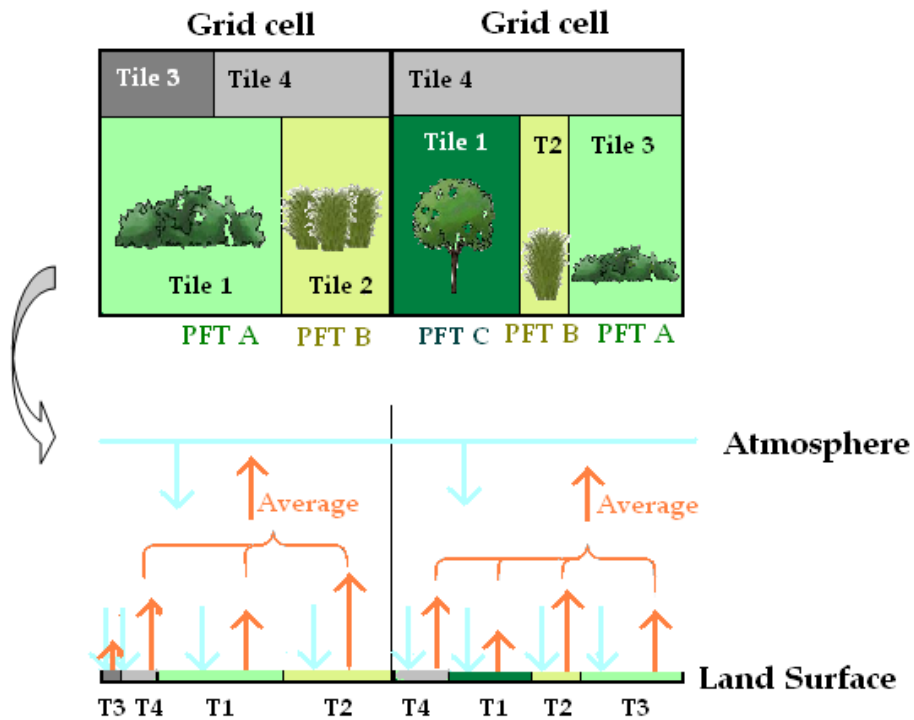


Figure 25 - The tilling approach (Source: Adapted from Brovnik *et al.*, 2009)

Summing up, the vegetation was described in a grid cell of different PFT, based on attributes which control the physiology and dynamics to which each PFT was assigned. Within this model 21 PFT were defined, as listed in the Table 26.

Table 26 - Plant Functional Types considered by JSBACH

No.	PFT	Biomass type
1	Glacier	-
2	Tropical evergreen trees	"Forest" Biomass
3	Tropical deciduous trees	"Forest" Biomass
4	Extra-tropical evergreen trees	"Forest" Biomass
5	Extra-tropical deciduous trees	"Forest" Biomass
6	Temperate broadleaf evergreen trees	"Forest" Biomass
7	Temperate broadleaf deciduous trees	"Forest" Biomass
8	Coniferous evergreen trees	"Forest" Biomass
9	Coniferous deciduous trees	"Forest" Biomass
10	Rain green shrubs	"Forest" Biomass
11	Deciduous shrubs	"Forest" Biomass
12	C3 grass	"Herbaceous" Biomass
13	C3 grass	"Herbaceous" Biomass
14	Pasture	"Herbaceous" Biomass
15	C3 Pasture	"Herbaceous" Biomass
16	C4 Pasture	"Herbaceous" Biomass
17	Tundra	-
18	Swamp	-
19	Crops	"Herbaceous" Biomass
20	C3 crop	"Herbaceous" Biomass
21	C4 crop	"Herbaceous" Biomass

The cover types of PFT for each one of four tiles existing in each grid cell, is presented in Figure 26 since the discrimination of vegetation type distribution might be useful for further interpretation of output data. (As explained before, the spatial distribution of PFT across the Iberian Peninsula is constant along the time, since JSBACH does not assume land use dynamics. Additionally for simplification matters, the results were aggregated in three main groups: (1) "*Forest biomass*" which includes the PFT listed from 2 to 11 (and hence trees and shrubs were accounted together); (2) "*Herbaceous biomass*", which comprises the rest of PFT excluding glacier, swamps and tundra and

(3)“All” - which regards all PFT together. Table 27 depicts some of the species that are found in IP, assigned to the major PFT from forest biomass :

Table 27- Major species existing in Iberian Peninsula assigned to forest type (Source: Alcaraz *et al.*, 2006)

PLANT FUNCTIONAL TYPE	SPECIES IN IBERIAN PENINSULA
Coniferous evergreen trees	Pine (<i>Pinus</i> spp), junipers (<i>Abies</i> spp), firs and spruces (<i>Picea</i> spp)
Temperate broadleaf trees	; <i>Quercus suber</i> ; <i>Quercus ilex</i> ; <i>Quercus petraea</i> ; <i>Quercus cerris</i> ; <i>Eucalyptus globulus</i> ; <i>Populus</i> ; <i>Fagus sylvatica</i>
Temperate Broadleaf deciduous trees	<i>Castanea sativa</i>

In Appendix A it can be found further information regarding the most common crops existing in the Iberian Peninsula, along with their spatial distribution.

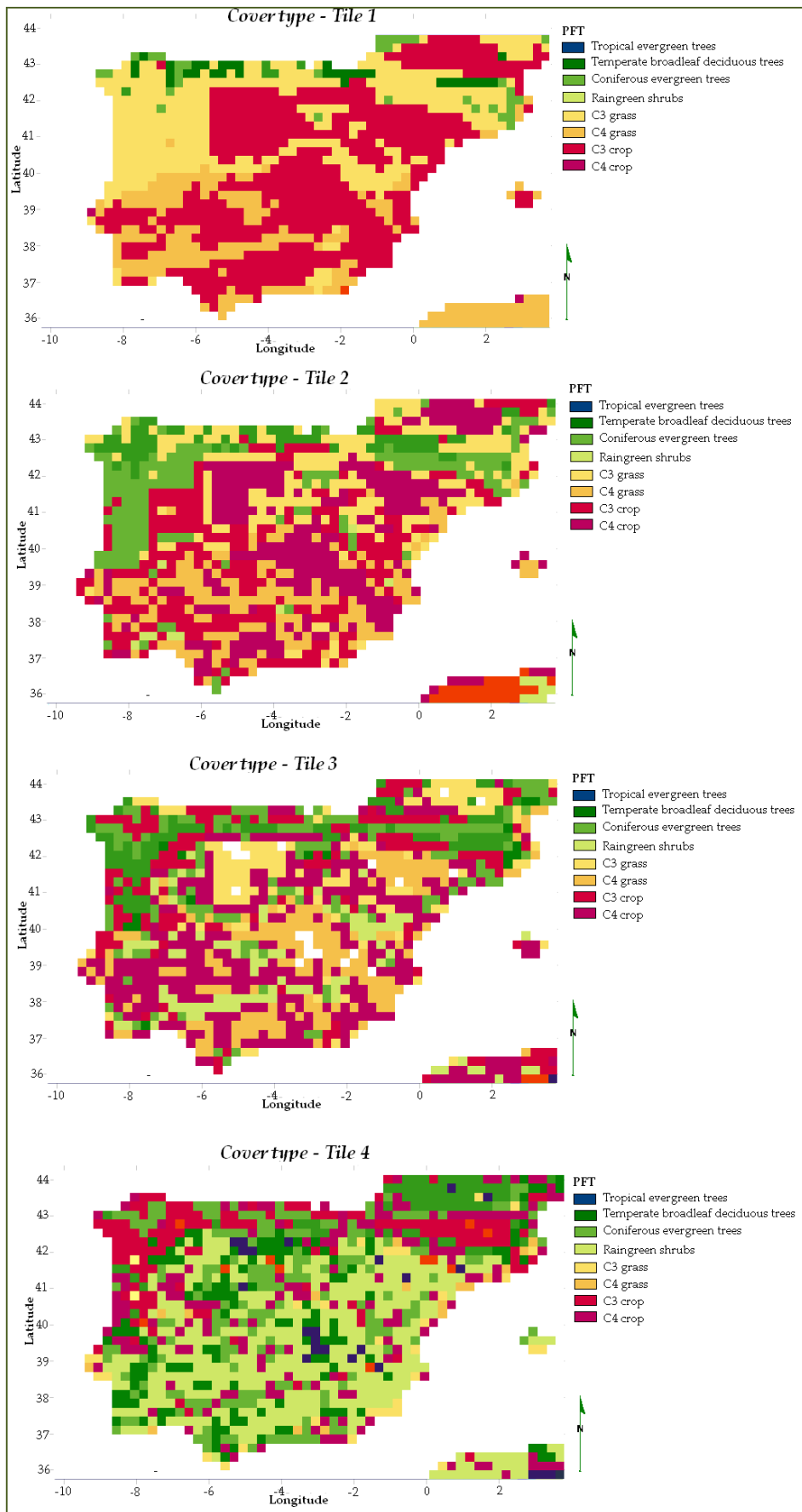


Figure 26- Cover Type per tile

3.2.3. CBALANCE module

The CBALANCE module regards the heterotrophic respiration (from soil), the net CO₂ exchange with atmosphere (NEP) and it also accounts with carbon in plants and soil pools, the so-called *C-pools*. Throughout this model, JSBACH simulates the carbon flow, more specifically the storage of carbon on land within five “pools” which are measured in mole of carbon per square meter (mol(C)/m²(canopy)) – translating thus in carbon density per square meter of canopy. However, only some of them (three, in fact) are regarded in this dissertation, namely the “Green pool”, the “Wood pool” and the “Reserve pool” – which consists of the state variables of the model (Reick, 2009).

The segregation of carbon pool is made upon the rate of carbon storage which is different from tissue to tissue within the same plant (Figure 27). The green pool is composed by the living parts of plants such as the leaves, the fine roots and sapwood and does not take into account reserves. The reserve pool is hence composed by sugar and starches that plants store as an energy reserve. Finally, the wood pool consists of the woody part of the plants, comprising thereby the stems, the branches and the roots.

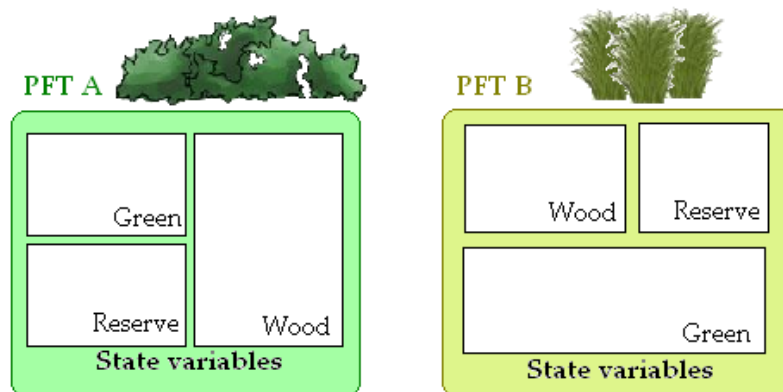


Figure 27 - Scheme of different Carbon pools for different PFTs

The green and reserve pools have a higher rate of carbon intake compared to wood pools, which are hence slower carbon pools. Thus, the JSBACH model simulates the growth of vegetation assuming certain percentage values of NPP assigned to each the pool composing each PFT in different percentages.

Figure 28 provides an illustrative interpretation of this explanation.

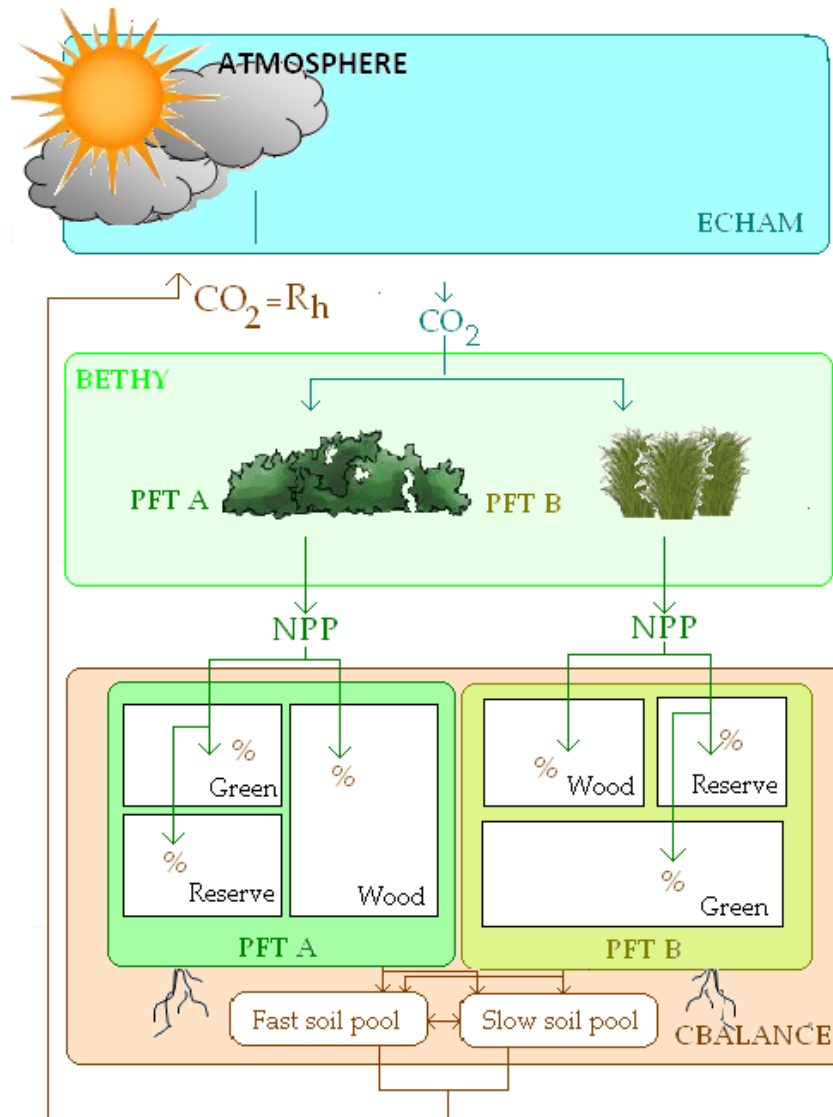


Figure 28 - CBALANCE Carbon Pool model

The calculated NPP (from BETHY module) is hence assigned to the three carbon pools. Each vegetation carbon pool will afterwards be assigned to other soil carbon pools: fast or slow soil pool (as it is shown in Figure 28) which is dependent on carbon pool, soil humidity surface temperature and time. Finally, these two soil carbon pools will contribute with carbon release onto the atmosphere, i.e., soil respiration (Reick, 2009). Therefore, the input data for CBALANCE model consists of NPP; LAI; soil moisture and temperature (Reick, 2009).

3.3. Model variables: inputs and outputs

The input data of JSBACH model (consisting in the mean annual climatology) used for this work is composed by six variables listed in Table 28, upon which the simulation in every single cell will be driven by – as illustrated in Figure 25:

Table 28 – Climate input variables

No.	Variable	Time
1	Air temperature at 2m above ground	30 min.
2	Downwards long-wave (infra-red) radiation flux	30 min.
3	Downwards short-wave (solar) radiation flux	30 min.
4	Precipitation (Rainfall)	30 min.
5	Specific humidity at 2m above ground	30 min.
6	Wind speed at 10m above ground	30 min.

The relevant output for this dissertation include: Gross Primary Productivity; Net Primary Productivity and Biomass.

3.4. Model datasets

The complete data set that composes the scheme supporting JSBACH, consisted of a fusion between the data sets provided by the Water and Global Change (WATCH) project and by the ERA INTERIM. The conjunction of both datasets comprises the climatic parameters which will be used as input data enabling thus to run the JSBACH. The nature of both data sets regards some attention, since a considerable part of JSBACH results reliability is dependent of the accuracy of forecasted results.

3.4.1. WATCH data sets

The Water and Global Change (WATCH) Project (which consisted in an Integrated Project funded under the Sixth Framework Program of European Union) gathers data regarding the components of current and future global water cycles as well as water resources states – for the recent past and the future. In short, the WATCH program provides an extensive analysis of the global water resources it also evaluates their

uncertainties and overall vulnerability of global water resources related to the main societal and economic sectors (Harding *et al.*, 2011).

WATCH was developed after having a consistent set of climate data input throughout an acquired understanding of water cycle in recent past. Therefore, the WATCH project comprises two different data set regarding past climate scenarios and predicted climate/hydrological scenarios, namely, “WATCH Forcing Data” and “WATCH Driving Data”, respectively.

The “WATCH Forcing data” covers the period 1901-2001 and it is based on a global 0,5 x 0,5 degree (approximately 50x50km) grid and the eight essential climate variables are comprised within it. These data result from merging observational dataset along the period; adding further observational procedures and are also subject of local validation against hourly meteorological data. These data can be hence, be used as input in several models, such as hydrological models which enable to produce comprehensive global water cycle data sets.

On the other hand, the “WATCH Driving Data” is covering the period 2001-2100, composing thus the 21st century data set. This data was created employing a novel bias-correction methodology which was trained on the 20th century WATCH Forcing Data. Hence, the WATCH Driving Data provides the same variables as the WATCH Forcing Data and use the same grid as well. These forecasted applied have been created from three well-established climate models which are running under two IPCC future emissions scenarios (Harding *et al.*, 2011). Hence, generally speaking, it evaluates the terrestrial water cycle throughout the use of land surface models as well as general hydrological models in order to asses significant variables (such as evaporation, runoff and soil moisture).

3.4.2. ERA interim data sets

Era-Interim consists in the latest global atmospheric reanalysis developed by the European Centre for Medium-Range Weather Forecasts (ECMWF). The ERA-Interim

project incorporates a forecast model with three fully coupled components for the atmosphere, land surface and ocean waves. It computes variation analysis of the basic upper air atmospheric fields (such as temperature, wind, humidity, ozone and surface pressure) as well as near-surface parameters (such as 2m temperature and 2m humidity); soil moisture and temperature; snow and ocean waves (Dee *et al.*, 2011).

Similarly to WATCH, ERA-Interim also covers a time period back at the 20th century (specifically from 1989 onwards) and it is extended forward in near-real time (Dee *et al.*, 2011). The data is also aggregated in a gridded scheme basis including 3-hourly surface parameters, although these parameters includes a bit wider range of parameters natures (e.g., such as the weather; the ocean-wave and land-surface conditions. The upper-air parameters (which cover both troposphere and stratosphere are run over a 6-hour scheme (Dee *et al.*, 2011). The forecasted information is possible through the model equations which enable extrapolating data from observed parameters, resulting in physically meaningful forecasted results. Reanalysis data provides a spatially complete and multivariate record of the global atmospheric circulation, and it is produced with a single version of a data assimilation system which includes the forecasted model used. This reanalysis provided by ERA-Interim was produced with a sequential assimilation scheme, advancing forward in time forward in time using hourly cycles.

JSBACH Storyline

The input data provided by the datasets, was selected according to the SRES scenario A1B, already mentioned. The A1 family was chosen, since it has the highest rates of technological change and economic development. Moreover, the trend of the global population growth is similar to some studies that regard these predictions (i.e. a growing population which peaks in the mid-century declining afterwards) (IPCC, 2000).

The A1 family and storyline also predicts a future world of rapid economic growth as well as the rapid introduction of new and more efficient technologies (IPCC; 2007). Although, the scenario A1B, (also known as the “balanced” scenario), in fact balances

across all energy sources. Hence, by being “balanced” means that this scenario does not rely too heavily on one particular energy source, assuming thus similar improvements rates applied to all energy supply and end-use technologies. This scenario, predicts a CO₂ increase until around 2050 and then decreasing after that (Figure 29).

Table 29 depicts some of the main driving forces responsible for the estimations of CO₂ emissions presented in the previous figure.

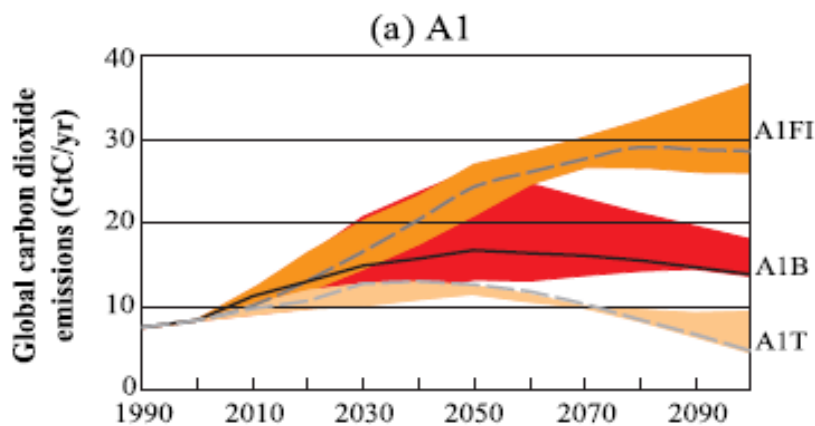


Figure 29 – Global carbon dioxide emissions (Gt(C)/year) for scenarios A1F1, A1R and A1B (IPCC, 2000)

Table 29 - Overview of main driving forces and CO₂ emissions across the years for A1B Scenario (Source: IPCC, 2000)

	Future	Reference: 1990	A1B Scenarios
Population (billion)	2020		7,5
	2050	5,3	8,7
	2100		7,1
World GDP (10 ¹² 1990US\$/yr)	2020		56
	2050	21	181
	2100		529
Per capita countries income ratio: Annex-I ¹² to Non-Annex-I ¹³	2020		6,4
	2050	16,1	2,8
	2100		1,6
CO ₂ fossil fuels (GtC/yr)	2020		12,1
	2050	6,0	16,0
	2100		13,1

3.5 Simulation Condition and Scenarios

¹² Developed countries and economies in transition

¹³ Developing countries

In order to accomplish the goals set for the present work, four different scenarios were considered as it is shown in Figure 30. The [1960-1990] period – hereafter also referred as “Reference Period” consists in a base time period regarding the recent past which will serve as a comparison period during the assessment of change in climate or carbon balance projected for future scenarios. Moreover, this reference period also enables to evaluate the model’s accuracy having recorded data for comparison purposes.

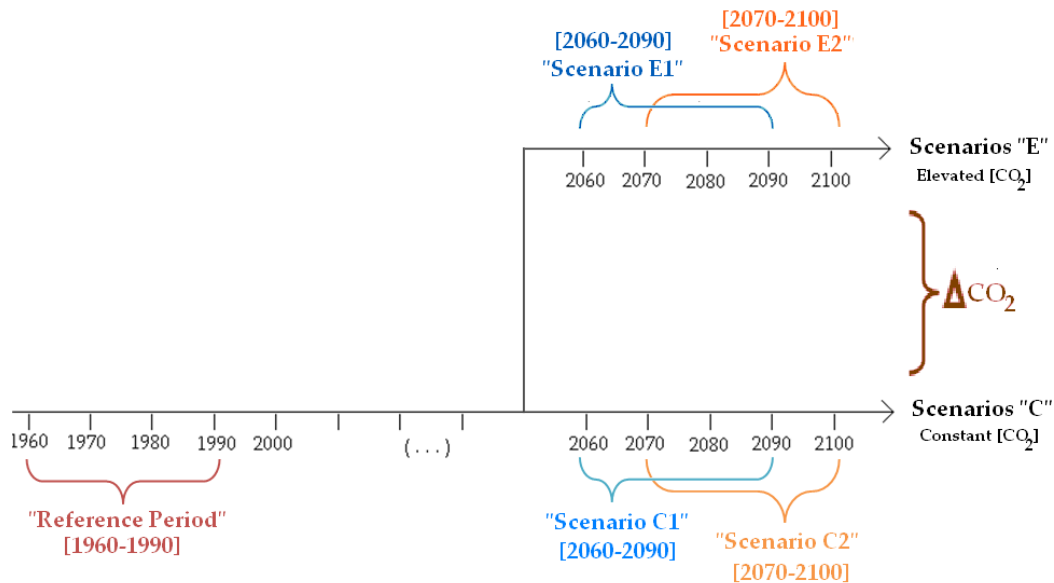


Figure 30 - Reference Period and Future Scenarios considered for the results

For the future prospects, two time periods were considered: covering the period from 2060 to 2090, and from 2070 to 2100. To each time period, two different conditions in atmospheric CO₂ concentration were assumed. The scenarios “C”, namely scenarios C1 (2060-2090) and C2 (2070-2100) assume constant atmospheric CO₂ concentrations, i.e.

these scenarios maintain the same CO₂ levels existing during the reference period ~296ppm. Conversely, the scenarios “E” account with a rise of CO₂ levels, namely of 88% in scenario

E1(2060-2090) and 99% in

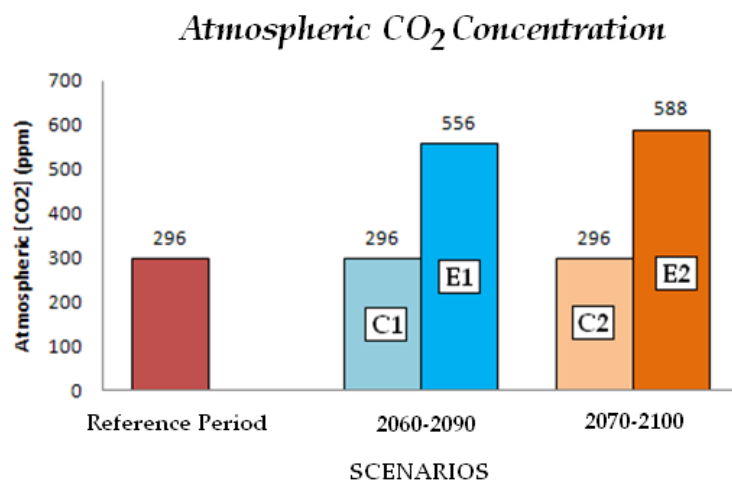


Figure 31 - Atmospheric CO₂ concentrations during the Reference Period and the Future Scenarios

scenario E2 (2070-2100) from reference period (Figure 31). Nevertheless both C and E scenarios assume the same climate changes.

The climate conditions characterizing the future scenario are in accordance with JSBACH storyline, (i.e. the A1B SRES scenario) meaning that climate changes are projected to occur in 2060-2090 and 2070-2100 and that both scenarios “C” and “E” are under the same changing climate conditions. The only difference (or varying variable) between “C” and “E” scenarios is thereby the concentration of atmospheric CO₂ and therefore the comparison analysis between a scenario of Constant CO₂ and a scenario of Elevated CO₂, enable to assess the solely impact of the CO₂ variable on an output result (Figure 32):

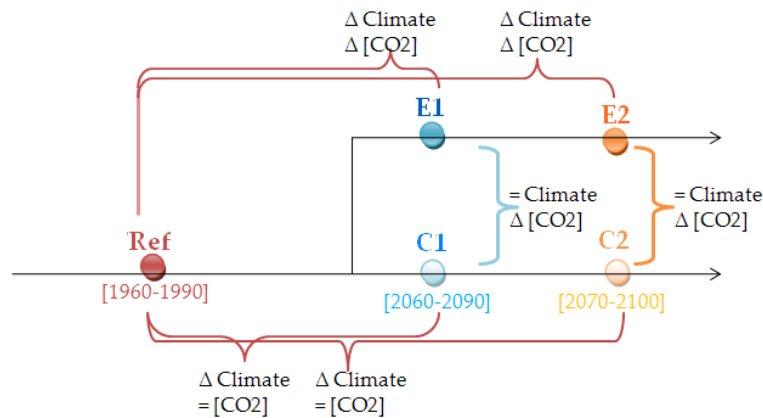


Figure 32 - Assessments from possible comparisons between Scenarios C1, C2, E1, E2 and the Reference Period

Figure 32 helps to illustrate the information that can be depicted from the comparison between a pair of scenarios. The comparisons between the output results from different scenarios (which consist in the variable mean of 30-years period scenario, over the IP) will be dependent on the information that it is expected to take from it. When it is aimed to understand the impact of CO₂ variation in productivity enhancement or biomass difference, for instance, the pairs of comparison are scenarios C1 and E1, and scenarios C2 and E2 (as there is no other variable varying between the scenarios besides CO₂). For realistic approaches, such as the assessment of biomass resource potential in future energy market, the comparisons rely on the E1 and E2 scenarios, as they meet the most likely future conditions (i.e. increase of CO₂ besides the changing climate variables).

3.6 Data handling and treatment

Data handling concerned the treatment of results regarding both the reference period and future scenarios: namely the results from climate variables and carbon balance variables yielded by JSBACH model. Table 30 and Table 31, describes the overall scheme setup of the work-flow concerning data handling and analysis:

Table 30 - Work flow of the three main stages of data treatment





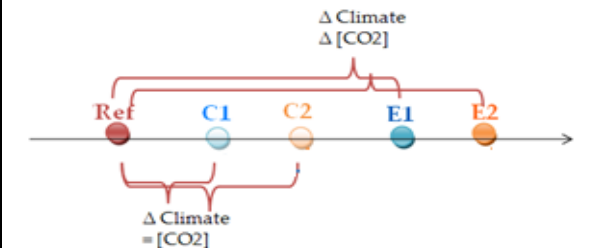
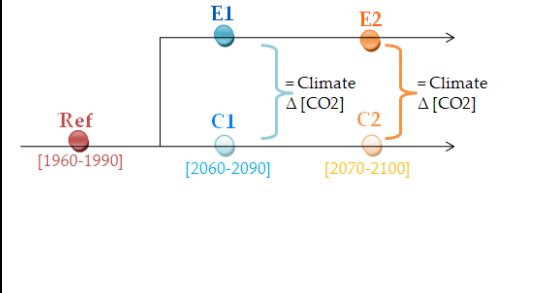
I – Reference Period: Climate variables* analysis	
<p>1 - Quantitative and qualitative analysis of spatial distribution of each climate variable during the period [1960-1990];</p> <p>2 - Spatial and qualitative comparison between climate patterns;</p> <p>3 - Assessment of correlation between spatial distributions of climate variables variable.</p> <p>*APAR and SWC are not climate variables</p>	<div style="border: 1px solid black; padding: 5px;"> <p>Variables under study:</p> <ul style="list-style-type: none"> • Land surface temperature  • Precipitation • Evapotranspiration • Soil moisture • Radiation (PAR and APAR) </div> <p style="text-align: center;">[1960-1990]</p>
II – Reference Period: Carbon balance assessment	
<p>1 - Quantitative and qualitative analysis of spatial distribution of each carbon-related variable during the period [1960-1990];</p> <p>2 - Spatial and qualitative comparison between climate patterns and PFT locations;</p> <p>3 - Assessment of correlation existing spatial distribution of GPP and climate variables;</p> <p>4 - Accounting of total biomass existing during the Reference period and discrimination of each PFT contribution;</p> <p>5 - Assessment of correlation existing spatial distribution of Biomass and climate variables;</p>	<div style="border: 1px solid black; padding: 5px;"> <p>Variables under study:</p> <ul style="list-style-type: none"> • GPP  • NPP  • Biomass (Herbaceous and Forest)  • WUE • LUE </div> <p style="text-align: center;">[1960-1990]</p>

Table 31- Work flow of the three main stages of data treatment (cont.)

III – Future Scenarios: Climate Change Assessment	
<p>1 - Spatial distribution comparison/analysis of quantitative alterations estimated for scenarios "C1", "C2", "E1", "E2" and reference period;</p> <p>2 - Analysis of differences and the magnitude of the annual mean changes of each variable;</p> <p>3 - Statistical comparison between results from future scenarios and Comparison of results with predictions studies made at global scale or IP scale, within the A1B scheme.</p>	<p>Variables under study:</p> <ul style="list-style-type: none"> • Δ Land surface temperature • Δ Precipitation • Δ Evapotranspiration • Δ Soil moisture • Δ Radiation (PAR and APAR) <p>Climate Changes comparisons:</p>  <p style="text-align: center;">([2060-2090] & [2070-2100])/ [1960-1990]</p>
IV – Future Scenarios: Carbon balance assessment	
<p>1 - Spatial distribution comparison/analysis of quantitative alterations estimated for scenarios "C1", "C2", "E1", "E2" and [1960-1990] time aggregation;</p> <p>2- Comparison of the magnitude of the annual mean change of change of variables;</p> <p>3- Analysis of correlation (between all Δ climate variable for ΔGPP and ; Forest and Herbaceous Biomass;</p> <p>4 -Statistical comparison between scenarios "Future C" and "Future E" (Δ GPP; ΔNPP and Δ Biomass</p> <p>5 – Predictions of biomass energy potentials (EJ) and analysis in terms of significance to the current energy system.</p>	<p>Variables under study:</p> <ul style="list-style-type: none"> • Δ GPP • ΔNPP • Δ Biomass • ΔWUE • ΔLUE <p>Comparisons between scenarios:</p>  <p style="text-align: center;">([2060-2090] & [2070-2100])/ [1960-1990]</p>

An overall setup of the methodology in regards to data treatment and final results is illustrated in Figure 33:

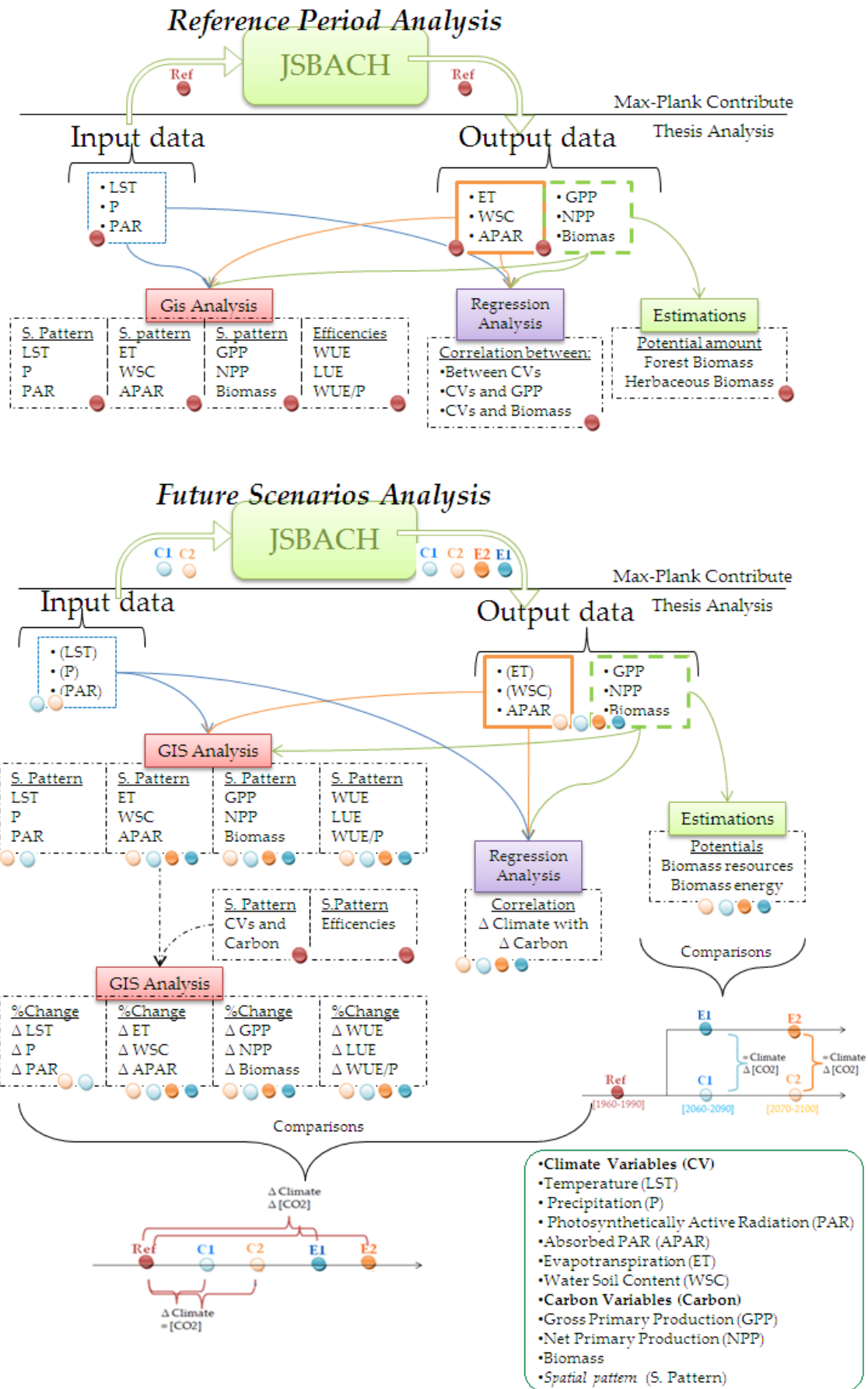


Figure 33 - Overall Methodology Scheme

3.6.1 GIS Analysis

The images created by JSBACH model as arithmetic variables were processed throughout map algebra operations under a GIS (Geographic Information System) tool (*IDRISI-Taiga*), enabling spatial modeling and visualization. In the following section, selected GIS analyses are presented to illustrate how JSBACH data was handled in a GIS.

Units Conversion

A major task performed in the GIS refers to units' conversion. For example, maps for *Mean Surface Temperature* units in Kelvin, were converted to maps in degree Celsius. Hence, as illustrated in the following *IDRISI* flowchart (Figure 34), a raster image (having the same spatial parameters than every map) was firstly created with initial single value set to be "273.15".

Afterwards, this new map (*273map*) was combined with the map of *Mean Surface Temperature* (in Kelvin) throughout a *overlay* operation enabling to create another map, by subtracting to each grid cell from the original map in Kelvin the value of 273,15 (since 1 degree Celsius corresponds to 273,15 degree Kelvin), resulting in a map unit of degree Celsius.

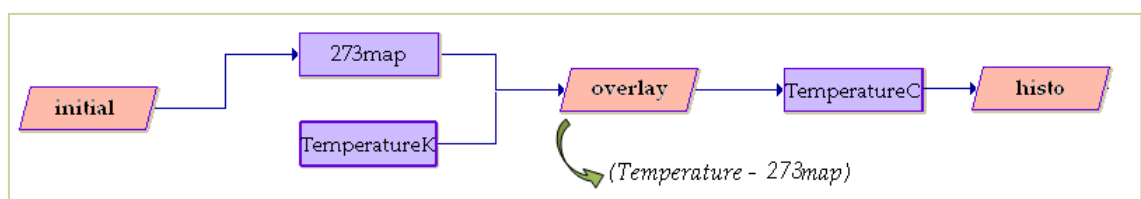


Figure 34 - Flowchart: creating an image with different units - example for temperature (degrees Kelvin to degrees Celsius conversion example)

The same procedure was applied for the different time aggregations, and after building up the new map. GIS also provide a graphic frequency histogram and statistics of the cell values for each image (Eastman, 2009), through the module *histo*. The number of classes and widths were defined similarly to each set of parameter, in order to facilitate visual interpretation and comparisons between eventual changes of static distribution.

A similar approach was made in order to convert precipitation and evapotranspiration maps (which units were initially expressed in kg/m²/s – and were converted to mm/year); as well as GPP; NPP and biomass maps (which was initially expressed in mol(CO₂)/m². . In some cases, such as soil moisture maps and biomass maps, the *overlay* module was also used in order to add or “sum” maps. In the case of soil moisture, several layers were added creating the final soil moisture map, whereas for the biomass map, *overlay* was applied to the three carbon pool of biomass (i.e. wood, green and reserve).

The *overlay* operations, also enable to create indexes based on prior maps. For example, to understand the water productivity over the IP during a certain time period – i.e. how much biomass would be created for a certain amount of water, the maps containing the evapotranspiration distribution and the GPP maps were related by using the division process.

Assessing percentage changes

In order to understand the scale of change between two different scenarios, map algebra operations (*imagediff*) were performed as shown in Figure 35, enabling to compare two quantitative images of the same variable for different dates (Eastman, 2009), to assess the percentage change between each image.

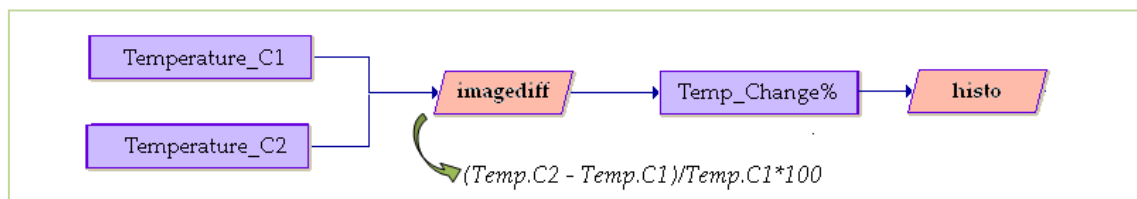


Figure 35 – Procedure to evaluate percentage change of land surface temperature between *Temperature C1* (Scenario C1) and *Temperature C2* (Scenario C2)

These procedures were used to assess the difference between a future scenario and the reference scenario, such as for instance the precipitation maps –which enable hence to understand “how less mm would rain within a 100 year time difference”.

Assessing images ratio changes: GPP example

Another procedure taken to assess changing variables over the time, was throughout the ratio between the later image (from a future scenario for instance), and the reference period. Figure 36 is illustrating this procedure as used for the visualization of overall changes (in terms of “positive” and “negative changes), such as increases or decreases of GPP over the Iberian Peninsula. This step as used whenever it was needed an clear visualization of overall changes (in terms of “positive” and “negative” changes), such increases or decreases of GPP over the Iberian Peninsula.

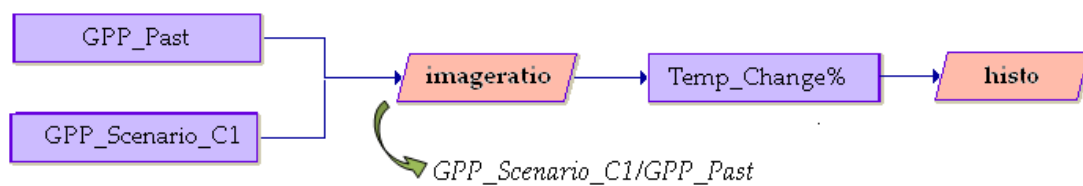


Figure 36 - Procedure to evaluate ratios GPP between reference period and scenario C1

3.6.2 Statistical Analysis

To evaluate the ecosystem response to climate variability, correlation analysis were performed between the mean annual carbon variables (i.e. GPP, NPP, forest and herbaceous biomass) and the mean annual climate variables, i.e. land surface temperature (T), precipitation (P), evapotranspiration (ET), soil water content (SWC), PAR and APAR, using data from each scenario. The results (i.e. correlation coefficients and determination coefficients) enabled to assess the relationship between the interannual variability in the carbon fluxes and climate variables, as well as the spatial pattern of pairs of variables during the reference period (e.g. between climate variables). The histograms created by the GIS tool, also enabled the statistical analyzes of the maps handled from the JSBACH model.

3.7 Estimations of the Potential Biomass for energy potentials

The estimations of biomass potentials were based in data from the literature, along with the biomass estimates yielded by JSBACH model. As explained before, the overall set of PFTs was segregated in two biomass types (“Forest” and “Herbaceous”). For each biomass type, JSBACH provided three types of maps (expressed in mol(C)/m²(grid box)) for each carbon pool (i.e. “green pool”, “reserve pool” and “wood pool” although for “herbaceous” biomass related maps, the wood pool had zero values).

3.7.1 Biomass Potentials

Each set of maps of carbon pools from each biomass type, were summed up, providing the overall biomass assigned to a biomass type for each scenario, expressed in section.3.5 In order to obtain biomass in terms of mass, the value of carbon molecular weight was used (Molar Mass of Carbon = 12,0107 g/mol, (Chang, 2005)).

Hence, multiplying the molar mass value by each value from the maps, biomass could now be expressed in terms of g(C)/m² – which represents the “areal density” of biomass. Afterwards, in order to depict the absolute values of biomass potentials, the following steps were taken:

- i) Since each grid box contains 4 tiles, and to every single tile a different PFT cover – with varying size is assigned, hence each cover fraction was multiplied against the value of the area of the corresponded grid box (this measure was necessary, since the grid box have different areas due to the curvature of the Earth), obtaining the total areas covered by each PFT (hereafter called as PFT areas).
- ii) PFT areas were multiplied by the value of “forest” or “herbaceous” biomass density assigned to that grid box – depending on the group that the PFT belongs to, obtaining the values of carbon mass that each PFT has.
- iii) The overall masses of each of the four tiles were summed up, resulting in the total amount of biomass of a certain PFT over the entire region under study (in terms of mass of C).

- iv) Finally, the final results obtained in the third step were multiplied by 2, since typically the carbon account up to approximately one-half of the dry “weight” of plants tissues (Broadmeadow & Matthews, 2003) obtaining thus the actual mass (or commonly referred as “weight”) of each total biomass assigned to each PFT.

3.7.2 Biomass Potential as Energy Resource

The effective potential contribute of biomass to energy production, was estimated after taking into account the amount of available residues recoverable for that purpose. For simplicity, the energy carrier considered for estimations is only electricity, although other energy uses can be considered from biomass. The data collected from literature (earlier presented in Table 8) regarded the rates of residues yielded from agriculture segregated by species. However, applying these ratios directly to the overall biomass yielded by JSBACH to each PFT after estimating the share of each species, would be subject of multiple uncertainties. Therefore, a wider approach was taken by considering the major residue produced in crop (straw) for the herbaceous biomass, while for forest biomass only two types of activity and residue (already reviewed in literature from Table 6), were taken as shown in Table 32.

Table 32 – Product/residue ratio (wet basis) of main agriculture crop residues for Southern Europe

	PRODUCT/ACTIVITY	RESIDUE	RPR	AUTHORS
HERBACEOUS BIOMASS	Cereals	Straw	0,9	Dalianis & Panoutsou (1995)
FOREST BIOMASS	Thinning	Top and Branches	0,1	Yoshida & Suzuki (2010)
	Logging residues	Top and Branches	0,3	Yoshida & Suzuki (2010)

Recovery rates vary with local practices as well as species, (for instance, according to BISIPLAN (2012) for maize residues values as low as 35% and as high as 75% have been reported, depending on the harvesting method employed). Thereby, no consistent data was found in literature regarding the recovery rates of residues for Iberian Peninsula. The rates of residues are dependent on multiple environmental, technical, social and economic constraints that reduce the amount of biomass that can be extracted from agriculture or forest. For that reason, the estimations were conducted

within two wide and general approaches aiming to explore the potential effects of selected environmental policy and resource management issues on land. The first approach, named as *Max Potential*, aimed to estimate the maximum theoretical electric potential possible, assessing thus the maximum contribution that forest biomass could have in electricity, by estimating the maximum electricity supply possible through the entire available potential of forest biomass from clear cuttings. However, it should be notice though that this approach is fairly unrealistic due to its inconceivability.

The other approach, named as *Plausible Potentials*, estimates the contribution of forest and agricultural residues under a set of three different scenarios assuming different rates of residues recovered for electricity production. These scenarios (namely *BAU*, *Low-Yield* and *High-Yield*) allow for plausible quantified projections, and therefore they do not intend to predict the future. Their purpose is to illustrate “what-would-happen-if” type of situations. The estimations of residues available for energy productivity were based on Table 33. It was assumed a removal rate of 90% for *Max Potential* approaches, since in accordance with Yoshida & Suzuki (2010), clear cuttings activities harvest 90% of biomass (Table 6).

Table 33- Scenarios to assess the effect of selected environmental policy and resource management options on soil organic matter levels in the EU for the 2030 horizon

Policy/Resource management issue	Plant Functional Type	Forests – resource management issues			
		<i>Max Potential</i>	<i>Plausible Potential</i>		
			<i>BAU*</i>	<i>Low-Yield</i>	<i>High-Yield</i>
Wood production	All forest biomass	90%			
Forest residues use for bioenergy	T. B. evergreen trees		10%	20%	40%
	T. B. deciduous trees				
	C. evergreen trees				
	Rain green shrubs				
	Deciduous shrubs				
Agriculture – resource management issues					
Crop residues and straw use for bioenergy	C3 crop		10%	20%	40%
	C4 crop				
Grass residues (straw) use for been.	C3 grass		10%	20%	40%
	C4 grass				

*According to IEA

The *BAU* scenario (which stands for “business-as-usual”) assumes a continuation of the current recovery rates of residues from major food crops and forestry industry

(assumed in IEA, (2003) study). On the other hand, both *Low-Yield* and *High-Yield* scenarios simulate ratios occurring in the future with increasing values, comparatively to the *BAU* scenario (since recovery of agro-forestry industry, are projected to increase. However, the magnitude of increase differs considerably between both scenarios. The *Low-Yield* scenario assumes lower residues recover rates than *High-Yield* scenario, being both inspired in Hogan *et al.* (2010) as follows. The later assumes an optimistic development of policy and resources management, which support the increase of residue collection. Hence, this scenario was mainly inspired in the forecasted forestry residue collection expected for Scandinavia (i.e. 40%) by 2030, while the *Low-yield* scenario assumes the projections for continental Europe (Hogan *et al.*, 2010). Afterwards, using the values provided in Table 33, the amount of residues recovered for energy production purpose from each PFT was estimated, throughout the following equations:

$$BIOMASS_R = BIOMASS \times RPR \quad (\text{Equation 5})$$

and

$$BIOMASS_{RR} = BIOMASS_R \times RR \quad (\text{Equation 6})$$

where BIOMASS is the total biomass assigned to each PFT (in tonnes); RPR is the residue production ratio (in %); BIOMASS_R is the total amount of residue yielded; RR is the recovery rate of residues (in %) and BIOMASS_{RR} is the total amount of residues recovered for energy production (in tonnes).

3.7.3 Biomass energy Potential – Conversion into energy

The total amounts of projected residues recoverable for electricity generation (BIOMASS_{RR}), refers to potential energy, computed by applying the following equation:

$$E_e = BIOMASS_{RR} \times LHV \times \eta_e \quad (\text{Equation 7})$$

where E_e is the electric energy; LHV represents the lower heating value and η_e represents the efficiency of the conversion pathway to generate electricity. Concerning

efficiency, it was assumed two different values (presented in Table 34) according to two different conversion pathways that can be deployed for these types of biomass:

Table 34 –Electrical efficiencies of conversions biomass types (Source: Nikolau *et al.*, 2003)

Conversion pathway	Electrical Efficiency (η_e)
Central combustion:	25%.
Gasification cycle combined:	35%

The range of the LHV values is wide due to the dependence of LHV on several factors. Even though the energy content of biomass (assuming a dry, ash-free basis) is similar to all plant species (i.e. lying in the range of 17-21 MJ/kg), it was assigned different LHV for the different biomass types – although not as specific as in the literature from Table 4, once again to avoid an increase of uncertainty. Thereby, LHV values used in Equation 7, were based in Table 35, allowing a more general approach to this assessment. As it is a common practice in literature, some general biomass properties (such as dry weight basis) were assumed in order to enable simpler estimations (and LHV assignments to each biomass type).

Table 35 - Lower Heating Values (LHV) of selected biomass

Biomass type	FOREST BIOMASS (wood)	FOREST BIOMASS (forest residues)	HERBACEOUS BIOMASS (crop residues)	HERBACEOUS BIOMASS (grasses)
Moisture content	<i>dry basis</i>	<i>dry basis</i>	<i>dry basis</i>	<i>dry basis</i>
Lower heating value (MJ/kg)	19,6 MJ/kg	15 MJ/kg 19* MJ/kg	17,6 MJ/kg	16,3 MJ/kg
Authors	HARC ESSOM	HARC ESSOM EEA (2006)*, RENREW(2007)*, Esteban <i>et al.</i> (2010)	Nicolau <i>et al.</i> (2003) EEA (2006) RENEW (2007) Esteban <i>et al.</i> (2010)	HARC ESSOM

The LHV of crops residues is lower than of wood, since they have a lower carbon content (about 45 percent) and higher oxygen content. The value presented for this type of energy resource consists in the average energy value of ash-free, oven-dry annual plant residues. For straw (as a result of crop residues) an average heating value of 15,2 MJ/kg was assumed, reported by Khan (2009), being very similar to the LHV of

three of the most widely produced crops in Iberian Peninsula (namely, wheat, barley and rice) and on the other hand, Nikolau *et al.* (2003), EEA (2006), RENEW (2007), Esteban *et al.* (2010) applied 17,5 to what they referred t be agricultural residues. The following Figure 37 illustrates the overall scheme of methodology applied to assess potential biomass resources for energy.

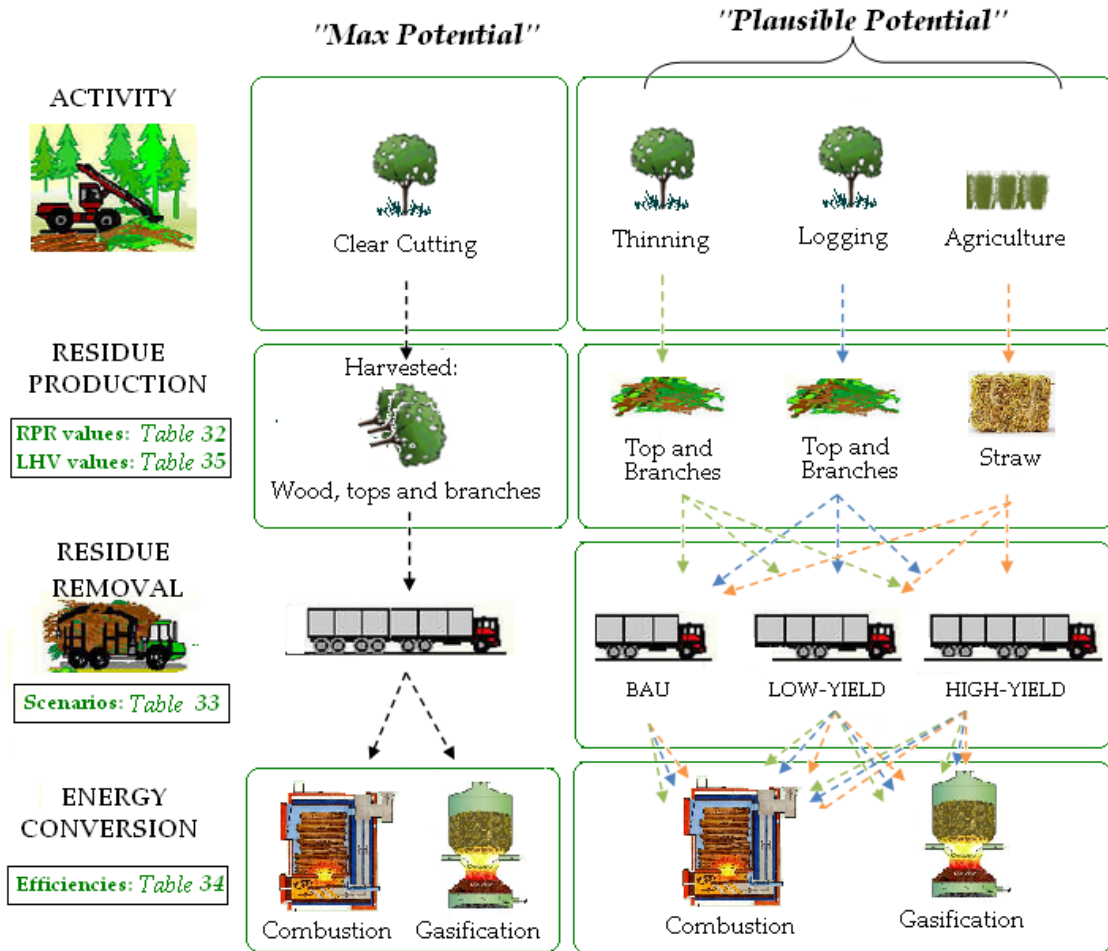


Figure 37 - Methodology applied to assessment of residue and energy potentials for forest biomass sources (Tree) and Herbaceous biomass sources (Grasses)

4. Results and Discussion

This chapter presents the whole set of results obtained and handled according to the methodology previously presented. The results yielded by the JSBACH model are hereafter considered separately by periods: the “Reference Period”, and the “Future Scenarios” (which comprises the two future scenarios of constant CO₂ levels – namely scenarios C1, C2, and the two future scenarios of elevated CO₂ - namely, E1 and E2 as described in section 3.6). The results for the Reference Period and the Future Scenarios are presented in a similar way. Firstly the spatial distributions patterns analyzes of the climatic variables (such as land surface temperature (LST), precipitation, evapotranspiration and photosynthetically active radiation (PAR)), under study across the Iberian Peninsula. The same study was applied to the other relevant environmental variables such as soil moisture and absorbed PAR (i.e. APAR). These sets of variables are assigned to three main groups starting with the land surface temperature, followed by the variables comprising the water balance and finally by those composing the radiation balance. The same scheme of results presentation is applied to the carbon balance variables.. Moreover a special focus is made on biomass response to climate change as well as on biomass energy potential under CO₂ fertilization scenarios.

It should be noticed that all climate variables (aside from evapotranspiration and soil moisture) were model input data, whereas the variables belonging to the carbon

balance analysis consists in model data output (along with evapotranspiration and soil moisture).

4.1 Climatic variables analysis – Reference Period

The analysis of the climate variables analysis during the 1960-1990 aims to disclose their spatial distribution as well as to understand their correlation with the orographic features characterizing the area under study and the correlation between them.

4.1.1 Land Surface Temperature (T)

For the Reference Period the geographic pattern of annual mean temperatures tended to have lower values at higher latitudes as shown in Figure 38. Land surface is strongly related to altitude (which coincides with Lutgens & Tarbuck (1995)), since it decreases at regions of high altitudes (as it can be compared with the Figure 16). Therefore, the lower temperatures (which are assigned to green) match the location of the many mountain ranges present in the territory of Spain (namely the Cantabrian Mountain Range and Central and Iberian Systems and the Penibetic Mountain Range in the Southeast region).

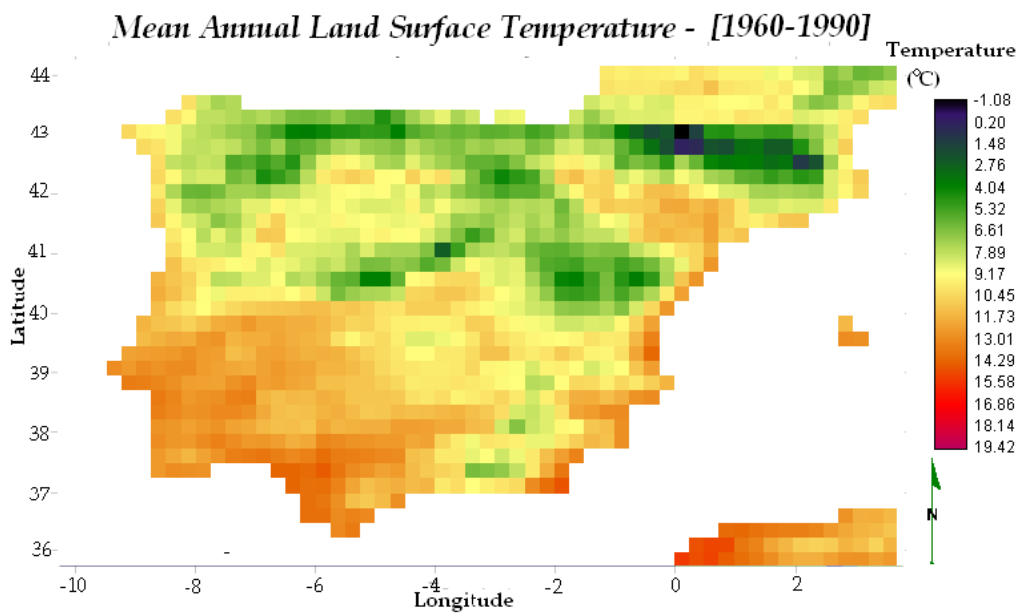


Figure 38 – Mean Annual Land Surface Temperature during the Reference Period [1960-1990]

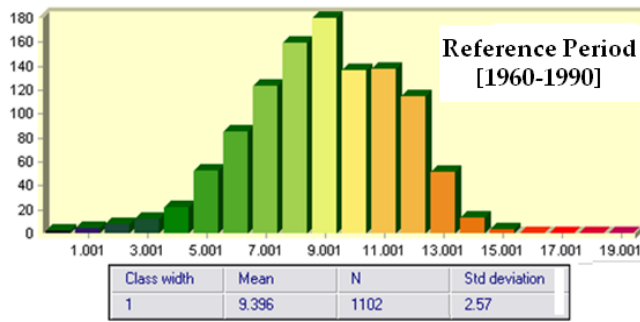


Figure 39 – Histogram and Statistical analysis of Mean Annual Land Surface Temperature over the Iberian Peninsula during the Reference Period [1960-1990]

During the reference period, the mean annual temperatures values shown to be normally distributed (Figure 39) and ranged between -1,08 and 15,4 degree Celsius (°C).

The overall mean land surface temperature for the reference period was around 9,4 °C. The lowest temperature occurred in the region of the Pyrenees, while the highest were present in southern IP (in Sierra Nevada).

4.1.2 Water balance (hydrology)

The water cycle inherent to the atmosphere is spatially highly influenced by the land morphology such as mountainous regions. The mountains modify the flow of air and respond differently from the surrounding atmosphere to solar radiation.

Precipitation (P)

The spatial distribution of the mean annual precipitation (mm/m²) is presented in Figure 40, showing distinctly changes with altitude revealing strong gradients.

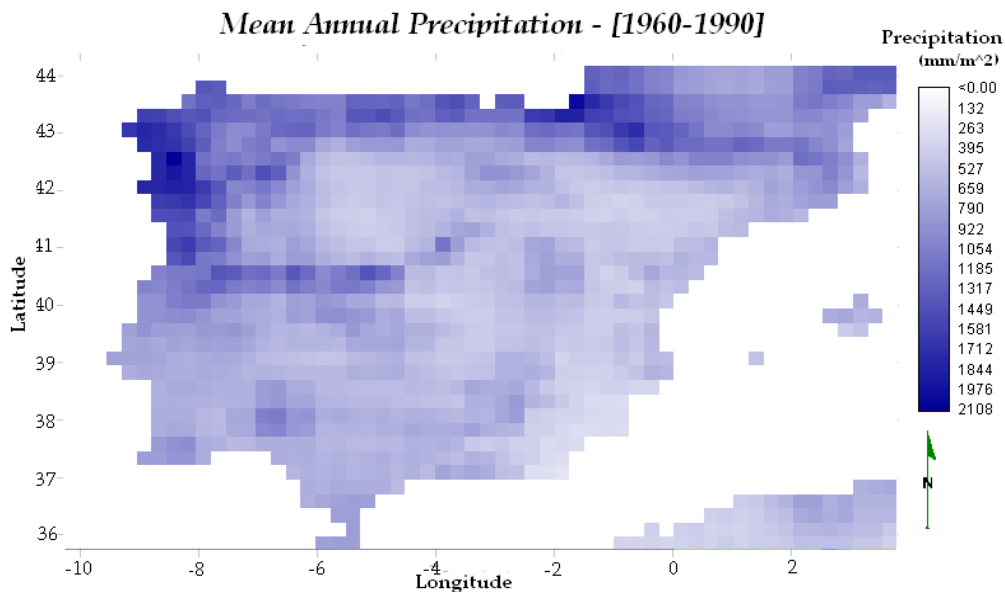


Figure 40 – Mean Annual Precipitation during the Reference Period [1960-1990]

The precipitation is enhanced in some of the mountainous environments present at the IP, having thus higher values in the west and the north of the IP as well as the Pyrenees (over 1.000 mm/year), and lower values (<400 mm/year) at lower latitudes, i.e. obtained toward the southeast of the IP.

There are also inland regions with a relatively low precipitation regime. The regions of Central Mountain Range and the Estrela Saw have also presented high precipitation values (agreeing with Daly *et al.* (1994) and Haiden & Postotnik (2008), which concluded that generally, precipitation increases with elevation - although the rate varies substantially). Moreover it is also interesting to notice the great variability of precipitation values in close regions: the region of northern Portugal and the Galicia region, as well as the orographic precipitation patterns in the Cantabrian region present values widely ranging: from ~500 up to ~2.100 mm/year. However, the relationship between precipitation and high altitudes reported in the northern regions is different at lower latitudes, i.e., there are regions where precipitation decreases in mountains environments. This difference of precipitation behavior relays on a phenomenon called *blocking* (Houze, 2012).

FACT BOX T: The Blocking Effect description

The so-called blocking effect occurs when an air mass flowing toward mountains flows up and over the mountain or slows down and turn to flow around them. The two difference scenarios are dependent on height of the topography along with the moisture content and resistance of air to rising causing different precipitation events. Generally, warmer air is less resistant to rising as it contains a bigger moisture content than colder air. When air flows over the mountains precipitation tends to concentrate in the wind facing side, leading to precipitation on this side. When moist air is forced up the windward slope it cools and expands causing water droplets to condense when the air is saturated triggering cloud formation which are responsible for rain (or snow) production over the windward side of the range (Houze, 2012).

The northern part of the IP is under conditions of consistent wind direction providing moist air continuously and where elevations are moderate (i.e. less than 2.500 meters), resulting in the previously discussed relationship existing between precipitation and topography (Houze, 2012). Moreover, the Coriolis effect acting over the trade winds

forces the air to turn when it slows (after approaching the topography), leading to increased precipitation on the windward side of the range - and decreased on the lee side (Houze, 2012).

Conversely, the precipitation decreases along the range of Iberian Mountain Range and Betic from northwest to southeast can be reflecting the decreasing of moisture supply as winds flows over the range (Houze, 2012). On the other hand, the higher precipitation rates located at the Northwest region of the IP are a fair example of blocked winds by the Cantabrian Mountain Ranges (which has higher latitudes than Iberian Mountain Range, for instance).

Conversely to what happened with the mean annual land surface temperature variable, annual mean precipitation values are not normally distributed (Figure 41) and instead of that the shape of the histogram suggests that this variable is lognormally distributed. The overall mean annual precipitation estimated during the 1960-1990 period for the IP region was ~767mm/year, and values ranged between 232 and 2.107 mm/year. The lowest value occurred in the southwest region of the Peninsula, in the region of Andalucía and in the region of Castilla y León located over the Central Upland. Part of the regions of Aragon, Catalonia and Castilla-La Mancha presented as well low values ($P < 500$ mm/year). These areas are another example of air moisture loss throughout flowing air masses.

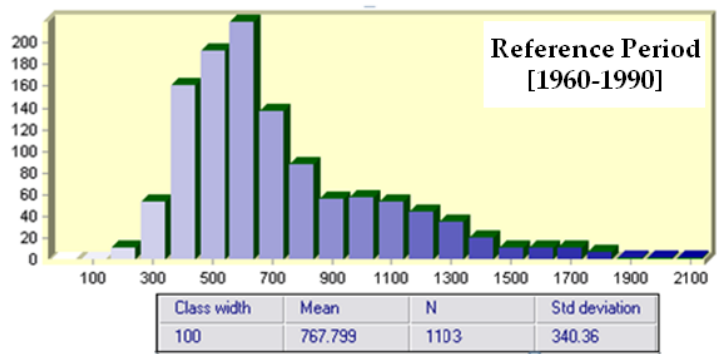


Figure 41 - Histogram and Statistical analysis of Mean Annual Precipitation over the Iberian Peninsula during the Reference Period [1960-1990]

Soil moisture (SWC)

The mean annual water content in the soil (SWC), or in other words soil moisture, was firstly analyzed at five vertical (layers), with the thicknesses and soil depths (of mid of the layer) disclosed in the following table:

Table 36 – Thicknesses and mid layer depth of the 5 layers of soil

	Layer 1	Layer 2	Layer 3	Layer 4	Layer 5
Thickness (m)	0,065	0,254	0,913	2,902	5,700
Mid depth (m)	0,033	0,192	0,775	2,683	6,984

It should be taken into account that, despite the soil layers in the model are always the same, if one layer is only 2 m deep, the following depths (deeper than 2 m) are not simulated. Therefore, the thicknesses of the soil vary, and the model uses this information for calculations. During the [1960-1990] period, the range of this variable has gotten notoriously wider as depth increases, and the pixel distribution changes considerably between each layer (Figure 42).

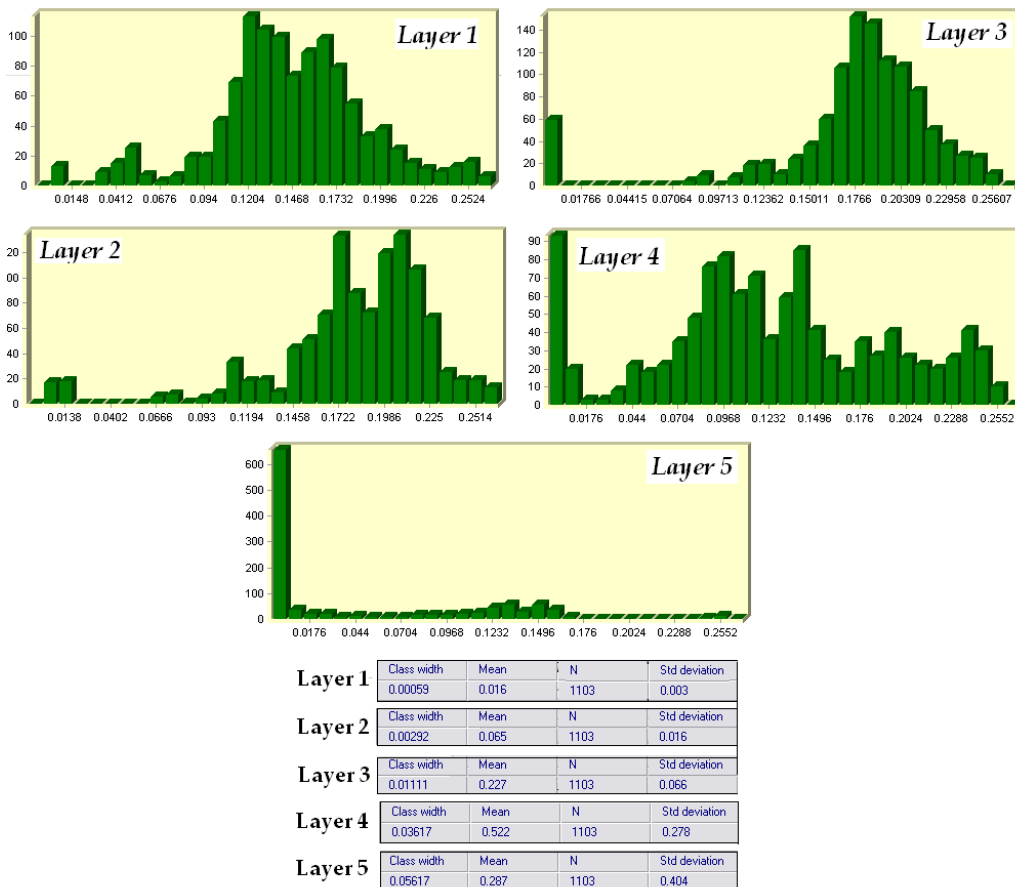
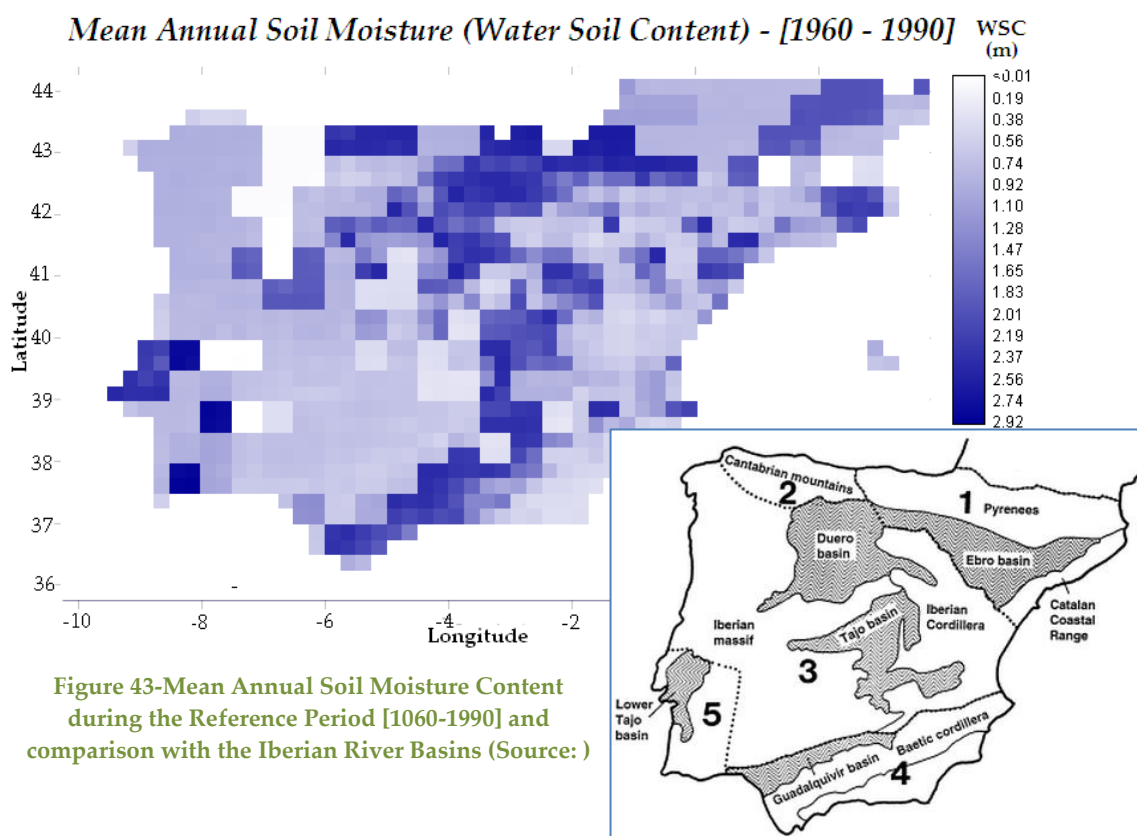


Figure 42 – Histogram of soil moisture content of layer I [m] of layers 1,2,3,4 and 5 during [1960-1990]

One of the most glaring differences consists of the absence of pixels with value “0” for the first two layers, contrarily to the considerable high amount existing in the layer 5, for instance. This translates a considerable decrease of water content as depth increases. The mean value tend to increase with depth, although the last layer (the fifth) had a lower value than the previous one.

Figure 43 presents the spatial pattern of the mean annual soil moisture over the IP, consisting in the combination of the soil water content from the five different layers, resulting thus in a general layer with 9, 8 meters depth. Conversely to precipitation, the



pattern of soil moisture does not seem to be related with the altitude. In fact, despite its lack of smooth change between SWC values, the pattern strongly resembles the shape of the several river basins present at the IP: in the center of Portugal, the highest darker colors would be placed over the Lower Tajo Basin; in the south of mainland Spain and spread towards the northeast direction, the shape of this wetter soil resembles the shape of the Guadalquivir basin, while the upper shapes further up

resemble the Tajo basin and upper north the Douro Basin. Close to the Pyrenees but not has demarked as the latter shapes, it would be the influence of the Ebro basin.

It is quite noticeable the very low SWC coming inwards from the northern shore, which is located over a region with high SWC (roughly were Asturias would sit). In fact, the lowest SWC values went lower than 0,015 m over that place, similarly to what occurred nearby the locations with the highest SWC in Portugal mainland. The higher SWC values occurred in Spain, namely over Asturias and Cantabria regions, where SWC reached up to 2,92m. The overall average annual soil water content in the IP during the Reference Period was estimated to be ~1,1m. The values from mean annual SWC variable, were not normally distributed, as shown in Figure 44.

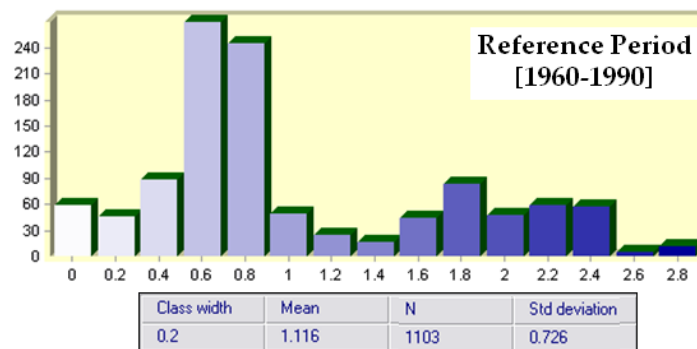


Figure 44 - Histogram and Statistical analysis of Mean Annual Water Soil Content over the Iberian Peninsula during the Reference Period [1960-1990]

Evapotranspiration (ET)

It is a common practice to set negative signal for all vertical upward fluxes as it is the meteorological convention (Bromwich, 2000), however, in order to enable a clear interpretation of results, the positive signal was assigned to upward fluxes in the map showing the mean annual evapotranspiration (ET)(mm/m²)(Figure 45). Hence, having this present, the lowest evaporation values can be found spread in several regions: roughly along the east Portuguese border (as well as in the south of this country) and in southeast region of Spain and in its central region as well. The higher values can be found in the northern regions of both countries.

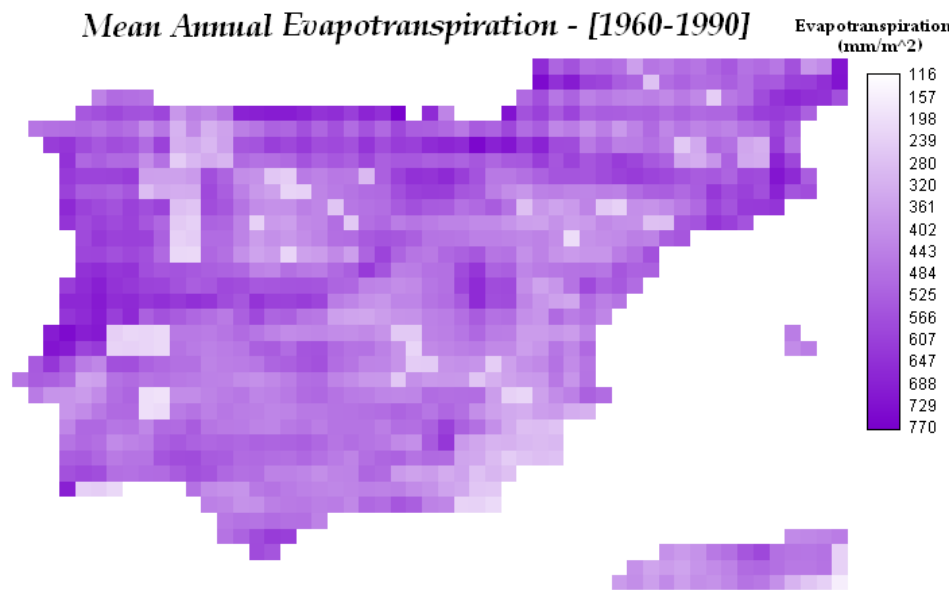


Figure 45 – Mean Annual Evapotranspiration during the Reference Period [1960-1990]

As a first approach, the spatial distribution of ET is moderately different from the rainfall (i.e. precipitation distribution), but it is also correlated with altitude. The mean annual ET distribution pattern slightly recall the spatial pattern of temperature (Figure 38), plus it also demonstrated a high correlation with the land cover type (Figure 26) Moreover, the location and shape of lower ET values, match the same existing in the SWC map (Figure 43).

Evaporation is also affected by the morphology since, the air consequently flows down the lee side, contracting and warming leading to the evaporation of the water droplets, suppressing thus precipitation (Houze, 2012).

ET changes from greater than 200 mm/year at the foot of the mountainous systems to about 700 mm/year at the highest locations, (whereas the precipitation changed from less than 200 mm/year at the foot of the mountain to more than 1.000 mm/year at the tops of the mountain. An important factor affecting this variable is the type and location of vegetation (described in Figure 26), since partly of this variable is composed by mainly transpiration (sourced by plants). For that reason this map should be addressed carefully since it comprises the transpiration rate as well, which is dependent on biologic factors (such as vegetation cover transpiration processes).

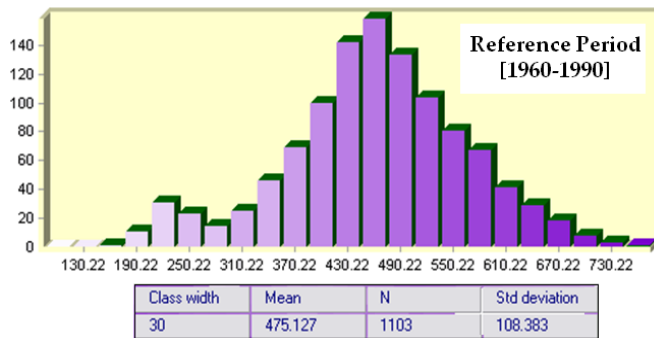


Figure 46 - Histogram and Statistical analysis of Mean Annual Evapotranspiration over the Iberian Peninsula during the Reference Period [1960-1990]

wide (in comparison to precipitation) range of values of mean annual evapotranspiration (between 160 and 761 mm/year) during the annual mean for the period from 1960 to 1990. The overall mean annual evapotranspiration was 474 mm/year (Figure 46).

4.1.3 Radiation balance

Photosynthetically Active Radiation (PAR)

The physical variable photosynthetically active radiation (PAR) over the IP is shown in Figure 48.

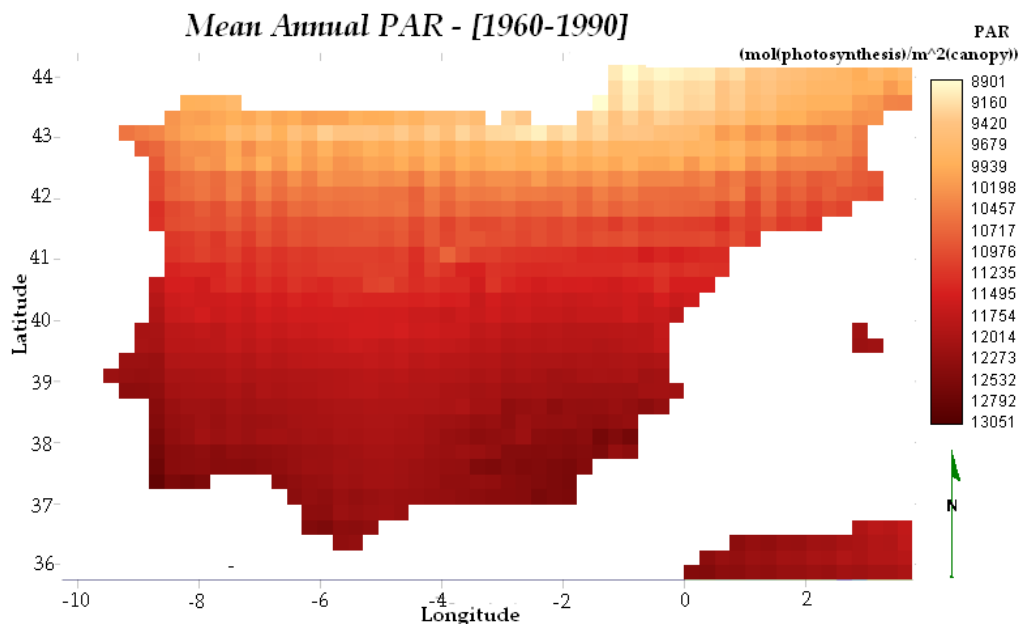


Figure 47 - Mean Annual Photosynthetically Active Radiation map during the Reference Scenario

Hence, the regions with coniferous evergreen trees and temperate broadleaf deciduous trees had the highest values, (with ET > 600 mm/year) whereas the ET in crop regions was relatively low (i.e. ET≈150 mm/year). Finally, the Iberian Peninsula presented a less

This variable can be measured either in radiometric units (W/m^2) - to determine its total energy value, or it can be measured in quantum terms, i.e. in terms of mol produced towards photosynthesis per square meter of canopy per year ($mol/m^2/year$) - in order to calculate the amount of the sunlight specifically available for plant growth during a year (Kania & Giacomelli., 2002).

Henceforth, the Figure 48 presents the spatial distribution of energy ranging between the 400 and 700 nm along the Iberian Peninsula, for the period of 1960-1990, in quantum terms.

The ranges of PAR values are uniformly and smoothly distributed along the latitudes, by increasing as latitudes increases and roughly maintaining constant along the longitudes. The lowest PAR value estimated was approximately $8.901 mol(photosynthesis)/m^2(canopy)/year$ while the highest value was $\sim 12.852 mol(photosynthesis)/m^2(canopy)/year$.

Absorbed Photosynthetically Active Radiation (APAR)

The pattern of the photosynthetically active radiation APAR (Figure 48) greatly differs from later image presented (PAR), since it is dependent on the existence of vegetation, as well as many other inherent factors to it (e.g. such as LAI or other features which characterizes each type of PFT, for instance). As it can be seen from the Figure 48, the pattern shows defined regions with higher or lower APAR values, in opposition to the smoothness characterizing the spatial pattern of the PAR values. As a matter of fact the pattern shown in this map strongly resembles the patterns existing in the ET map (as well in GPP map, which will be shown afterwards).

The north and center of Portugal shown to have high rates o absorbed PAR, since throughout roughly the entire area, APAR was above $5.205 mol(photosynthesis)/m^2(canopy)/year$. In what concerns the largest areas of lower APAR values, these regions match the same regions pointed out in Figure 41, as regions with some of the lowest precipitation rate values.

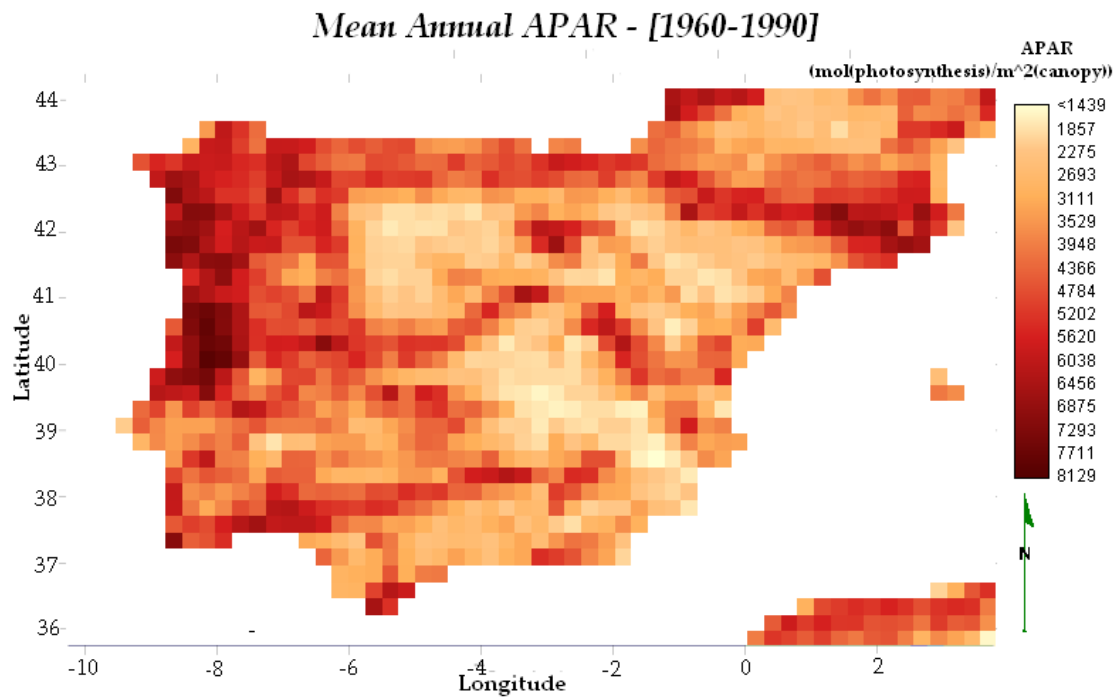


Figure 48 - - Mean Annual Absorbed Photosynthetically Active Radiation during the Reference Period

The values estimated by the model, do not show a normal distribution. The lowest value obtained for the period 1960-1990 was ~1.434 mol (photosynthesis/m²/year) and the highest value was ~7.974 (mol (photosynthesis)/m²(canopy)/year). The overall mean absorbed photosynthetically active radiation throughout the entire Peninsula during the reference period was around 3.979 mol (photosynthesis)/m²(canopy)/year(Figure 49).

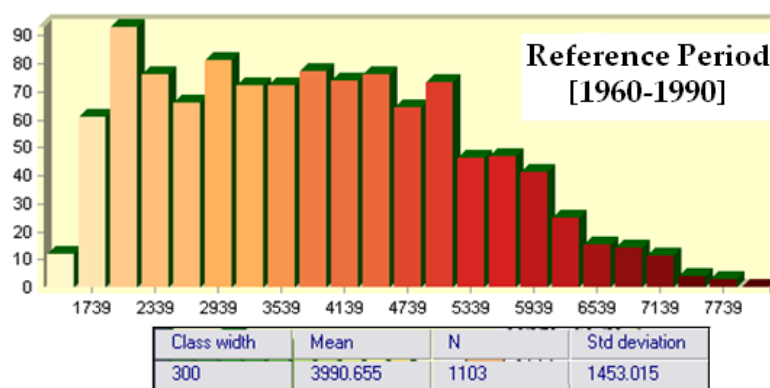


Figure 49 - Histogram and Statistical analysis of Mean Annual APAR over the Iberian Peninsula during the Reference Period [1960-1990]

In some areas – (such as the reddish over the Northern region of Portugal) the rate of absorbed by canopy goes up to 60% of the maximum of PAR incident, while in other areas – such as the blue ones in Spain presents values under the 20% of absorption of total PAR over the place (Figure 50).

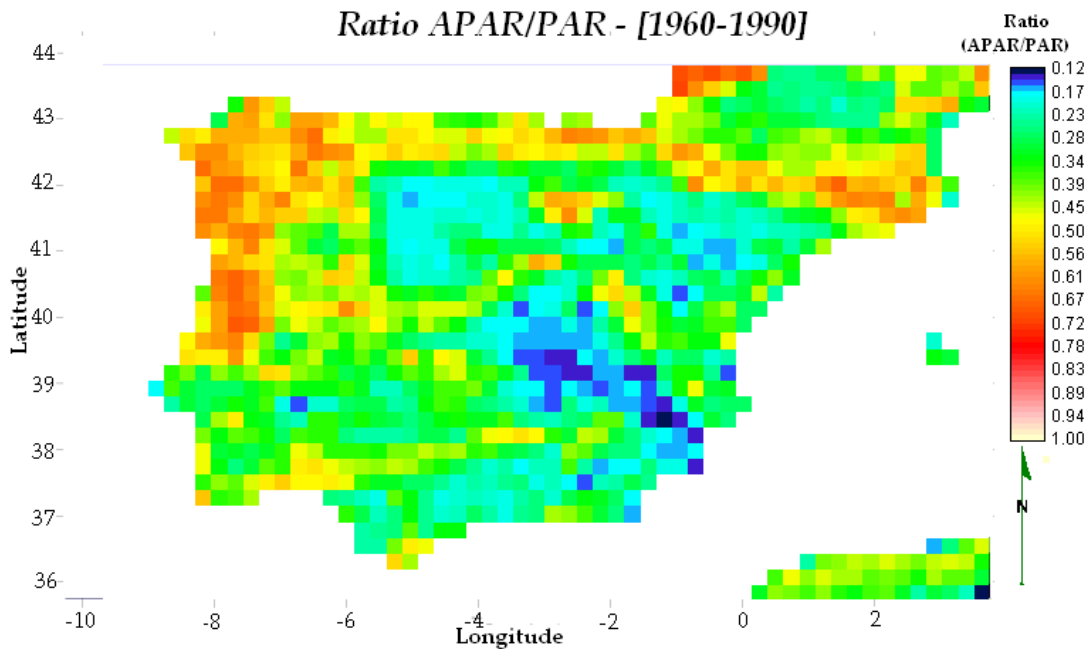


Figure 50 - Ratio APAR/PAR during the Reference Period

4.1.4 Climate variables interactions

In this section, the spatial correlation between each pair of climatic variables, over the Iberian Peninsula during the 1960-1990 period is analyzed. Therefore, Table 37 presents the Pearson's Correlation Coefficients (R) between each possible combination of the previously analyzed variables (where stronger correlations are highlighted in bold). It should be taken into account that this correlation coefficient consists in a simplified manner of measuring the strength of the association between two quantitative and continuous variables – as is the case.

Table 37 - Coefficient correlation between climate variables estimated by JSBACH model for the Reference period

	Temperature (T)	PAR	APAR	Precipitation (P)	Evapotranspiration (ET)
T					
PAR	0,63				
APAR	- 0,10	- 0,11			
P	- 0,40	- 0,53	0,55		
ET	- 0,22	- 0,28	0,54	0,49	
SWC	- 0,12	- 0,13	- 0,12	0,06	0,3

Temperature and other variables correlation

The mean annual land surface temperature extracted across the Iberian Peninsula during the 1960-1990 period showed a positive (+) and significant ($R = 0,63$) interaction with the mean annual PAR. Roughly speaking, there was an increase of temperature by 5 degrees driven by each increase of 1.000 mol (photosynthesis)/m²/year of PAR, as it can be seen from the figure (Figure 51). This positive relationship was expected since increased income of solar radiation boosts an increase of land surface temperature as a result of radiation absorption. Furthermore, it is easily perceived from the comparison between both PAR and T map (Figure 48 and Figure 39), that mean values tend to increase at southern latitudes. The results of the correlation between land surface temperature and the rest of the variables i.e., APAR, precipitation, evapotranspiration and soil moisture presented a negative (-) and less strong relationship.

Another moderate (but less strong) correlation is the interaction between temperature-precipitation, which is shown in Figure 51. The result of this negative relationship also makes sense since these two variables are closely related due to being strongly dependent on each other. Comparing the temperature and precipitation maps (Figure 38 and Figure 40), the highest precipitation occurred roughly in the regions with lower mean annual land surface temperature such as at higher latitudes, and vice-versa for southern regions. The strength of this relationship (i.e., the fact of being moderate $R=0,40$) results from the fact that there are multiple places where higher temperatures do not imply lower precipitations

Nevertheless, temperature and precipitation spatial patterns should be interpreted considering the strong co variability that exists (Kevin *et al.*, 2005). In order to rain the temperature needs to rise so that water evaporates generating clouds formation (Buishand & Brandsa, 1999). However, as it can be seen in the south Portugal and the region of Andalusia, higher temperature did not lead to higher precipitation. The explanation for this fact could rely on the fact that higher temperatures lead to higher saturate vapor levels causing a higher capacity of the warm air to contain higher moisture amount than cold air

The negative (even though small) relationship existing between temperature and evapotranspiration, is a reasonable result, since higher rates of evapotranspiration promote cloud formation causing less radiation penetration into the atmosphere resulting in lower land surface temperatures. Similarly to others, this interaction is no linear since there are many other factors affecting both variables such as the precipitation and heat latent flux, for instance.

PAR, APAR and other variables correlation

The second stronger relationship occurred between PAR and precipitation ($R=-0,53$), being negatively correlatd. As it can be interpreted from the comparison of Figure 41 and 48, higher rates of income PAR over certain areas, driven lower precipitation rates there.

The PAR and APAR relationship is positive (+)– since the latter consist in the amount from PAR which was actually absorbed by the plant, hence higher incomes of PAR will enhance photosynthetic processes resulting in greater amounts of radiation being absorbed during that process. These two variables are moderately correlated ($R=0,55$), since the spatial distribution of APAR is constrained mostly by vegetation cover – thus, APAR spatial distribution do not follow the same patter as PAR.

The positive (+) relationship existing between both precipitation and evapotranspiration and the APAR variable, is expected, since APAR denotes the existence of vegetation. Hence, more precipitation will enhance photosynthesis, triggering the increase of photosynthetically active radiation being absorbed by plants

leading to a. higher the rate of photosynthetically processes and ultimately a higher transpiration rate by plants as a consequence of that process.

Evapotranspiration and other variables correlation

Finally, the comparison of the spatial patterns of mean annual precipitation and mean annual evapotranspiration (Figure 40 and Figure 45) shows that areas where precipitation rate is higher evapotranspiration rate tend to be higher: the higher the water supply throughout rainfall processes, the bigger the amount of water possible to be evapotranspired resulting in a positive and moderate relationship ($R=0,49$). As it can be seen from the Figure 51, this interaction is stronger when precipitation rate ranges between ~250 and ~800 mm/m²/year.

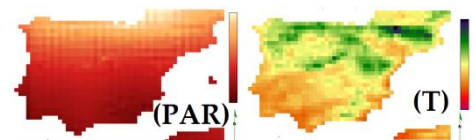
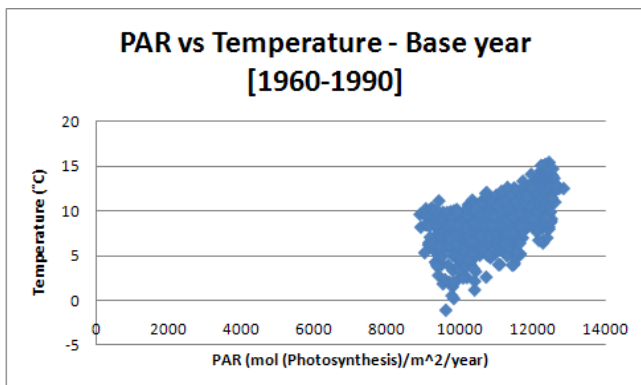
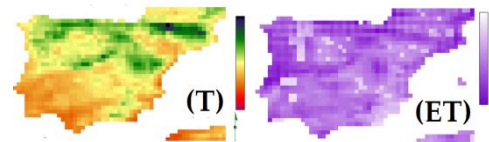
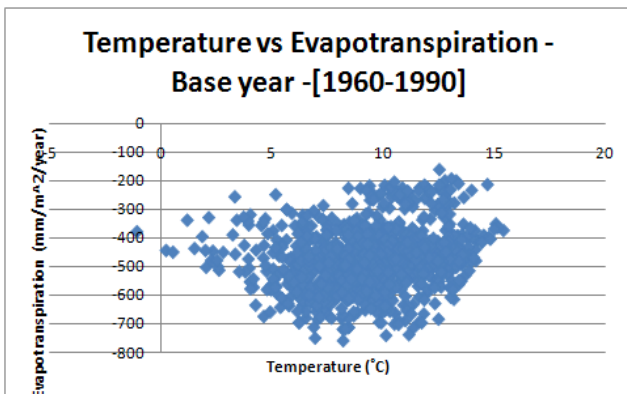
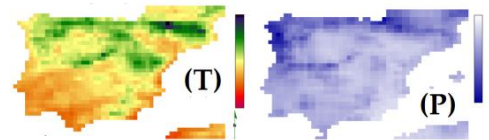
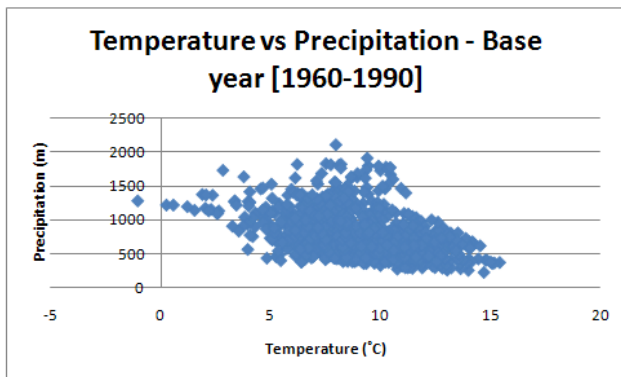
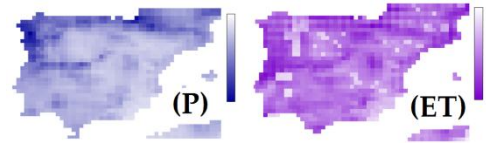
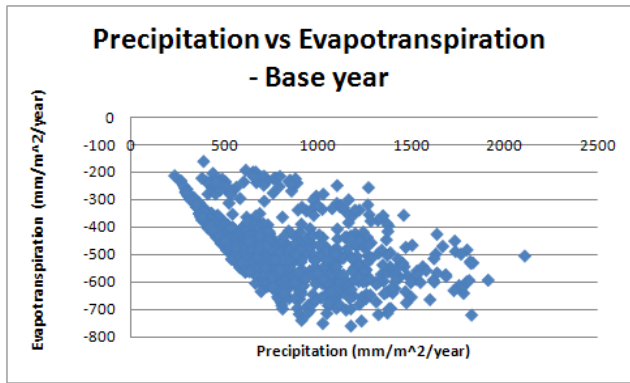


Figure 51 - Correlation between climate variables during the Reference Period

4.2 Carbon balance analysis – Reference Period

The analysis of the carbon balance during the reference period aims to assess the spatial distribution of carbon uptake and productivity of vegetation across the Iberian Peninsula. The variables taken into account are the gross primary production, the net primary production and biomass spatial distribution during the 1960-1990 period. Both productivity and biomass are segregated by herbaceous and forest biomass types. This set of results will serve as reference to the assessment of change in vegetation response to the climate changes projected in future scenarios. The spatial correlation of carbon variables and climate variables are also assessed for the reference period.

4.2.1 Gross Primary Production (GPP)

Corroborating Polley *et al.* (2011), the gross primary productivity (GPP) map consists in a key component of the carbon (C) cycle, enabling the understanding of spatial patterns in C fluxes. Consequently, the map shown below (Figure 52), depicts the areas with higher carbon production (and therefore higher carbon uptakes). The highest rates of GPP are located in the north of Portugal (more specifically the region above the

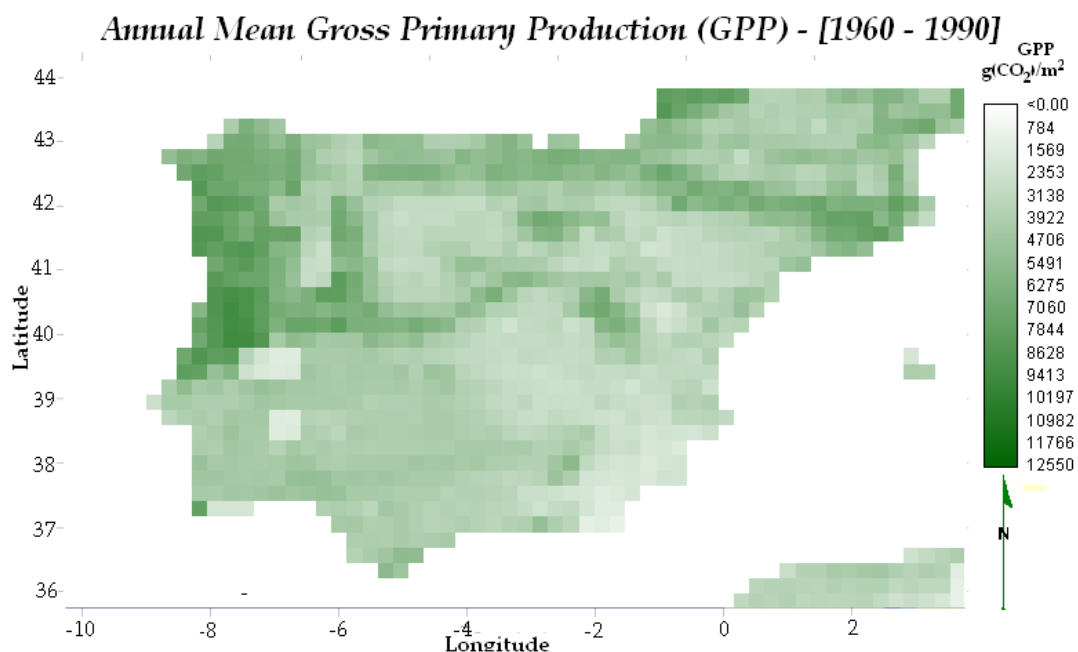


Figure 52 – Mean Annual Gross Primary Production (GPP) during the Reference Period [1960-1990]

Tejo river); in Galicia, along the north shore of Spain (including the Pyrenees) and along the Central Mountain System. This pattern resembles thus the temperate zone,

which matches the areas of higher precipitation and APAR rates. The mean annual GPP during the Reference period ranged between ~1.141 and ~9.373 g(CO₂)/m², having an overall mean of ~4.422 g(CO₂)/m².

Environmental Controls on GPP

In order to assess how is GPP controlled by the previously regarded climate factors, the spatial correlations between GPP and temperature, precipitation, evapotranspiration, soil moisture, PAR and APAR were evaluated by calculating the correlation coefficients (*R*) over the Iberian Peninsula (Table 38), enabling hence to take conclusions regarding the strength of relationship of their spatial patterns.

Table 38- Correlation coefficients for GPP and climate variables during the Reference Period [1960-1990]

	Temperature	Water Balance			Radiation	
		P	ET	SWC	PAR	APAR
GPP	-0.25	0.65	0.76	0.12	-0.36	0.81

Among all the factors, precipitation, evapotranspiration and APAR were more strongly correlated with GPP during the 1060-1990 period. On the other hand, the impact of land surface temperature (T) and PAR had a weak and negative (-) correlation with the GPP, meaning that these environmental variables were the least significant among all. The negative relationship means that, spatially, the GPP increased in regions where temperature and PAR mean values lowered.

In what concerns soil moisture or soil water content (SWC), the resulting relationship was considerably lower than expected (since soil water content plays such an important role on productivity). The relationship is positive (+) and one of the most probable reasons for the evident low relationship, is the fact that this variable is not regarding merely the amount of water which is actually available to the roots. Moreover, the relationship between GPP and soil water content vary: trees are able to store water and nutrients and to tap water from deeper soil horizons (Davis *et al.*, 1998; Oliveira *et al.*, 2005). For the same reason earlier explained, precipitation is not equal to water available to vegetation (Liu *et al.*, 2011) and hence that would explain the less strong correlation between the pair GPP vs precipitation than the pairs GPP vs ET and

GPP vs APAR - even though water is known to be a limiting factor in this environment and that it plays a great impact on the interannual variability. Notwithstanding this variable was shown to be linearly correlated with GPP (Figure 53) and its coefficient of determination R^2 shows in fact that this linear regression fits moderately to the relationship between GPP and P.

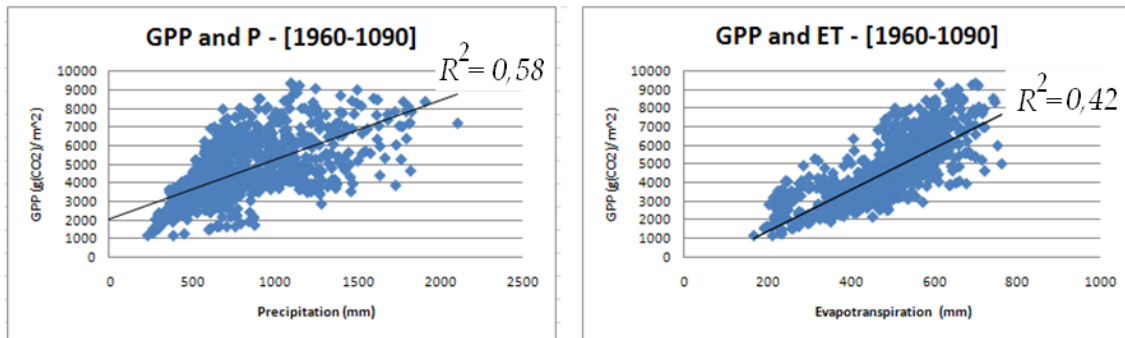


Figure 53 - Relationship between GPP and Precipitation and GPP and Evapotranspiration during the Reference Period [1960-1990]

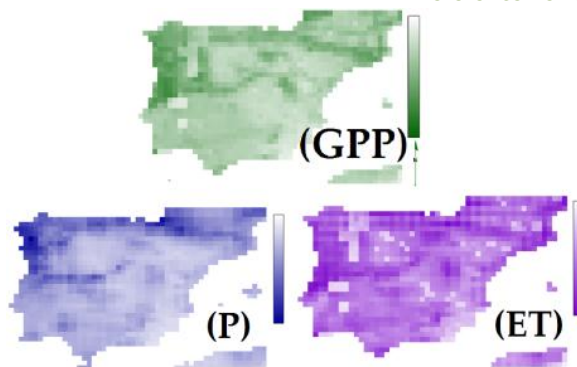


Figure 54 - Comparison of spatial distribution between GPP, P and ET during [1960-1990]

The strong relationship between GPP and ET is explained by the fact that plant transpiration and photosynthesis are strongly coupled as well as due the fact that stomata are the pathway for absorbing CO_2 and releasing water vapor by transpiration. Hence this strong and positive correlation is in

accordance with the expected (i.e. high GPP corresponding with high ET, and vice versa (Lu & Zhuang, 2010; Running & Zhao, 2005). The correlation between these two variables will hence be used as another source of information to depict the water use efficiency, i.e. the ratio of GPP to ET, in a forthcoming chapter. Looking closely to the pattern of ET and P maps (Figure 40 and Figure 45) and comparing them with the GPP map (Figure 52), in fact the ET pattern is noticeable far more resembling (namely the existing areas of considerable lower values from both variables)(Figure 54).

Moreover, as it can be also seen, the southeastern quadrant of the P map, lacks some patterns that are present in ET and P maps. Similarly to the precipitation variable, the

evapotranspiration also present a linear correlation with GPP (Figure 53), although it is less well explained by the linear functions (since the coefficient of determination is smaller, i.e. $R^2 = 0,42$). The coefficients correlations between annual GPP, precipitation and temperature are in accordance with Jung *et al.* (2011) (since these correlations are positive and higher than 0,4).

The strongest relationship (i.e. correlation between GPP and APAR) is expected, since GPP describes the total light energy that has been converted to plant biomass (Anderson *et al.*, 2009). Furthermore, GPP and APAR can be combined as

$$GPP = \varepsilon \times APAR \quad (\text{Equation 8})$$

(where ε stands for conversion efficiency which is dependent upon vegetation type (Anderson *et al.*, 2009.)). Since GPP is proportional to the APAR (Monteith, 1972; Xiao *et al.*, 2005) these two variables showed - not surprisingly - to be strongly and positively correlated ($R=0,81$) (Figure 55) and present the greatest R^2 among all variables relationship. The evident strong relationship among these two variables has also driven the interest on studying forwardly, the so-called light-use efficiency (LUE), which is derived from empirical observations of GPP and APAR (Monteith, 1972).

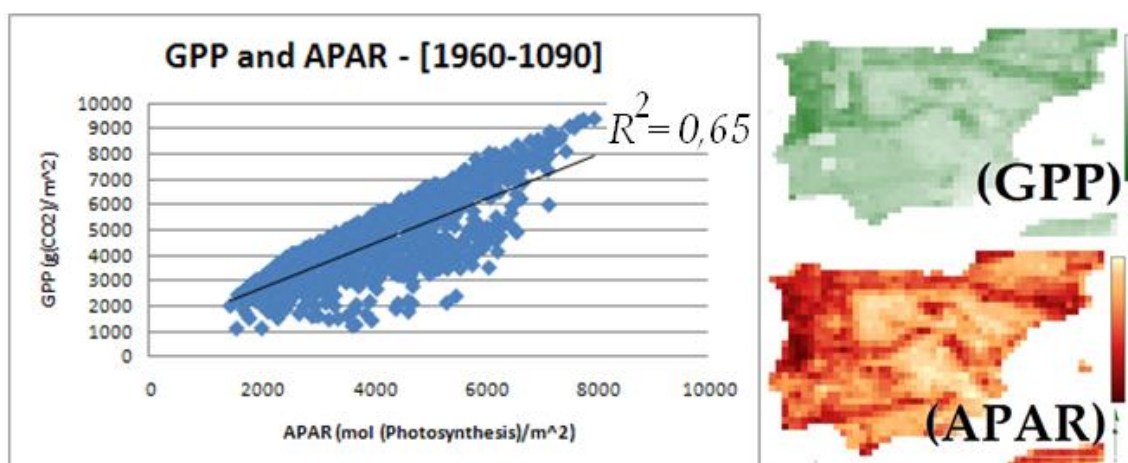


Figure 55 –The relationship between GPP and APAR at the IP during the 1960-1990 period.

Water-Use Efficiency (WUE) during the Reference Period

The water-use efficiency across the IP, during the [1960-1990] period is found in Figure 56 and it is expressed in terms of grams of CO₂ uptake for each mm of water from evapotranspiration flux. By visual interpretation of Figure 26, the plant functional type is an important factor to determine the spatial pattern. For the northern region of Portugal (which is a C3 grass dominated system – followed by coniferous evergreen trees) the WUE showed higher values – greater than 11 g(CO₂)/mm(H₂O). The region located in the south and southwestern part of the IP (bordered by the Baetic Mountain Range and the Central Mountain System), showed evenly WUE values ranging between 8 and 9 g(CO₂)/mm(H₂O) consisting thus in a significant difference between this C4 grass and C3 crop dominated site and the site firstly addressed. These WUE differences are because of PFT-oriented parameterizations .

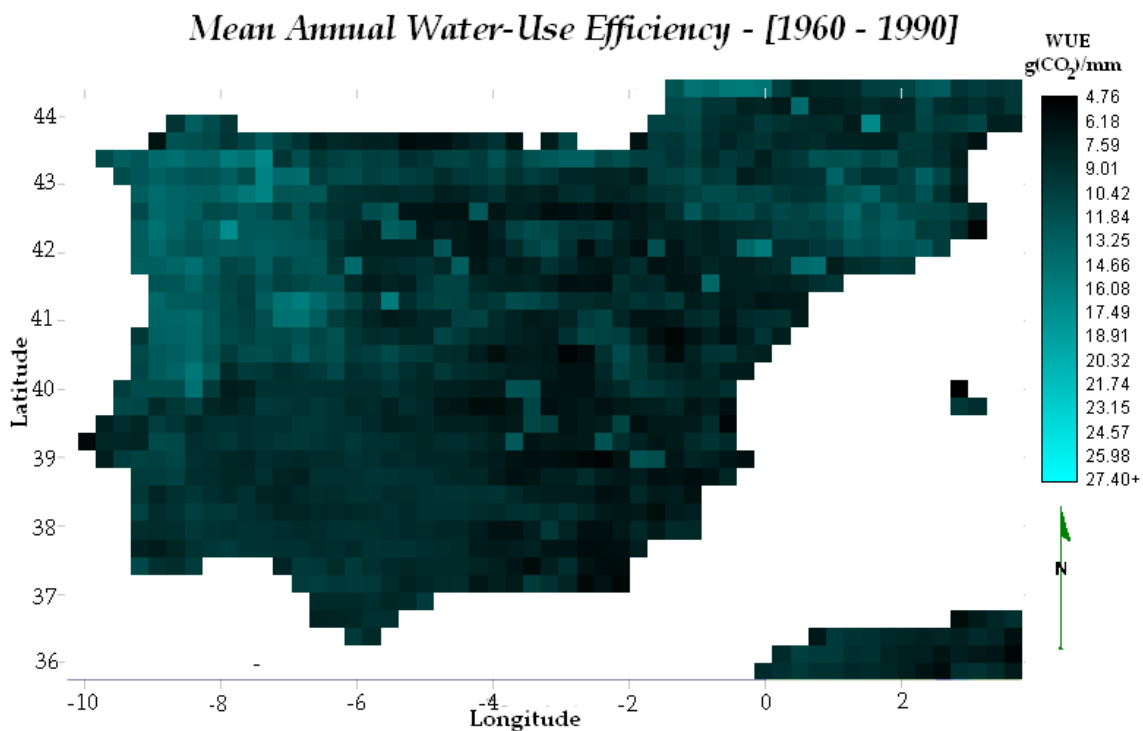


Figure 56 - Mean Annual WUE during reference period

The right half of the IP presented mainly lower WUE values (consisting mainly in a C3 crop dominated site), but there are also areas of great WUE (greater than 14 g(CO₂)/mm(H₂O)). The overall mean value of WUE over the area of study was around 9,2 g(CO₂)/mm(H₂O).

Hence, these results mean that even though that mean annual precipitation and ET are similar over these areas, the higher WUE existing over some region, enable them to uptake more carbon during the growing seasons than regions with lower WUE values. Another important result that can be taken from here is that once again the ecosystem difference in atmospheric CO₂ concentration as well as CO₂ and water fluxes, have important management implications including primary productivity, C sequestration and rangeland health.

Light-Use Efficiency (LUE) during the Reference Period

There were significant differences in LUE occurred during the 1960-1990 period over the territory due to differences in soil water content (as it resembles this map, when it comes to pattern distribution) (Figure 43). It also corroborates the findings of Polley *et al.* (2011), who have depicted the existence of a great relationship among these LUE and soil water content.

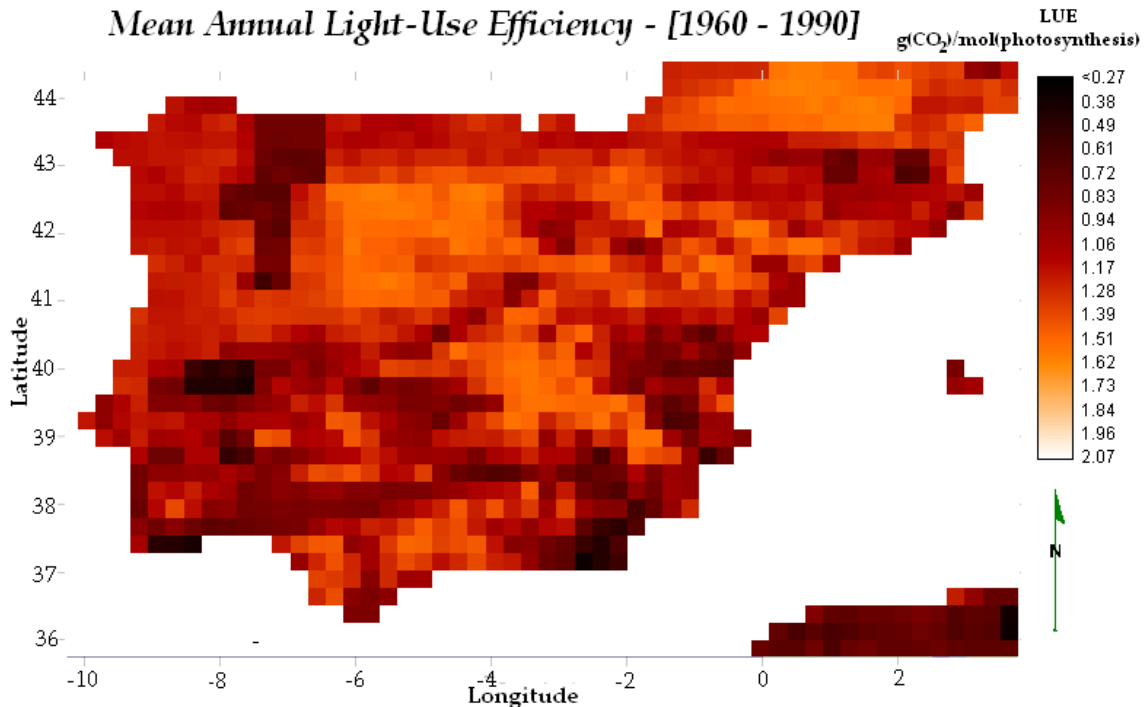


Figure 57 - Mean Annual LUE during the Reference Period

For the reference period, the values of LUE varied between 0.34 and 1.62 $\text{g}(\text{CO}_2)/\text{mol}(\text{photosynthesis})$ and the overall mean LUE was $\sim 1.16 \text{g}(\text{CO}_2)/\text{mol}(\text{photosynthesis})$ (Figure 57).

4.2.2 Net Primary Production (NPP)

The results regarding the Net Primary Production (NPP) are segregated by forest and herbaceous biomass (Figure 59 and Figure 60) – and NPP is expressed similarly to GPP. The spatial patterns of both biomass types are considerably different. The NPP from forest biomass varies more abruptly and the higher values are located along the Temperate zone of the IP. The herbaceous biomass has shown to be more evenly distributed across the territory, showing less evidently the pattern of bioclimatic zones, although it discriminates better locations with lower annual SWC and evapotranspiration regions (which could mean that grasses are more responsive to water scarcity than forest biomass).

The highest mean annual NPP for forest biomass were found in the northwest part of the Iberian Peninsula (accounting with $\sim 2.699 \text{g}(\text{CO}_2)/\text{m}^2(\text{grid box})$ whereas in some areas namely over the Southern Plateau showed no existence of NPP. The overall mean annual NPP over the IP during the reference period was approximately $450 \text{g}(\text{CO}_2)/\text{m}^2(\text{grid box})$.

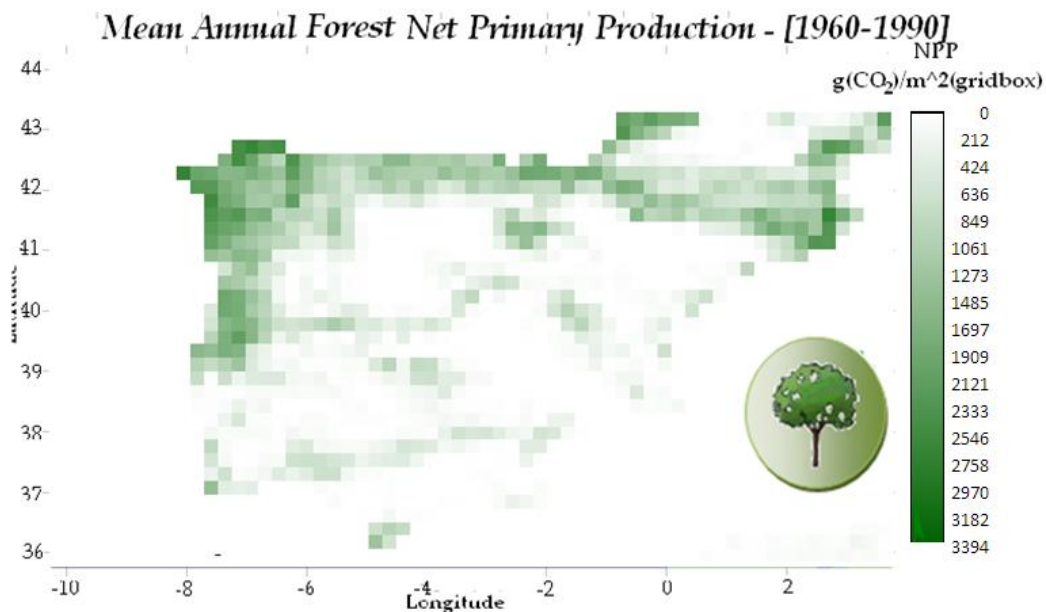


Figure 58- Mean Annual Forest Net Primary Production (NPP) during the Reference Period [1960-1990]

The mean annual NPP underlying the herbaceous biomass during the same period, reached higher values (up to 2.890 g(CO₂)/m²(grid box) and having an overall mean of ~1.531 g(CO₂)/m²(grid box).

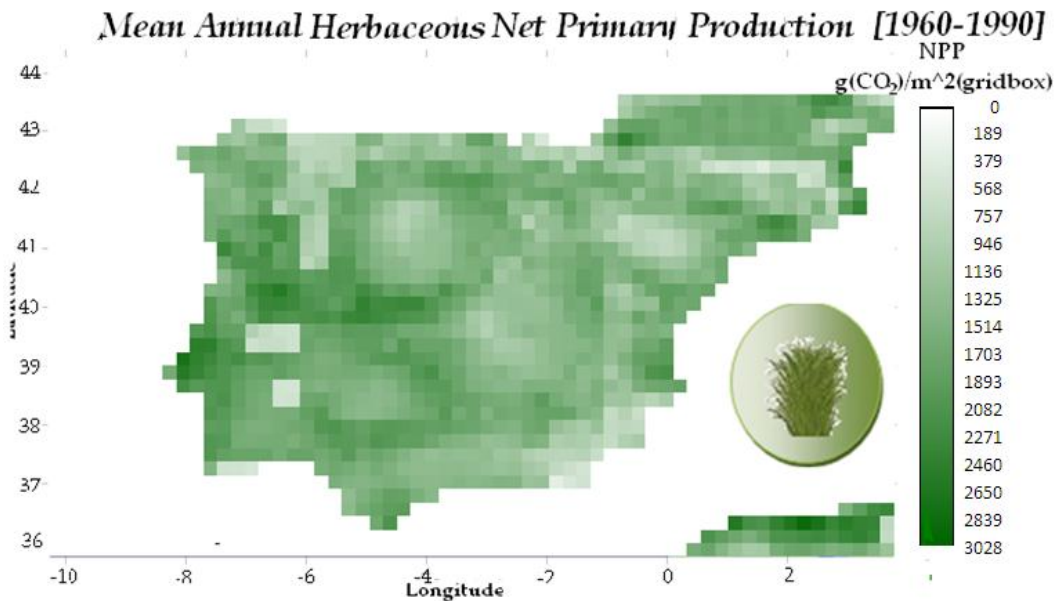


Figure 59 - Mean Annual Herbaceous Net Primary Production (NPP) during the Reference Period [1960-1990]

The spatial distribution of NPP did not show the same pattern as ET across this large elevation range.. These different spatial patterns might be due several processes, such as the autotrophic respiration and the intersectional water loss and evaporation from soil (Sun *et al.*, 2004).

NPP and GPP correlation

The mean annual NPP of all biomass present at the IP (i.e. both herbaceous and forest biomass) was, as expected, strongly and positively correlated with the mean annual GPP, having a great coefficient correlation, $R = 0,88$. From the picture below (Figure 60), (along with the coefficient of determination R^2) denotes that the linear association between NPP and GPP is very strong since ($R^2 = 78\%$).

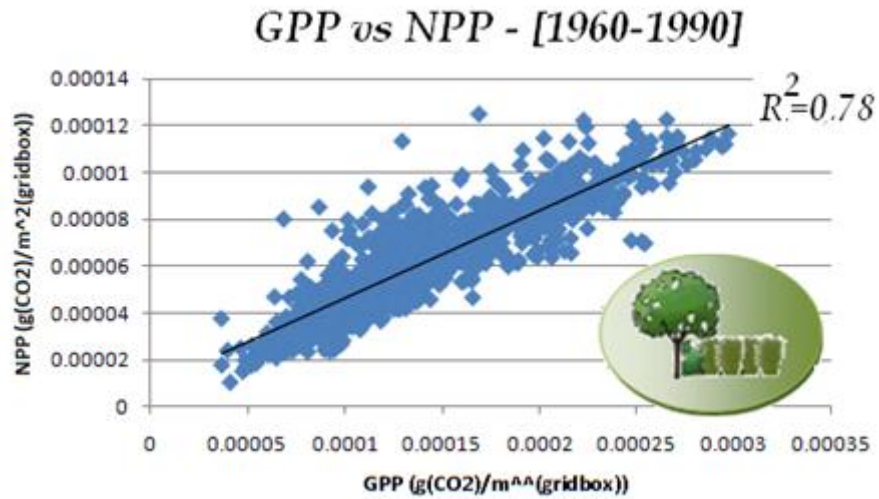


Figure 60 - Regression analysis between mean annual GPP and NPP (from all biomass) over the Iberian Peninsula during the Reference Period

4.2.3 Biomass

The following figures, present the biomass estimations over the IP, segregated in “Forest” biomass (Figure 61) and “Herbaceous” biomass (Figure 62). These maps do not present biomass in absolute terms, but in “areal density” of biomass, since it expresses the amount of mass of carbon per unit area.

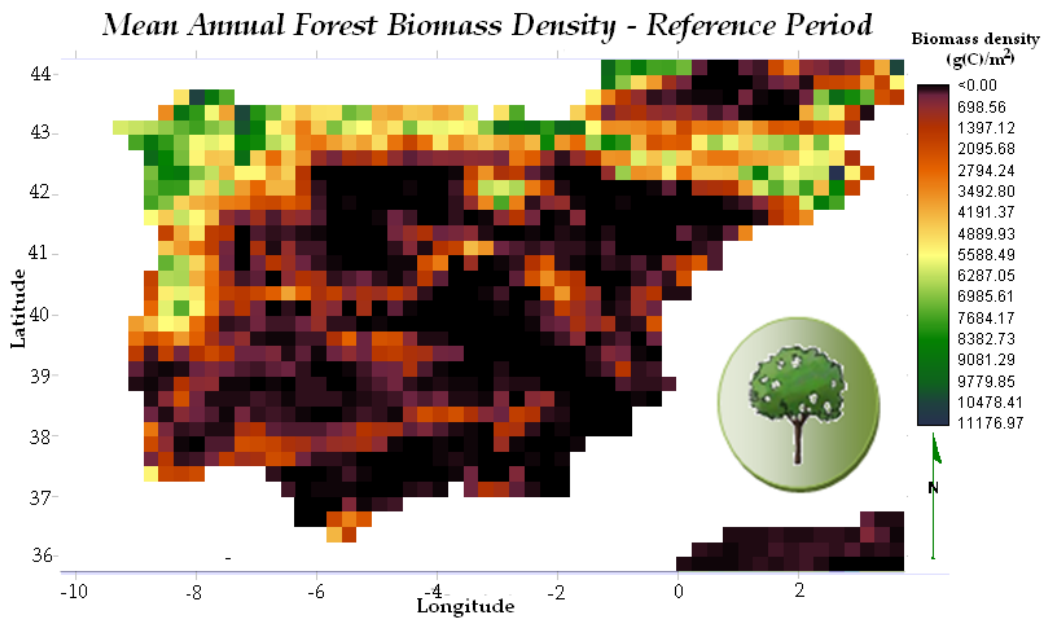


Figure 61 - Mean Annual Forest Biomass Density during Reference Period [1960-1990]

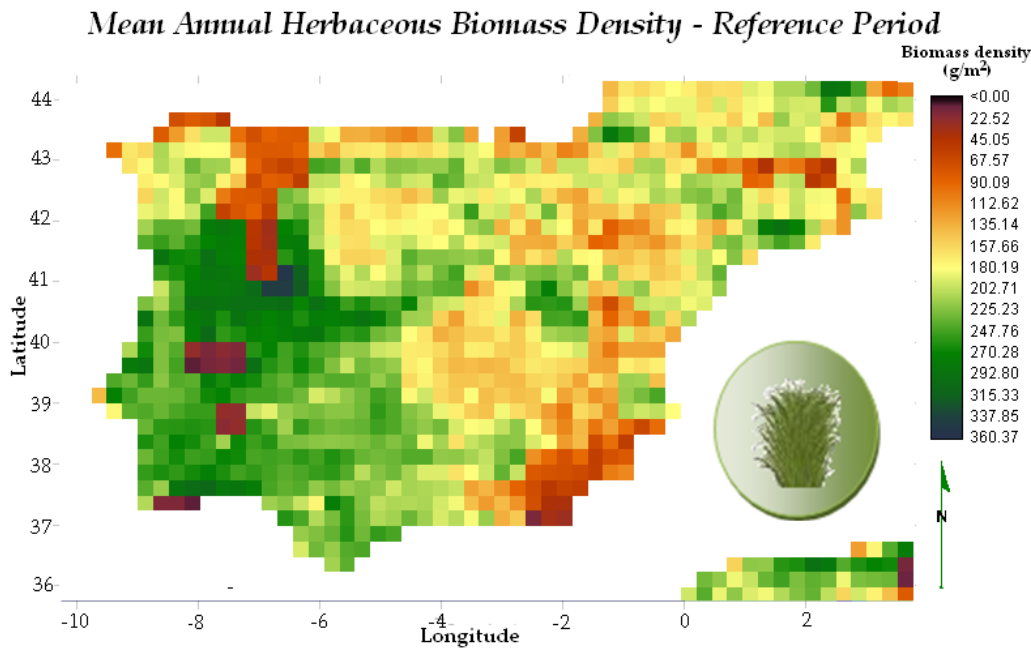


Figure 62 - Mean Annual Herbaceous Biomass Density during Reference Period [1960-1990]

The regions with higher densities of forest biomass (i.e. amounting above $5.500 \text{ g(C)}/\text{m}^2$) are located in the northern IP; in the northern regions of Portugal and at the highest altitudes from the Central Mountain Range, matching the Temperate bioclimatic zone (Figure 17), where mean annual precipitation values were above $1.000 \text{ mm}/\text{year}$. The Mediterranean regions present hence lower densities of forest biomass density. The locations with lower density values are shown to be over the Central Plateau and also over the river basins of Tejo, Douro, Ebro and Guadalquivir rivers (see Figure 43 for comparison), with values below $600 \text{ g(C)}/\text{m}^2$. Although some variables have a similar pattern (such as mean annual APAR), the mean annual precipitation spatial pattern (Figure 40) has the most similar pattern to forest biomass areal density.

Multiple cells (537), corresponding nearly to 50% of the Iberian territory, have shown values densities of forest biomass to be zero $\text{g(C)}/\text{m}^2$ – which denotes an absence of forest biomass. The maximum value of annual mean forest biomass during the reference period was $\sim 9.744 \text{ g(C)}/\text{m}^2$ and the overall mean was $\sim 1.503 \text{ g(C)}/\text{m}^2$ (Figure 63).

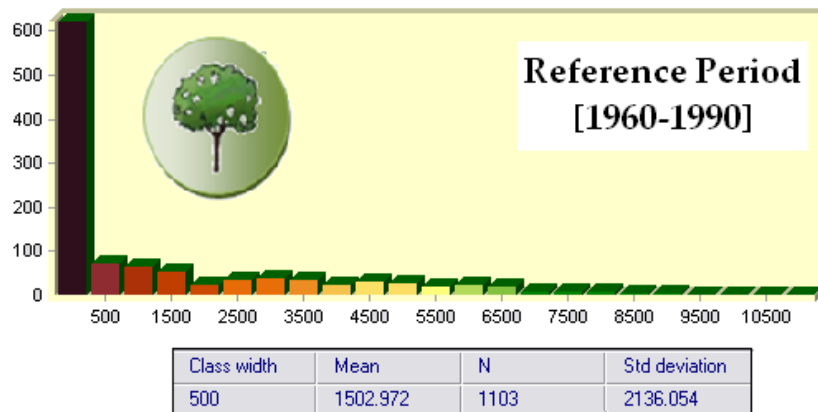


Figure 63 - Statistical analysis of Mean Annual Forest Biomass during [1960-1990]

The spatial pattern of herbaceous aerial densities did not show to be correlated with bioclimatic zones as forest biomass did. Both northern part and southeastern quadrant of the IP shown to have low values of herbaceous biomass density, and the lowest values were located in the territory of Portugal. The location of low densities of herbaceous biomass strongly resembles the map of the spatial pattern of mean annual soil moisture and evapotranspiration (Figure 43 and Figure 45), which could indicate that these type of biomass is strongly affected by water scarcity. The highest values accounted with $\sim 353 \text{ g (C)/m}^2$ while the lowest densities of herbaceous biomass were $\sim 10 \text{ g (C)/m}^2$. The overall mean annual herbaceous biomass density during the reference period was $\sim 190 \text{ g(C)/m}^2$ (Figure 64).

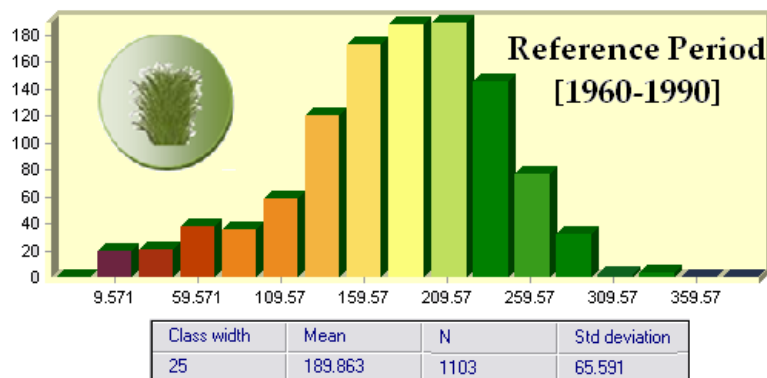


Figure 64 - Statistical analysis of Mean Annual Herbaceous Biomass during [1960-1990]

In terms of absolute biomass, i.e. total amount of biomass estimated for the 1960-1990 period in terms of mass, as fairly expected, the “Forest” biomass presented a much larger contribute (up to 78%) than “Herbaceous” biomass, which accounted with 22% of the total biomass estimated over the Iberian Peninsula during the Reference period. Figure 65 shows a chart pie summarizing the overall results from “Forest” biomass and “Herbaceous” biomass. Despite the large land areas with agriculture, the higher enrichment in fiber of trees results in a much greater mass.

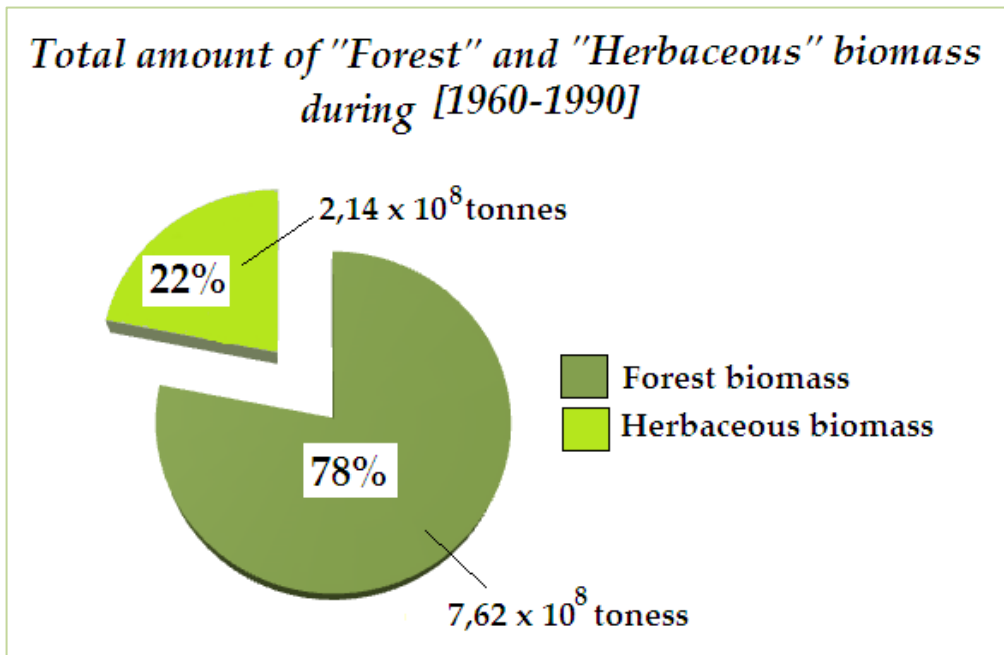


Figure 65 - Percentage and absolute values of Forest and Herbaceous Biomass during the Reference Period [1960-1990]

The mass of biomass discriminated for each PFT presented in IP is shown in Figure 66. The greater biomass contributing to the overall scheme, are from Coniferous evergreen trees (which accounted in 1960-1990 period with $\sim 4,24 \times 10^8$ tonnes) and broadleaf deciduous trees (accounting with $3,02 \times 10^8$ tonnes). In fact, together these two PFT accounted with 95% of the overall “Forest” biomass type. Within the same biomass type, both temperate broadleaf evergreen trees and rain green shrubs accounted each one of them with 2% of the overall biomass from forests. In last place comes the deciduous shrubs, which contribute was almost negligible.

Biomass estimations for each PFT during 1960-1990

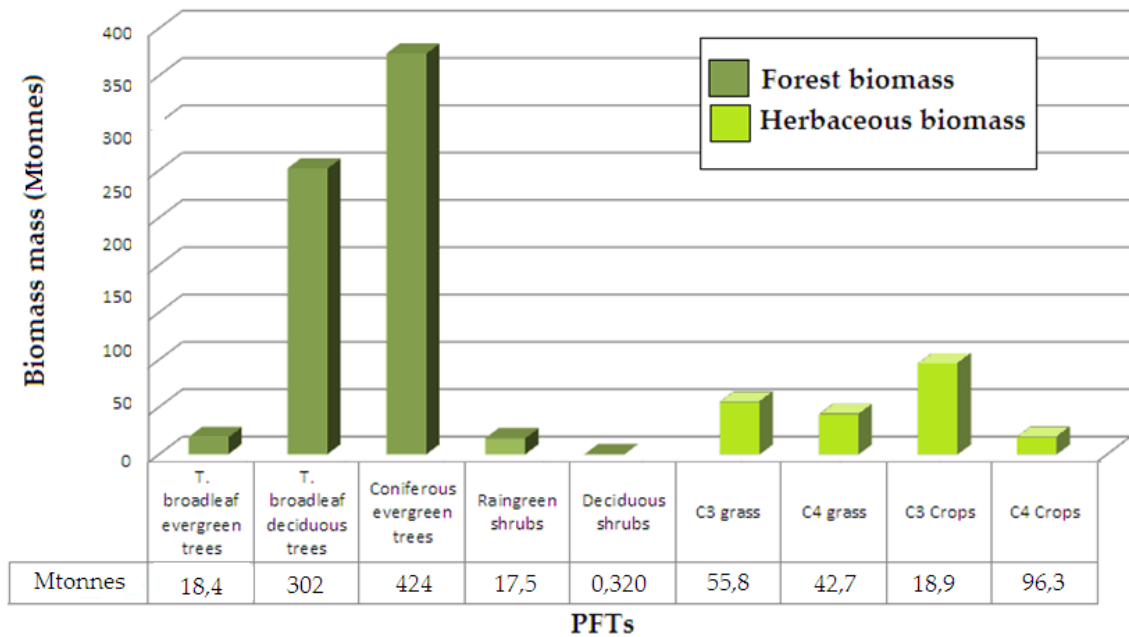


Figure 66 - Estimations of Biomass assigned to each PFT, during the Reference Period [1960-1990]

In what concerns the “Herbaceous” biomass, the contribution of each PFT to the overall amount of biomass was more even: 45, 26, 20 and 9% for C3 crops, C3 grasses, C4 grasses and C4 crops, respectively.

Environmental Controls on Forest and Herbaceous Biomass

Similarly to the section assessing the environmental controls on GPP, this section assesses how climate variables are correlated (in spatial patterns) to both sets of biomass (herbaceous and forest biomass) through the correlation coefficient R (as well as the graphic visualization of each variable against the other). These comparisons enable to understand the strength of the relationships between the two sets of biomass and climate variables existing back in 1960-1990 period – and their differences. Table 39 shows the summary of the coefficient correlation each climate variable-biomass type pair (the strongest correlations are highlighted in bold).

Table 39 - Correlation coefficients between Biomass and Climate Variables during the Reference Period

	Water Balance			Radiation		
	T	P	ET	SWC	PAR	APAR
FOREST BIOMASS	-0,436	0,692	-0,457	0,184	-0,536	0,702
HERBACEOUS BIOMASS	0,175	0,097	-0,059	-0,049	-0,024	0,028

Forest biomass shown to be moderately and negatively correlated with land surface temperature distribution (Table 39) which is explained by the fact that the locations with higher amounts of forest biomass which are located in the temperate zone – where mean annual temperatures are lower (Figure 38). These areas of lower temperatures (i.e. $T < 9^{\circ}\text{C}$) are wider and more disperse than the locations with high densities of forest biomass. Herbaceous biomass shown to have a weak (and positive) relationship with land surface temperature.

The comparison of the correlation coefficients between precipitation-forest biomass and precipitation-herbaceous biomass (Table 39), confirms the assumption earlier made in 4.2.3, i.e. forest biomass is likely to be more strongly spatially affected by precipitation than herbaceous biomass. Forest biomass shows hence a negative and moderate correlation with mean annual evapotranspiration (while herbaceous biomass relationship was negligible).

Hence, summarizing and rating all the significant correlations (i.e. which upward the value of 0,4), it comes that forest biomass mostly depends on APAR, followed closely by precipitation and then PAR, temperature and finally evapotranspiration, having a negative relationship with the three later. On the other hand, herbaceous biomass showed to be no meaningfully correlated with the climate variables (Table 39).

Figures 68, 69, 70, 71 and 72 provide a graphical analyzes of the correlation between the climate and environmental variables and the biomass variables. Henceforth, The correlation of mean annual land surface temperature and the amount of biomass modeled for the reference period, showed that both biomass types are likely to be able to harvest carbon, (i.e. to generate biomass) under a optimal range of annual land surface temperature between 10 and 15°C degrees – (the extremes of this range in fact nearly match the total and maximum mean temperature verified during 1960-1990).

However for the herbaceous biomass, the amount of biomass does not seem to vary considerable during this range of temperatures. On the other hand, the forest biomass seems to have higher rates of biomass generation between ~ 6 and 9 °C degrees, and after the 14 °C biomass rates tend to decrease (Figure 67). For the biomass-precipitation interaction, it is noticeable a difference of the response between the herbaceous and forest biomass to the mean annual precipitation during the reference period. The interaction of the herbaceous biomass resembles a logarithmic behavior – the biomass increase rapidly until the ~ 600 mm/year and after this, the maximum values tend to stabilize (Figure 69). Forest biomass increases less rapidly for small mean annual precipitation values, (i.e. until ~ 500 mm/year) after which it starts to increase reaching the maximum values between the ~ 1.000 and ~ 4.000 mm/year of precipitation (Figure 69).

In what concerns the response of biomass to the mean annual evapotranspiration, the herbaceous biomass behaves smoothly having a biomass rate ranging between ~ 9 and ~ 28 mol(C)/m² within the approximate range of evapotranspiration 700 and 500 mm/year, after which tends to decrease (Figure 70). Conversely, the forest biomass showed a general decrease tendency of biomass values as evaporation rates decrease. Furthermore, for values higher than 600 mm/year, the biomass values are greater than 100 mol(C)/m², however, after this evaporation values, the range of biomass becomes wider (reaching the lowest values estimated for biomass). The maximum values of biomass for forest biomass were estimated to occur for evaporation rates ranging between 600 and 500 mm/m² (Figure 70).

Finally, for soil water content, both herbaceous and forest biomass, showed to be poorly related to this variable, since it the values ranged around the same values. Forest biomass showed though three peaks of lower biomass values for the ranges $\sim 0,25-0,500$, $\sim 1,00-1,30$ and $1,60-1,75$ m of soil water content (for the first soil layer).

Finally, the response of herbaceous to mean annual PAR seems was barely noticeable, conversely to forest biomass which seems to have slight increase of biomass production for lower values of PAR (i.e., the highest biomass values were found to occur within the range of ~ 8.900 and 11.000 mol(C)/m² of PAR). For APAR variable

(and similarly to what occurred with the response to the annual precipitation rate variable), the herbaceous biomass response to APAR resemble a logarithmic behavior while the forest transpired an tendency of increasing biomass values with increasing APAR rates resembling a exponential behavior. Forest biomass shows increasingly higher values after the ~ 4.000 mol (photosynthesis)/ m^2 . After the ~ 6500 mol (photosynthesis)/ m^2 biomass values are higher than 200 mol(C)/ m^2 (Figure 72).

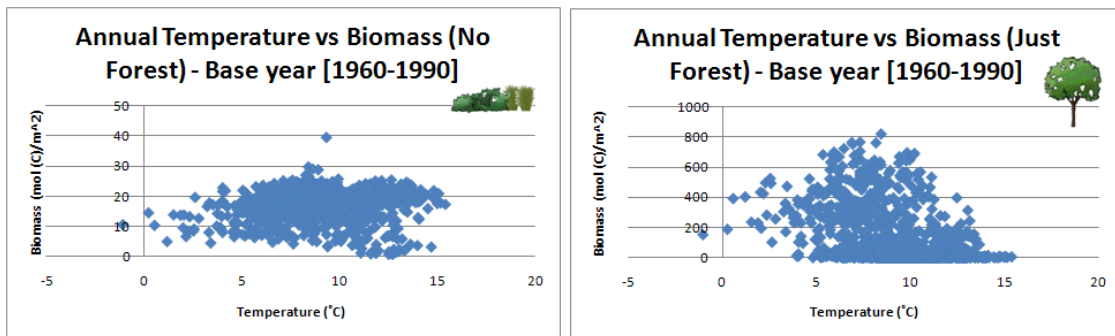


Figure 67 - Correlation between mean annual temperature and herbaceous/forest biomass during the Reference Period [1960-1990]

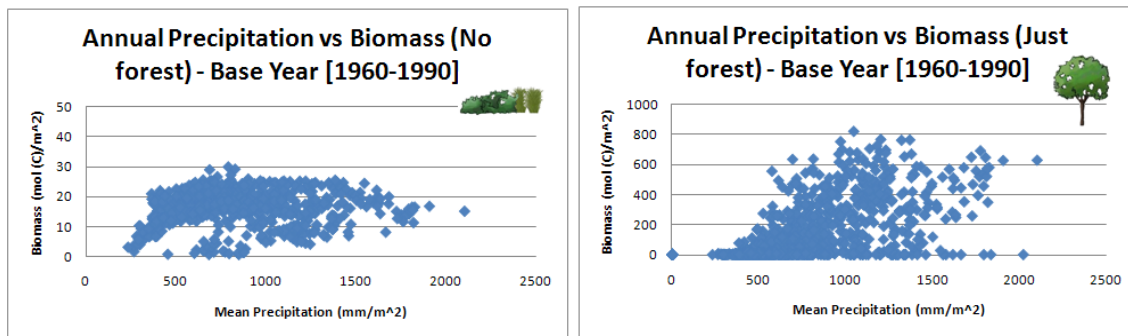


Figure 68 - Correlation between mean annual precipitation and herbaceous/forest biomass during the Reference Period [1960-1990]

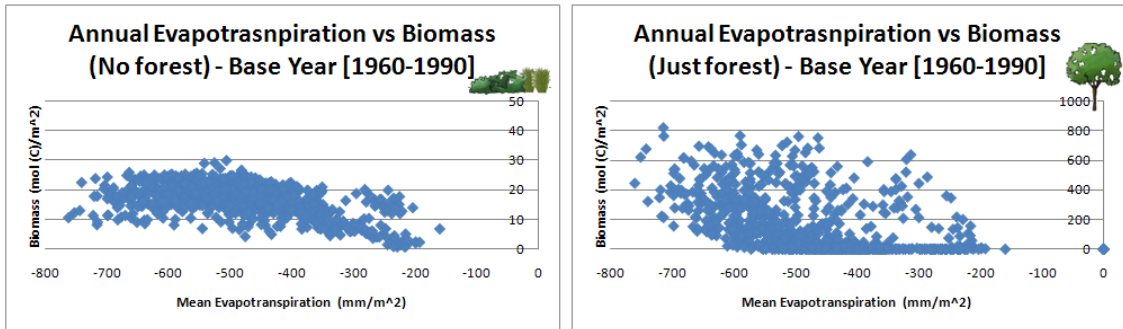


Figure 69 - Correlation between mean annual ET and herbaceous/forest biomass during the Reference Period [1960-1990]

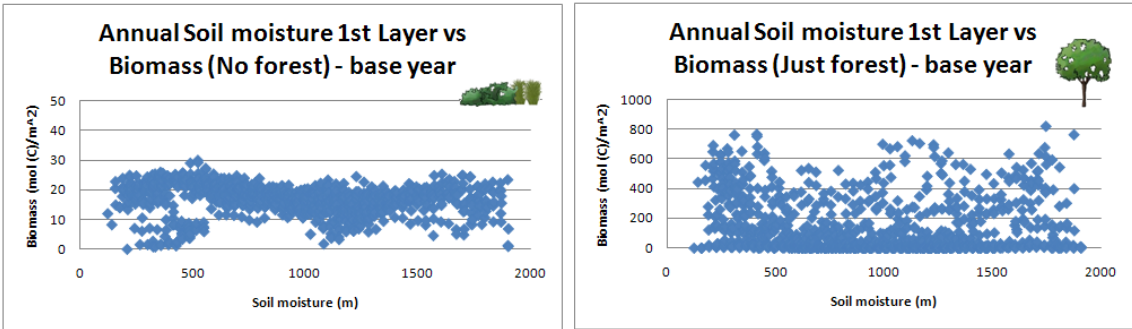


Figure 70 - Correlation between mean annual SWC and herbaceous/forest biomass during the Reference Period [1960-1990]

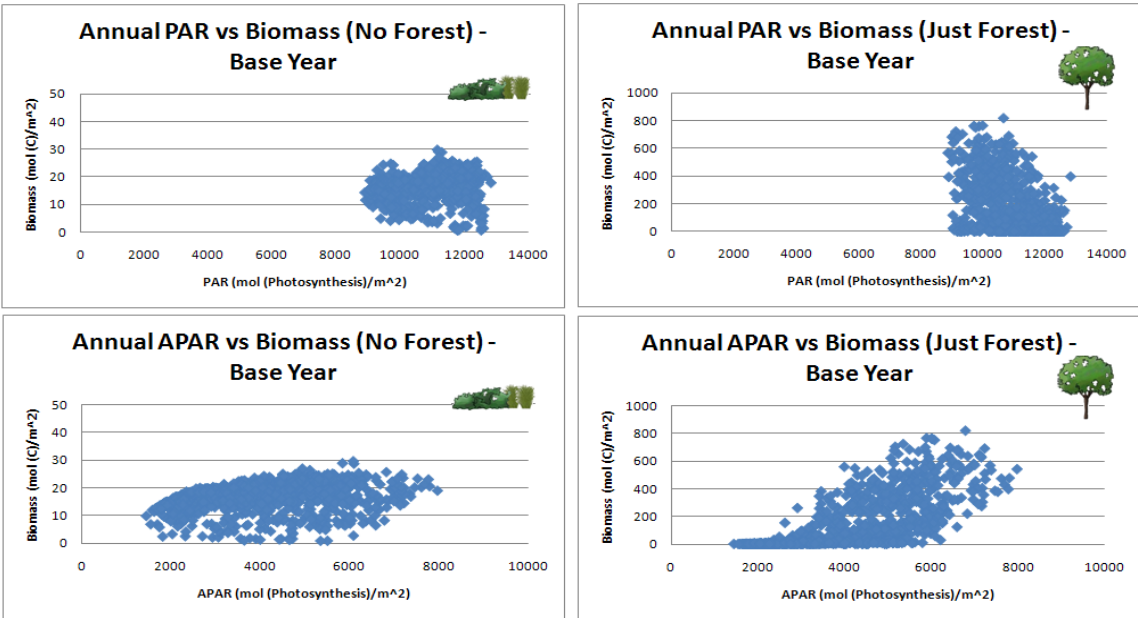


Figure 71 - Correlation between radiation variables and herbaceous/forest biomass during the Reference Period [1960-1990]

4.3 Climate Variables Change Analysis – Futures Scenarios

The climate variable change analysis performed in this section assesses the changes occurred for each climate (and environmental) variable earlier addressed, projected for the future time periods, in comparison with the reference period. Hence, (similarly as in the climate variables analysis for the reference period), the spatial pattern of each projected climate variable is analyzed along with its magnitude of change. In some cases (whenever meaningful) its absolute difference from reference period is also analyzed. These analyzes enable to assess the locations subject of greater changes which will ultimately enable the understanding of how these changes in climate will likely affect future vegetation productivity and biomass (which will be addressed in the carbon balance analysis for future scenarios).

It should be noticed though that the variables that are model data inputs refer to two future scenarios, namely 2060-2090 and 2070-2100. However, the climate variables that are model data outputs (e.g. soil moisture, evapotranspiration, APAR, productivity and biomass variables) are regarded in four future scenarios, namely 2060-2090 and 2070-2100 with CO₂ levels assumed to be constant (C1 and C2 scenarios, respectively), and future scenarios 2060-2090 and 2070-2100 with CO₂ levels considered to rise (E1 and E2 scenarios, respectively). After each climate variable change analysis, a comparison of other studies (which regarded climate variables for the same IPCC scenario, i.e. A1B scenario) was made at an Iberian and global scale, allowing understanding how different or accurate JSBACH results are in comparison with literature results.

4.3.1 Land surface temperature (T)

The mean annual land surface temperature variable is projected to maintain the same general geographic pattern existing in the 1960-1990 period, as it can be compared with Figure 38, for both future time aggregations scenarios 2060-2090 and 2070-2100 (which will be hereafter addressed as C1 and C2 scenario whenever the CO₂ level is not relevant as is the case of every variable consisting in model data input). Although, the main difference between these two scenarios and the reference period, consists in the fact that the mean land surface temperature values have increased throughout the

whole region under study (Figure 72) (the map regarding scenario C2 is not shown, since it was visually similar to scenario C1). The average annual land surface temperature during the reference period for the Iberian Peninsula, is estimated to increase by 3,5°C for the scenario C1 and by 3,8°C for the scenario C2.

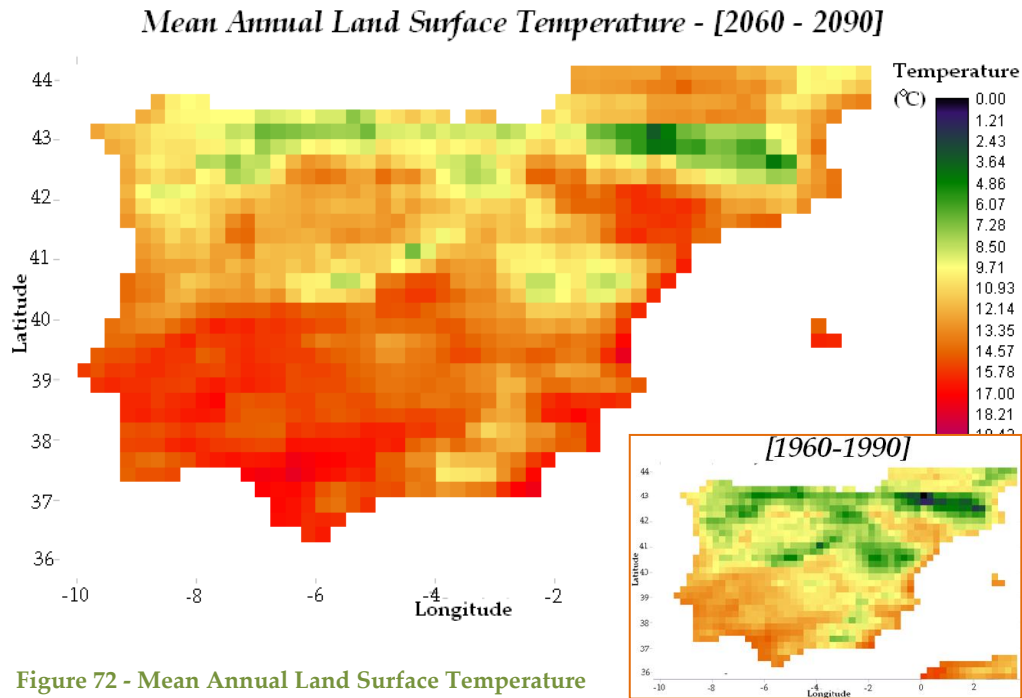


Figure 72 - Mean Annual Land Surface Temperature projected for scenario C1 [2060-2090]

Due to the increase of mean values, the histograms are dislocated to the right (comparatively to the histogram of the reference period).. The maximum temperature estimated was approximately 4°C higher than the maximum estimated during the 1960-1990 period, while the lowest temperatures estimated were 4,5 and 4,9 higher than the minimum temperature recorded during the reference period, for scenarios C1 and C2, respectively (Figure 73). These last results do not agree with Jerez *et al.* (2012), which stated that maximum temperatures would be more affected than minima.

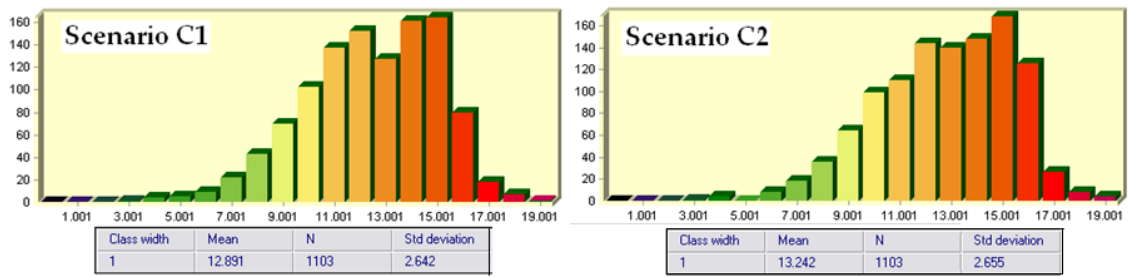


Figure 73 – Histograms and Statistical analysis of Land Surface Temperature for Scenarios C1 and C2

As shown in Figure 74, under the scenario C1, the overall increase of annual mean land surface temperature over the IP, is higher than the global temperatures predicted within the A1B scenario for global surface warming (which ranges between 2,3 and 2,8°C) (IPCC, 2007). Furthermore, Figure 74 enables as well to understand that the highest changes in temperature are expected to occur in the center and Northeast region of the Iberian Peninsula, while the smaller changes are associated to regions closer to the shore.

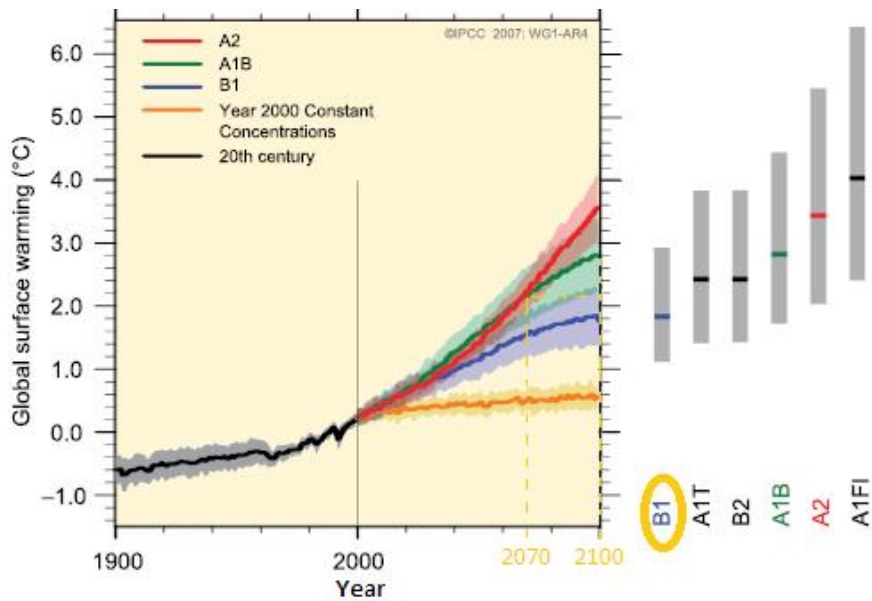


Figure 74 – Multi-Model Averages and Assessed Ranges for Surface Warming (Source: Adapted from IPCC, 2007)

The Pyrenees and the highest points of the Iberian Peninsula exhibit considerable strong mean annual land surface temperature changes. Some pixels of the image showed a percentage change upper than 100% in Scenario C1, when comparing to the reference period. The image below (Figure 75) shows the difference in percentages

between future scenarios against the reference period. Moreover, the results show that in fact, the temperature rise occurs in all parts of the region under study.

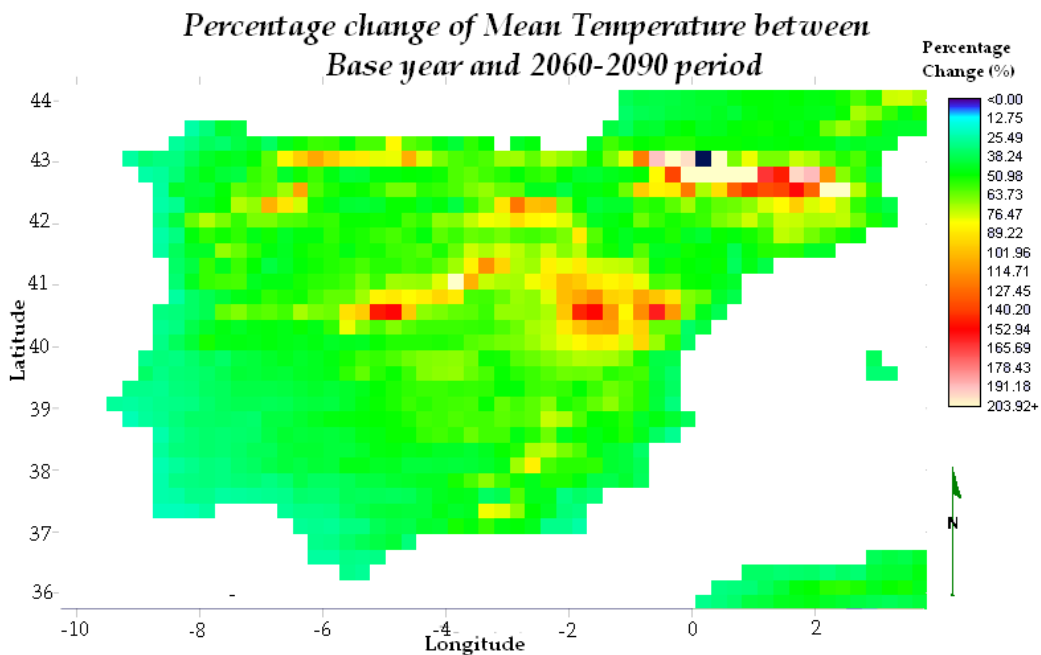


Figure 75 - Percentage Change of Mean Annual Land Surface Temperature between Reference Period [1960-1990] and Scenario C1 [2060-2090]

Both maps regarding the percentage changes of differences between the future period scenarios [2060-2090] and [2070-2100] and the reference period ranges from 16 up to nearly 300%. The strongest changes occurred mainly over the mountain ranges existing in mainland Spain (being spatially wider in Iberian Mountain Range) as well as in the Pyrenees. Warming temperatures are thus, likely to become more pronounced in the mid continental areas at higher altitudes; whereas the lower rises are located in the North and South Portuguese shore (ranging roughly between 17 and 25%).

Figure 76 presents the pattern of change between both future scenarios, showing that the areas with greater percentage changes are wider over the mountain ranges. The maximum change occurring between 2060-2090 and 2070-2100 periods is around 11 %.

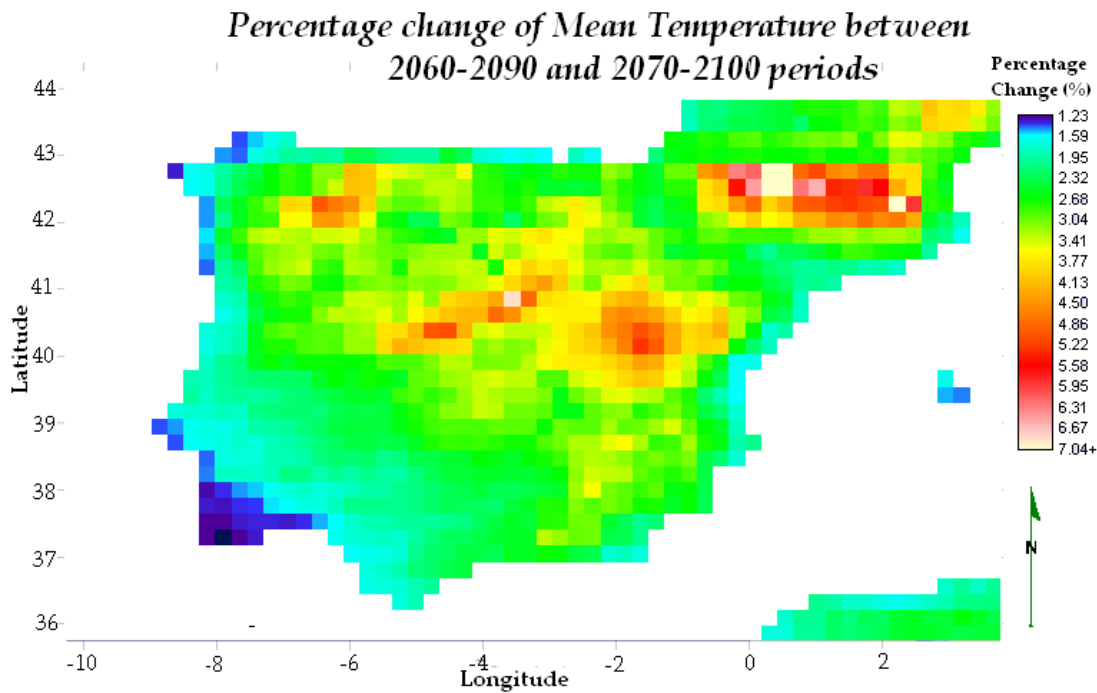


Figure 76 - Percentage Change of Mean Annual Land Surface Temperature between Scenario C1 [2060-2090] and Scenario C2 [2070-2100]

The overall mean of percentage change of land surface temperature for the scenario C1 in comparison to the reference period was estimated to be around 38% (and 41% for scenario C2-Reference period comparison). In coastal areas the percentage change has a percentage changes ranging between 17 and 25% approximately, while the inner land areas have stronger changes, between 40 and 55%. Although the most accentuated changes occurred at regions with higher altitudes such as the highest points in the cordilleras (with temperature changes going further than 170% percentage change of temperature), and basically along the Pyrenees. In fact there were verified the highest temperature changes of the Iberian Peninsula (some grid cells presented values around 200%). The percentage change of land surface between the scenario 2 and 1 has also verified positive changes although considerably lower than the first comparison, with values ranging between ~1% and 11%. The mean change between the two futures scenarios was ~3% and the pattern of percentage change was similar to the previously addressed.

4.3.2 Water balance

Precipitation (P)

Similarly to the previous variable, the mean annual precipitation during both future C1 and C2 scenarios across the Iberian Peninsula keeps the same pattern as in reference period (Figure 77). Despite the same pattern, annual precipitation is projected to decrease. Overall, across the Iberian Peninsula, the mean rate was estimated to drop by ~195 and ~206 mm by 2060-2090 and 2070-2100, respectively.

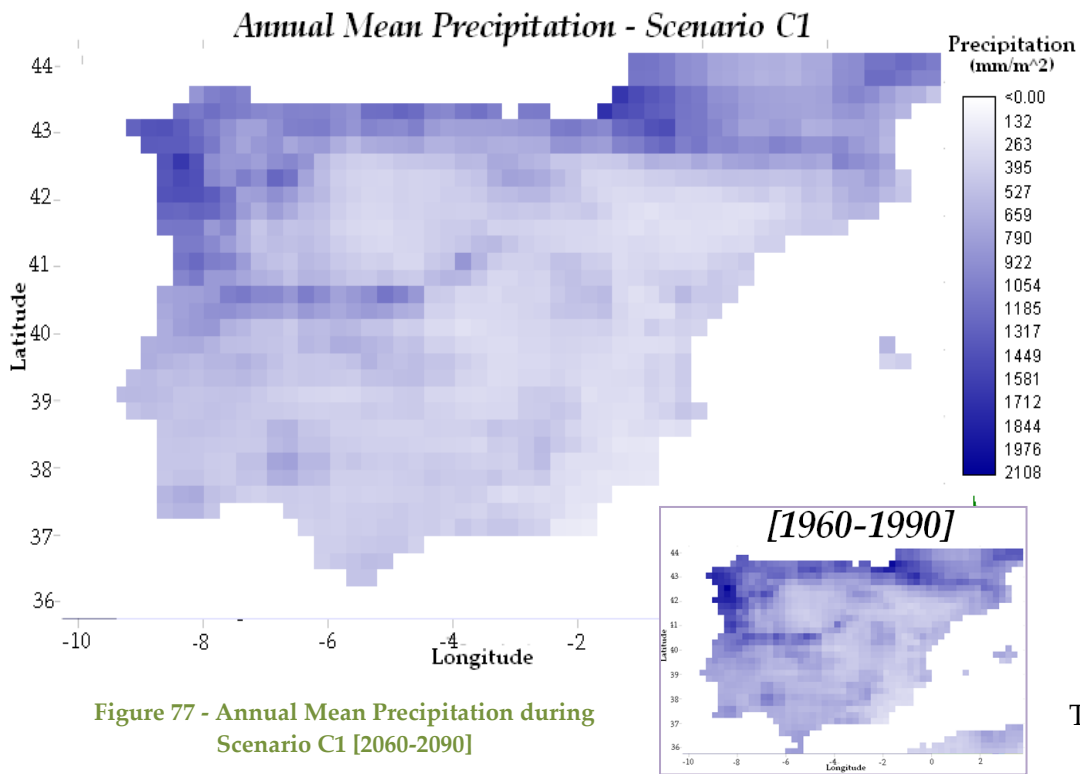


Figure 77 - Annual Mean Precipitation during Scenario C1 [2060-2090]

The

histograms are dislocated to the left – since the mean precipitation rates decreases in 2060-2090 and 2070-2100 periods (Figure 78), but still they maintain a shape resembling a lognormal distribution.

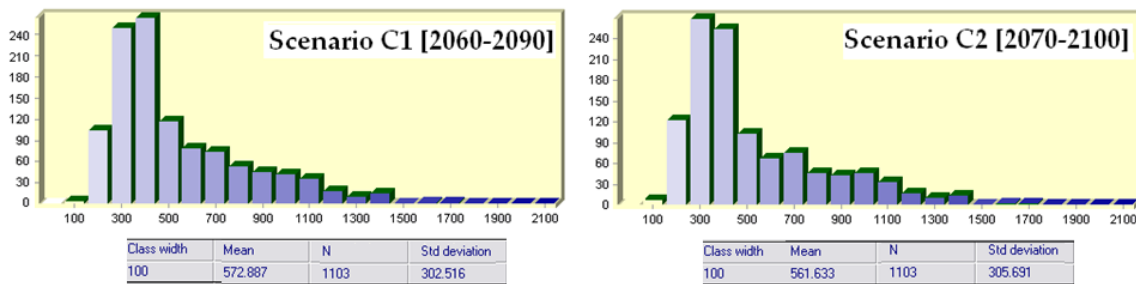


Figure 78 - Histograms and Statistical analysis of Precipitation for Scenarios C1 and C2

The following images (Figure 79), presents the percentage change existing between the reference period, and each of the future scenarios. The percentages are represented as positive values, and they translate into the amount of the precipitation rate that has decreased from the reference period. For instance, if the value of a grid cell existing in the reference period decreased its precipitation rate from 1.000 mm/m²/year to 200 mm/year, which would imply a decrease of precipitation rate (within that grid cell) of 80%.

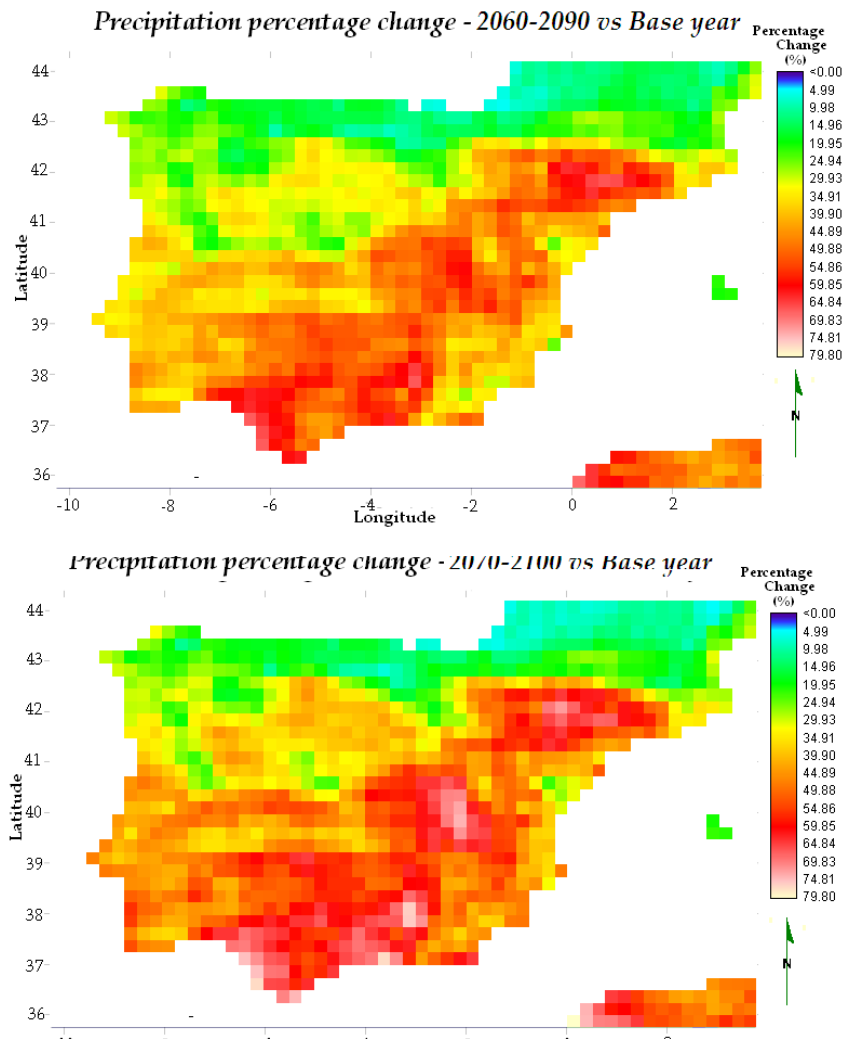


Figure 79 - Percentage Change of Mean Annual Precipitation between Reference Period [1960-1990] and Scenarios C1 (upper image) and Scenario C2 (bottom). In this case, positive change refers to decrease in precipitation. Redish areas present higher decreases in precipitation and greenish areas present lower decreases in precipitation.

The entire southern and most of eastern quadrant of Spain, were the regions with the biggest decreases in precipitation rate from reference period to scenarios C1 and C2. In fact, in the latter period, the decrease in precipitation went up to 70% of the precipitation value existing during the reference period.

The northern regions – matching with the Iberian Temperate Climate region consisted thus in the region with the least changes – ranging between ~5 to ~30%. The low range of change at these places may be due to the fact, that those areas had in fact the highest precipitation rates in the Iberian Peninsula during the reference period - and thus, in terms of absolute values, a considerable decrease will not result in terms of percentage, in a significant change when compared to a place with lower precipitation rates (Figure 79). In what concerns the summary statistics (Figure 80), the overall change results across the entire Peninsula are that the mean annual precipitation is expected to decrease in roughly 37% of its value from the 1960-1990 period, while this value decreases for up to nearly 40% by 2070-2100. Furthermore, the entire area will have a decrease of at least 5% of the average annual precipitation existing during the reference period.

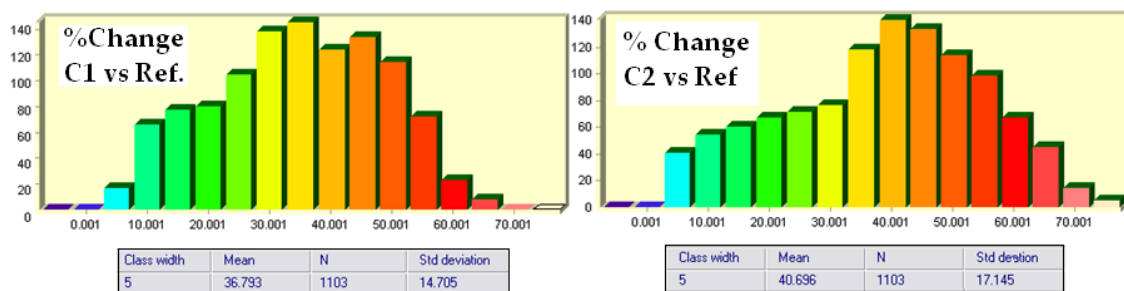


Figure 80 - min c1~5,2 mm/m²/year min c24,8

The previous results for Iberian Peninsula are contrary to some published results. As it can be seen from the picture below (Figure 81), at least one climate model has predicted rises in precipitation (i.e. $\Delta P > 0$) rates for the northern part of the IP region (orange color is assigned to one model).

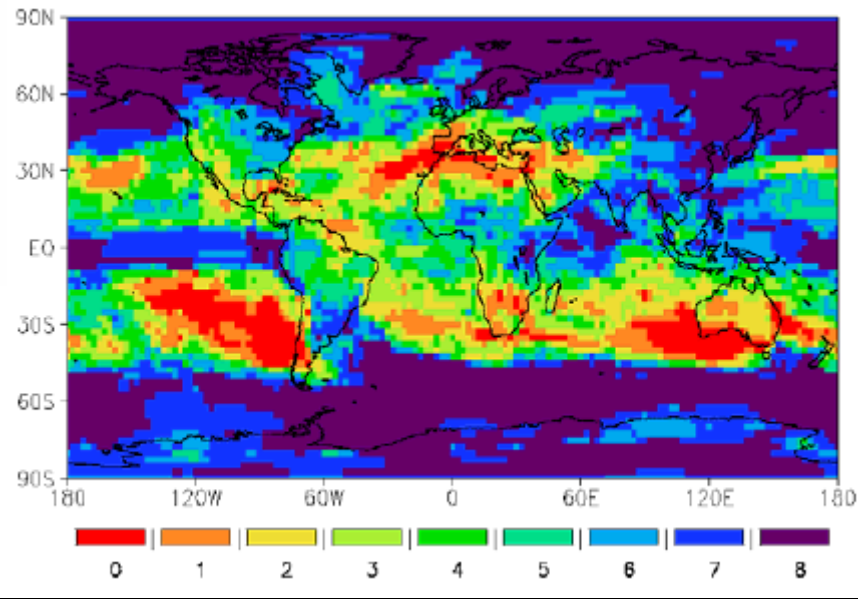


Figure 81 – Number of models which simulate a precipitation increase between the time periods 2080-2099 and 1980-1999 for the scenario A1B (Source: Höschel *et al.*, n.d.)

Moreover, comparing the trends of mean annual global precipitation and mean annual global precipitation over the IP by the next century and under a A1B scenarios projections, the results are considerable different (Figure 82): they predicted an overall increase in precipitation by 5 and 4,5% between the period 2060-2090 and the period 1980-1990 and between the period 2070-2100 and the period 1980-1990, respectively.

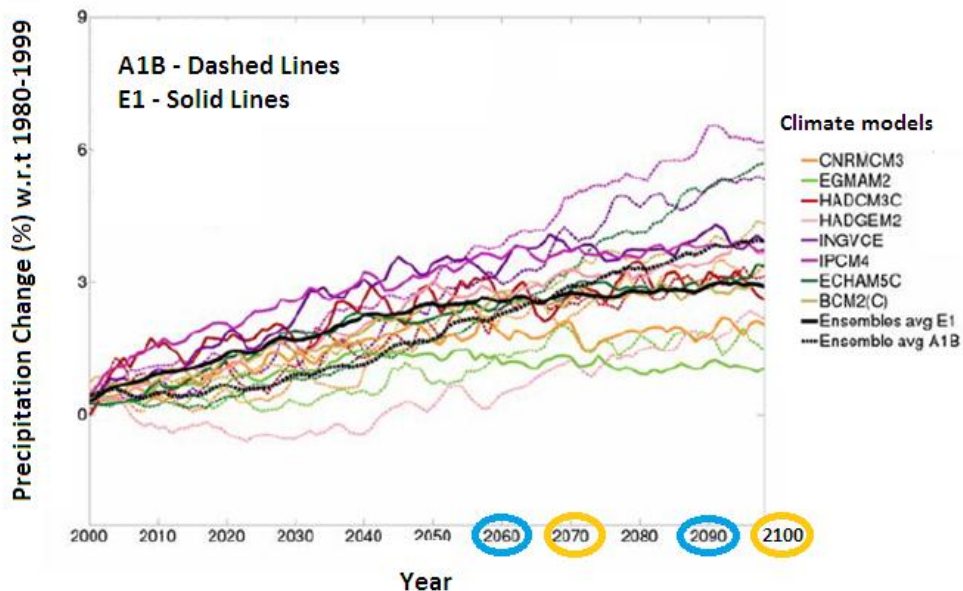


Figure 82 - Time series of globally averaged precipitation change (%) from various coupled models for Scenario A1B and E1, relative to the 1980-1999 annual average (Source: Adapted from Höschel *et al.*, n.d.)

Soil moisture (SWC)

The mean annual soil moisture modeled by JSBACH model for the scenario C1 (Figure 83) does not present great visual differences from the remaining scenarios C2, E1 and E2. The maximum values of SWC have decreased for the scenarios "C": from 2,74 to 2,72m – corresponding to scenarios C1 and C2; and remained roughly constant for both scenarios E1 and E2 (i.e. SWC \approx 2,82m). The minimum values remained roughly constant as well, for the overall set of future scenarios (i.e. SWC \approx 0,013m).

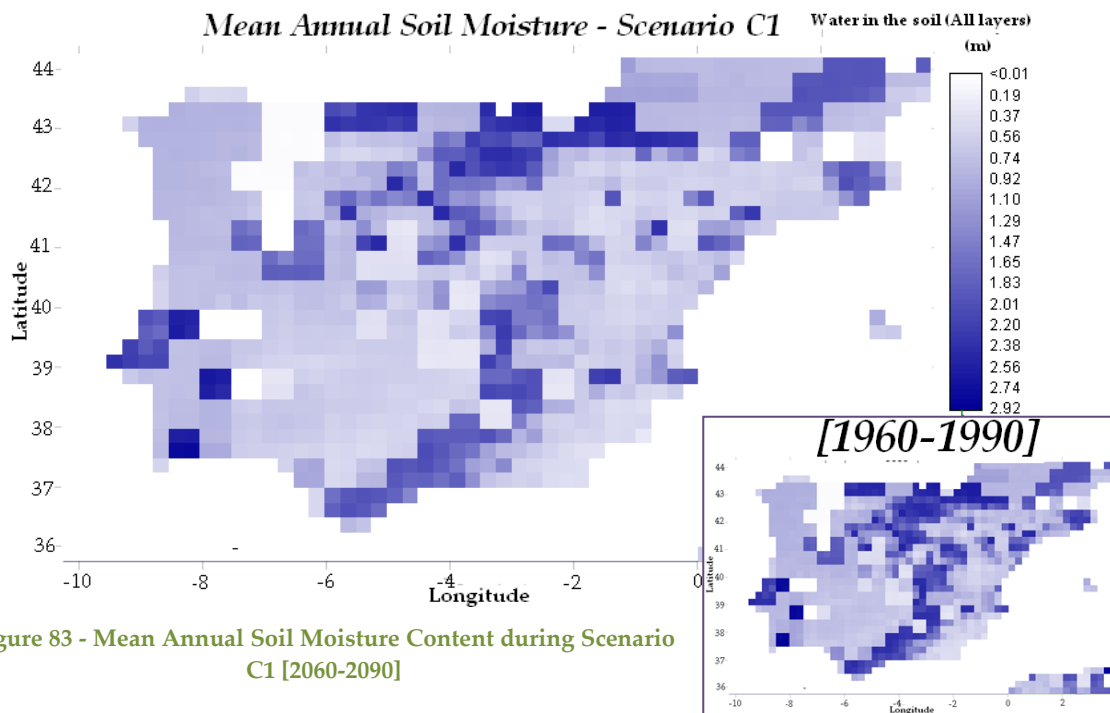


Figure 83 - Mean Annual Soil Moisture Content during Scenario C1 [2060-2090]

The overall mean annual SWC values, have also decreased for all scenarios even though the scenarios "C" showed higher decreases, namely 0,86 and 0,84 for C1 and C2, respectively – and 0,93 to 0,91 from scenario E1 to E2 (Figure 84).

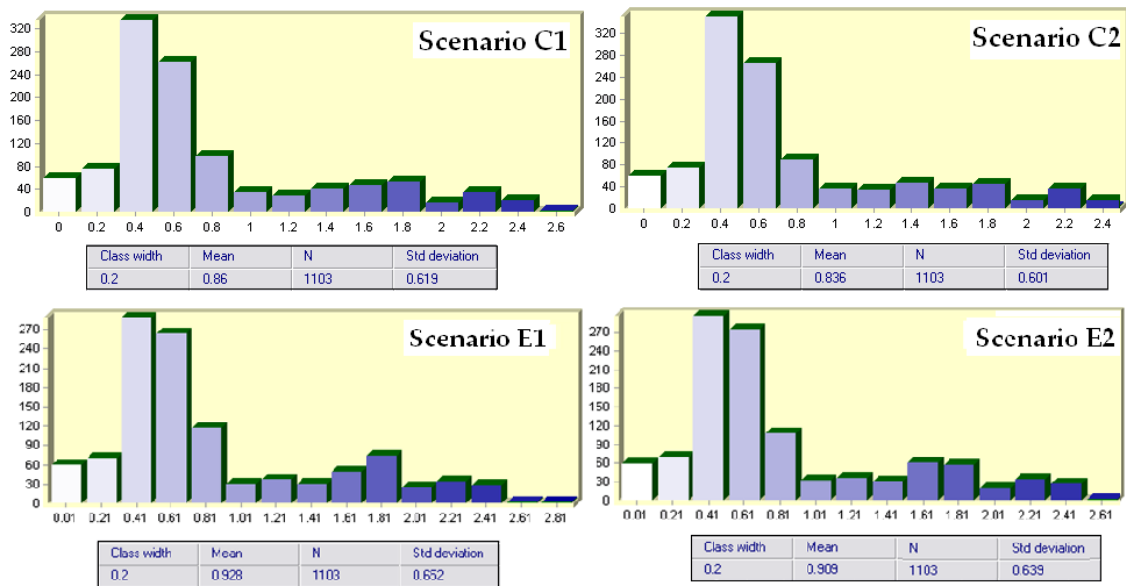


Figure 84 - Histograms and Statistical Analysis of Mean Annual SWC during Scenarios C1, C2, E1 and E2

Hence, regarding now the overall average magnitude of change, there was a notable reduction of average SWC over the IP in the Scenario C1 and C2 – i.e. -22% and 25%, having the 1960-1990 as basis. Although not so strong, the decline of SWC also occurred for Scenarios “E” (a reduction by 16 and 18% of decline, for scenario E1 and E2, respectively). Comparing now the Scenarios “E” and “C”, the scenarios assuming rising CO₂ depict hence a less strong loss of soil water content than the scenarios of constant atmospheric CO₂. The difference between scenario E1 and C1, and the scenarios E2 and C2 were respectively 8 and 9%.

The overall tendency of decreasing soil moisture was fairly expected, due to the decrease of water input (since precipitation rates were projected to decrease was well i.e. this variable is mainly controlled by water supply). In fact, the percentage changes of both precipitation and SWC for 2060-2090 and 2070-2100 periods are in the same order of magnitude (i.e. above 20% of change).

In comparison with IPCC (2007), the results modeled by JSBACH model were substantially the same: as it can be depicted from the Figure 85, the IP region was modeled to suffer a decline by 20% (reddish colors in the map),

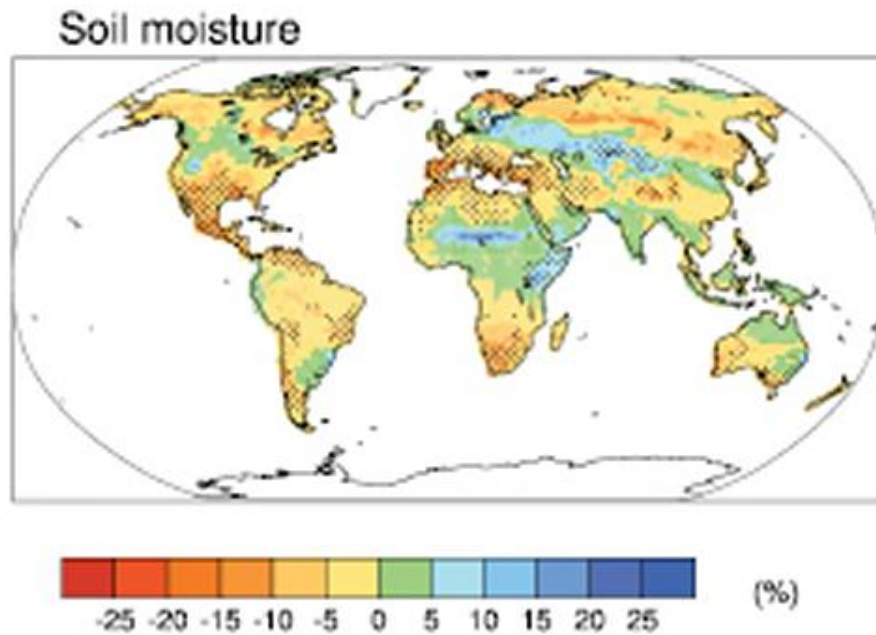


Figure 85 - Multi-model (10 models) mean change in soil moisture content (%). Changes are annual means for the SRES A1B scenario for the period 2080 to 2099 relative to 1980 to 1999. The stippled marks the locations where at least 80% of models agree on the sign of the mean change (Source: IPCC, 2007)

Evapotranspiration (ET)

In the mean annual evapotranspiration forecasted for scenarios C1, C2, E1 and E2 scenarios, the Spanish territory verifies the most accentuated changes, mainly in the regions of Castilla y León, Aragon, Castilla-La Mancha, Extremadura and Andalucía (as it can be seen in the Figure 86 the color became "brighter", meaning a decrease evapotranspiration over the region)

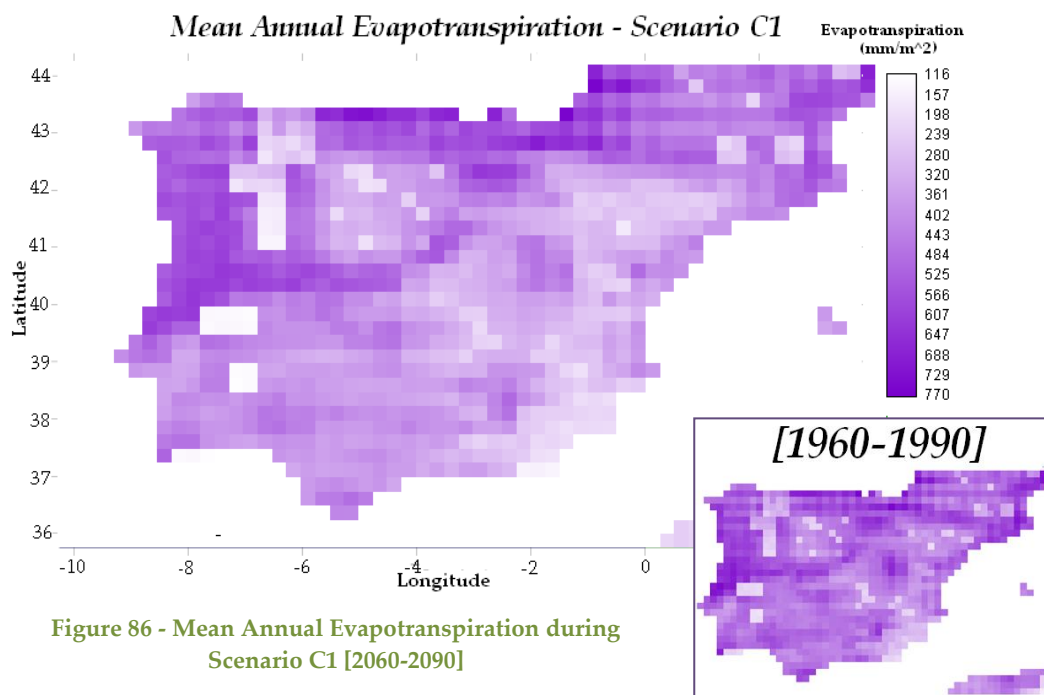


Figure 86 - Mean Annual Evapotranspiration during Scenario C1 [2060-2090]

The changes consisted mainly in the decrease of evapotranspiration in the regions mentioned above – for the Scenario C1 the overall annual mean evapotranspiration was projected to be ~415 mm/year, and ~407 mm/year for Scenario C2, whereas for the E1 and E2 scenarios these values drop to ~401 and ~393mm/year (Figure 87). The difference between the maximum and minimum value of evapotranspiration rate, became wider during the scenario C1 (ranging approximately between ~125 and 810 mm/year) (while for the scenario C2 the values ranged between ~118 and ~809 mm/year), which means, that the minimum rate value became lower and the maximum rate value became higher. In other words, the rates became more extreme. While for the E1 and E2 scenarios the evapotranspiration variable ranges between [123 – 776]mm/year and [116-769]mm/year, respectively.

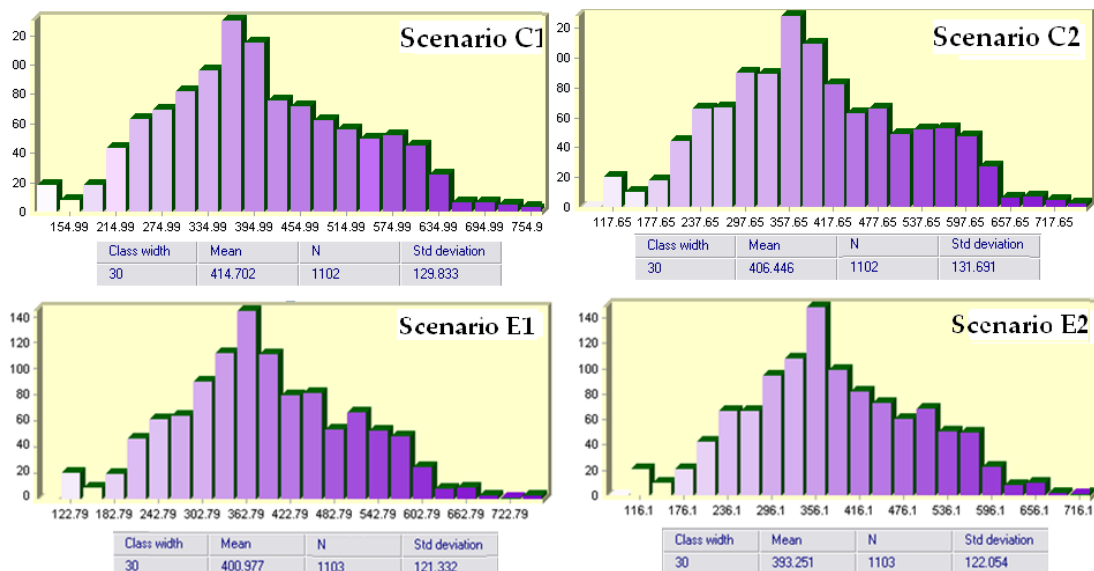


Figure 87 - Histograms and Statistical Analysis of Mean Annual Evapotranspiration during Scenarios C1, C2, E1 and E2

The overall decrease trend can be due to the fact that evapotranspiration are potentially driven by changes in mean temperature and precipitation (besides other factors). Therefore, since as presented in earlier results, once that that precipitation is decreasing and temperature are rising it could lead to less water supply resulting in lower levels of evapotranspiration processes (lower levels of evapotranspiration lead to less cloud formation, boosting the income of radiation). In terms of magnitude of change (i.e. in percentage change), the scenarios C1 and C2 showed a decrease of 15 and 16%, respectively whereas the scenarios E1 and E2 had a higher decrease: -16 and -

18% of the mean annual evapotranspiration during the reference period. Comparing this to other values, the overall trend of decreasing evapotranspiration rate across the IP is similar to what was forecasted by Kim *et al.*(2002.)(Figure 88).

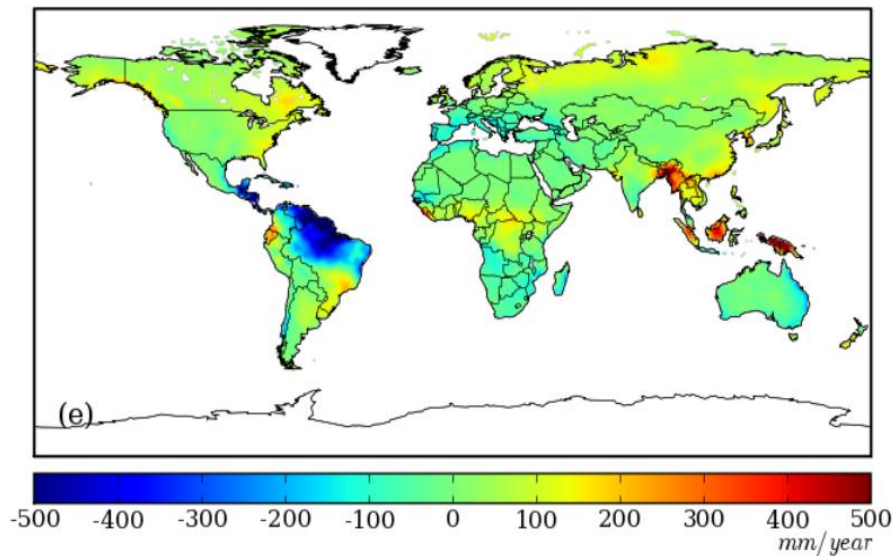


Figure 88 - Differences between global mean ET during the period 1960-1990 and 2070-2100. Simulation results from ECHAM5 with IPCC climate scenario A1B (Source: Kim *et al.*, 2002)

The greenish-blue color even though it is hard to define by the greenish-blue color over the IP region, the value ranges match approximately the same range that the previous map presented (i.e. decrease of evapotranspiration around ~70mm/year). However, the changes in evapotranspiration rate have different behaviors throughout the rest of the world, due to the different hydrological (and biological factor presents in each one of them (Kim *et al.*, 2002)).

A plausible reason that could explain the differences between the Scenarios “C” and “E” (i.e., the higher decreases in the scenarios assuming elevation of atmospheric CO₂ concentration compared to “C” scenarios) could be the direct effect of atmospheric CO₂ enrichment. Under elevated CO₂ concentrations conditions, the plants do not open their leaf stomatal pores as wide as they do, under lower levels of atmospheric CO₂ concentration. Moreover, they also tend to produce less stomata per unit area of leaf surface at higher levels of atmospheric CO₂. Both changes will hence reduce the rate of transpiration, implying does the greater decrease forecasted to Scenarios “E” in comparison the scenarios “C”, where CO₂ rise is not taken into account.

4.3.3 Radiation Balance

Photosynthetically Active Radiation (PAR) and Absorbed PAR (APAR)

Although the PAR is presenting the same patter distribution over the IP (Figure 90), the changes between the periods 2060-2090 and 2070-2100, are considerably different. The latter showed the lowest mean of PAR (~9.114 mol(photosynthesis)/m²/year), while the 2060-2090 period presented a mean of approximately 11.412 mol(photosynthesis)/m²/year, which is higher than what was estimated for the 1960-1990 period.

The highest changes (i.e. ranging between 2,60 and 4,14% of increased PAR) are located above the 40 latitude and they are located in the Northern Plateau, along both Central and Cantabrian Mountain System and in the Pyrenees. The highest changes occurred at

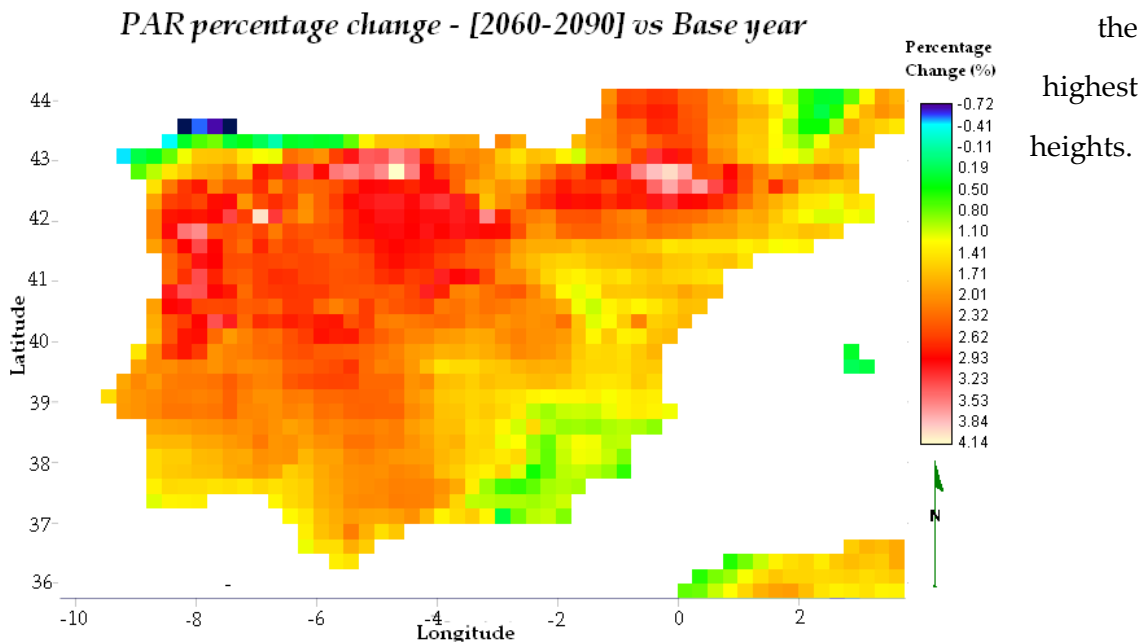
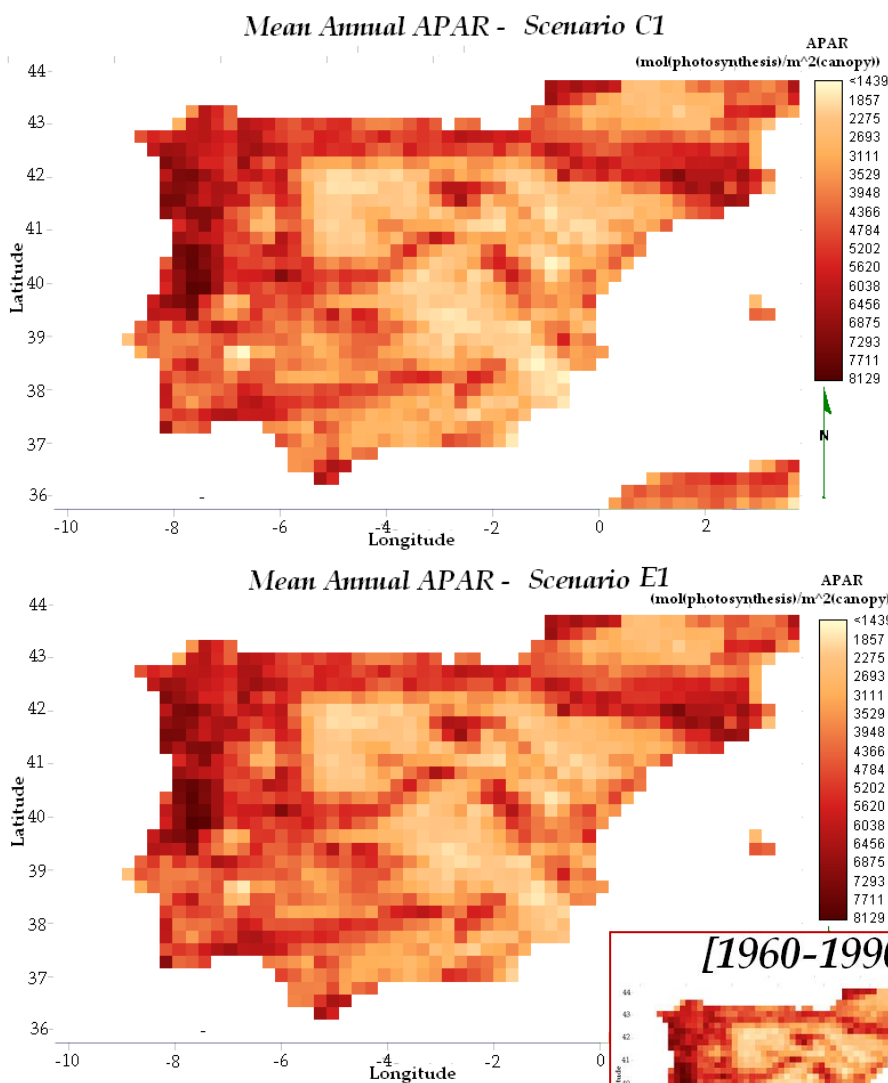


Figure 89 - Percentage Change of Mean Annual PAR between the Reference Period and Scenario C1 [2060-2090]

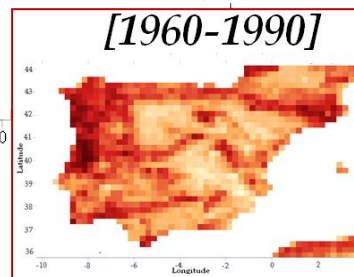
The overall increase in PAR over the IP region in terms of magnitude change from the reference period was 1,98% and 2,22%, for periods 2060-2090 and 2070-2100, respectively.

One of the likely explanations for the increase in those areas might be linked to the changes in mean annual evapotranspiration, due to the lower water available cause by lower precipitation rates. The less water vapor (and therefore clouds) in the atmosphere will enable a higher rate of solar radiation to go toward, which could explain as well the boosting temperatures earlier verified for this area. Similarly to what happen with the PAR variable, the same pattern of APAR remained for the simulations of the four future scenarios. There were very small changes between the



scenarios and the reference period, – and between the future scenarios themselves. As it can be seen from the Figure 90, the changes are barely perceived.

Figure 90 - Mean Annual APAR during Scenarios C1 and Scenario E1 [2060-2090]



For the scenarios C1 and E1, the mean absorbed PAR rate modeled by JSBACH was ~ 3.938 and 4.103 mol (photosynthesis)/ m^2/year by 2060-2090, respectively) and ~ 3.936 and 4.131 mol(photosynthesis)/ m^2/year (for the scenarios C2 and E2).

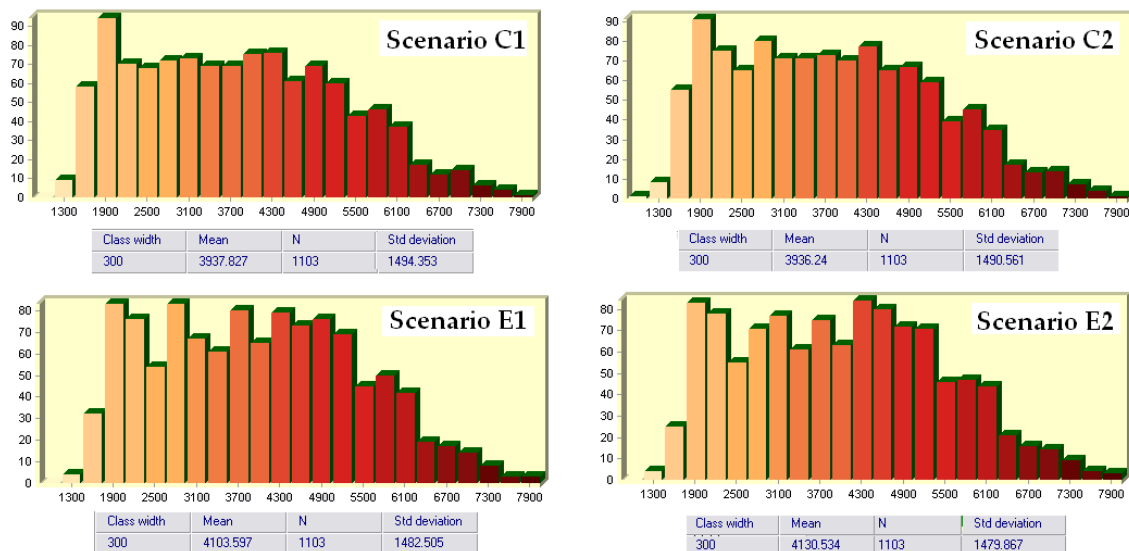


Figure 91 -Histograms and Statistical Analysis of Mean Annual APAR during Scenarios C1, C2, E1 and E2

Furthermore, within the Scenarios “C”, the minimum APAR values have decreased while the maximum values have increase from the reference period to the scenario C1, and slightly decrease from scenario C1 to scenario C2. Conversely, the Scenarios “E”, disclosed an increase of maximum values and an increase between the maximum from reference period to scenario E1, and a decrease from scenario E1 to scenario E2.

In what concerns the distribution pattern of the difference of APAR between the scenarios E1 and E2 and the reference period in means of percentage change, the following images (Figure 92) shows the spatial and quantitative percentage changes. Both scenarios were estimated to undergo positive and negatives changes i.e. to have increases and reductions of absorbed PAR rates at different places. As such, the Scenario E1 shows changes ranging between approximately -16 and 36%, while for the Scenario E2, this range becomes a bit wider: -20 to 38% of change compared to the reference period.

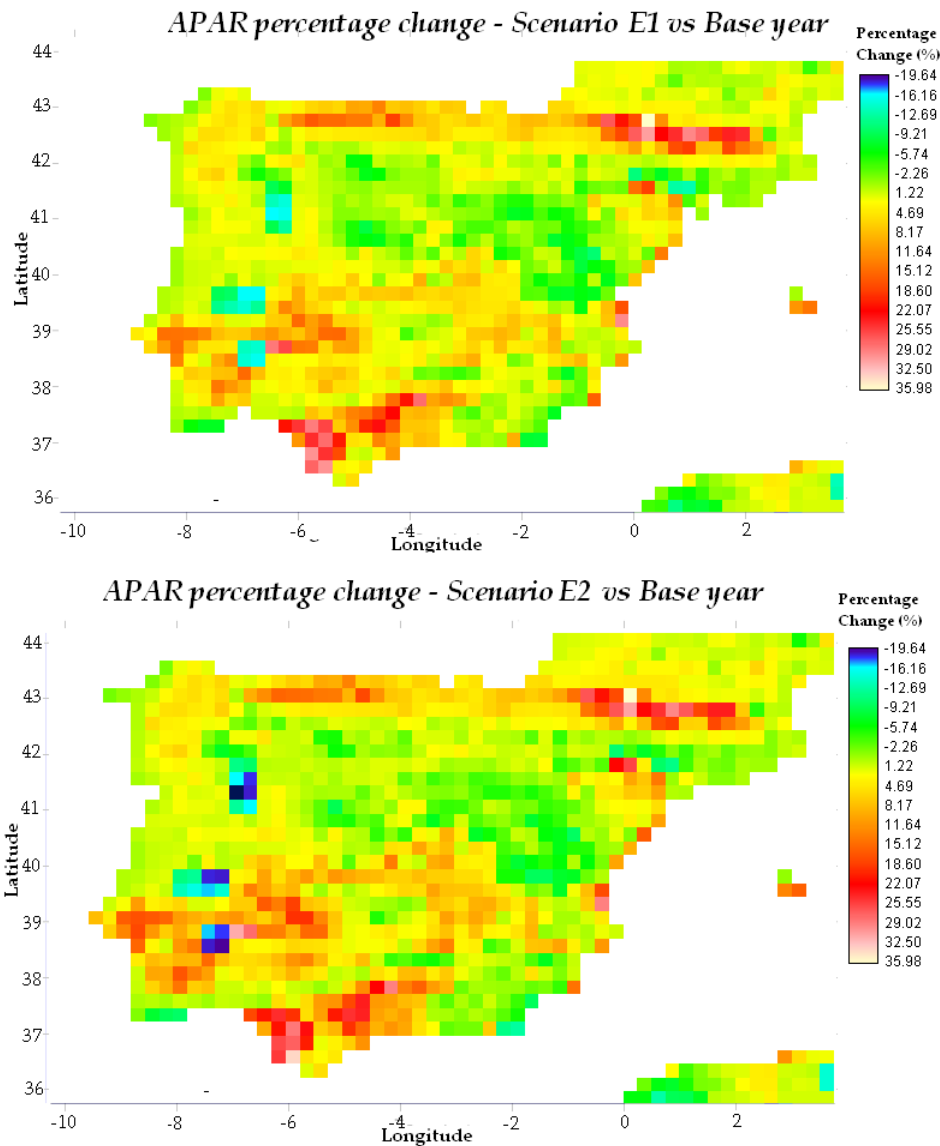


Figure 92 - Percentage Change of Mean Annual APAR between the Scenario E1 and E2 and the Reference Period

The areas with higher positive changes (assigned to reddish areas) lie in northern regions of the Peninsula, as well as in the regions of South Portugal and Alentejo region in the same country.. For the negative percentage changes, i.e. decrease in APAR rates, the greenish areas are spread all over the Peninsula, although the highest decreases are likely to occur in three different spots across the boundary between Portugal and Spain (dark and light blue areas).

Hence the model has simulated a small decrease of the mean value (~-1%) for the scenarios admitting constant atmospheric CO₂ concentration. For the scenarios E1 and E2, the change of APAR was positive and a bit higher (~3 and 4%, respectively).

Reference period The different behaviors of APAR tendency in scenarios “C” and “E” is likely to be the result from an increase of vegetation productivity (since the higher the rate of production, the higher the photosynthetically processes, and hence, the higher the solar radiation absorbed). Although this issue will be carefully addressed in forthcoming chapter.

4.4 Carbon Balance Analysis– Future Scenarios

The approach made to the variables belonging to the carbon balance (GPP, NPP and biomass) is similar to the one made when assessing changes in climate and environmental variables for the future scenarios. This chapter presents the assessment of the spatial patterns and magnitudes of change (having the reference period as basis), although it is empathized the role of carbon dioxide in those changes. Hence, this final section aims to assess biomass and vegetation productivity response to changes in climate variables (and how strongly are they correlated) and aims to understand and quantify the effect of fertilization of CO₂, i.e. to understand how this physical variable is affecting vegetation – namely herbaceous and forest biomass.

The potential biomass (from herbaceous and forest resources) modeled by JSBACH will also be addressed in means of energy source by computing the energy potentials of biomass modeled by JSBACH assuming the most plausible scenario, i.e. assuming the increase of atmospheric CO₂ concentration (and the climate change scenario A1B), under different approaches assuming different politic and management of resources.

4.4.1 Gross Primary Production (GPP)

The maps projected by JSBACH regarding the Gross Primary Production for both constant and changing atmospheric CO₂ scenarios present the same pattern distribution as in Figure 52. The average productivity as well as the maximum and minimum GPP values vary considerably between each other, as well as between the GPP estimated during the reference period. According to the results from the model, during the scenario C1, in general, the GPP decreases its rates values (Figure 94). The mean annual GPP decreases hence from 4.422 to ~4.007 g(CO₂)/m²/year. The actual maximum for this scenario is ~8.764 g(CO₂)/m²/year and the actual minimum modeled was ~715 g(CO₂)/m²/year.

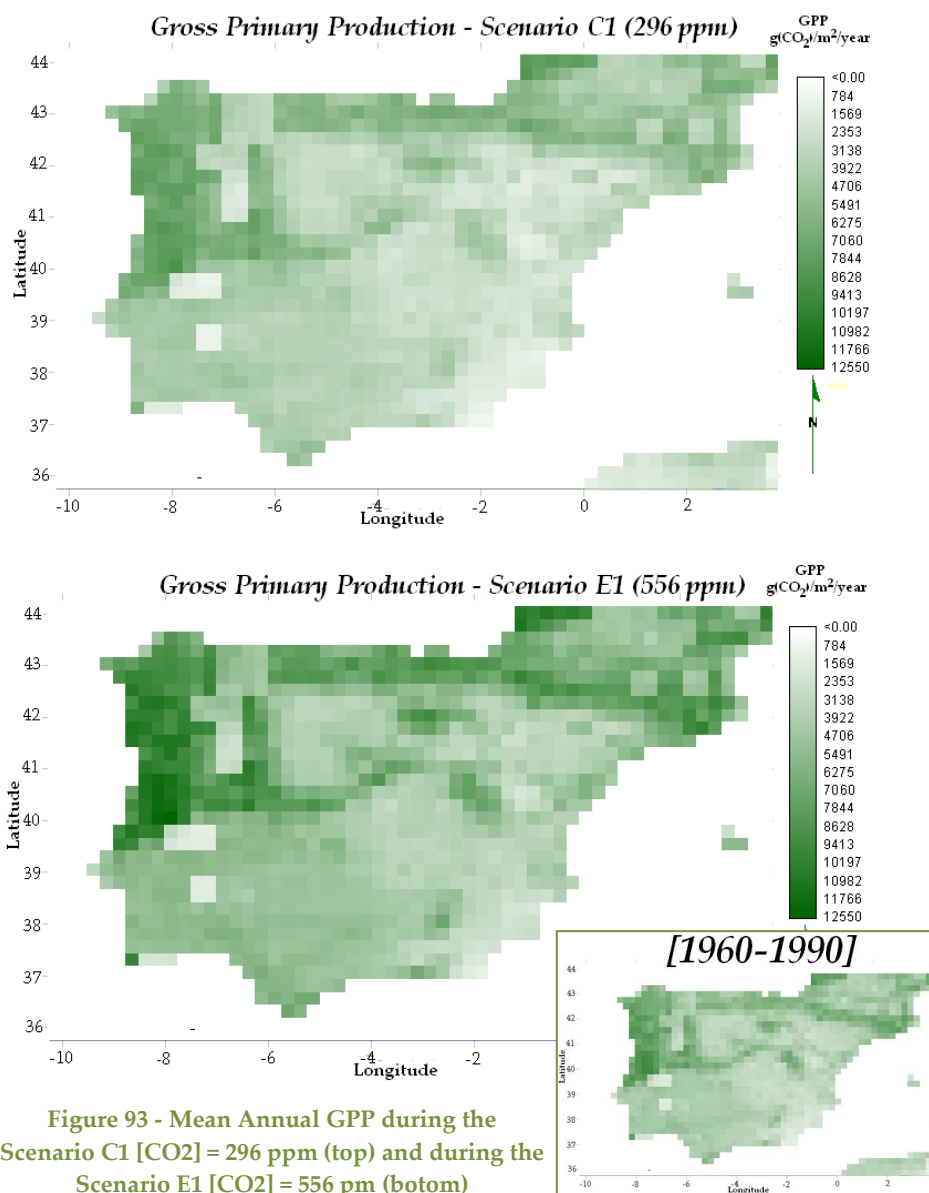


Figure 93 - Mean Annual GPP during the Scenario C1 [CO₂] = 296 ppm (top) and during the Scenario E1 [CO₂] = 556 pm (botom)

Conversely to what JSBACH modeled for the Scenario C1, the Scenario E1 presents a different trend on GPP change – instead of decreasing, it increases substantially. Hence, the mean productivity projected for a scenario admitting and increase by 88% of atmospheric CO₂ concentration is ~5.575 g(CO₂)/m²/year. The actual maximum and minimum estimated change considerably as well: ~12.456 and 1.131 g(CO₂)/m²/year, respectively (Figure 95).

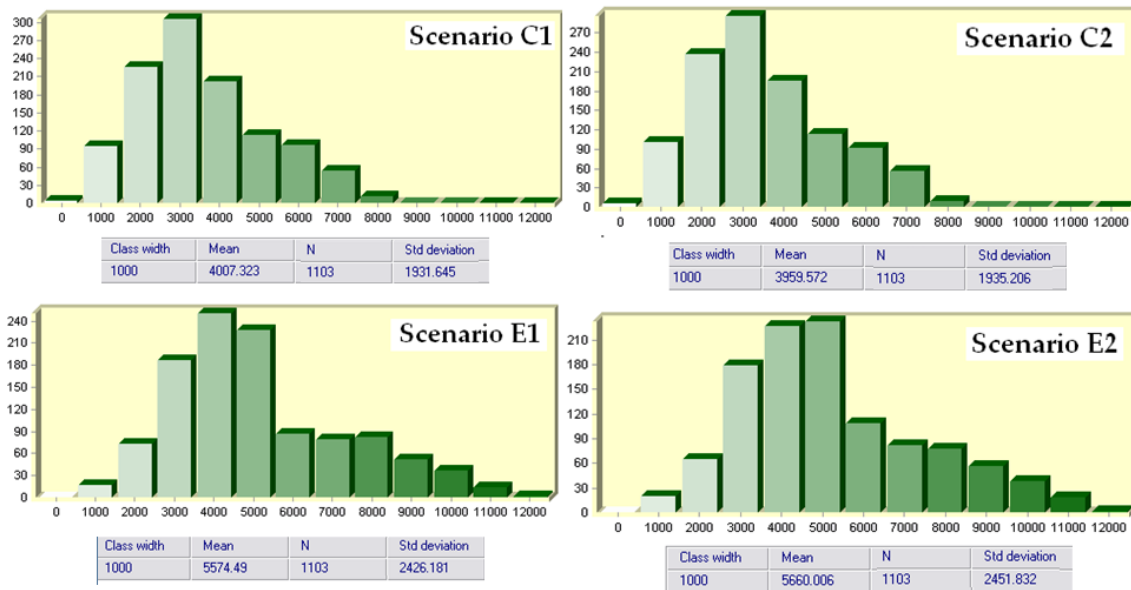


Figure 95 - Histograms and Statistical Analysis of GPP during the Future Scenarios C1, C2, E1 and #E2

As it can be perceived from the Figure 96, the greatest differences occurred at higher latitudes – approximately above the latitude 40 and associated to topographic features – namely associated to the mountain ranges presented in the territory.

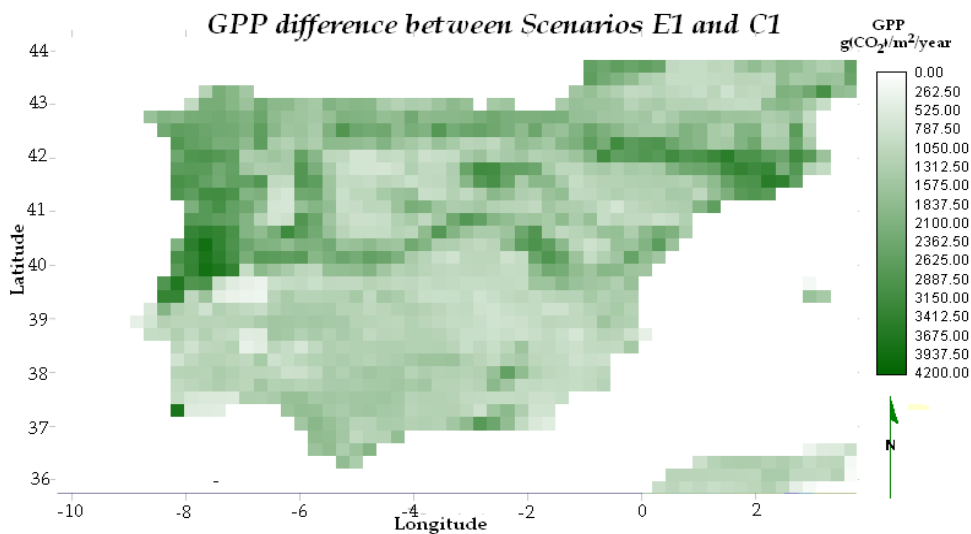


Figure 96 - Mean Annual GPP differences between Scenario E1 [CO₂]=556ppm and Scenario C1[CO₂]=296ppm

The Portuguese territory (along with the region of Galicia and the Pyrenees mountain range) verify some of the strongest differences in GPP (above $\sim 3.500 \text{ g}(\text{CO}_2)/\text{m}^2/\text{year}$, occurring overall across the northern part of the territory (i.e. above the Tejo River). The mean difference between scenarios E1 and C1 is $\sim 1.567 \text{ g}(\text{CO}_2)/\text{m}^2/\text{year}$, and $\sim 1.700 \text{ g}(\text{CO}_2)/\text{m}^2/\text{year}$ between scenarios E2 and C2 (Figure 97).

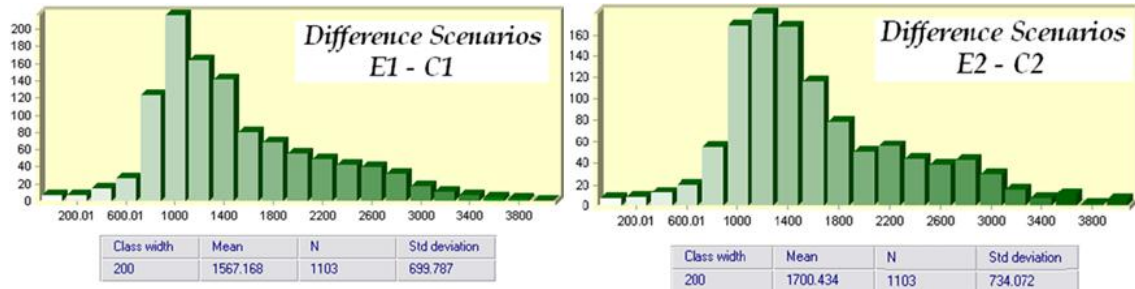


Figure 94 - Histograms and Statistical Analysis of the differences of GPP between Scenarios E1 and C1 (top) and Scenarios E2 and C2

Despite the location of the wider differences, the pattern of percentage change is different, since the greatest percentage changes (above 70% change) are mainly located over the east side of the IP constrained though by the Penibetic and Iberian mountain ranges. The maximum percentage change verified between the GPP modeled for scenario C1 and scenario E1 was $\sim 83\%$ and the overall mean percentage change between both scenarios is $\sim 41\%$ (Figure 95). The same map for percentage change between scenario E2 and C2 showed similar results. The overall mean percentage change was higher for the period 2070-2100: approximately 45% (Figure 99).

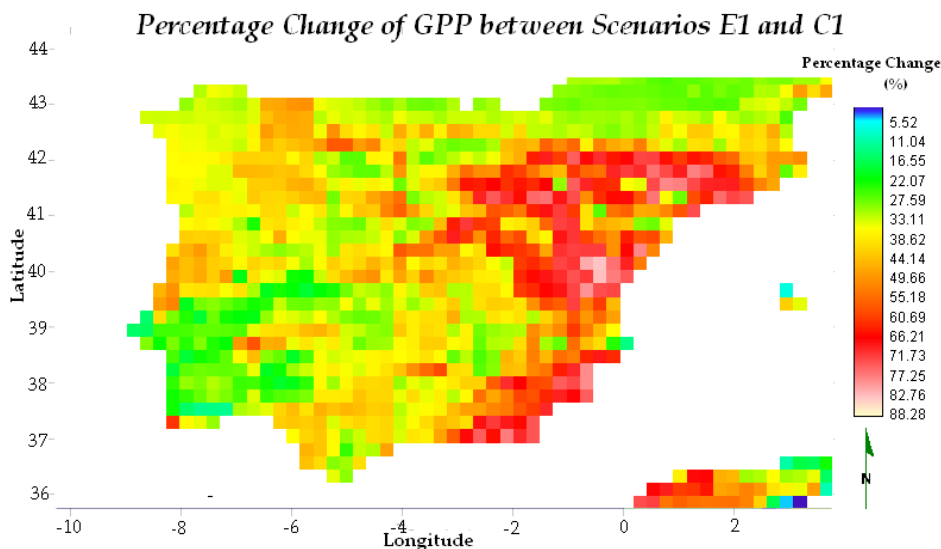


Figure 95 - Percentage Change of Mean Annual GPP between Scenario E1 and C1

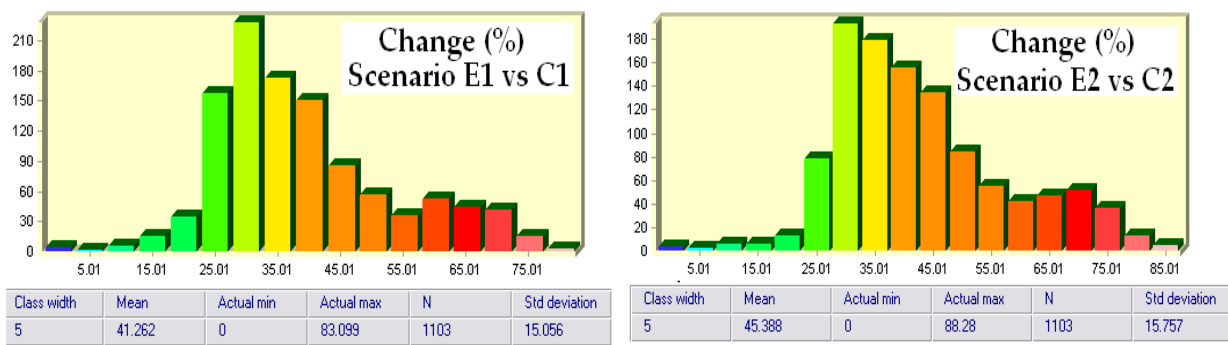


Figure 96 - Histograms and Statistical analysis of percentage change of GPP in period 2060-2090 (left) and 2070-2100 (right)

The considerably higher CO₂ uptake was thus a result of elevated atmospheric CO₂, since it was the only variable changed between the two scenarios meaning that the results yielded by JSBACH model are in accordance with several authors (e.g. Amthor, 1998; DeLucia et al., 1999; Schaphoff *et al.*, 2006, and many others).

Hence, despite the overall decreases of water supply (through precipitation) expected to occur within roughly almost a century, the fertilization effect was modeled by JSBACH, since plants uptake more CO₂ from the atmosphere – resulting in increased yields. Moreover, taking in consideration the former results from evapotranspiration (i.e. the decreasing tendency in evapotranspiration mean annual values), these results are also corroborated by Kimball *et al.* (2002), whom have concluded that as a result of CO₂ fertilization – the stomatal conductance tend to decrease, leading to decreases in evapotranspiration. Furthermore, Kimball *et al.* (2002) (along with many other authors, such as Amthor, 1998; DeLucia et al., 1999; Schaphoff *et al.*, 2006) have also depicted an improvement of water-use efficiency (as a result from what was explained) – which drawn even more interested to get this variable analyzed (in following chapter).

Changing Environmental Controls on GPP

From the correlation coefficients presented in Table 40, the relationship between mean annual GPP and every variable climate (aside from mean annual temperature and APAR), tend to get considerably stronger for future scenarios assuming elevated CO₂ and constant CO₂ levels – although during the later scenarios the increase of correlation was more considerable. The mean annual temperature correlation with mean annual

GPP showed a slightly different trend: despite the relationship got stronger for future scenarios, the relationship was stronger for scenarios of elevated CO₂. The mean annual APAR stands out, since it was the only variable which got less spatially correlated with GPP for future scenarios (and even lesser for scenarios elevated CO₂). Every relationship kept the same signal than in the reference period for all climate variables (Table 40).

Table 40 – Comparison of Correlation coefficients for GPP and Climate Variables during the Reference Period and the Future Scenarios

	Response variable	Water Cycle				Radiation	
		T	P	ET	SWC	PAR	APAR
Ref. Period		-0.25	0.65	0.76	0.12	-0.36	0.81
C1		-0.40	0.73	0.88	0.32	-0.40	0.79
C2	GPP	-0.42	0.73	0.89	0.35	-0.41	0.79
E1		-0.42	0.68	0.84	0.23	-0.39	0.78
E2		-0.43	0.67	0.85	0.26	-0.39	0.78

Table 41 presents the correlation analysis related to the interannual variability of the mean annual GPP to the climate variables, showing thus the relationship between the interannual variability of GPP and climate change (under scenarios of elevated and constant CO₂ levels). GPP was highly and positively correlated with changing ET ($R_{C1}=0,79$ and $R_{C2}=0,80$) and APAR ($R_{C1}=0,79$ and $R_{C2}=0,78$) variables for scenarios where atmospheric CO₂ rising is disregarded. For scenarios assuming elevated CO₂, GPP stills highly correlated with ET and APAR, although the relationships are less strong. These findings, i.e. the strong influence of ET and APAR in the interannual variability of GPP are in accordance with Liu *et al.* (2011).

Table 41 - Correlation coefficients for variability of GPP in response to varying climate variables

Δ SCENARIOS	Response variable	Water Balance				Radiation	
		ΔT	ΔP	ΔET	ΔSWC	$\Delta APAR$	ΔPAR
C1-Ref. Period		-0.30	-0.02	0.79	0.15	0.79	0.02
C2- Ref. Period		-0.30	0.05	0.80	0.11	0.78	0.00
C2-C1	ΔGPP	-0.30	0.52	0.83	0.12	0.72	-0.05
E1- Ref. Period		-0.47	-0.32	0.65	0.10	0.62	0.18
E2- Ref. Period		-0.47	-0.27	0.65	0.08	0.61	0.20
E2-E1		-0.36	0.27	0.70	-0.07	0.73	0.06

Despite the fact that mean annual precipitation has a great impact on the interannual variability of primary production (Liu *et al.*, 2011), this variable is not equal to water available to vegetation. For that reason, the changing precipitation events throughout the future scenarios and the reference period shown to be poorly and negatively correlated under both “E” and “C” scenarios (although GPP was fairly more sensitive to changing mean annual precipitation under scenarios of elevated CO₂).

The negligible *R* computed for mean annual PAR suggests that GPP has a null relationship with changing mean values of PAR. The almost absent relationship could be due the fact that this variable does not go under considerable changes. Conversely to APAR, SWC is subject of considerable changes although there is also an almost null relationship with GPP (which can be explained as well by the same reason given for weak correlation between mean annual precipitation and mean annual GPP). The graphical correlation assessed in Table 40 and Table 41, are found in Figure 97 and Figure 98. These graphics regard the variability between scenario C1 and the reference period (i.e. 2060-2090/1960-1990), under scenarios assuming constant CO₂ levels and elevated CO₂ levels (296ppm and 556ppm, respectively).

Among the variables composing the water balance, the correlation between evapotranspiration and GPP resembles a linear correlation – the greater the values of

evapotranspiration variations between the scenario C1 and the reference period, the greater the amount of GPP variability, i.e. evapotranspiration decrease, GPP also decreases which shows its sensitivity to the variability of this climate variable. Both precipitation and soil moisture (besides their lack of defined pattern), drove more positive values for GPP (reflecting a greater increase in GPP during the [2060-2090/1960-1990] period considered) for the scenario assuming rising CO₂. (i.e. scenario E1).

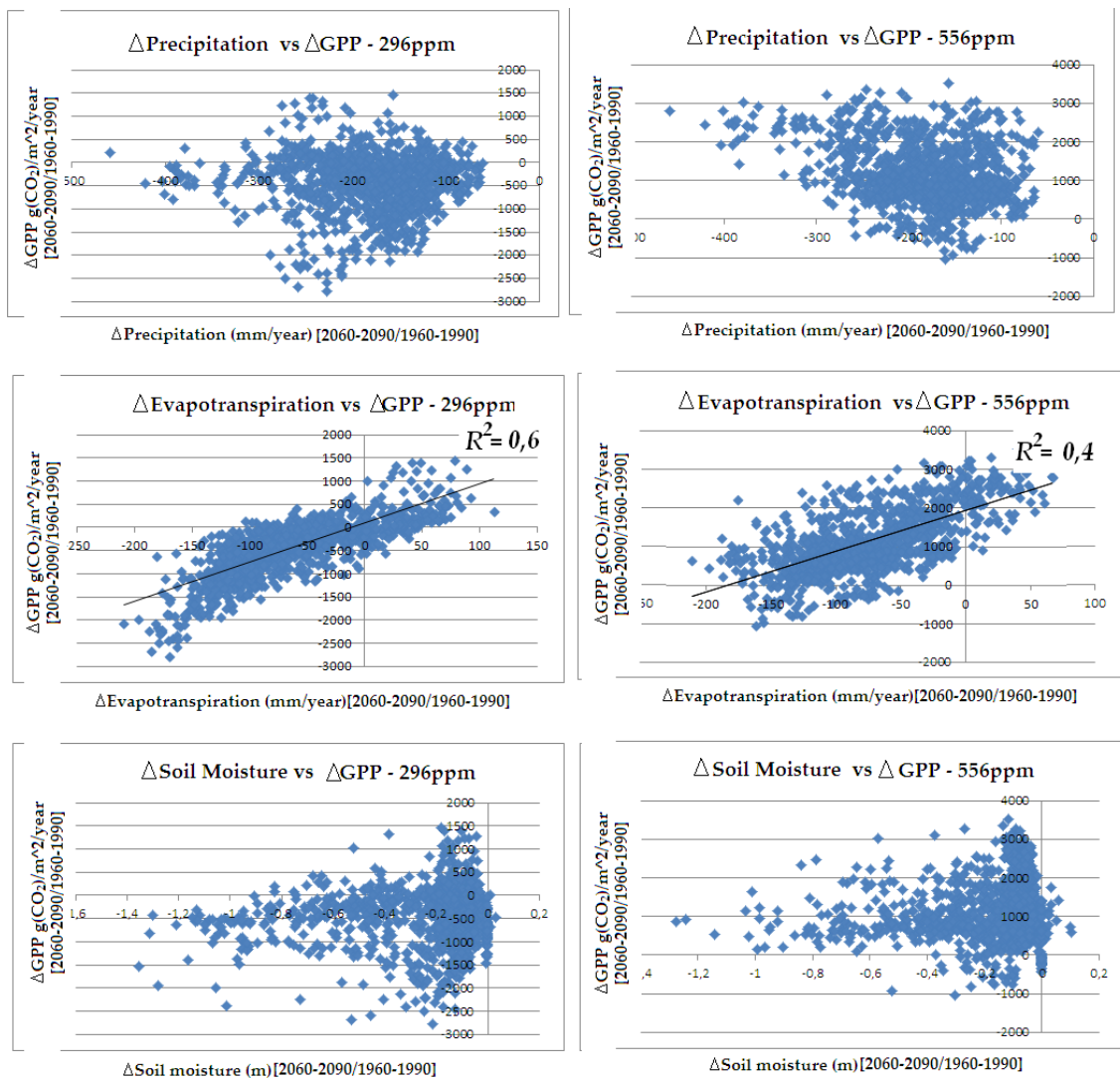


Figure 97 – Correlation between interannual variability of mean annual GPP and mean annual variables from water balance (i.e. precipitation (top); evapotranspiration (middle); soil moisture content (bottom) – between Scenarios E1 and C1 and Reference Period [1960-1990]

Similarly to the mean annual precipitation and mean annual soil moisture, both mean annual temperature and PAR variables shown a similar tendency, (i.e. lack of pattern, but a wider locations with increased GPP under the scenario E1). As expected the mean annual APAR variability is likely linearly correlated with GPP Figure 98 .

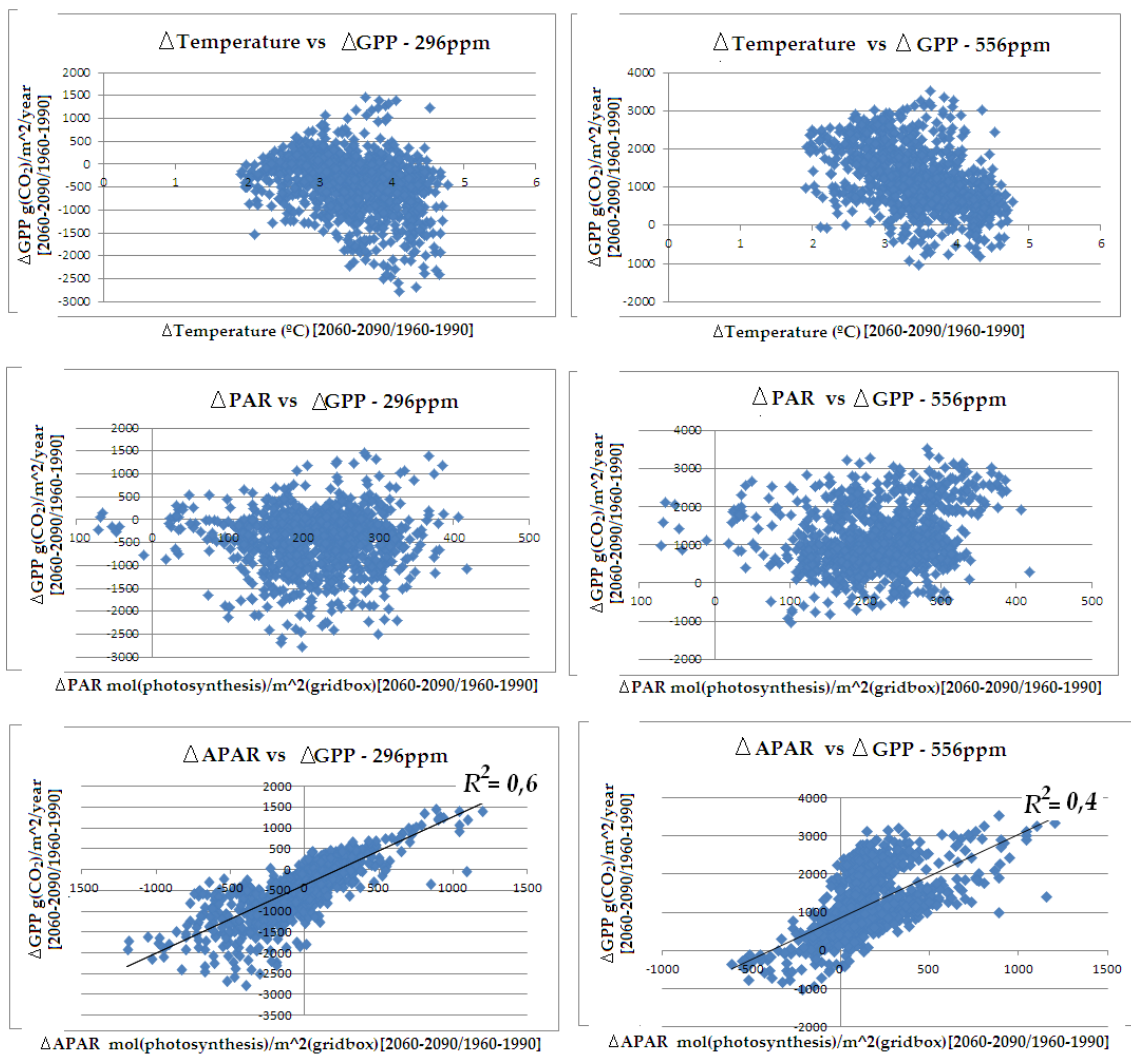


Figure 98 - Correlation between interannual variability of mean annual GPP and mean annual temperature (top) and variables from radiation balance (i.e. PAR (middle) and APAR (bottom) – between Scenarios E1 and C1 and Reference Period [1960-1990]

Water-Use Efficiency (WUE) during Future Scenarios

As previously found throughout the analysis of water balance, the climate change expected for the future scenarios aggravate the problem of water shortages. When temperature rises and precipitation decreases, water requirements increase and hence it is necessary to evaluate this increase. The changes suffered by herbaceous plants and forest as a consequence of the changing environmental patterns referring to yield are mainly caused by variations in water availability (when CO₂ elevation is disregarded).

Nowadays it is well documented that high yield potentials as well as high yield under water-limited conditions are generally associated with reduced WUE (Blum, 2005), mainly due to the higher water use. Associated with low WUE, is also the enhanced capture of soil moisture by roots (which enables dehydration avoidance). On the other hand, the reduction of transpiration and evapotranspiration is generally associated with higher WUE (Kobata *et al.*, 1996; Tolk & Howell, 2003). This last fact was actually the main result from the scenarios modeled for the future periods 2060-2090 and 2070-2100, (which are presenting the same pattern of WUE distribution). However, both Scenarios "C" and "E" project an increase of mean WUE values. The scenario C1 and C2, account with an overall mean of 9,8 and 9,9 g(CO₂)/mm(H₂O), respectively (Figure 99), while the scenarios E1 and E2 depict a considerable higher change of WUE, namely 13,8 and 13,9 g(CO₂)/mm(H₂O)(Figure 100).

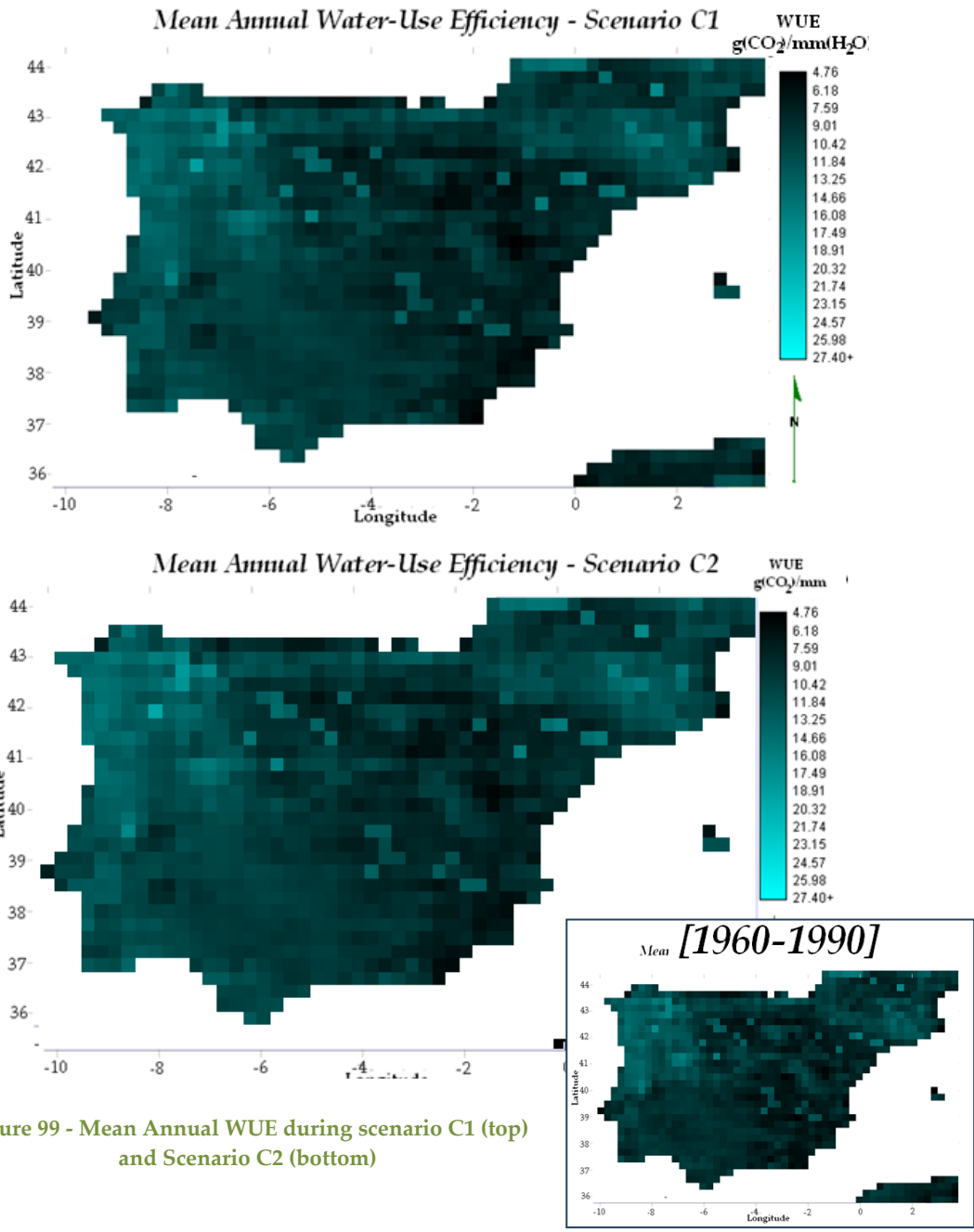


Figure 99 - Mean Annual WUE during scenario C1 (top) and Scenario C2 (bottom)

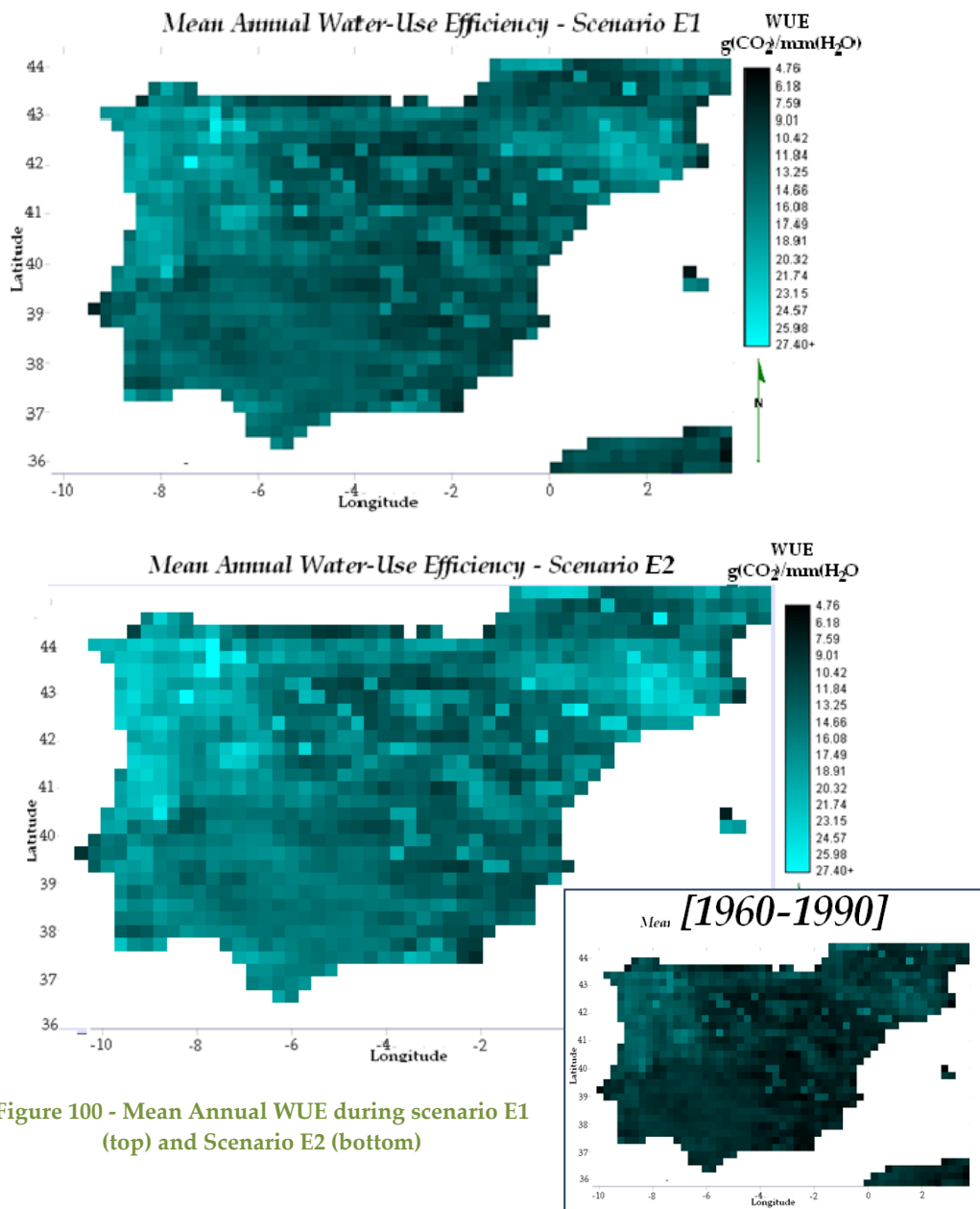


Figure 100 - Mean Annual WUE during scenario E1 (top) and Scenario E2 (bottom)

The minimum WUE values have also increased in 2060-2090 (4,48 and 6,17 $g(CO_2)/mm(H_2O)$, for scenarios C1 and E1, respectively) and slightly decreased in the 2070-2100 period (4,76 and 6,16 $g(CO_2)/mm(H_2O)$ – scenarios C2 and E2, respectively). The maximum values of WUE presented a similar tendency ($máxWUE_{C1}=18,9$; $máxWUE_{C2}=19,2$; $máxWUE_{E1}=27,4$; $máxWUE_{E2}=26,1$ – all in $g(CO_2)/mm(H_2O)$).

In terms of magnitude of change in respect to the Reference period, the overall mean WUE over the IP tend to increase by 6 and 7%, for the scenarios admitting constant atmospheric CO_2 concentration (for scenarios C1 and C2, respectively), whereas for the for the scenarios E1 and E2, WUE greatly changes it tendency: it also increases but the

difference is substantial - 48 and 50%. Hence, comparing Scenarios "C" against Scenarios "E", the effect of rising atmospheric CO₂ contributes to an increase of WUE by 40% from scenario E1 to scenario C1 (within the 2060-2090 period), and 41% for the 2070-2100 period.

From these results, there is clear evidence that the CO₂ elevation does have - within its complex interactions with the water cycle and the productivity - a considerable influence on water use efficiency. As it was previously explained for decreasing evapotranspiration rates, this tendency of rising WUE levels is due, to the two changes driven by atmospheric CO₂ enrichment, i.e., the smaller stomata opening and lower produce of stomata per unit of leaf area, which tend to reduce the rate of transpiration whereas the amount of carbon they gain per unit of water lost (i.e. the WUE) rises - which will greatly increase their ability to withstand drought.

Other valuable explanations of how will the atmospheric CO₂ enrichment improve the relationship between plant and water, are (1) the increase of plant turgor: the leaf osmotic potential is enhanced by leaf carbohydrate concentration, which is CO₂ induced, and ultimately helps to maintain a proper leaf water content for continued photosynthesis and growth - facing thus the decay of soil moisture availability); and the (2) reduced water use (WU). Plants were designed by evolution to be capable of controlling - and hence reduce the WU under drought stress. Moreover, even though its genetics influence, when a plant is exposed to dry soil conditions, root morphology and growth can change (i.e. increase under drought stress) to the extent that the potential root length becomes irrelevant (Blum, 2005). One of the main reasons can rely on the so-called "dehydration avoidance", which is defined as the plant capacity to sustain high cellular hydration under the effect of drought. This mechanism enables that plant avoid dehydration by enhancing for instance the capture of soil moisture, by limiting crop water loss, and also by retaining cellular hydration despite the overall reduction in plant water potential (Blum, 2005).

Hence, regardless the CO₂ variability, the overall water use efficiency of the Iberian Peninsula tends to increase considering the climate changes modeled by JSBACH.

When the atmospheric CO₂ elevation is taken into account the water-use efficiency doubles its overall value. Which mean, that the increase of nearly 88% of the concentration of dioxide carbon in the atmosphere, leads to a doubled biomass production per unit of water. According to Emmrich (2007) the C₄ grasses have higher water-use efficiency (WUE) than do C₃ shrubs, although on the other hand, the C₄ plants are believed to lose this known advantage (Emmrich, 2007) due to the rising atmospheric CO₂ concentration. Even though, for that reason, the C₄-grass-dominated ecosystems are usually expected to present a higher WUE than C₃-shrub dominated ecosystems under same CO₂ concentration and climatic variability (Emmrich, 2007).

Despite the previous findings it should be noticed that due to the multiple environmental factors influencing the WUE and the complex relationship existing between the carbon and water cycles, the spatial dynamics (as well as the variability between each time period) should be addressed carefully (Tian *et al.*, 2010). For instance, WUE can be affected by soil fertility (which is linked to roots and water and nutrients availability)(Stewart, 2001). Nevertheless, several studies corroborate these results. In fact, Policy *et al.* (1993), have found results indicating that the increase in CO₂ since the Glacial time to at the time (1993) CO₂ concentrations have enhanced biospheric carbon fixation by increasing the WUE of biomass production of C₃ plants (the bulk of the vegetation of the Earth). It also matches some other findings that predict that an increase in atmospheric CO₂ concentration is proposed to have an effect on both the hydrological cycle and ecosystem productivity (Gelfand & Robertson, n.d.).

Light-Use Efficiency (LUE) during Future Scenarios

For the scenarios assuming constant atmospheric CO₂ concentration, the light-use efficiency tend to decrease contrarily to what happened with the scenarios E1 and E2, where LUE shown to increase. Hence, the overall mean of LUE for scenarios C1 and C2 are projected to be ~1.00 and 0.98 g(CO₂)/mol(photosynthesis)(Figure 101), representing a decrease of -13 and -15%, respectively, from the reference period. This decrease means that within these scenarios, there is a lower carbon uptake per unit of absorbed photosynthetically radiation –which means that in order to produce the same amount

of carbons than during the reference period, there is a need of more ~13 and 15% of APAR during the future scenarios (assuming that the other conditions maintains).

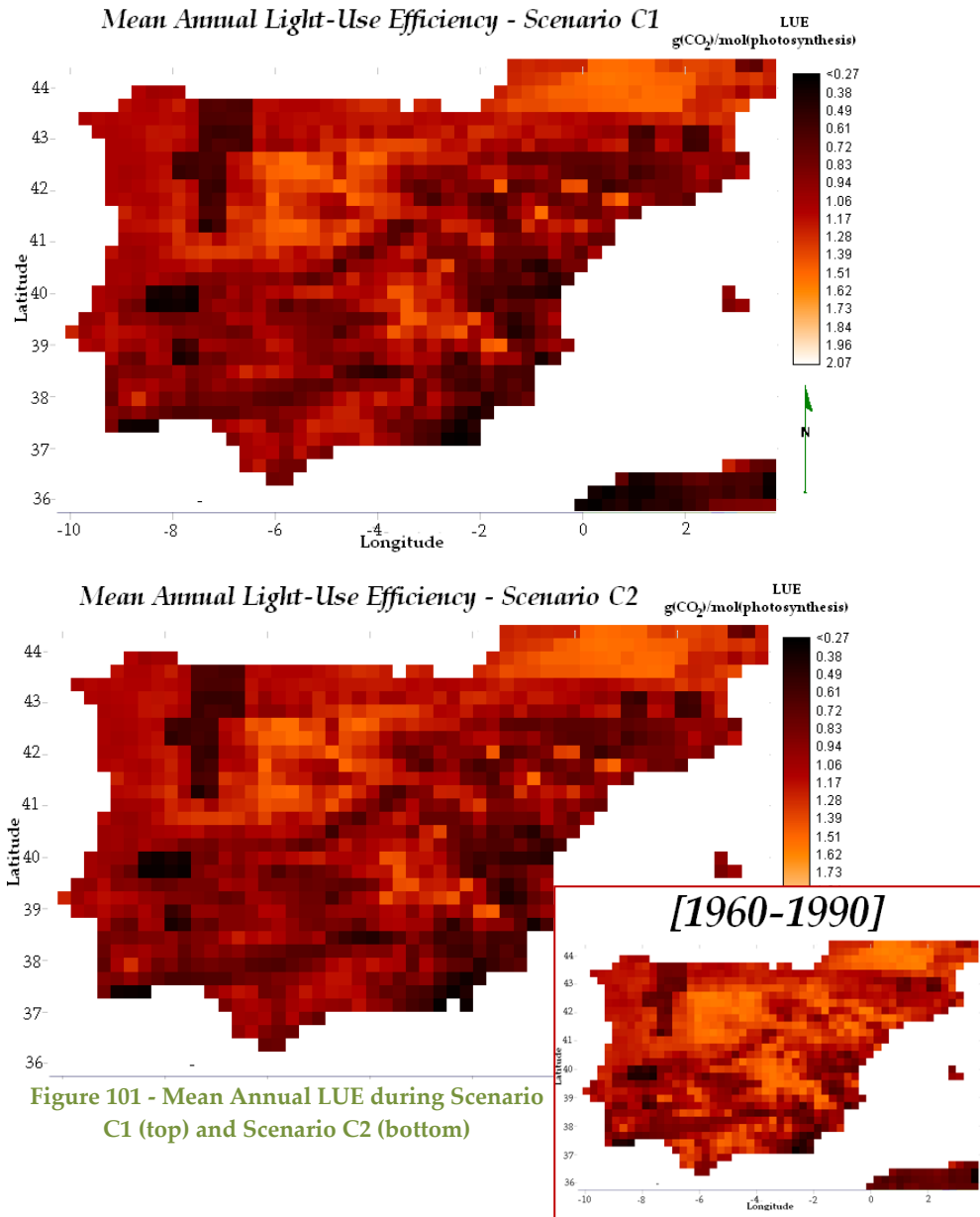


Figure 101 - Mean Annual LUE during Scenario C1 (top) and Scenario C2 (bottom)

On the other hand, the scenarios E1 and E2 (Figure 102), depict increases of 26 and 28% compared to the Reference period (meaning LUE values of 1.46 and 1.48, respectively). Thereby, for the same amount of APAR, the vegetation over IP during these scenarios produces more 26 and 28% of carbon.

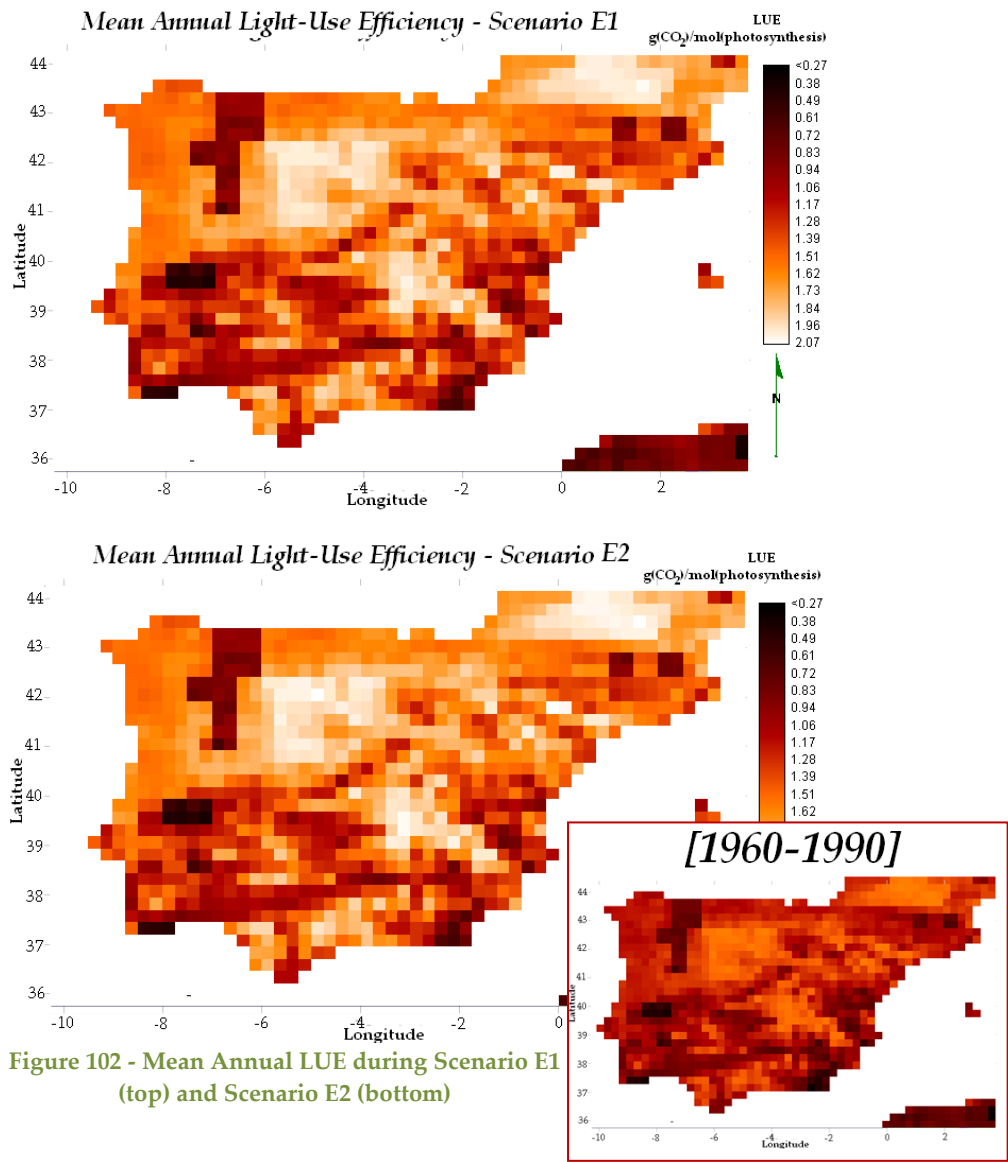


Figure 102 - Mean Annual LUE during Scenario E1 (top) and Scenario E2 (bottom)

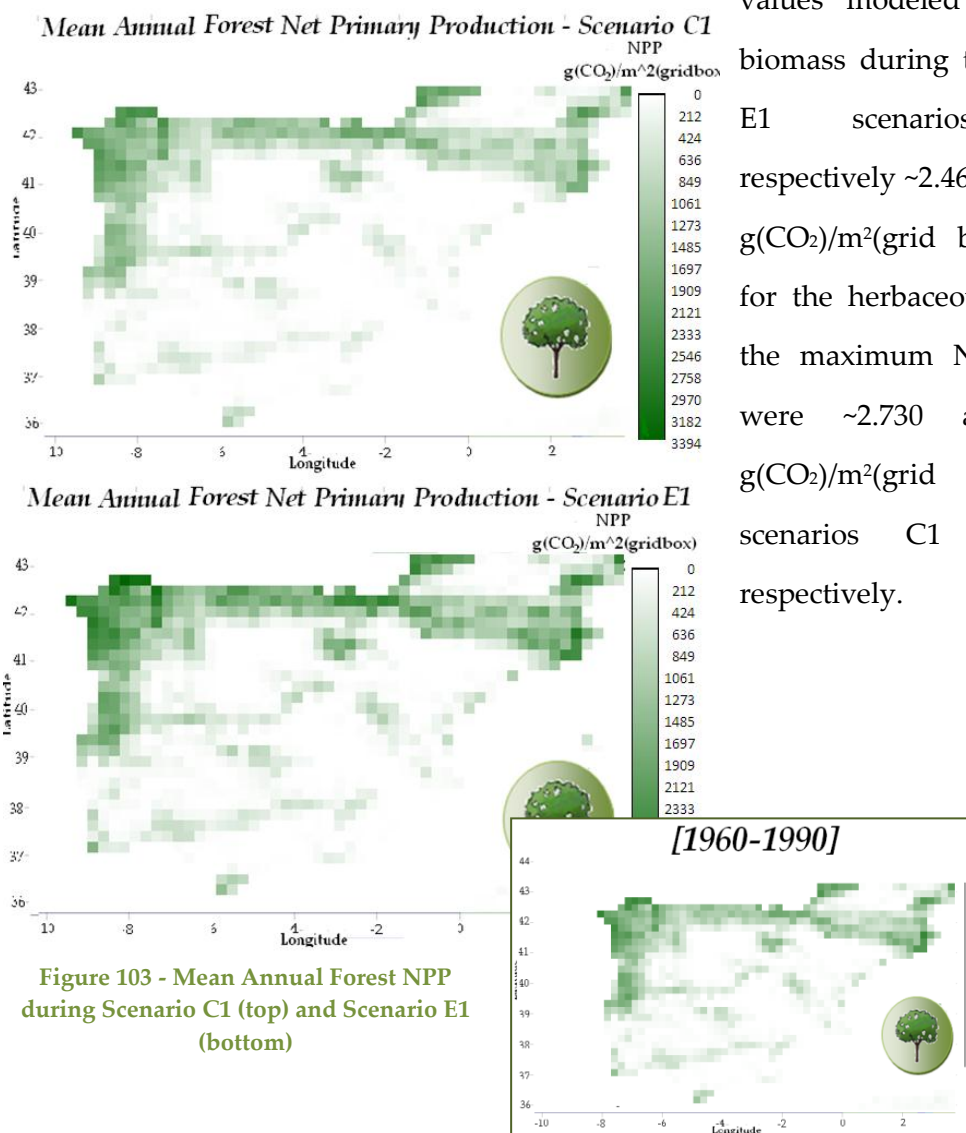
Light-use efficiency was not greatly affected by the transition between the periods of 2060-2090 and 2070-2100, whether it was assumed a constant level of atmospheric CO₂ concentration, or not. Hence, between the scenario C1 and C2, LUE resisted a decrease of 2%, while for the scenarios E1 and E2 this difference was only 1%. Although the magnitude of difference between scenarios “C” and “E” was considerable: between

scenario E1 and C1, there was an increase of 46% of light-use efficiency, and this value reaches 51% for the comparison of scenarios E2 and C2.

4.4.2 Net Primary Production (NPP)

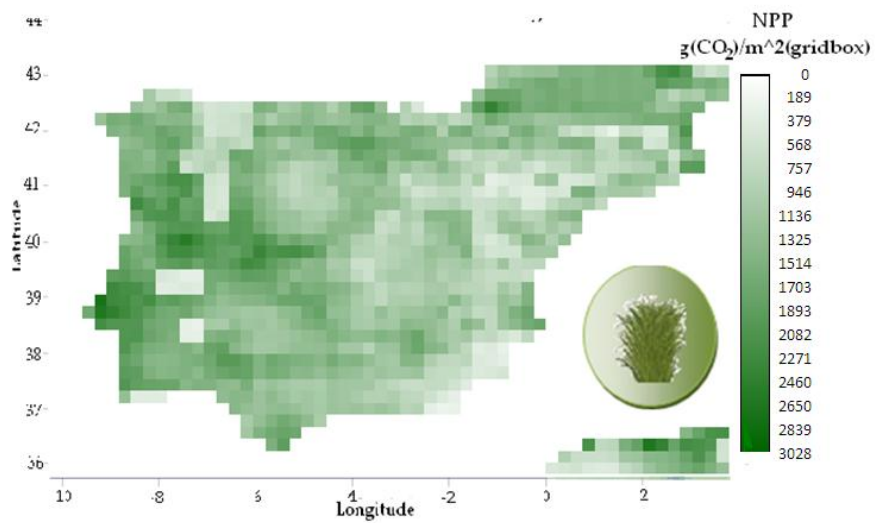
Both forest and herbaceous NPP have shown similar tendencies: comparatively to the reference period the NPP decreased for scenarios "C" (Figure 103) and increased substantially for scenarios "E" (Figure 104) for both biomass types .The maximum NPP

values modeled for forest biomass during the C1 and E1 scenarios were respectively ~2.465 and 3.394 g(CO₂)/m²(grid box), while for the herbaceous biomass the maximum NPP values were ~2.730 and 3.028 g(CO₂)/m²(grid box) for scenarios C1 and E1 respectively.



Both biomass types had a considerable increment in the overall mean NPP. From the scenario C1 to the scenario E1: herbaceous biomass' NPP increased from 1.260 to 2.028 g(CO₂)/m²(grid box), whereas for forest biomass it increased from 389 to 539 g(CO₂)/m²(grid box).

Mean Annual Herbaceous Net Primary Production - Scenario C1



Mean Annual Herbaceous Net Primary Production - Scenario E1

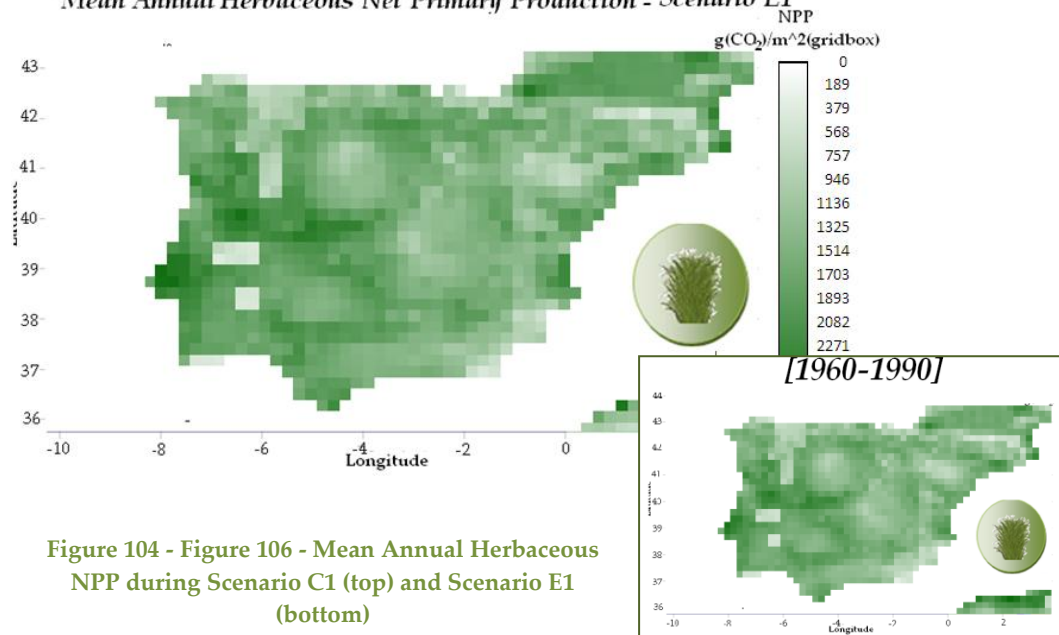


Figure 104 - Figure 106 - Mean Annual Herbaceous NPP during Scenario C1 (top) and Scenario E1 (bottom)

The difference in both biomass types in means of percentage is shown in Figure 105. The NPP underlying forest biomass verified more impact of CO₂, as the maximum

percentage change occurring reached up to ~170%, while the maximum verified for herbaceous biomass was around 136%. The areas subject to most changes in NPP are similar for both forest and herbaceous biomass and it resembles the same spatial pattern of percentage change of GPP during a scenario of constant CO₂ and elevated CO₂ (Figure 105).

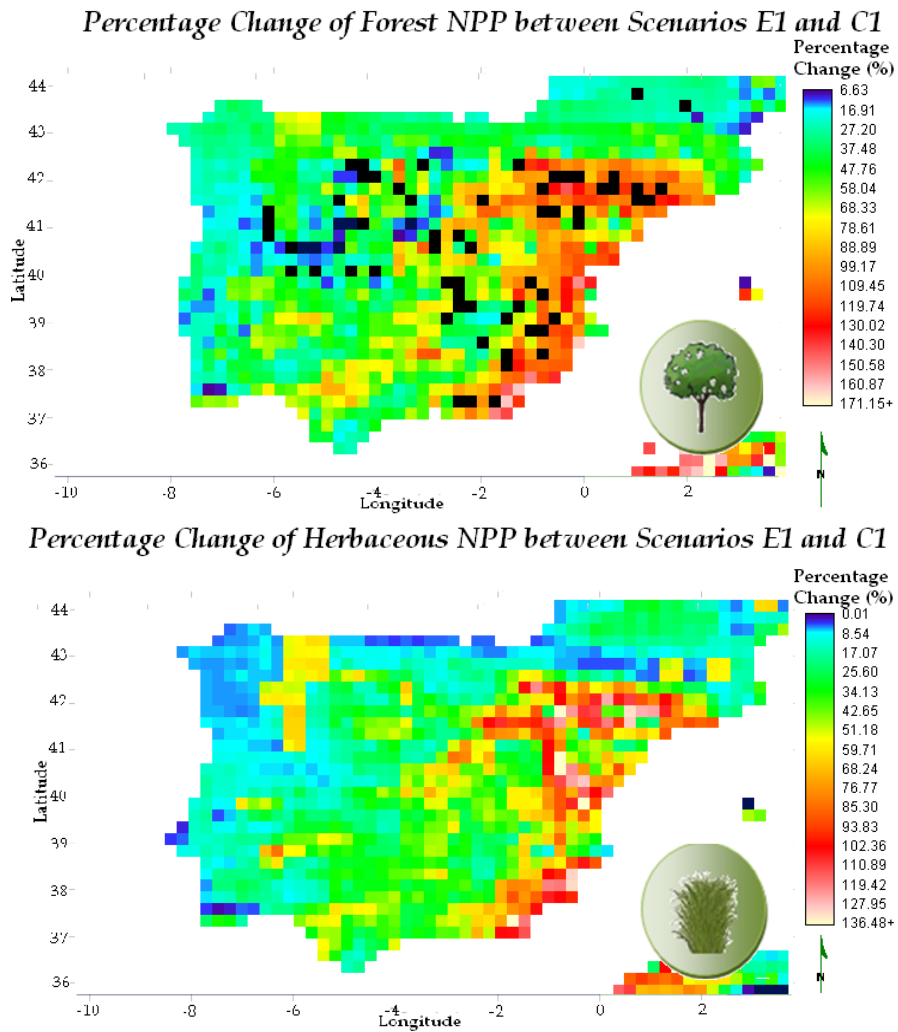


Figure 105 - Percentage change of forest (top) and herbaceous (bottom) NPP between Scenario E1 and C1

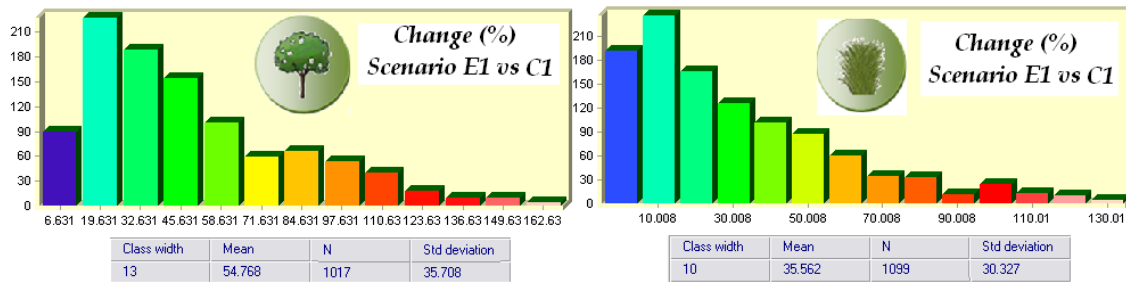


Figure 106 - Histograms and statistical analysis of Percentage Change of Forest (left) and Herbaceous (right) NPP between Scenario E1 and C1

NPP and GPP interannual correlation

From the analysis of coefficient correlations (provided in Table 42) between the mean annual NPP and the mean annual GPP (considering all biomass) over the IP during the future scenarios, it is noticeable an increase of strength of the relationship of these two variables in comparison to the reference period. The scenarios disregarding CO₂ rise are those where NPP and GPP are more correlated, although there is not a considerable change between each period (i.e. 2060-2090 and 2070-2100).

Table 42 - Parson's coefficients between NPP and GPP over the IP, during Future Scenarios

SCENARIOS	Reference Period	C1	C2	E1	E2
Coefficient of Correlation "R"	0,88	0.91	0.92	0.89	0.89

Figure 107 also enables to understand (through the value of R^2), that the NPP and GPP relationship can be "more explained" as a linear relationship, as the regression line fits better the correlation between these two variables. The considerable change in NPP and GPP correlation might be linked to the response of autotrophic respiration to climate change. This process is an important component of vegetation carbon balance (as well as the CO₂ budget), although so far the autotrophic respiration response to increasing concentrations of CO₂ in the atmosphere is not fully understood (Bunce, 2004).

Mean annual NPP vs Mean annual GPP

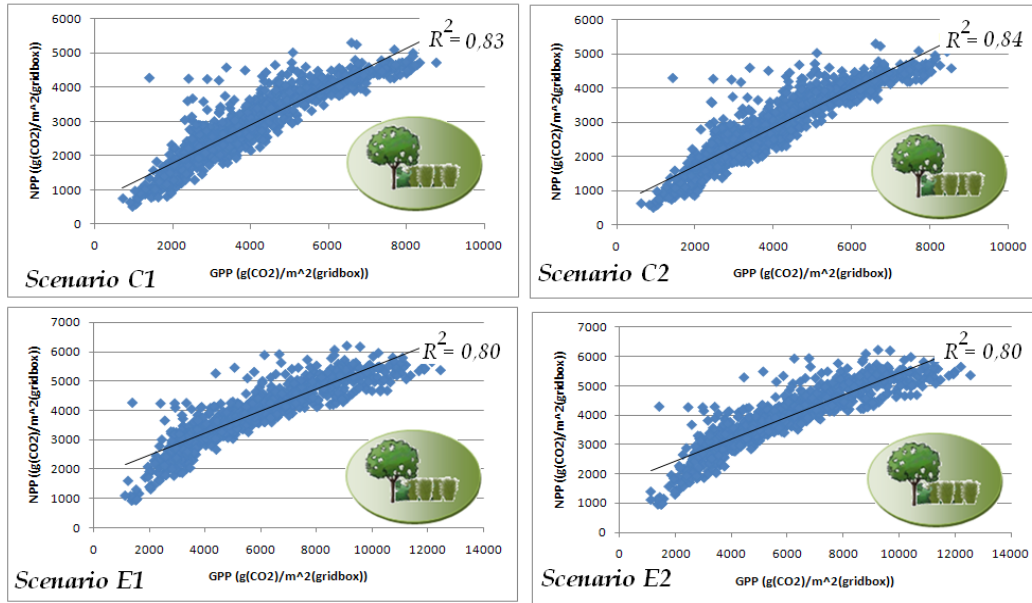


Figure 107 - Regression analysis and coefficients of determination between NPP and GPP during Future Scenarios

Comparison of results with other studies

The conclusions concerning productivity response to climate change in regions such as Iberian Peninsula widely different from author to author. For instance, the IPCC (2001) stated with a medium confidence¹⁴ that the increase of agricultural yields for most crops as a result of increasing atmospheric CO₂ concentration would be counteracted by the risk of water shortage in southern and Eastern Europe, and hence this regions would have decreases in productivity. These projections are supported by other authors (e.g. Rost *et al.*, 2009). On the other hand, Reyer & Gutsch (n.d.) stated that in the Mediterranean forests, the effect of elevated concentration of atmospheric CO₂ on stomatal conductance, will lead to enhanced water-use-efficiency (which is consistent with the findings present in section regarding the WUE during future scenarios) resulting in increased productivity and biomass production. Reyer & Gutsch (n.d.) also stated that despite the key limiting factors for each forest (such as temperature for Temperate forests or water availability for Mediterranean forest), both biomes'

¹⁴ The authors of the report assign a confidence level that represents the degree of belief among the authors in the validity of a conclusion. A quantitative confidence level of 33-67%, was assigned to "medium confidence level".

responsiveness to [CO₂] reveal to be very consistent and positively related to productivity and biomass changes.

Since despite the decreases in ET, rainfall and soil moisture, the productivity is expected to increase considerably, perhaps we could assume that the JSBACH model hence, attributes a considerable weight on CO₂ fertilization (at least high enough to offset the water scarcity conditions), comparatively to other studies.

4.4.3 Biomass Potentials for Future Scenarios

Both sets of herbaceous and biomass maps results provided by the JSBACH model, have no visual expression in what concerns a perceptible change in aerial densities as they look similar to the maps obtained in Figure 61 and Figure 62, respectively, and hence they are not here disclosed. Notwithstanding, the results of forest and herbaceous biomass are significantly different in future scenarios when compared to the reference period.

In terms of absolute biomass, the shares of forest and herbaceous biomass differed from what was estimated for the 1960-1990 period (i.e. 78% and 22% for forest and herbaceous biomass, respectively). For both scenarios C1 and C2, the contribution of herbaceous biomass has decreased by 6% compared to the reference period, while the forest biomass accounted with more of the same percentage for the overall biomass over the IP. On the other hand, for the scenarios assuming elevated concentrations of atmospheric CO₂, the change in contribution of each biomass type to the overall scheme just differed by 1% from the reference period (decreasing for herbaceous and increasing for forest biomass) (Figure 108). In terms of absolute biomass values, these values can be found in the table below (Table 43).

*Percentage of "Forest" and "Herbaceous" biomass
in future scenarios "C" and "E"*

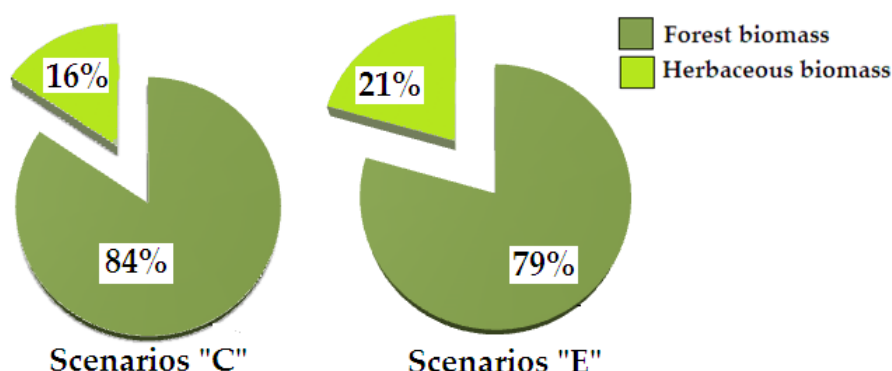


Figure 108 –Share of Herbaceous and Forest Biomass to the overall amount during Scenarios "C" (left) and Scenarios "E" (right)

Table 43 –Absolute amounts of Forest and Herbaceous Biomass (tonnes) during the Future Scenarios C1, C2, E1 and E2

	C1	C2	E1	E2	"E" / "C"
FOREST BIOMASS	7,46 x 10 ⁸ (tonnes)	7,42 x 10 ⁸ (tonnes)	8,68 x 10 ⁸ (tonnes)	8,73 x 10 ⁸ (tonnes)	16-17%
HERBACEOUS BIOMASS	1,43 x 10 ⁸ (tonnes)	1,36 x 10 ⁸ (tonnes)	2,26 x 10 ⁸ (tonnes)	2,25 x 10 ⁸ (tonnes)	55-65%

The comparison between the forest biomass from the reference period and the futures scenarios "C" and "E" discriminated by PFT (Figure 109), enable to understand that the major differences occurred in temperate broadleaf deciduous trees and coniferous evergreen trees. These two PFT showed a considerable increase in biomass in response to elevation of CO₂ levels, especially the latter, which biomass increased over 50.000.000 tonnes between the reference period and the both future scenarios E1 and E2. The most significant difference in biomass from the reference period to the future scenarios with constant CO₂ levels occurred for the coniferous evergreen trees, which verified a reduction by approximately 25.000.000 tonnes, whereas the remaining PFT presented a considerably lower change (even though the temperate broadleaf deciduous trees had an almost negligible increase).

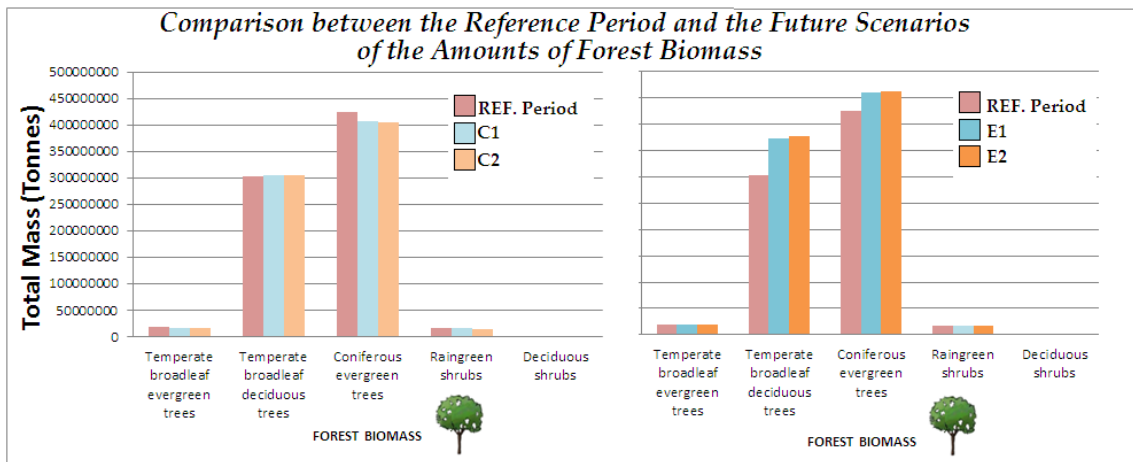


Figure 109 – Comparison of Absolute Amounts of Forest Biomass between Reference Period and Scenarios “C” (left) and between Reference Period and Scenarios “E”(right) segregated by PFTs

The amount of herbaceous biomass presented noticeable differences for the future scenarios assuming constant CO₂. All the four PFTs considered, shown decreases in biomass (Figure 110), being the C3 crops the one most affected by the climate variables, having decreases of approximately 40.000.000 tonnes. This PFT was also the most affected by the variable CO₂ concentration, showing as response to that, an increase of ~10.000.000 tonnes (from the reference period). The remaining PFT did not present significant changes in their biomass: C4 grasses continued to present a decrease as in the constant CO₂ assumptions (although considerably lower), while the C3 grasses and C4 crops have both presented small increases.

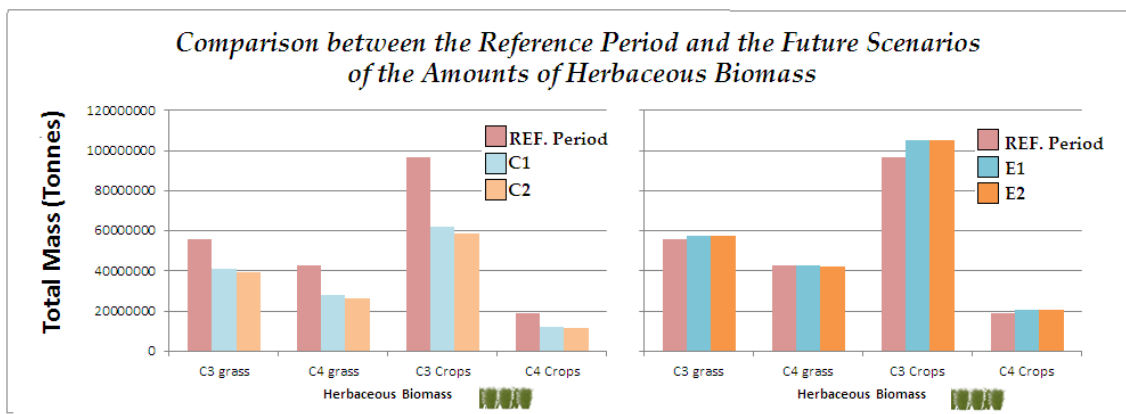


Figure 110 – Comparison of Absolute Amounts of Herbaceous Biomass between Reference Period and Scenarios “C” (left) and between Reference Period and Scenarios “E”(right) segregated by PFTs

Since the scenarios “C” and scenarios “E” differ on the concentration of atmospheric CO₂, the comparison of biomass change between these scenarios enable to depict

differences between the responses of each PFT to the rising CO₂ (since the climate variables are assumed to be changing equally). The Table 44 shows the percentage of change between the scenarios C1 and E1 and scenarios C2 and E2. All PFT (aside deciduous shrubs) showed higher changes for the period 2070-2100 (i.e. between C2 and E2) than the period 2060-2090. The percentage changes of biomass forest and herbaceous biomass between scenarios assuming constant CO₂ and elevated CO₂ concentrations, is disclosed in the Table 44 by PFT.

Table 44 Percentage of Change of Forest and Herbaceous Biomass between Scenarios "C" and Scenarios "E" – Effect of rising CO₂ levels

	(%) CHANGE	E1 vs C1	E2 vs C2
FOREST BIOMASS	Temperate broadleaf evergreen trees	11%	13%
	Temperate broadleaf deciduous trees	22%	23%
	Coniferous evergreen trees	13%	14%
	Rain green shrubs	13%	15%
	Deciduous shrubs	5%	5%
HERBACEOUS BIOMASS	C3 grass	41%	45%
	C4 grass	52%	61%
	C3 Crops	69%	79%
	C4 Crops	67%	76%

The PFT from forest biomass with higher impacts of elevated CO₂ were the temperate broadleaf deciduous trees, followed by rain green shrubs, coniferous evergreen trees, temperate broadleaf evergreen trees and finally deciduous shrubs. By 2060-2090 (C1), approximately 22% of the deciduous forest growth could be attributed to the variation in CO₂ – whereas for deciduous shrubs only 5% of its biomass increase resulted from that.

A possible reason for these tendencies showing different sensitivity of these forests to CO₂ change, could rely on the type and structure of the ecosystem. The results are in accordance with many authors (e.g. Hui *et al.*, 2003; Richardson *et al.*, 2007)), since their studies have ordered the decrease of impact on forest in the following way: deciduous forest, mixed forest, coniferous and peat land – although they refer to environmental changes in general (not highlighting the solely effect of CO₂). For that reason the

findings disclosed in Table 44 should not be compared straightforwardly with the later studies.

Herbaceous biomass showed to be highly CO₂-responsive. The PFTs with higher responses were by order, C3 crops, C4 crops, C4 grasses and C3 grasses. Typically C3 plants are responding better to atmospheric CO₂ increasing, due to the CO₂ saturation effect on C4 leaves. For instance Wand *et al.* (1999) estimated biomass enhancements of 44 and 33%, respectively, for C3 and C4 plants for a doubling atmospheric CO₂ concentration; while Poorter (1993) and Wand *et al.* (1999) concluded that on average the growth stimulation of C4 plants in response to a doubling ambient CO₂ was about 22-33%, compared with 40-44% for C3 plant. Those studies do not correspond to the findings on Table 44: firstly, the increases in biomass (where CO₂ almost reaches the doubling concentrations from the reference period) present at the table are considerably higher, and the other noticeable difference regards the grasses response (i.e. C4 grasses were more sensitive to CO₂ than C3 grasses).

An advantage that may come to C4 grasses (explaining their enhanced CO₂-responsiveness compared to C3 grasses), could be the fact that the ongoing rise in the air (which was verified in) enhances the ability of C4 grass to increase its uptake for some nutrients (BassiriRad *et al.*, 1998). Moreover, Poorter (1993) and Wand *et al.* (1999) concluded that the magnitude of the growth stimulation of C4 plants to elevated CO₂ increases with decreasing soil water availability. Therefore, those results and the findings in Table 44 cannot be considered mutually exclusive in terms of final conclusions (since SWC is projected to decrease Figure 43 and Figure 84). In fact, Wand *et al.* (1999) suggested that under water-stress conditions, C4 species end up to be more competitive than C3 – which in fact characterize the region in the IP where this conditions are more likely to occur (as can be compared from Figure 26 and Figure 84). Many authors (e.g. Berry & Downton, 1982; Cure & Acock, 1986), generally assumed that C4 plants do not respond to elevated CO₂ under well-watered conditions. C4 plants are known to better cope with water stress (Wand *et al.*, 1999), which may be the reason why Campbell *et al.* (2000) concluded that the growth of C4 species in grasslands is more responsive to CO₂ concentration than C3 species.

The magnitude of biomass change (i.e. values and patterns) is different between forest biomass and herbaceous biomass meaning that they have different responses to changes in climate variables and atmospheric CO₂ levels. For the 2060-2090 period, forest biomass showed considerable changes between scenarios C1 and E1, and it present higher values for the later scenario. The highest changes (ranging between approximately 70 and 100%) occur in several areas located along the eastern region of Spain as it can be depicted from the map (Figure 111).

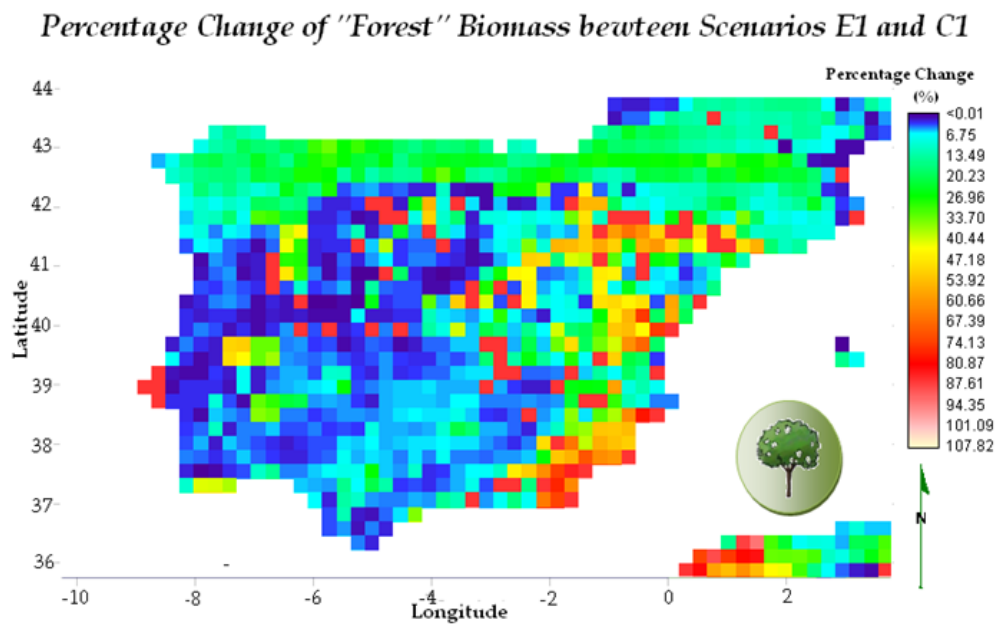


Figure 111 – Percentage of Change of Forest Biomass between Scenario E1 [CO₂]=556ppm and Scenario C1 [CO₂]=296ppm

The green colored area existing evenly along the entire north of Spain (green zone), shows that the forest biomass located at the Temperate zone responded with increases of 20-30% to the elevation of CO₂. The central and southeastern of the IP shows very low percentage changes, lower than 6%. The mean percentage change of biomass response to elevated CO₂ is 23%. The pattern and magnitude change between scenarios C2 and E2 had similar results), although the overall percentage increase is higher (~25%) (Figure 112).

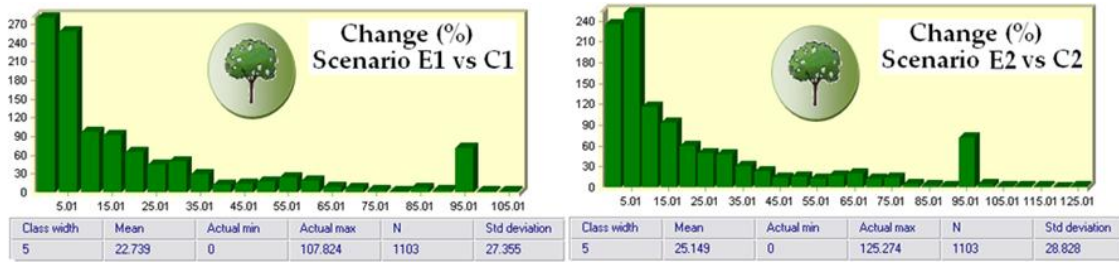


Figure 112 – Histograms and Statistical Analysis of Percentage Change of Forest Biomass between Scenarios E1 and C1 (left) and between Scenarios E2 and C2 (right)

The results of magnitude of change of herbaceous biomass between a scenario of elevated and constant atmospheric CO₂ was considerably greater than in the previous case. The pattern also seems to be smoother between percentage changes. Almost the entire territory of Portugal verified percentage changes smaller than 7% between scenarios C1 and E1 (Figure 113) as well as the Temperate zone (aside from that area coming inwards from the northern shore (close to Asturias) which has presented lower SWC and evapotranspiration values (Figure 43 and Figure 45)). In this area (as well in the southeast shore and Aragón and Cataluña regions) JSBACH modeled a change by over 215% of herbaceous biomass. In some areas, this biomass type has reached over 500% of percentage of increase (between a scenario of constant and elevated CO₂ levels).

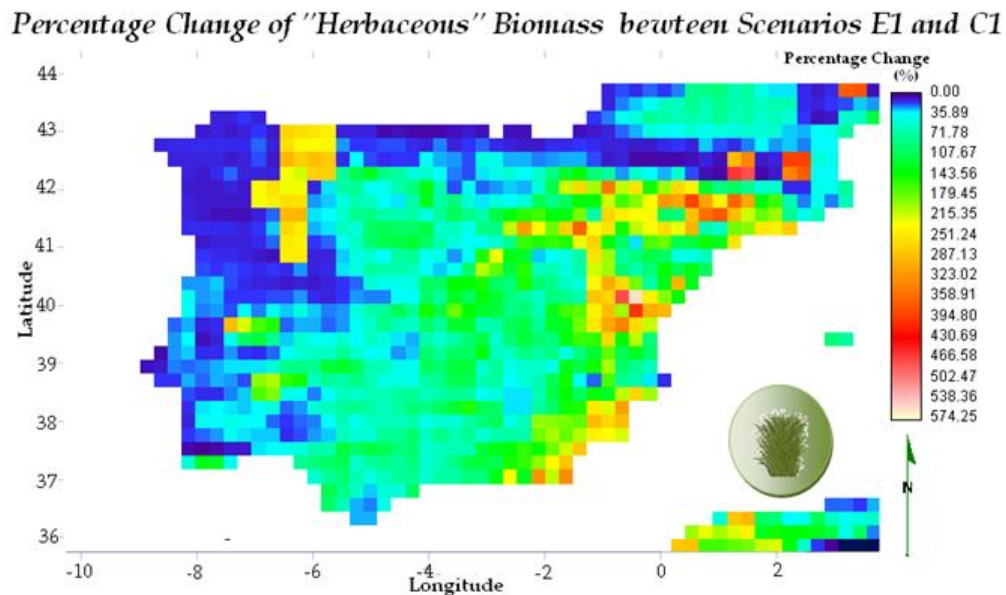


Figure 113 - Percentage of Change of Herbaceous Biomass between Scenario E1 [CO₂]=556ppm and Scenario C1 [CO₂]=296ppm

The overall mean of increase in herbaceous biomass for a elevated CO₂ scenario for the period 2060-2090 was around 89%, although the values of percentage increase more common ranged around 30% (Figure 114). The map of percentage change of

herbaceous biomass between scenarios E2 and C2 had similar results (and for that reason they are not here disclosed). The herbaceous biomass of IP for the period 2070-2100, showed an overall mean of ~100% increase of biomass as a response to elevated atmospheric CO₂ concentration (Figure 114).

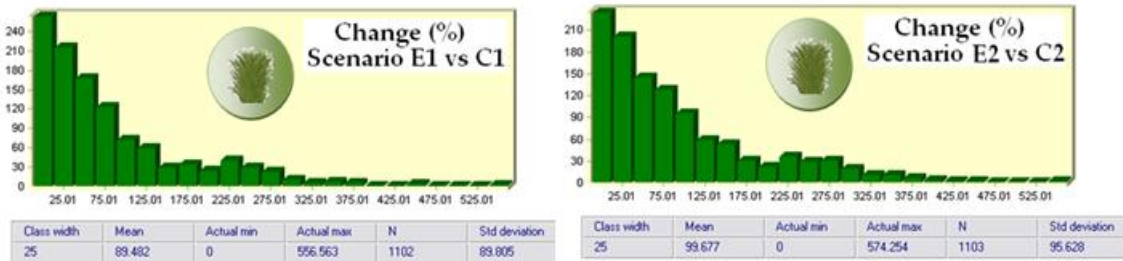


Figure 114 - Histograms and Statistical Analysis of Percentage Change of Herbaceous Biomass between Scenarios E1 and C1 (left) and between Scenarios E2 and C2 (right)

In terms of percentage change of all biomass across the IP between the scenarios assuming constant and elevated CO₂ levels, the set of all PFT has presented an increase of biomass for the later scenarios (Figure 115). The map for the percentage change between scenarios E2 and C2 has presented a similar pattern.

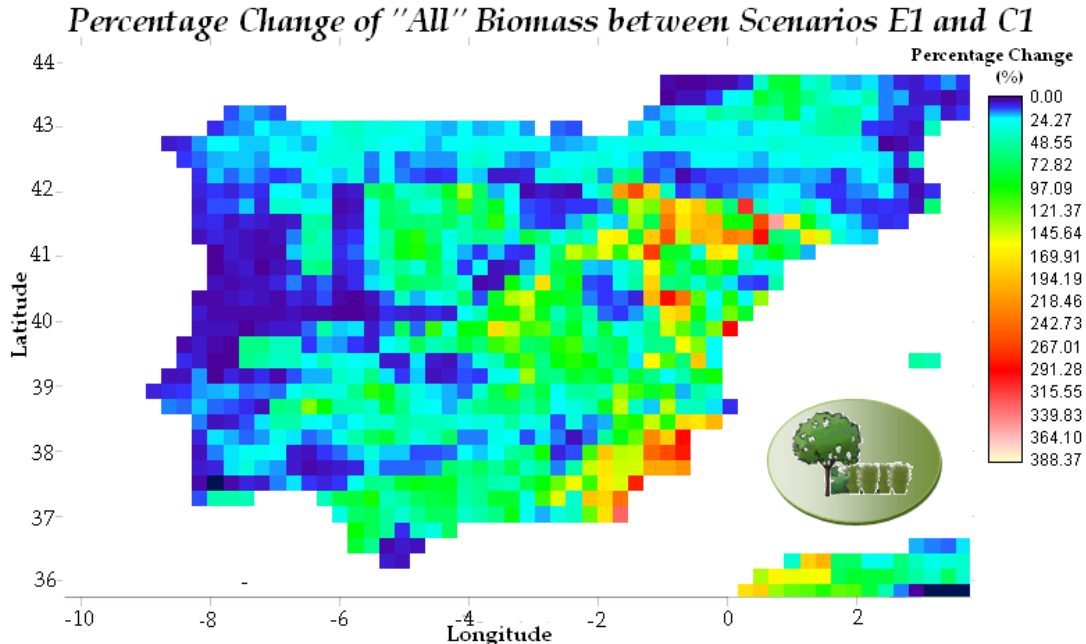


Figure 115 - Percentage of Change of Total Biomass between Scenario E1 [CO₂]=556ppm and Scenario C1 [CO₂]=296ppm

The map above, is considering both biomass types together and for that reason the overall mean percentage change of biomass is higher than when considering solely

forest biomass and lower than considering only herbaceous biomass, i.e. ~49% (Figure 116). For the period 2070-2100, this value reaches up to ~56%.

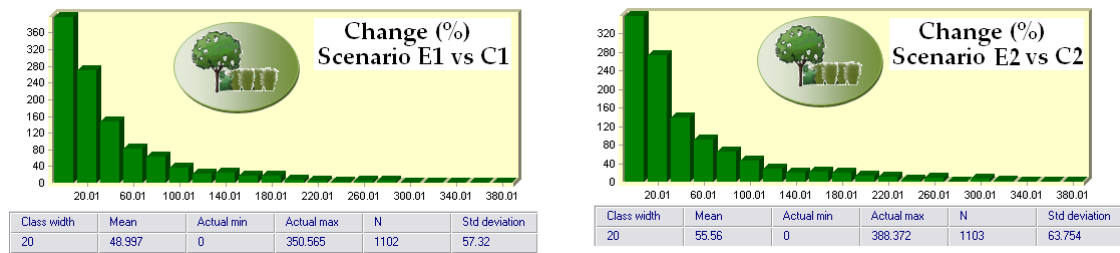


Figure 116 - Histograms and Statistical Analysis of Percentage Change of Total Biomass between Scenarios E1 and C1 (left) and between Scenarios E2 and C2 (right)

4.5 Biomass Response to Climate Change

This section aims to understand how changing climate variables are projected to affect both forest and herbaceous biomass changes under scenarios with constant CO₂ and elevated CO₂ levels. Table 45 presents the correlations coefficients between the variation of each climate variable and the variation of biomass density (in gC/m²) (this variation regards changes between future scenarios and the reference period). The stronger correlations (i.e. $R > 0,4$) are highlighted in bold).

Table 45 - Correlation coefficients between Changing Biomass and Changing Climate Variables

Scenarios	Biomass	Climate variables					
		ΔT	ΔP	ΔET	ΔSWC	ΔPAR	$\Delta APAR$
	$\Delta FOREST$						
Constant CO ₂	C1[2060-2090] – Ref	0,13	0,11	0,38	-0,02	0,03	0,44
	C2[2070-2100] – Ref	0,11	0,13	0,39	-0,04	0,00	0,44
Elevated CO ₂	E1[2060-2090] – Ref	-0,37	-0,07	0,53	0,18	-0,11	0,49
	E2[2070-2100] – Ref	-0,36	0,00	0,52	0,20	-0,06	0,45
	$\Delta HERBACEOUS$	ΔT	ΔP	ΔET	ΔSWC	ΔPAR	$\Delta APAR$
Constant CO ₂	C1[2060-2090] – Ref	-0,51	-0,04	0,77	0,21	-0,0041	0,58
	C2[2070-2100] – Ref	-0,51	0,02	0,76	0,21	-0,02	0,55
Elevated CO ₂	E1[2060-2090] – Ref	-0,10	0,27	0,39	0,00	-0,03	0,31
	E2[2070-2100] – Ref	-0,10	0,30	0,38	-0,03	-0,11	0,31

Forest biomass presents stronger (and positive) relationships with APAR and evapotranspiration and these relationships are likely to become even stronger under

scenarios assuming the CO₂ fertilization effect. On the other hand, the strongest responses of herbaceous biomass occur for changes in ET, APAR and temperature (having a negative relationship with the later) and these variables are (conversely to forest biomass) considerably stronger under scenarios assuming constant CO₂ and the impact of changing precipitation, SWC and PAR on herbaceous biomass trend is, according to the model, negligible. Figure 17 and Figure 118 illustrate the correlation between variation of each biomass type and variations in climate variables - between the period 2060-2090 and the reference period, and under scenarios of constant and rising CO₂ levels (scenarios C1 and E1, respectively).

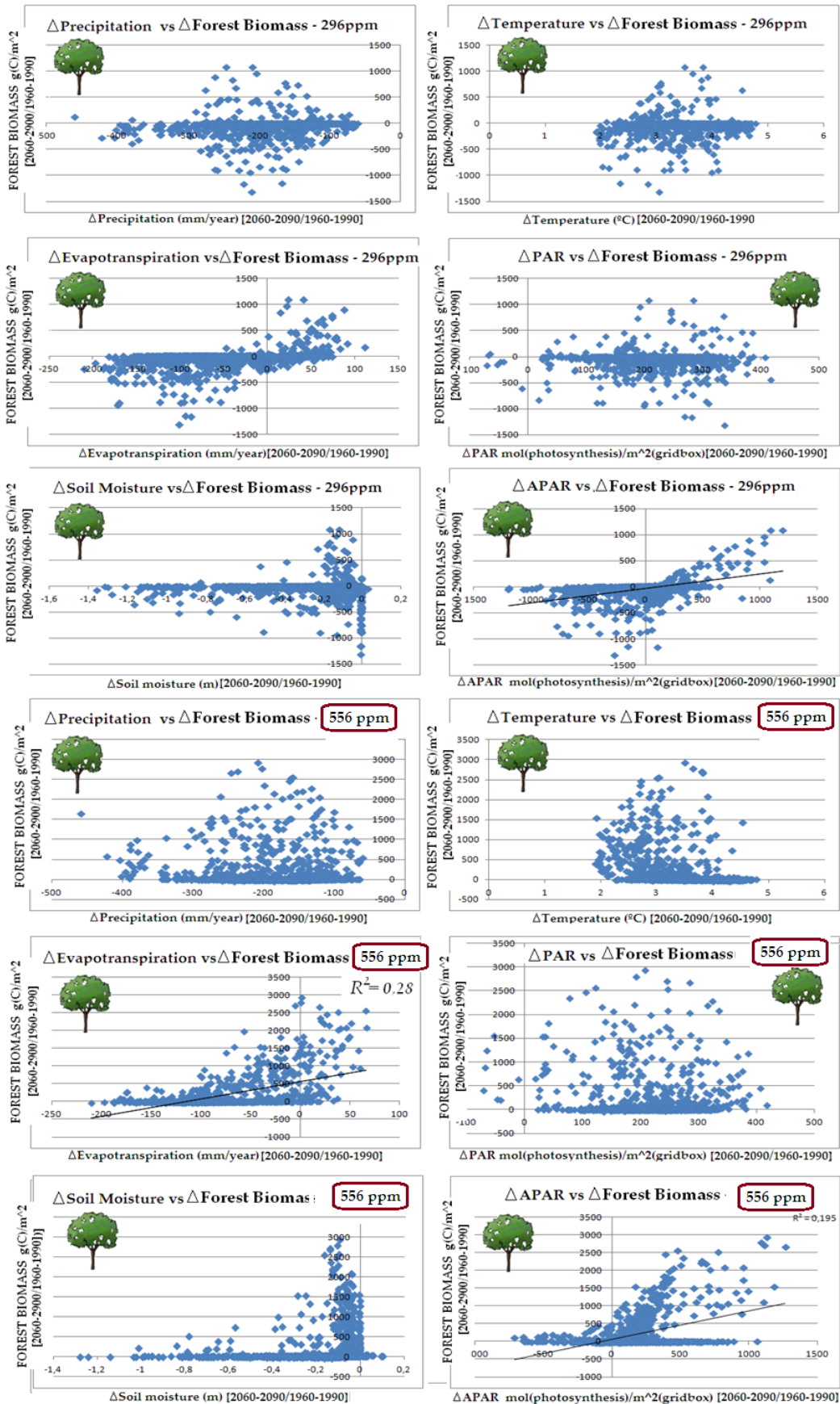


Figure 117- Correlation between interannual variability of Forest Biomass and climate variables – between Scenario C1 and Ref. Period (top six) and between Scenario E1 and Ref. Period (bottom six)

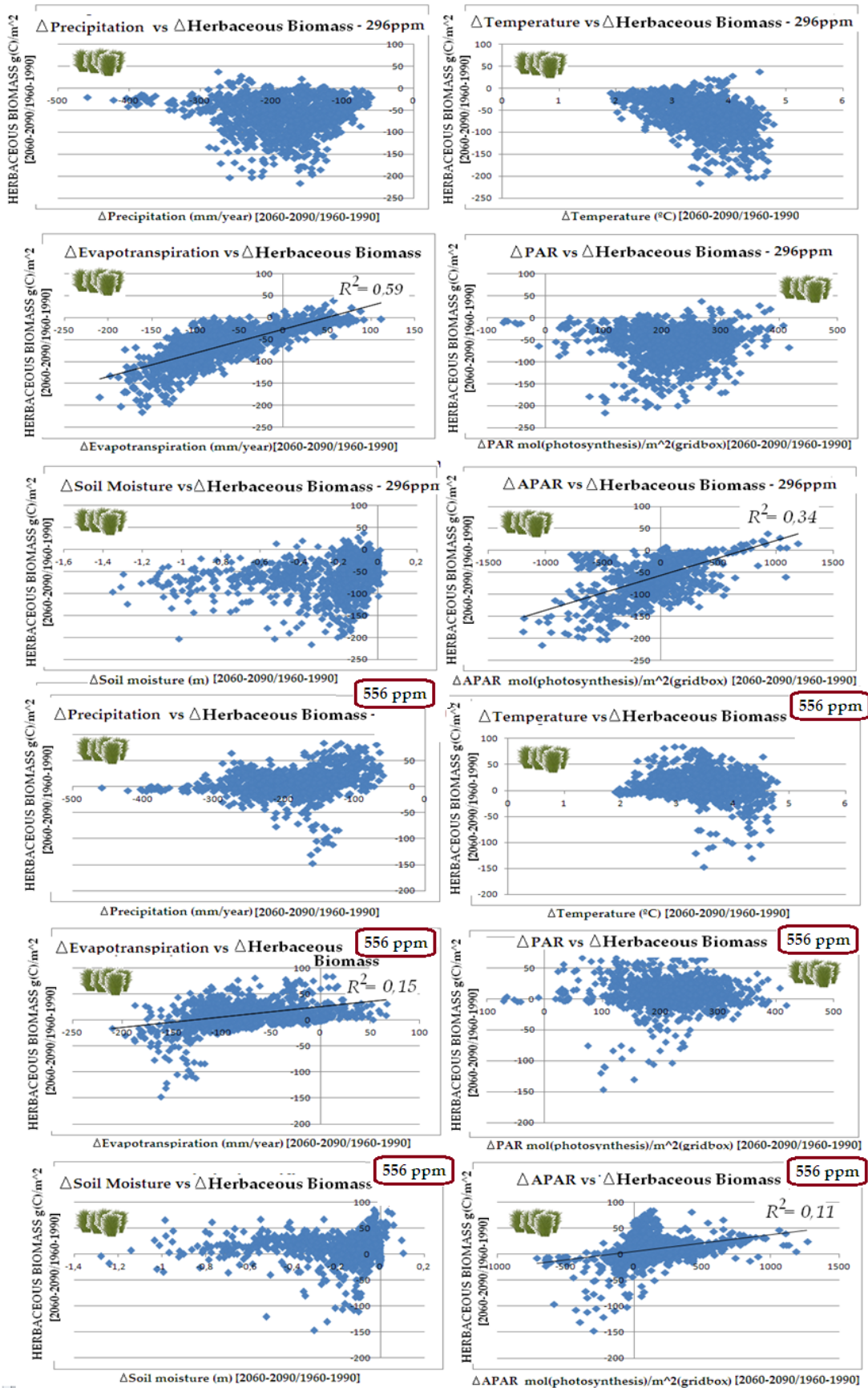


Figure 118 - Correlation between interannual variability of Herbaceous Biomass and climate variables – between Scenario C1 and Ref. Period (top six) and between Scenario E1 and Ref. Period (bottom six)

Regarding firstly the responses of biomass to warming temperature, herbaceous biomass presented in stronger correlation between its interannual variability and interannual change in temperature for scenarios of constant CO₂ levels. The correlation present in the top right graph in Figure 118, roughly resembles a linear relationship. Forest biomass shows no pattern for scenarios of constant CO₂ levels, justifying the negligible correlation between it and temperature ($R=0,13$). For scenarios of elevated CO₂ the response of interannual variability of forest biomass to warming temperatures suffers a considerably shift as it can be depicted from the Figure 120 – where data points above the line illustrates a positive response to warming temperatures.

In what concerns the water balance variables (i.e. precipitation, evapotranspiration and soil moisture), as expected from previous results for impact of climate variables in GPP, the graphs showing the correlation between these variables showed no resembling pattern with exception to the evapotranspiration, which presented a roughly linear shaped pattern. However, the only significant determination coefficient was assigned to the relationship between changing herbaceous biomass and changing evapotranspiration for scenarios assuming constant CO₂ ($R^2 = 0,59$). Despite the negligible correlations with soil moisture, both forest and herbaceous biomass, showed to be more responsive to smaller decreases in soil moisture (i.e. around -0,2m of SWC), although herbaceous were more negatively affected, by decreasing its biomass whereas forest showed mostly increases.

The responses to the variable PAR, lacked a traceable pattern for responses of both forest and herbaceous biomass. From the graphs present in Figure 117 (third graph from the right top, and bottom right graph), for positive change in APAR, the response of forest biomass seems to be roughly linear (although its determination coefficients R^2 negligible). Herbaceous biomass presented higher R^2 (although very small), since its interannual variability shows a smooth linear relationship with interannual variability of APAR (Figure 118).


4.6 Biomass energy Potentials

As described in methodology, the assessment of biomass energy potentials was conducted under two distinct approaches: “*Max Potentials*” consisting in the estimations of forest biomass energy potential derived from clear cuttings activities and “*Plausible Potentials*”, a more realistic approach assuming several scenarios of forest and herbaceous residues use for energy purposes.

Max potential

The “*Max Potential*” approach was broken at the level of some PFT (or group of PFT) depending on being or not subject of interest to be analyzed. The main results can be found in Table 46:

Table 46 –Biomass and Herbaceous Energy Potential from Clear Cutting activities (*Max Potential*) for all scenarios

BIOMASS TYPE	PFT	CONVERSION PATHWAY	POTENTIAL ENERGY (EJ)				
			Ref.	C1	C2	E1	E2
 FOREST BIOMASS (Clear cutting)	ALL*	Combustion	3,362	3,289	3,274	3,828	3,850
		Gasification	4,706	4,604	4,583	5,359	5,389
	Temperate Broadleaf Deciduous Trees	Combustion	1,333	1,345	1,346	1,639	1,656
		Gasification	1,866	1,883	1,884	2,295	2,318
	Coniferous evergreen trees	Combustion	1,868	1,796	1,783	2,023	2,029
		Gasification					
				2,616	2,515	2,496	2,833

*ALL = “All” stands for all the PFT belonging to the biomass type.

The coniferous evergreen trees consist in the PFT accounting with more energy potential, followed by the temperate broadleaf deciduous trees. As expected from the earlier assessment of biomass potential for scenarios C and E, the later present a considerable rise in energy potential when compared to the reference period or scenarios disregarding elevated CO₂. As a result from rising atmospheric CO₂ concentration, the energy potential from a “max potential” perspective increase by 13% from the reference period – and decreases by 2% when CO₂ is assumed to remain constant (Figure 122), considering all forest biomass (i.e. all PTF are accounted).

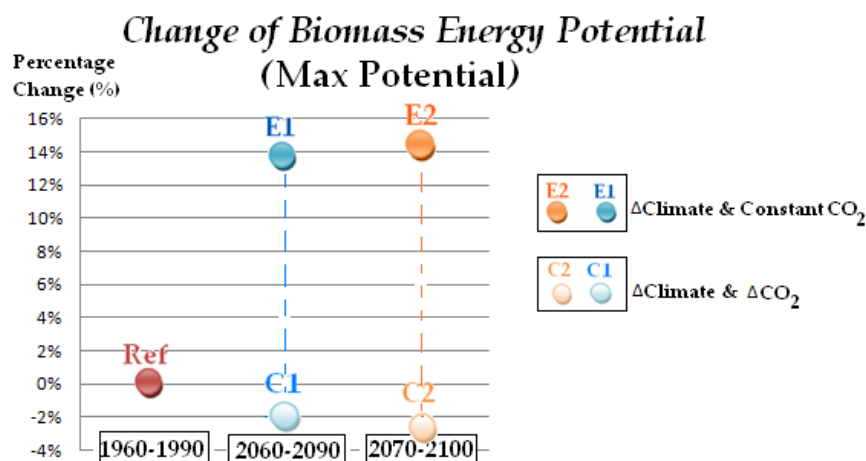


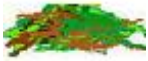
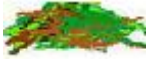

Figure 119- Percentage Change of Biomass Energy Potential from Forest Biomass under a "Max Potential" approach

The energy potential assessment made through the *Max Potential* shows that the forest of the Iberian Peninsula contain an overall mean energy potential of approximately 3,8 EJ for the scenario E1 (when assuming combustion as the conversion pathway).

Plausible Potentials

The biomass energy potential assessment (within a plausible approach) is presented in Table 47, regarding only the scenarios E1 and E2 since they represent the most probable future conditions (in regard of climate variables as well atmospheric CO₂ concentration)(similar tables regarding the results achieved for reference period and scenarios C1 and C2 can be found in Appendix B). The forest residues were accounted separately, in order to avoid double-counting of residues from both activities (i.e. thinning and logging). The energy potentials do not verify a great change between the periods 2060-2090 and 2070-2100. Within the forest biomass group, the PFT comprising shrubs, had the lowest contribute to overall results while the temperate broadleaf deciduous trees and coniferous evergreen trees accounted for most of the total result. The herbaceous biomass has a much lower energy potential due to its considerable lower biomass potential (even though this biomass produces a higher amount of residue per unit of biomass). The crops are among the herbaceous biomass, the PFT with higher energy potential once again due to its greater biomass potential along with its higher LHV value.

Table 47- Plausible approach results for Forest and Herbaceous Biomass under scenarios assuming climate change and elevated CO₂

RESIDUE REMOVAL SCENARIO	BIOMASS TYPE SOURCE	PFT	ENERGY POTENTIAL (EJ)			
			SCENARIO E1		SCENARIO E2	
			Combustion	Gasification	Combustion	Gasification
BAU (10%)	FOREST RESIDUES	All	0,041	0,058	0,041	0,058
		T. B. Deciduous Trees	0,018	0,025	0,018	0,025
		C. evergreen trees	0,022	0,031	0,022	0,031
LOW-YIELD (20%)	 (Top and branches from thinning)	All	0,082	0,115	0,083	0,116
		T. B. Deciduous Trees	0,035	0,049	0,036	0,050
		C. evergreen trees	0,044	0,061	0,044	0,060
HIGH- YIELD (40%)		All	0,165	0,231	0,166	0,1232
		T. B. Deciduous Trees	0,071	0,099	0,071	0,100
		C. evergreen trees	0,087	0,122	0,087	0,122
BAU (10%)	FOREST RESIDUES	All	0,124	0,173	0,124	0,174
		T. B. Deciduous Trees	0,052	0,074	0,054	0,075
		C. evergreen trees	0,065	0,092	0,066	0,092
LOW-YIELD (20%)	 (Logging residues)	All	0,247	0,346	0,249	0,348
		T. B. Deciduous Trees	0,106	0,120	0,107	0,149
		C. evergreen trees	0,131	0,148	0,131	0,149
HIGH- YIELD (40%)		All	0,495	0,693	0,498	0,697
		T. B. Deciduous Trees	0,212	0,297	0,214	0,300
		C. evergreen trees	0,262	0,366	0,262	0,367
BAU (10%)	HERBACEOUS RESIDUES	All	0,086	0,121	0,086	0,121
		C3 and C4 grass	0,037	0,051	0,037	0,051
		C3 and C4 crops	0,050	0,070	0,050	0,070
LOW-YIELD (20%)	 (Straw from agriculture)	All	0,173	0,242	0,173	0,242
		C3 and C4 grass	0,073	0,103	0,073	0,102
		C3 and C4 crops	0,099	0,139	0,099	0,139
HIGH- YIELD (40%)		All	0,346	0,484	0,345	0,483
		C3 and C4 grass	0,147	0,206	0,146	0,205
		C3 and C4 crops	0,199	0,279	0,199	0,278

Comparison with other studies

Table 48 contains results of energy potentials from forest and agricultural residues estimated for the Iberian Peninsula from four studies. The first one was conducted by CRES (Nikolau *et al.*, 2003), the second by the European Environment Agency (EEA, 2006); the third by the RENEW project and the last and more recent one by CHRIGAS (Esteban *et al.*, 2008; Esteban *et al.*, 2010). Despite the use of the same LHV values, the several studies should not be straightforwardly compared due to the lack of information on the methodology followed in most of the works and production values used for the crops involved. Moreover, different time periods are being regarded. In order to compare more proximate results from this dissertation, the table is presenting

the results obtained from biomass residues available during the reference period, since the amount of biomass available then is likely to be similar to the studies (instead of the future biomass potentials where CO₂ has enhanced further biomass generation). This table serve hence as a raw approach to the evaluation of the reliability of the achieved results.

Table 48 - Comparison between assessments on biomass resources (data in EJ/year) estimated by other authors and for the reference period

FOREST RESIDUES			
Authors	Energy Potential (EJ)		
Nikolau <i>et al.</i> (2003)	0,126		
EEA (2006)	0,081		
RENEW (n.d.)	0,068		
Esteban <i>et al.</i> (2010)	0,103		
Aparício (2012)	SCENARIOS	<i>Thinning</i>	<i>Logging</i>
Results from: Reference Period [1960-1990]	BAU	0.036	0.109
Conversion Pathway: Combustion	LOW-YIELD	0.072	0.217
	HIGH-YIELD	0.142	0.435
AGRICULTURAL RESIDUES			
Authors	Energy Potential (EJ)		
Nikolau <i>et al.</i> (2003)	0,150		
EEA (2006)	0,392		
RENEW	0,128		
Esteban <i>et al.</i> (2010)	0,266		
Aparício (2012)	SCENARIOS	<i>Agriculture</i>	
Results from: Reference Period [1960-1990]	BAU	0,082	
Conversion Pathway: Combustion	LOW-YIELD	0,164	
	HIGH-YIELD	0,327	

Concerning forestry, in the present work the values obtained for the available biomass assuming the *BAU* scenario are generally lower than the obtained by other authors. For *LOW-YIELD* scenarios, the energy potential assessed for the reference period is in the range of the other studies, whereas for *HIGH-YIELD* scenarios the results from are considerably higher (which is fairly reasonable, since the removal rates assumed in *HIGH-YIELD* were not applied in Iberian Peninsula at the time that the other studies were developed). Generally, these comparisons state the reasonability of the estimations achieved at the present work.

5 Conclusions

The goals stated for this work include: (1) the understanding of the magnitude of the impact that climate changes and the solely effect of rising CO₂ (in accordance to the prescribed in A1B scenario from IPCC) have in biomass and productivity over the Iberian Peninsula (IP), by (2) modeling the interannual variability in terrestrial productivity and biomass across de region (having the period 1960-1990 as reference) depicting from there (3) the energy potentials derived by biomass in future scenarios (2060-2090 and 2070-2100 periods). The carbon fluxes were modeled by JSBACH model and its results were handled using GIS and statistical analysis. A better understanding of the applicability (and reliability) of this model on achieving the latter stated goals was gained (by comparisons of some results with other authors), reaching this way another goal purposed in this work. This chapter presents the main conclusions achieved regarding those goals.

5.1 Climate change and CO₂ fertilization impact on productivity and biomass

The scenarios "E1" and "E2" (2060-2090 and 2070-2100 periods, respectively) were modeled taking into account the CO₂ fertilization effect while scenarios "C1" and "C2" (2060-2090 and 2070-2100 periods, respectively) kept atmospheric CO₂ constant at 296 ppm. In the latter case, productivity changes were only driven by the modeled changes in climate variables, whereas the first case the full effect of changes in temperature, precipitation and atmospheric CO₂ level is taken into account.

According to the JSBACH model, most regions experience significant increases in productivity (GPP and NPP) under assumed CO₂ fertilization, while for scenarios disregarding elevated CO₂ the productivity and biomass were modeled to decrease (although not as significantly as in scenarios of elevated CO₂). The Temperate Zone presented considerably higher productivity rates comparatively to the Mediterranean zone, due to the greater concentration of forest biomass in the first. Although the spatial distribution of changes in GPP, NPP and biomass across the IP are very similar, (i.e. higher changes were modeled to occur in the eastern and southeastern quadrant of the region), the magnitude of change varied considerably among these three variables. The comparison between “E” and “C” scenarios enabled the understanding of the magnitude of the impact that roughly doubling the CO₂ from 296ppm to 556 ppm and to 598ppm (scenario E1 and E2, respectively) had on productivity. The GPP had an overall mean annual increase by ~41 and ~45% across the IP, whereas forest biomass NPP increased by ~54% and herbaceous biomass NPP by ~36% (between scenarios E1 and C1. In what concerns to the percentage change in forest and herbaceous biomass, Figure 120 illustrates the changes between future scenarios and the reference period, as well as the change in biomass between scenarios assuming constant CO₂ and scenarios accounting with rising CO₂.

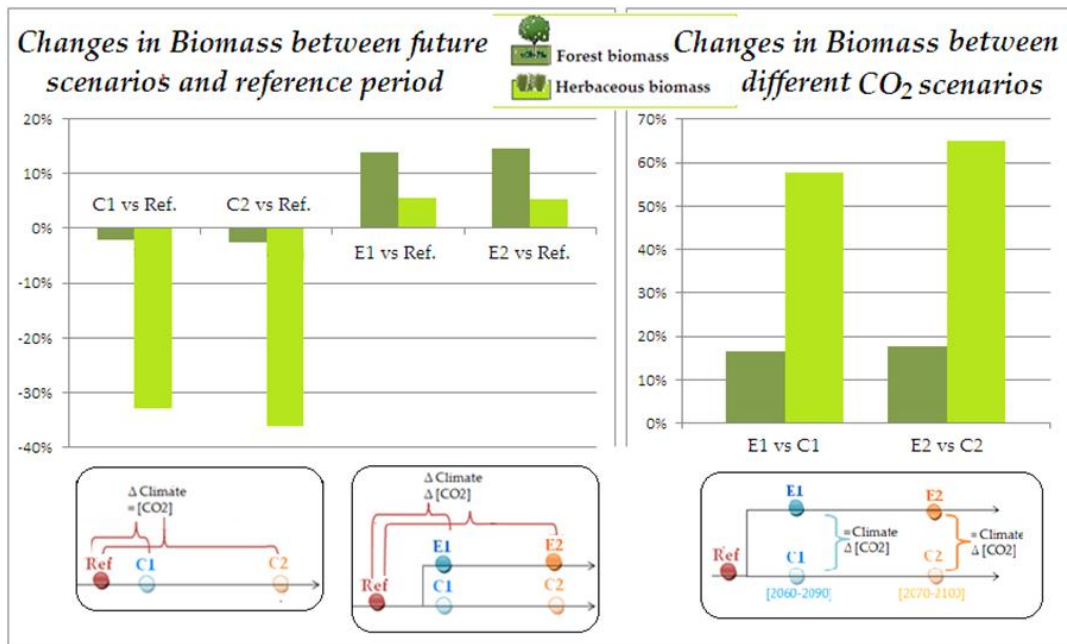


Figure 120 – Comparison of Forest and Herbaceous Biomass changes between futures scenarios and reference period (left) and between elevated atmospheric CO₂ concentration scenarios (E1 & E2) and constant atmospheric CO₂ concentration (C1 and C2) (right)

The climate variables affecting productivity were mostly APAR, followed by evapotranspiration (ET) and precipitation, whereas forest biomass shown to be more affected by APAR, followed by precipitation, ET and temperature. Another major difference was the greater susceptibility of herbaceous biomass to increased temperature (which showed a moderate negative response) under constant CO₂ scenarios, while for forest biomass this correlation was less strong, and positive, under elevated CO₂ scenarios. Despite that, generally the JSBACH model did not enabled to understand the relationship between environmental factors and herbaceous biomass, since the correlations achieved among them were mostly negligible, which could be interpreted as one limitation of the model. Scenarios "C" and "E" also presented differences concerning how productivity (and biomass) were related with climate variables, and how strongly is the variation productivity affected by the variation of climate. GPP showed to be strongly correlated with climate variables for scenarios of constant CO₂, although GPP interannual variation shown to be strongly affected by ET and APAR changes.

The water-use efficiency (WUE) increased for both futures scenarios "C" and "E" comparatively to the reference period. However, the increase verified for elevated CO₂ scenarios was considerably higher than the for constant CO₂ scenarios (WUE > 58% and WUE > 7%, respectively). This rise in WUE explains the great increase in productivity. On the other hand, the light-use efficiency (LUE) decreased for scenarios "C" (LUE < -13%) and increased considerably for scenarios "E" (LUE > 28%). Although WUE tendencies were in accordance with multiple authors, the findings concerning the increase of productivity as a result of the CO₂ fertilization effect over the IP, were not in accordance with multiple authors that predicted instead, lowering productivity rates for the region as a consequence of water shortage driven by climate change. Henceforth, it has to be noted that the beneficial effect of CO₂ fertilization is subject to heavy debate, specially taking into account that the model (comparatively with other research results, is considerably overestimating the effect of CO₂ fertilization), since the IP region is stated as being water-limited and the decrease in water supply (for rising

CO₂ scenarios) is not evidently affecting productivity and biomass growth. On the other hand, besides the assessment of carbon fluxes, the modeled output climate variables (i.e. ET, APAR and soil moisture) enabled to assess the model in what concerns its applicability to projected climate variables (as these results were compared with other authors which considered as well the A1B scenario). Hence, based on these comparisons, the JSBACH model showed an acceptable reliability.

5.2 Biomass Energy Potentials

Under a scenario of elevated CO₂ (the likely trend in future), the biomass energy potentials did not greatly differ between the periods 2060-2090 and 2070-2100. Therefore, for the scenario E1 (2060-2090 period), and assuming combustion as the energy conversion pathway (since this shown to be the one providing more proximate results to other similar studies for the reference period), from forest biomass, the estimations for thinning activities accounted for 0,041 and 0,165 EJ (under *BAU* and *HIGH-YIELD* scenarios – which assume 10 and 40% of removal rate, respectively). For logging activities the estimations under the same scenarios were 0,124 and 0,495 EJ, respectively and the potential biomass energy estimated for herbaceous biomass, as a result of agricultural activities were 0,086 and 0,346 EJ, under scenarios *BAU* and *HIGH-YIELD*. Since these results concern annual averages, herbaceous biomass results are more meaningful for future projections, since unlikely forest biomass activities, agricultural activities mostly have an annual seasonality (i.e. thinning and logging activities are not commonly an annual process).

Assuming the stabilization of both population and consumption per capita for the year 2011 for the next century (i.e. Table 49), just for comparison purposes, the potential energy results would have the share in the total electric consumption presented in Figure 124.

Table 49 - Energy consumption in 2010 in Portugal and Spain (Source:INE, 2010; Pordata, 2012)

	PORTUGAL	SPAIN
Population (millions of inhabitants)	10,6	44,7
Consumption per capita	4.772 (kWh/inhabitant)	6.000 (kWh/inhabitant)
Total annual consumption (EJ)		1,14 EJ

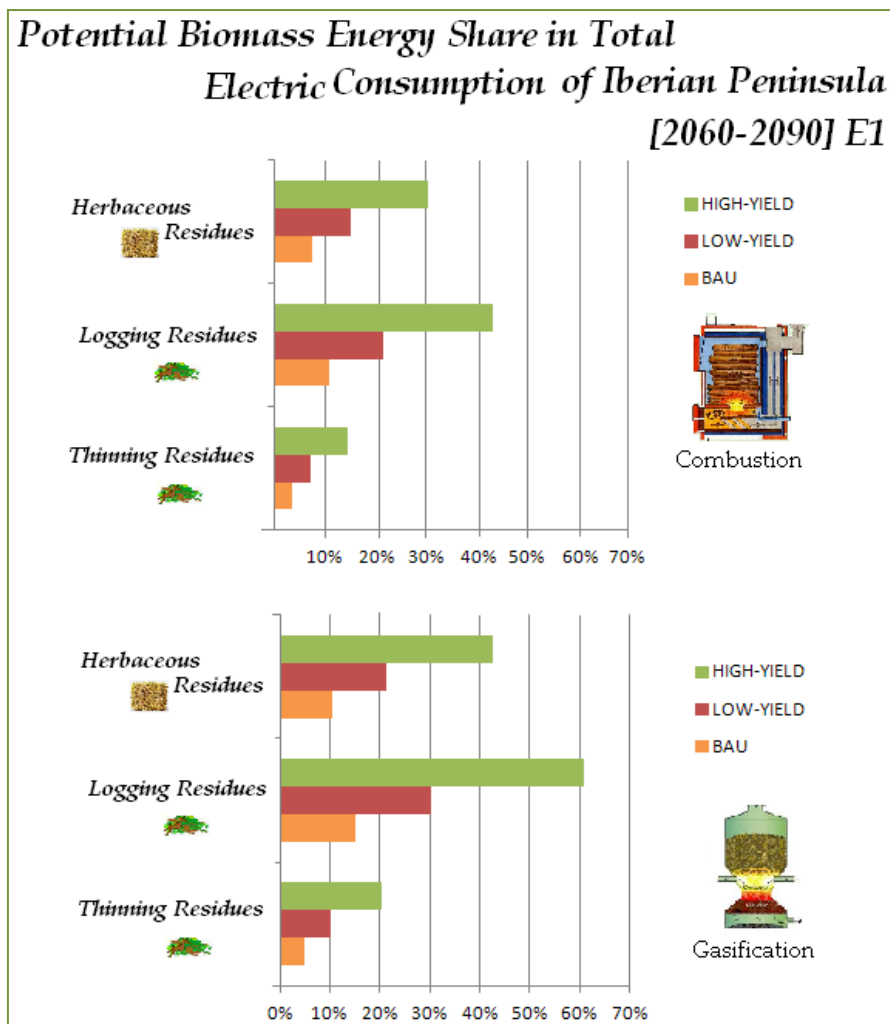


Figure 121 - Potential biomass energy share in total electric consumption of Iberian Peninsula for the Scenario E1 through combustion (top) and gasification (bottom) as conversion pathway processes.

From the overall results provided in Figure 121, in accordance with the results of the present work, the EU target of 20% of renewable energy share in total consumption for the short-term (2020) appears to be achieved assuming a *LOW-YIELD* scenario using solely the herbaceous residues by the time period of 2060-2090 (when gasification is assumed as the conversion pathway of biomass into energy). Nevertheless, in addition to modeling uncertainties, it should be bear in mind that, the methodology applied, along with the assigned dry weight conditions; LHV values and removal rates are subjected of considerable uncertainty as well. On top of that, the total energy consumption upon which the shares of biomass potentials were estimated, refer to 2010 and 2012 demographic and energy consumption in Portugal and Spain,

respectively, and hence they are assumed to remain constant, which is fairly unlikely to happen.

Being bioenergy a strong driver to decarbonize European economies in the long-term, and taking into account the role of biomass, one can state that the *HIGH-YIELD* scenario should be considered in the future, as well as more efficient technologies like gasification. The results achieved with this work show that, an elevated CO₂ concentration will induce an overall increase of the contribution from biomass (both from forestry and herbaceous) to energy use of about 14% and 15% for forest biomass - an increase of EJ (i.e. energy from biomass source) by 2060-2090 and 2070-2100, respectively, when compared with the reference period estimations, and 6% for herbaceous biomass for both future periods. It should also be noticed, that the sole effect of CO₂ fertilization has a meaningful contribution to the increase of EJ, i.e. nearly doubling CO₂ concentration drives an increase around 16% and 38% for forest and herbaceous biomass potential energy comparatively to the reference period.

5.3 Considerations about the model and further research

Besides uncertainties in future developments of drivers (such as climate change, CO₂ fertilization effect, management, technological change), modeling of forest and herbaceous productivity at large scales encompasses an overall uncertainty as many processes are necessarily implemented in a simplified manner. Some of the uncertainties of productivity and biomass results are justified by limitations of the JSBACH model. For instance, according to Alton (2011), current PFT schemes are insufficient for representing the full variability of vegetation parameters necessary to accurately represent carbon cycle processes.

Another constraint of the model is the fact that it does not regard land-use dynamics. Therefore it does not accommodate changes in vegetation cover derived by temperature (e.g. IPCC (2007) stated that a temperature increase greater than 2 °C can result in desert and grassland expansion at the expense of shrublands, as mixed deciduous forest expansion at the expense of evergreen conifer forest); nor competition

between plants; nor decay due to pests benefiting with warmer temperatures. Other limitations of the model include the disregard of the contribution from anthropogenic CO₂ emissions; and the ocean carbon cycle.

Another limitation of the JSBACH model is the absence of nitrogen cycle which also poses great constraints to the acceptance of results. The CO₂ fertilization effect was responsible for broadly increase vegetation yields due to enhanced carbon assimilation rates as well as improved water-use efficiency. However, increased carbon assimilation rates can only be converted into productive plant tissue or the harvested storage organs, if sufficient nutrients are available to sustain additional growth. Hence, even though water supply decreases, the model does not accommodates the less nutrient availability resulting from that, and therefore plant growth is only being constrained by water and not nutrient availability as well. Giving the considerable increase of productivity over the entire region of the IP, it also contributes to the concern whether the model is overestimating the CO₂ fertilization effect or not.

The results of the magnitude of energy potential from biomass resource by 2060-2090 and 2070-2100 periods is likely to be strongly affected by the need to produce feed for livestock, as a result for food competition – and hence, in future research it is recommended careful considerations of biomass in the Iberian food system, in particular in the livestock system – since it is highly important in deriving realistic potentials for future energy from biomass resources supply, i.e. it should be considered a “food first” approach. It is also recommended analysis of carbon fluxes but segregated monthly means, in order to understand as well in annual variability of productivity.

6 References

- AEMET - Agencia Estatal de Climatología. (2012). (Agencia Estatal de Climatología). <<http://www.aemet.es/es/serviciosclimaticos/datosclimatologicos>> (visited 21, September, 2012).
- Ahl, D. E., Gower, S. T., Burrows, S. N., ^a, Sean Shabanov, N. V., Myneni, R. B. & Knyazikhin, Y. (2006). Monitoring spring canopy phenology of a deciduous broadleaf forest using MODIS. *Remote Sensing of Environment*, **104**, 88–95.
- AEBIOM - European Biomass Association (AEBIOM) (2011). Annual Statistical Report on the contribution of Biomass to the Energy System in the EU27. <<http://pt.scribd.com/doc/73012151/2011-AEBIOM-Annual-Statistical-Report>>. (visited 5, May, 2012).
- Ainsworth, E. A. & Long, S. P. (2005). What have we learned from 15 years of free-air CO₂ enrichment (FACE)? A meta-analytic review of the responses of photosynthesis, canopy properties and plant production to rising CO₂. *The New Phytologist*, **165**, 351-71.
- Alcaraz, D., Paruelo, J. & Cabello, J. (2006). Identification of current ecosystem functional types in the Iberian Peninsula. *Global Ecology and Biogeography*, **15**, 200 – 212.
- Alton, P. B. (2011). How useful are plant functional types in global simulations of the carbon, water and energy cycles? *J. Geophys. Res.*, **116**, G01030.
- Amthor, J.S. *et al.* (1998). *Terrestrial Ecosystem Responses to Global Change: a research strategy*. ORNL Technical Memorandum 1998/27, Oak Ridge National Laboratory, Oak Ridge, Tennessee. 37 pp.

- Amthor, J.S. & Baldocchi, D.D. (2001) Terrestrial Higher Plant Respiration and Net Primary Production. *Terrestrial Global Productivity*, [in Academic Press], 35 – 59.
- Anderson, J., Tibbitts, J. & Weber, K. T. (2009). *2007 Range Vegetation Assessment at the O'Neal Ecological Reserve, Idaho*. Pages 3 – 14 in K.T. Weber and K. Davis (Eds.), *Final Report: Comparing Effects of Management Practices on Rangeland Health with Geospatial Technologies (NNX06QE47G)*, 168 pp.
- Atkin, O. K. & Tjoelker, M. G. (2003). Thermal acclimation and the dynamic response of plant respiration to temperature. *Trends Plant Sci.*, **8** (7), 343 – 51.
- Bacaria, J. et al. (1999). *Environmental Atlas of the Mediterranean*. Fundació Territori i Paisatge Eds.
- BassiriRad, H., Reynolds, J. F., Virginia, R. A. & Brunelle, M. H. (1998). Growth and root No-3 and Po-42 uptake capacity of three desert species in response to atmospheric CO₂ enrichment. *Australian Journal of Plant Physiology*, **24**, 353 – 358.
- Berndes, G. (2003) The contribution of biomass in the future global energy supply: a review of 17 studies. *Biomass and Bioenergy*, **25**, (1), 1- 28.
- Berndes, G. & Hanson, J. (2007). Bioenergy expansion in the EU: Cost-effective climate change mitigation, employment creation and reduced dependency on imported fuels. *Energy Policy*, **35**, 5965-5979.
- Berry, J. A. & Downton, J. S. (1982). Environmental regulation of the photosynthesis. In *Photosynthesis, Development, Carbon Metabolism and Plant Productivity* (ed. Govindjee), Academic Press, New York, pp. 263 – 343.
- BISYPLAN *Web-based Handbook*. (2012). <<http://bisyplan.bioenarea.eu/>> (visited 27th,September, 2012).
- Blum, A. (2005). Drought resistance, water-use efficiency, and yield potential – are they compatible, dissonant, or mutually exclusive? *Australian Journal of Agricultural Research*, **2005**, 1159 – 1168.
- Boberg, F. & Christensen, J. H. (2012). Overestimation of Mediterranean summer temperature projections due to model deficiencies. *Nature Climate Change*, **2**, 433 – 436.
- Boer, G. J. (1993). Climate change and the regulation of the surface moisture and energy budgets. *Clim Dyn*, **8**, 225–239.

- Bohn, U., Gollub, G. & Hettwer, C. (2000). *Reduced general map of the natural vegetation of Europe. 1:10 million*. Bonn-Bad Godesberg.
- Bonan, G. B. (2002). *Ecological Climatology: Concepts and Applications*. Cambridge: Cambridge University Press, 678 pp.
- Bondeau, A., Smith, P.C., Zaehle, S., Schaphoff, S., Lucht, W., Cramer, W., Gerten, D., Lotze-Campen, H., Müller, C., Reichstein, M., Smith, B. (2007). Modelling the role of agri- culture for the 20th century global terrestrial carbon balance. *Glob. Change Biol*, **13**, 679- 706.
- Bosetti, V., Paltsev, S., Reilly, J. & Carraro, C. (2012). Emissions Pricing to Stabilize Global Climate. *MIT Join Program on the Science and Policy of Global Change*, Report **211**.
- Bowes G. (1991). Growth at elevated CO₂: photosynthetic responses mediated through Rubisco. *Plant Cell Environ*, **14**,795–806.
- BP (2006). Quantifying energy BP Statistical Review of World Energy. <http://www.bp.com/liveassets/bp_internet/russia/bp_russia_english/STAGING/local_assets/downloads_pdfs/s/Stat_Rev_2006_eng.pdf> (visited 6, May, 2012).
- Blanco, E., Casado, M.A., Costa, M., Escribano, R., García, M., Génova, M., Gómez, A., Gómez, F., Moreno, J. C., Morla, C., Regato, P., Sainz, H. & Sain Ollero, H. (1998) *Los bosques ibéricos.*, Barcelona: Geoplaneta.
- Brand, M. A. (2007). *Fontes de biomassa para a geração de energia*, Brasil: Universidade do Estado de Santa Catarina Brito, J.O. & Barrichelo, L.E.G. *Química da madeira*. Piracicaba: ESALQ/DS, (1983): 136pp..
- Buishand & Brandsa. (1999) Dependence of precipitation on temperature at Florence and Livorno (Italy). *Clim Res*, **12**, 53–63.
- Broadmeadow, M. & Matthews, R. (2003). Forests, Carbon and Climate Change: the UK Contribution. *Information Note 48*. Edinburgh: Forestry Commission.
- Bromwich, D. H., Rogers, A. N., Kallberg, P., Cullather, R. I., White, J. W. C., & Kretz, K. J. (2000). *Journal of Climate*, **13**, 1406 – 1420.
- Bushnell, D.J., Haluzok, C. & Dadkhah-Nikoo, A. (1989). *Biomass fuel characterization, testing and evaluating the combustion characteristics of selected biomass fuels*. Bonneville Power Administration, Corvallis, OR.

- Campbell, J. E., Lobell, D. B., Genova, R. C., Field, C. B. (2008) The global potential of bioenergy on abandoned agriculture lands. *Environ Sci Technol*, **42** (15), 5791–5794.
- Campbell, B. D., Stafford, S., Ash, D. M., Fuhrer, J. Gifford, R. M., Hiernaux, P., Howden, S. M., Jones, M. B., Ludwig, J. A., Manderscheid, R., Morgan, J. A., Newton, P. C. D., Nosberger, J., Owensby, C. E., Soussana, J. F., Tuba, Z. & ZuoZhong, C. (2000). A synthesis of recent global change research on pasture and rangeland production: reduced uncertainties and their management implications. *Agriculture, Ecosystems and Environment*, **82**, 39 – 55.
- Canadell, J.G., Pataki, D., Gifford, R., Houghton, R. A., Lou, Y, Raupach, M. R., Smith, P. & Steffen, W. (2007) in *Terrestrial Ecosystems in a Changing World*, International Geosphere–Biosphere Programme Series, eds Canadell, J. G., Pataki. D., Pitelka, L. Berlin: Springer, 59–78 pp.
- Cartalis, C., Synodinou, A., Proedrou, M., Tsangrassoulis, A. & Santamouris, M. (2001). Modifications in energy demand in urban areas as a result of climate changes: An assessment for the southeast Mediterranean region. *Energy Conversion and Management*, **42** (14), 1647-1656.
- Chang, R. (2005). *Chemistry*, Williams College, 8 ed.
- Chasmer, L., C. Hopkinson, P. Treitz, H. McCaughey, A. Barr, and A. Black. (2008). A lidar-based hierarchical approach for assessing MODIS fPAR. *Remote Sensing of Environment*, **112**, 4344–4357.
- Climate Change Science Program (CCSP) L. Clarke *et al.* (2006). CCSP Synthesis and Assessment Product 2.1, Part A: Scenarios of Greenhouse Gas Emissions and Atmospheric Concentrations., US Climate Change Science Program, Draft for CCSP Review.
- Collatz, G. J., Ribas-Carbo M. & Berry, J. A. (1992) Coupled photosynthesis-stomatal conductance model for leaves of C4 plants. *Aust J Plant Physiol*, **19**, 519 – 538.
- Cramer, W., Bondeau, A., Woodward, I., Prentice, C., Betts, R., Brovkin, V., Cox, P., Fisher, V., Foley, J., Friend, A., Kucharik, C., Lomas, M., Ramankutty, N., Sitch, S., Smith, B., White, A. & Young, C. (2001). Global response of terrestrial

- ecosystem structure and function to CO₂ and climate change: results from six dynamic global vegetation models. *Global Change Biology*, **7**, 357-373.
- Cure, J. D. & Acock, B. (1986). Crop responses to carbon dioxide doubling: a literature survey. *Agriculture and Forest Meteorology*, **38**, 127 – 145.
- Dam, J. M. C., Faaij, A. P. C., Lewandowski, I. M. & Fischer, G. (2007). Biomass production potentials in Central and Eastern Europe under different scenarios. *Biomass & Bioenergy*, **31** (6), 345-417.
- Dalianis, C. & Panoutsou, C. (1995). Energy potential of agricultural residues in EY. EUREC Network on Biomass (Bioelectrecity) Final Report. Contract No: RENA CT 94-0053.
- Daly, C., Neilson, R. P. & Phillips, D. L. (1994). A statistical-topographic model for mapping climatological precipitation over mountainous terrain. *J. Appl. Meteor.*, **33**, 113 - 120
- Davis, M. A., Wrage, K. J., & Reich, P. B. (1998). Competition between tree seedlings and herbaceous vegetation: support for a theory of resource supply and demand. *Journal of Ecology*, **86** (4), 652–661, 1998.
- De Saussure, T. (1804) *Recherches chimiques sur la végétation*. Chez la Ve Nyon, Paris.
- Dee, D. et al., (2011) The ERA-Interim reanalysis: Configuration and performance of the data assimilation system. *Quart. J. Roy. Meteor. Soc.*, **137**, 553-597.
- Delmas, R. J., Ascencio, J. M. & Legrand, M. (1980). Polar ice evidence that atmospheric CO₂ concentration 20.000 year BP was 50% of present. *Nature*, **285**, 155-157.
- DeLucia, E. H., Hamilton, J. G., Naidu, S. L., Thomas, R. B., Andrews, J. A., Finzi, A., Lavine, M., Matamala, R., Mohan, J. E., Hendrey, G. R. & Schlesinger, W. H. (1999). Net primary production of a forest ecosystem with experimental CO₂ enrichment. *Science*, **284**, 1177-1179.
- Di Blasi, C., Tanzi, V., Lanzetta, M. (1997), A study for the production of agricultural residues in Italy. *Biomass and Bioenergy*, **12**, 321-331.
- Dixon, R. K., Brown, S., Houghton, R. A., Solomon, A. M., Trexler, M. C. & Wisniewski, J. (1994). Carbon pools and flux of global forest ecosystems. *Science*, **263**, 185–190.
- Dornburg, V. & Faaij, A. P. C. (2007). Review of biomass potential studies and their links to food, water, biodiversity, energy modeling and economy. Scientific Assessment and Policy Analysis for Climate Change (WAB).

- Eastman, J. R. (2009). *IDRISI 16: The Taiga Edition*. Worcester, MA: Clark University
- Ebinger, J. & Vergara, W. (2010). *Climate Impacts on Energy Systems: Key Issues for Energy Sector Adaptation*. World Bank Study. Washington DC: World Bank Publications.
- European Environmental Agency (EEA). (2006). How much bioenergy can Europe~ produce without harming the environment? Copenhagen, Report No.
- EPA (2010). *Inventory of U.S. Greenhouse Gas Emissions and Sinks: 1990-2008* (PDF). U.S. Environmental Protection Agency (EPA).
- Elbersen, B., Boywer, C. & Kretschmer, B. (2012). Atlas of EU biomass potentials: Summary for policy makers – Policy briefing under D6.4. *Biomass Futures project*.
- Emmerich, W. E. (2007). Ecosystem Water Use Efficiency in a Semiarid Shrubland and Graassland Community. *Rangeland Ecol Manage*, **60**, 464 – 470.
- Engel, R. E., Long, D. S. & Carlson, G. R. (2003). Predicting Straw Yield of Hard Red Spring Wheat. *Agron. J.*, **95**, 1454 – 1460.
- Erbs, M. & Fangmeier, A. (2006). Atmospheric carbon dioxide enrichment effects on ecosystems – experiments and the real world. *Progress in Botany*, **67** (5), 441 – 459.
- Ericsson, K. & Nilson, J. (2004). International Biofuel Trade – A Study of the Swedish Import. *Biomasse & Bioenergy*, **24**, 205 – 220.
- Essenwanger, O. M. (2001) Classification of Climates, World Survey of Climatology 1C General Climatology – Amsterdam: Elsevier, 102 pp.
- Esteban, L. S., Ciria, P. & Carrasco, J. E. (2008). Surveying sustainable biomass. *BioResources*, **3** (3), 910 -928.
- Esteban, L. S., Ciria, P., Maletta, E., García, R. & Carrasco. (2010). Biomass Resources and Costs in Spain and Southern EU Countries. *Clean Hydrogen-rich Synthesis Gas (CHRISGAS)*, Report Deliverable **D36**.
- EUBIA - European Biomass Industry Association. (2007). <www.eubia.org> (visited 7, June, 2012).
- EUROSTAT (2003) – *EUROSTAT Yearbook 2003 - The statistical guide to Europe*, publishe. Luxembourg: Office for Official Publications of the European Communities.

- Falkenmark, M. (1990). Global Water Issues Facing Humanity. *Journal of Peace Research*, **27**, (2), 177-190.
- Farquhar, G. D., von Caemmerer, S. & Berry, J. A. (1980). A biochemical model of photosynthetic CO₂ assimilation in leaves of C₃ species. *Planta*, **149**, 78 – 90.
- FAO 2006 – Food and Agriculture Organization (FAO) *The State of Food Insecurity in the World 2006. Eradicating world hunger – taking stock ten years after the World Food Summit*.
- Fischer G. & Schrattenholzer, L. (2001) Global bioenergy potentials through 2050. *Biomass Bioenergy*, **20**(3), 151–159.
- Field et al. (2008). Biomass energy: the scale of the potential resource. *Trends Ecol. Evol.*, **23** (2), 65 – 72.
- Gelfand, I. & Robertson, G. P. (n.d.) *Positive feedback between increase of CO₂ concentration in the atmosphere and ecosystem productivity*, in Kellogg Biological Station and Long-Term Ecological Research <<http://lter.kbs.msu.edu/abstracts/330>> (visited 28, August, 2012).
- Gerten, D., Heinke, J., Hoff, H., Biemans, H., Fader, M., Waha, K. (2011). Global water availability and requirements for future food production. *J. Hydrometeor*, **12**, 885-899.
- Gerten, D., Schaphoff, S. & Lucht, W. (2007). Potential future changes in water limitations of the terrestrial biosphere. *Climatic Change*, **80**, 277-299.
- Gielen, D.J. , de Feber, M. A. P. C., Bos, A. J. M. & Gerlagh T. (2001) Biomass for energy or materials? A Western European systems engineering perspective. *Energy Policy*, **29**, 29 – 302.
- Gielen, D., Fujino, J., Hashimoto, S. & Moriguchi, Y. (2003). Modeling of global biomass policies. *Biomass and Bioenergy*, **25** , 177 – 195.
- Grainger, A. (1988). Estimating areas of degraded tropical lands requiring replenishment of forest cover. *Int. Tree Crops J*, **5**, 31 – 61.
- Guisan, A. & Zimmermann, N. E. (2000). Predictive habitat distribution models in ecology. *Ecological Modelling*, **135**, 147 – 186.

- Gregory, P.J. (1989). Water-Use-Efficiency of crops in the semi-arid tropics. In: *Soil, Crop and Water Management in the Soudano-Sahelian zone*. ICRISAT. Patancheru, India, 85 – 98.
- Haberl, H., Erb, K-H., Krausmann, F., Bondeau, A., Lauk, C., Müller, C., Plutzer, C. & Steinberger, J. K. (2011). Global bioenergy potentials from agricultural land in 2050: Sensitivity to climate change, diets and yields. *Biomass and Bioenergy*, **35**, 4753 – 4769.
- Haberl, H., Erb, K-H., Krausmann, F., Gaube, V., Bondeau, A. Plutzer, C., *et al.* (2007). Quantifying and mapping the human appropriation of net primary production in earth's terrestrial ecosystems. *Proc Natl Acad Sci*, **104** , 12942-7.
- Haiden, T. & Pistotnik, G. (2008). Parameterization of elevation effects in short-duration precipitation analysis. Preprints, *13th Conference on Mountain Meteorology*, Amer. Meteor. Soc., Whistler, Canada, 4pp.
- Hall, J. Peter. (2002). Sustainable production of forest biomass for energy. *The Forestry Chronicle*, **78**(3)1-6.
- Hall, D. O. & Scrase, J. I. (1998). Will Biomass be the Environmentally Friendly Fuel of the Future. *Biomass and Bioenergy*, **15** (4/5), 357-367.
- Hogan, M., Otterstedt, J., Morin, R. & Wilde, J. (Eds.). 2010. Biomass for Heat and Power. Opportunity and economics. European Commission . Report from the Commission to the Council and the European Parliament on sustainability requirements for the use of solid and gaseous biomass sources in electricity, heating and cooling. 72 pp.
- Hogan, M.. (2011). *Encyclopedia of Earth*. Eds. Mark McGinley and C.J.Cleveland. National Council for Science and the Environment, Washington DC.
- Hongqing, W., Halla, C. A. S., Scatenab, F. N., Fetcherc, N. & Wu, W. (2003). Modeling the spatial and temporal variability in climate and primary productivity across the Luquillo Mountains, Puerto Rico. *Forest Ecology and Management*, **179**, 69 – 94.
- Hoogwijk, M., Faaij, A., van den Broek, R., Berndes, G., Gielen, D., & Turkenburg, W. (2003) Exploration of the ranges of the global potential of biomass for energy. *Biomass Bioenergy*, **25**(2), 119–133.

- Hoogwijk, M., Faaij, A., Eickhout, B., de Vries, B. & Turkenburg, W. (2005). Potential of biomass energy out to 2100, for four IPCC SRES land-use scenarios. *Biomass Bioenergy*, **29**(4), 225–257.
- Houghton, R. A. (1990). The future-role of tropical forests in affecting the carbon-dioxide concentration of the atmosphere. *Ambio*, **19** (4), 4 204 – 210.
- Houze, R. A. (2012). Orographic effects on precipitating clouds. *Rev. Geophys.*, **50**, RG1001.
- Höschel, I., Körper, J. & Cubasch, U (n.d.) Temperature and Precipitation Response in Scenarios A1B and E1 (WP2A.3).EU FP6 Integrated Project ESSEMBLES Freie Universität Berlin.
- Hui, D., Luo, Y. & Katul, G. (2003). Partitioning interannual variability in net ecosystem exchange between climatic variability and functional change, *Tree Physiol.*, **23**, 433 – 442.
- Hughes, E. (2000). Biomass coffering: economics, policy, and opportunities. *Biomass and Bioenergy*, **19** (6), 457-465.
- Hulme, M. (1994). Validation of large-scale precipitation fields in general circulation models. *NATO ASI Series I: Global environmental change*, **26**, 389–405.
- Hulme, M., Osborn, T. J., Johns, T. C. (1998). Precipitation sensitivity to global warming: comparison of observations with HadCM2 simulations. *Geophys Res Lett*, **25**, 3379–3382.
- Hulme, M., Jenkins, G J., Lu, X., Turnpenny, J. R., Mitchell, T. D., Jones, R. G, Lowe, J., Murphy, J. M., Hassell, D., Boorman, P., McDonald, R. & Hill, S. (2002). Climate Change Scenarios for the United Kingdom: The UKCIP02 Scientific Report. Norwich, UK: Tyndall Centre for Climate Change Research.
- IEA - International Energy Agency. (2003): *Renewables for Power Generation*. France: IEA Publications.
- IEA - International Energy Agency. (2008).Energy Technology Perspectives – In support of the G8 Plan of Action: Scenarios & Strategies to 2050. France: IEA Publications.
- INE – Instituto Nacional de Estadística <www.ine.es>. (visited 3; August; 2012).

- Inman, M. (2011). Opening the future – Box 1: Representative concentrations pathways. *Nature Climate Change*, **1**, 7 -9.
- Intergovernmental Panel on Climate Change - IPCC (1990) *Climate change: the IPCC scientific assessment*. Houghton JT, Jenkins GJ, Ephraums JJ (eds). Cambridge: Cambridge University Press.
- Intergovernmental Panel on Climate Change - IPCC (1992) *Climate change 1992: the supplementary report to the IPCC scientific assessment*. Houghton JT, Callander BA, Varney SK (eds). Cambridge: Cambridge University Press.
- Intergovernmental Panel on Climate Change - IPCC (2000) *Special Report on Emissions Scenarios: A Special Report of Working Group III of the Intergovernmental Panel on Climate Change*, N. Nakicenovic, and R. Swart, Eds., Cambridge: Cambridge University Press.
- Intergovernmental Panel on Climate Change - IPCC (2001). *Third Assessment Report Annex B. Glossary of Terms* Cambridge: Cambridge University Press.
- Intergovernmental Panel on Climate Change – IPCC. Easterling, W.E., P.K. Aggarwal, P. Batima, K.M. Brander, L. Erda, S.M. Howden, A. Kirilenko, J. Morton, J.-F. Soussana, J. Schmidhuber and F.N. Tubiello, 2007: Food, fibre and forest products. *Climate Change 2007: Impacts, Adaptation and Vulnerability. Contribution of Working Group II to the Fourth Assessment Report of the Intergovernmental Panel on Climate Change*, M.L. Parry, O.F. Canziani, J.P. Palutikof, P.J. van der Linden and C.E. Hanson, Eds., Cambridge: Cambridge University Press., 273-313.
- Intergovernmental Panel on Climate Change – IPCC (2011). O. Edenhofer, R. Pichs-Madruga, Y. Sokona, K. Seyboth, P. Matschoss, S. Kadner, T. Zwickel, P. Eickemeier, G. Hansen, S. Schlömer, C. von Stechow (eds). *IPCC Special Report on Renewable Energy Sources and Climate Change Mitigation*. Prepared by Working Group III of the Intergovernmental Panel on Climate Change. Cambridge University Press, Cambridge, United Kingdom and New York, NY, USA, 1075 pp.
- Ito, A. & Oikawa, T. (2002) A simulation model of the carbon cycle in land ecosystems (Sim-CYCLE): A description based on dry-matter production theory and plot-scale validation. *Ecological Modelling*, **151**, 147-179.

- Jansson, C., Wulschleger, S D., Kalluri, U. C. & Tuskan, G. A. (2010). Phytosequestration: Carbon Biosequestration by Plants and the Prospects of Genetic Engineering. *BioScience*, **60**, 685 – 696.
- Jenkins, B.M. (1993). Properties of biomass. In: Wiltsee, G. (ed), Biomass energy fundamentals, **22**: Appendices. EPRI TR-102107, Electric Power Research Institute, Palo Alto, California.
- Jenkins, B. M, Baxter, L.L,, Miles, T. R. & Miles, T. R. (1998). Combustion properties of biomass. *Fuel Process. Technol.*, **54**, 17 – 46.
- Jerez, S., Montavez, J. P., Gomez-Navarro, J. J., Jimenez, P. A., Jimenez-Guerrero, P., Lorente, R. & Gonzalez-Rouco, J. F. (2012). The role of the land-surface model for climate change projections over the Iberian Peninsula. *Journal of Geophysical Research*, **11**, 1109-15.
- Johansson, D. J. A. & Azar, C. (2007). A scenario based analysis of land competition between food and bioenergy production in the US. *Climatic Change*, **82** (4), 267 – 291.
- Jung, M. *et al.* (2011). Global patterns of land-atmosphere fluxes of carbon dioxide, latent heat, and sensible heat derived from eddy covariance, satellite and meteorological observations. *Journal of Geophysical Research*, **116**, G00J07.
- Jurevics, A. (2010). *A comparison of harvesting residue yield and recovery rates for energy policy development*. Second cycle, A2E University essay from SLU/Southern Swedish Forest Research Centre, North Carolina State University, 26 pp.
- Kaltschmitt M, Hartmann H, Hofbauer H (eds) (2009) *Energie aus Biomasse: Grundlagen, Techniken und Verfahren*, 2nd ed. Springer, Dordrecht.
- Kania, S. & Giacomelli, G. (2002). Solar Radiation Availability for Plant Growth in Arizona controlled environment Agriculture Systems. *CCEA Newsletter*, **11** (2), 2 – 8.
- Kevin, E., Trenberth, K. E. & Dennis J. Shea, D. J. (2005). Relationships between precipitation and surface temperature. *Geophysical Research Letters*, **32**.
- Keeling, H. C. & Phillips, O. P. (2007). The global relationship between forest productivity and biomass. *Global Ecology and Biogeography*, **16**, 618 – 631.

- Khan, A. A. (2009). Potential to use biomass for bio-energy in Ontario. *Guelph Engineerng Journal*, **2**, 39-44.
- Kim, J., T.-K. Kim, R.W. Arritt, & N.L. Miller, (2002). Impacts of increased atmospheric CO₂ on the hydroclimate of the Western United States. *J. Clim.*, **15**(14), 1926–1942
- Kimball, B. A., Kobayashi, K. & Bindi, M. (2002). Response of agricultural crops to free-air CO₂ enrichment. *Advances in Agronomy*, **77**, 293 – 368.
- Kimball, B. A., Zhu, J., Cheng, L., Kobayashi, K. & Bindi M. (2002). Responses of agricultural crops of free-air CO₂ enrichment. *Ying Yong Sheng Tai Xue Bao.*, **10**, 1323-38.
- Kobata, T., Okuno, T. & Yamamoto, T. (1996). Contributions of capacity for soil water extraction and water use efficiency to maintenance of dry matter production in rice subjected to drought. *Nihon Sakumotsu Gakkai Kiji*, **65**, 652 – 662.
- Knorr, W. (2000). Annual and interannual CO₂ exchanges of the terrestrial biosphere: process-based simulations and uncertainties. *Global Ecol. Biogeogr.* **9**, 225–252.
- Knorr, W. & Kattge, J. (2005). Inversion of terrestrial ecosystem model parameter values against eddy covariance measurements by Monte Carlo sampling. *Global Change Biology*, **11**, 1333-1351.
- Kosa, P. (2009). Air Temperature and Actual Evapotranspiration Correlation Using Landsat 5 TM Satellite Imagery. *Nat. Sci.*, **43**, 605 – 611.
- Kottek, M., Grieser, J., Beck, C., Rudolf, B. & Rubel, F. (2006). World Map of the Köppen-Geiger climate classification updated. *Meteorologische Zeitschrift*, **15** (3), 3 259 -263.
- Krausmann, F., Gingrich, S., Lauk, C. & Haberl, H. (2008). Global patterns of socioeconomic biomass flows in the year 2000: a comprehensive assessment of supply, consumption and constraints. *Ecol Econ*, **65**, 471-87.
- Landsberg, J.J. & Waring, R.H. (1997). A generalized model of forest productivity using simplified concepts of radiation-use efficiency, carbon balance and partitioning. *For. Ecol. Manage.*, **95**, 209-228.
- Latzka, A. (2009). *Estimating the Potential Supply of Biomass for Cofiring in Electricity Production in New York State*, Honors Thesis Presented to the College of

Agriculture and Life Science, Social Sciences of Cornell University in Partial Fulfillment of the Requirements for the Research Honors Program

- Lavorel, S., Díaz, S., Cornelissen, J.H.C., Garnier, E., Harrison, S.P., McIntyre, S., Pausas, J.G., Pérez-Harguindeguy, N., Roumet, C. & Urcelay, C. (2007). Plant Functional Types: Are We Getting Any Closer to the Holy Grail? In: Canadell, J.G., Pitelka, L.F. and Pataki, D. (eds.) *Terrestrial Ecosystems in a Changing World*. The IGBP Series, Springer-Verlag, Berlin Heidelberg.
- Leakey, A. D. B. (2009). Rising atmospheric carbon dioxide concentration and the future of C₄ crops for food and fuel. *Proc Biol Sci*, **276** (1666), 2333 – 2343.
- Leonidas, P.A., Gilberto, C., Sedyama, Everardo C. Mantovain & Martinez, M. A. (2011). Tendências recentes nos elementos do clima e suas implicações na evapotranspiração da agricultura do milho em Viçosa. *Eng. Agríc*, **31** (4), 631-642.
- Linder, K. P., et al. (1990). National impacts of climate change on electric utilities. *The Potential Effects of Global Warming on the United States*, J. B. Smith and D. A. Tirpak, Eds., Washington, D.C.: Environmental Protection Agency.
- Lillesand, T. M. & Kiefer, R. W. (2000). *Remote Sensing and Image Interpretation*, 763 5th ed., New York: Wiley & Sons.
- Liu, S., Oliver, A., Chadwick, D., Roberts, A. & Chris, J. (2011). Relationships between GPP, Satellite Measures of Greenness and Canopy Water Content with Soil Moisture in Mediterranean-Climate Grassland and Oak Savanna. *Applied and Environmental Soil Science*, 14 pp.
- LOT5. (2003): Bioenergy's role in the EU Energy Market. Biomass availability in Europe. Report to the European Commission. CRES, BTG, ESD.
- Lu, X., & Zhuang, Q. (2010). Evaluating evapotranspiration and water-use efficiency of terrestrial ecosystems in the conterminous United States using MODIS and AmeriFlux data. *Remote Sensing of Environment*, **114**, 1924–1939.
- Lutgens, F. K. & Tarbuck, E. J. (1995). Increase of precipitation with altitude. *Mon Weather Rev*, **47**, 33–41.
- Mayeux, H. S., Johnson, H. B., Polley, H. W. & Malone, S. R. (1997). Yield of wheat across a subambient carbon dioxide gradient. *Global Change Biology*, **3**, 269 – 278.

- McCown, R. L. & Williams, J. (1990). Savanna Ecology and Management: Australian Perspectives and Intercontinental Comparisons. *Journal of Biogeography*, **17** (4), 513 – 520.
- McKendry, P. (2002). Energy production from biomass (part 1): overview of biomass. *Bioresource Technology*, **83**, 37-46.
- Mirasgedis, S., Sarafidis, Y., Gerogopoulou, E., Kotroni, V., Lagouvarods, K. & Lala, D. P. (2007). Modeling Framework for estimating impacts of climate change on electricity demand at regional level: Case of Greece. *Energy Conversion and Management*, **48**, 1737 – 1750.
- Monfreda, C., Ramankutty, N. & Foley, J. A. (2008). Farming the planet: 2. geographic distribution of crop areas, yields, physiological types, and net primary production in the year 2000. *Glob. Biogeochem. Cycles*, **22**, GB1022.
- Monteith, J. L. (1965) Evaporation and environment: the state and movement of water in living organisms. *Symp. Soc. Exp. Biol.*, **19**, 250 – 234.
- Morita, T. *et al.* (2010). Greenhouse Gas Emission Mitigation Scenarios and Implications. in *Climate Change 2001: Mitigation, Contribution of Working Group III to the Third Assessment Report of the Intergovernmental Panel on Climate Change*. Cambridge University Press, Cambridge, U.K., and New York, N.Y., U.S.A.
- Nakicenovic, N., J. Alcamo, G. Davis, B. de Vries, J. Fenham, S. Gaffin, K. Gregory, A. Grübler, T.-Y. Jung, T. Kram, E.L. La Rovere, L. Michaelis, S. Mori, T. Morita, W. Pepper, H. Pitcher, L. Price, K. Riahi, A. Reohrl, H.H. Rogner, A. Sankovski, M. Schlesinger, P. Shukla, S. Smith, R. Swart, S. van Rooijen, N. Victor, and Z. Dadi, (2000). *Special report on emissions scenarios*. Working Group III, Intergovernmental Panel on Climate Change (IPCC). Cambridge: Cambridge University Press, 595 pp.
- Neftel, A., Oeschger, H., Staffelbacj, T. & Stayffer, B. (1988). CO₂ record in the Byrd ice core 50.000 year BP. *Nature*, **331**, 609-611.
- Nikolau, A., Remrova, M. & Jeliaskov, L. (2003). Biomass availability in Europe. < <http://www.biomatnet.org/publications/2119rep.pdf>> (visited 12, September, 2012).

- Nogueira, L.A.H. & Lora, E.E.S.(2003). Dendoenergia: fundamentos e aplicações - 2 ed., Rio de Janeiro: Interciência
- Norby, R. J. *et al.* (2005). Forest response to elevated CO₂ is conserved a broad range of productivity. *Proc. Natl Acad. Sci.*, **102**, 18052 – 06.
- O'Connor, E. (2003). Energy Crops | Biomass production. *Encyclopedia of Applied Plant Sciences*, 266-273.
- O'Neill, R.V. & De Angelis, D.L. (1981). Comparative productivity and biomass relations of forest ecosystems. Dynamic properties of forest ecosystems. Cambridge: *Cambridge University Press*, [ed. by D.E. Reichle] pp. 411– 449.
- OECD. (2000). Agricultural Policies in OECD Countries: Monitoring and Evaluation: Glossary of Agricultural Policy Terms.
- Oldeman, L. R., Hakkeling, R. T. A. & Sombroek, W. G. (1990) World Map of the Status of Human-Induced Soil Degradation – An Explanatory Note (Global Assessment of Soil Degradation GLASOD). ISRIC: Wageningen.
- Oliveira, R. S., Bezerra, L., Davidson, E. A. *et al.* (2005). Deep root function in soil water dynamics in cerrado savannas of central Brazil. *Functional Ecology*, **19** (4), 574– 581.
- Panoutsou, Calliope (n.d.) *Biomass potentials of Europe* Imperial College London, <http://213.133.109.5/video/energy1tv/Jan%20NEU/Konferenz/Wirtschaft/FNR_BT_L_08/T1/3_Roh/1_Panoutsou.pdf> (visted 14, September, 2012).
- Parkpoom, S. & Harrison, G. P. (2008). Analyzing the Impact of Climate Change on Future Electricity Demand in Thailand. *IEEE Transactions on Power Systems*, **23** (3), 1441 – 1448.
- Parry, M. L., Rosenzweig, C., Iglesias, A., Livermore, M. & Fischer, G. (2004). Effects of climate change on global food production under SRES emissions and socio-economic scenarios. *Glob. Environ. Change*, **14**, 53 – 67.
- Pavlick, R., Drewry, D. T., Bohn, K., Reu, B. & Kleidon, A. (2012). The Jena Diversity-Dynamic Global Vegetation Model (JeDI-DGVM): a diverse approach to representing terrestrial biogeography and biogeochemistry based on plant functional trade-offs. *Biogeosciences Discuss*, **9**, 4627-4726.

- PIK – Postdam Institute for Climate Impact Research. (2012). <<http://www.pik-potsdam.de/research/climate-impacts-and-vulnerabilities/models/lpjml>> (visited 2, June, 2012).
- Policy, H. W., Johnson, H. B. & Marinot, B.D., *et al.* (1993). Increase in C3 plant water-use efficiency and biomass over Glacial to present CO₂ concentrations. *Nature*, **361**, 61 – 64.
- Polley, H. W., Phillips, R. L., Frank, A. B., Bradford, J. A., Sims, P. L. Morgan, J. A. & Kiniry, J. R. (2011). Variability in Light-Use Efficiency for Gross Primary Productivity on Great Plains Grasslands. *Ecosystems*, **14**, 15 – 27.
- Poorter, H. (1993). Interspecific variation in the growth response of plants to an elevated ambient CO₂ concentration. *Vegetatio*, **104/105**, 77 – 97.
- PORDATA – Base de Dados Portugal Contemporâneo. Available at <www.pordata.pt> (visited 3rd, August, 2012).
- Potter, C., J. Randerson, C. Field, P. A. Matson, P. Vitousek, H. Mooney & Klooster, S. (1993). Terrestrial ecosystem production: A process model based on global satellite and surface data. *Global Biogeochemical Cycles*, **7** (4), 811 – 841.
- Potter, C. S. & Klooster, S. A. (1997). Global model estimates of carbon and nitrogen storage in litter and soil pools: response to changes in vegetation quality and biomass allocation. *Tellus B*, **49** (1), 1 – 17.
- Potter, C. S., Davidson, E., Klooster, S., Nepstad, D., Negreiros, G. & Brooks, V. (1998). Regional application of an ecosystem production model for studies of biogeochemistry in Brazilian Amazonia. *Global Change Biology*, **4**, 315 – 333.
- Potter, C., Genovese, V. B., Klooster, S., Bobo, M. & Torregrosa, A. (2001). Biomass burning losses of carbon estimated from ecosystem modeling and satellite data analysis for the Brazilian Amazon region. *Atmospheric Environment*, **35**, 1773 – 1781.
- Pregitzer, K. S. & Euskirchen, E. S. (2004). Carbon cycling and storage in world forests: biome patterns related to forest age. *Glob Change Biol*, **10**, 2052–2077.
- Prentice, I. C. *et al.* (2001). The carbon cycle and atmospheric CO. In: Houghton J. T., Yihui, D., (eds) The Intergovernmental Panel on Climate Change (IPCC) Third Assessment Report. New York: Cambridge University Press, **3**, 185 – 237.

- Prentice, I. C., Bondeau, A., Cramer, W., Harrison, S. P., Hickler, T., Lucht, W., Sitch, S., Smith, B. & Sykes, M.T. (2007) Dynamic vegetation modelling: quantifying terrestrial ecosystem responses to large scale environmental change. In: Canadell J, Pitelka LF, Pataki D. (eds) *Terrestrial ecosystems in a changing world*. Berlin: Springer, 175–192.
- Puebla C. R., Encinas, A. H., Nieto S., & Garmendia, J. (1998). Spatial and temporal patterns over the Iberian Peninsula. *Int. J. Climatol*, **18**, 299–316.
- Raddatz, T. J., Reick, C. H., Knorr, W., Kattge, J., Roeckner, E., Schnur, R., Schnitzler, K. G., Wetzell, P. & Jungclaus, J. (2007). Will the tropical land biosphere dominate the climate-carbon cycle feedback during the twenty-first century. *Climate Dynamics*, **29**, 565-574.
- Ramankutty, N., Evan, A. T., Monfreda, C. & Foley, J. A. (2008). Farming the planet. Part 1: the geographic distribution of global agricultural lands in the year 2000. *Glob. Biogeochem. Cycles*, **22**.
- Raven, J.A. & Edwards, D. (2001). Roots: evolutionary origins and biogeochemical significance. *Journal of Experimental Botany*, **52**, 381–401.
- Renewable Energy Directive (RED) 2009/28/EC, April 2009.
- Regato-Pajares, P., *et al.* (2004). Recent landscape evolution in Dehesa woodlands of Western Spain. In: S. Mazzoleni, P. *et al.* (editors), *Recent Dynamics of the Mediterranean Vegetation and Landscape*. Gordon and Breach Pub., Reading, U.K.
- Reyer, C. & Gutsch, M. (n.d.). Meta-analysis of simulated forest productivity and biomass changes under global change. *PIK Research Domain II: Climate Impacts & Vulnerabilities*.
 <<http://www.isa.utl.pt/def/fp0603forestmodels/PDF/Posters/Reyer.pdf>> (visited 29, August, 2012).
- Riedy, M. J. & Stone, T. C. (2010). Defining Biomass – A Comparison Of Definitions In Legislation. Mintz, Levin, Cohn, Ferris, Glovsky, and Popeo, P. C.
- Rios-Enteza, A. & Miguez-Macho. (2012). Moisture recycling and the maximum of precipitation in the Spring in the Iberian Peninsula. *Geophysical Research Abstracts*, **12**, EGU2010-14072.

- Reick, C. (2009). *The JSBACH Model or The Land-Biosphere on the COSMOS Model*. Research Unit Global Vegetation Modelling. Max Planck Institute for Meteorology Hamburg. < <http://issmes.enes.org/uploads/media/reick.pdf>> (visited 28, April, 2012).
- Reilly, J. & Paltsev, S. (2008). Biomass Energy and Competition for Land. *Joint Program on the Science and Policy of Global Change*, Working Paper No. 46.
- Reilly, J. & Paltsev, S. (2008) *Biomass Energy and Competition for Land*, Joint Program on the Science and Policy for Global Change, GTAP Working Paper No. 46 [Chapter 8 of the book *Economic Analysis of Land Use in Global Climate Change Policy*].
- Richardson, A. D., Hollinger, A. Y., Aber, J. D., Ollinger, S. V. & Braswell, B. H. (2007). Environmental variation is directly responsible for short – but not long-term variation in forest-atmosphere carbon exchange. *Global Change Biol.*, **13**, 788 – 803.
- Rivas-Martínez, S., Penas, A. & Díaz, T. E. (2004). *Bioclimatic Map of Europe*. Cartographic Service. University of León, Spain.
- Rockström, J., M. Falkenmark, & M. Lannerstad. (2007). Assessing the water challenge of a new green revolution in developing countries. *Proceedings of the National Academy of Sciences*, **104**, 6253–6260.
- Rojstaczer, S., Sterling, S. M. & Moore, N. J. (2001). Human appropriation of photosynthesis products. *Science*, **294**, 2549 – 52.
- Rost, S., Gerten, D., Bondeau, A., Lucht, W., Rohwer, J. & Schaphoff, S. (2008). Agricultural green and blue water consumption and its influence on the global water system. *Water Resource*, **44**.
- Rost, S., Gerten, D., Hoff, H., Lucht, W., Falkenmark, M. & Rockström, J. (2009) Global potential to increase crop production through water management in rainfed agriculture. *Environ. Res. Lett.*, **4**, 1 – 9.
- Running, S. W., Thornton, P. E., Nemani, R. R., & Glassy, J. (2000). Global Terrestrial Gross and Net Primary Productivity from the Earth Observing System. *Methods in Ecosystem Science*, **3**, 44-45.
- Running, S. W. & Zhao, M. (2005). Global Primary Production and Evapotranspiration. *Ecological Applications*, **15** (3), 954–969.

- Ruth, M. & Lin, A. C. (2006). Regional energy demand and adaptations to climate change: Methodology and application to the state of Maryland, USA. *Energy Policy*, **34**, 2820 – 2833.
- Schaphoff, S., Lucht, W., Gerten, D., Stich, S., Cramer, W. & Prentice, C. (2006). Terrestrial Biosphere Carbon Storage under alternative Climate Projections. *Climatic Change*, **74**, 97-122.
- Segal, M., Shafir, H., Mandel, M., Alpert, P. & Balmor, Y. (1992). Climatic-related evaluations of the summer peak-hours' electric load in Israel. *J. Applied Metereology*, **31** (12), 1492 – 1498.
- Henderson-Sellers, A., Howe, W. & McGuffie, K. (1995). The MECCA analysis project. *Global Planet Change*, **10**, 3–21.
- Shiklomanov, I. A. (1993). World fresh Water Resources. *Water in Crisis: A Guide to the World's Fresh Water Resources*. New York: Oxford Univ. Press., 12 – 24pp.
- Siebert, S. & Döll, P. (2009). Quantifying blue and green virtual water contents in global crop production as well as potential production losses without irrigation. *J. Hydrol.*, **384**, 198 – 217.
- Singh, A., Sharma, J., Rexer, K. & Varma, A. (2000) Plant productivity determinants beyond minerals, water and light: *Piriformospora indica* – A revolutionary plant growth promoting fungus. *Current Science*, **79** (11), 1548 – 1554.
- Sitch, S., Smith, B., Prentice, I C., Arneth, A., Bondeau, A., Cramer, W., Kaplans, J.O., Levis, S., Lucht, W., Sykes, M. T., Thonicke, K. & Venevsky, S.(2003). Evaluation of ecosystem dynamics, plant geography and terrestrial carbon cycling in the LPJ dynamic global vegetation model. *Global Change Biology*, **9**, 161-185.
- Smeets, E., Faaij, A. & Lewandowski, I. (2004). A quickscan of global bio-energy potentials to 2050: An analysis of the regional availability of biomass resources for export in relation to the underlying factors. *Netherlands Organization for Energy and the Environment Report NWS* (2004): 0 – 121.
- Smeets, E. & Faaij, A. (2007). Bioenergy potentials from forestry in 2050: An assessment of the drivers that determine the potentials. *Climatic Change*, **81**, 353 – 390.

- Smeets, E. M., Faaij, A. P., Lewandowski, I. M., Turkenburg, W. C. (2007) A bottom-up assessment and review of global bio-energy potentials to 2050. *Prog Energy Combust Sci* **33**(1), 56–106.
- Smeets, E. M. & Faaij, A. P. (2007) Bioenergy potentials from forestry in 2050. *Clim Change*, **81**(3), 353–390.
- Sørensen, B. (1999). Long-term scenarios for global energy demand and supply: Four global greenhouse mitigation scenarios. *Energy & Environment Group Roskilde: Roskilde University*, 426 pp.
- Sterner, M. & Fritsche, U. (2011). Greenhouse gas balances and mitigation costs of 70 modern Germany-focused and 4 traditional biomass pathways including land-use change effects. *Biomass and Bioenergy*, **35**, 4797 – 4814.
- Stewart, B.A. & Nielsen, D. R. (1990). Irrigation of agricultural crops. *Agron. Monogr.* **20** (4), 341 – 342.
- Stewart, W. M. (2001). Balanced fertilization increases water use efficiency. *News & Views. Potash & Phosphate Institute. GA.* <[http://www.ipni.net/ppiweb/ppinews.nsf/\\$webcontents/736A94E12DC4646D85256A0300522826/\\$file/Water+Use+Efficiency.pdf](http://www.ipni.net/ppiweb/ppinews.nsf/$webcontents/736A94E12DC4646D85256A0300522826/$file/Water+Use+Efficiency.pdf)>.
- Tolk, J. A. & Howell, H. A. (2003). Water use efficiencies of grain sorghum grown in three USA southern Great Plains soils. *Agricultural Water Management*, **59**, 97 – 111.
- Thum, T., Räisänen, P., Sevanto, S., Tuomi, M., Reick, C., Vesala, T., Raddatz, T., Aalto, T., Järvinen, H., Altimir, N., Pilegaard, K., Nagy, Z., Rambal, S. & Lski, J. (2011). Soil carbon model alternatives for ECHAM5/JSBACH climate model: Evaluation and impacts on global carbon cycle estimates. *Journal of Geophysical Research: Biogeosciences*, **116**(G2), G02028.
- Tian, H., *et al.*, (2010). Environmental controls over carbon dioxide and water vapor exchange of terrestrial vegetation. *Agric. For. Meteorol.*, **113**, 97 – 120.
- Tilman, D. A. (1978). *Wood as an energy resource*. New York: Academic Press, 252 pp.
- Tubiello, F. N., Soussana, J. F. & Howden, S. M. (2007). Climate change and food security special feature: crop and pasture response to climate change. *Proc Natl Acad Sci*, **104**, 19686 - 90.

- Turkenburg, W. C. (2000). Renewable energy technologies. World Energy Assessment. J. Goldemberg. Washington, D.C., U.S.A., UNPD: 220-72.
- Turner, W., S. Specter, N. Gardiner, M. Fladeland, E. Sterling, & M. Steininger. (2003). Remote sensing for biodiversity science and conservation. *Trends in Ecology & Evolution*, **18**, 306–314.
- United Nations, Department of Economic and Social Affairs, Population Division (2007). *World Population Prospects: The 2006 Revision*, vol. I *Comprehensive Tables* (United publications, Sales No. E.07.XIII.2).
- United States Global Change Research Program - USGRP. (2009). Global Climate Change Impacts in the United States (2009).
- Venäläinen, A., Tammelin, B., Tuomenvirta, H., Jylhä, K., Koskela, J., Turunen, M. A., Vehviläinen, B., Forsius, J. & Järvinen, P. (2004). The influence of climate change on energy production and heating energy demand in Finland. *Energy and Environment*, **15**(1), 93-109.
- Voivontas, D., Assimacopoulos, D. & Koukios, E. G. (2001). Assessment of biomass potential for power production: a GIS based method. *Biom. Bioenergy*, **20**, 101-112.
- Wang, P., Yamanaka, T., Qiu, G. Y. (2012). Causes of decreased reference evapotranspiration and pan evaporation in the Jinghe River catchment, northern China. *Environmentalist*, **32**, 1–10.
- Harding, R. et al. (2011). Current Knowledge of the Terrestrial Global Water Cycle. *J. Hydrometeor*, **12**, 1149–1156.
- Ward, S. J. E., Midgley, G. F, Jones, M. H. & Curtis, P. S. (1999). Responses of wild C4 and C3 grass (Poaceae) species to elevated atmospheric CO₂ concentration: a test of current theories and perceptions. *Global Change Biology*, **5**, 723 – 741.
- Wiegmann, K., Fritsche, U. & Elberse, B. (2005). Environmentally compatible biomass potential from agriculture. *Consultancy report to the EEA*.
- Whitmarsh, J. & Govindjee. (1995). Concepts in Photobiology: Photosynthesis and Photomorphogenesis. *Encyclopedia of Applied Physics*, **13**, 513-532.
- Whittaker, R.H. & Likens, G.E. (1973). *Carbon in the biota*. Carbon and the biosphere: proceedings of the 24th Brookhaven Symposium in Biology, Upton, N.Y., May 16 –18, 1972 (ed. by G.M.).

- Whitmarsh, J. & Govindjee. (1995). Concepts in Photobiology: Photosynthesis and Photomorphogenesis. *Encyclopedia of Applied Physics*, **13**, 513-532.
- Wit, M. P. & Faaij, A. P. C. (2008) Potential and Related Costs: Assessment of the EU-27, Switzerland, Norway and Ukraine. *Refuel Work Package 3 final report*.
- de Wit, M. & Faaij, A. (2010). European biomass resource potential and costs. *Biomass and Bioenergy*, **34** (2), 188 – 202.
- World Bank Annual Report (2009) – Year in review. Cathy Lips (ed.): Washington DC
- Xiao, X., Zhang, Q., Hollinger, D., Aber, J. & Moore, B. (2005). Modeling gross primary production of an evergreen needleleaf forest using modis and climate data. *Nature*, **361**, 61 – 64.
- Xiao, J. & Chen, j., *Global Patterns and Interannual Variability of Water Use Efficiency*, (n.d). <
<http://www.fluxdata.org/DataInfo/Paperwriting%20Proposals/Xiao%20Global%20Patterns%20and%20Interannual%20Variability%20of%20Water%20Use%20Efficiency.pdf>>(visited 27, August, 2012).
- Xu, C. Y., Gong, L. B., Tong, J. & Chen, D. L. (2006) Ecreasing reference evapotranspiration in a warming climate - A case of Changjiang (Yangtze) River catchment during 1970-2000. *Advances in Atmospheric Sciences*, **23** (4),513-520.
- Yoshida & Suzuki, H. (2010). Current Status of Woody Biomass Utilization in ASEAN Countries., *Biomass*, Ed. Maggy Ndombo Benteke Momba, Available format <<http://www.intechopen.com/books/biomass/current-status-of-woody-biomass-utilization-in-asean-countries>>Zaehle, S., Friedlingstein, P. & Friend, D. Terrestrial nitrogen feedbacks may accelerate future climate change. *Geophysical Research Letters*, **37**, L01401.
- Zomer, R. J., Trabuco, A., Verchot, L. V. & Muys, B. *Land*. (2008). Area Eligible for Afforestation and Reforestation within the Clean Development Mechanism: A Global Analysis of the Impact of Forest Definition. *Mitigation and Adaptation Strategies for Global Change*, **13** (3), 219 – 239.

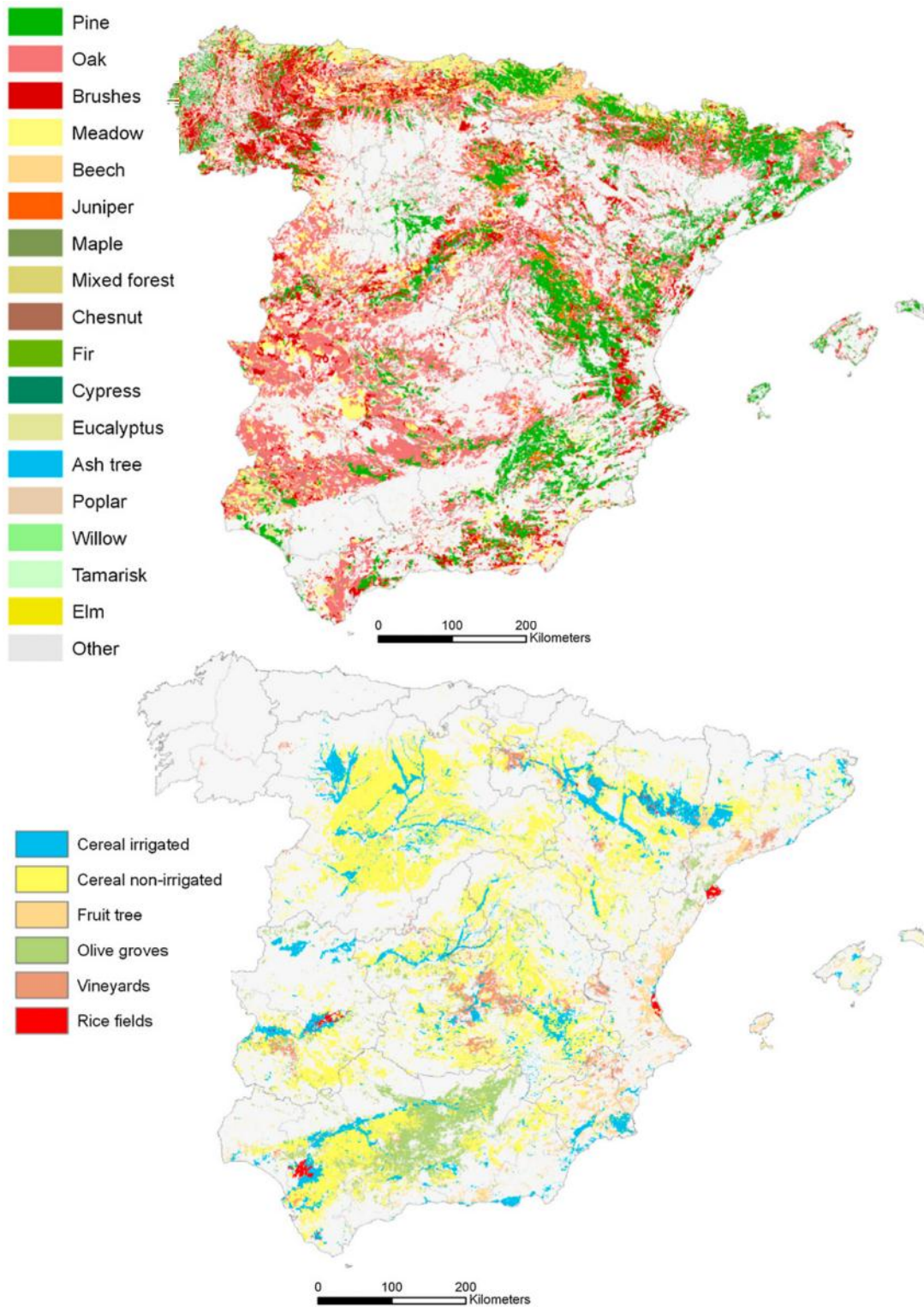
7 . Appendix

APPENDIX A

Crops in Iberian Peninsula

In Portugal the main crops grown are cereals (namely, wheat, barley, corn and rice), potatoes, grapes (for wine), tomatoes and olives (Portugal-live.net). Other crops widely produced are green vegetables, oilseeds, nuts and cherries. Crops of wheat and barley are mostly located in three regions, highlighting the Alentejo (which presents a cultivated area of more than 180.000 hectares). The barley crop is restricted to the Alentejo and Lisboa and Tejo Valley). Contrarily to the two previous, corn crop can be found in all regions of Portugal – having more importance in Minho, Beira Litoral, Lisbon and Alentejo (accounting with respective weight percentages of 26, 23, 22 and 14%). The potato crop as also a wide location, even though it predominates in Trás-os-Montes (28%), in Beira Litoral (24%) and Lisboa and Tejo Valley (20%). The beet crop is done almost exclusively in the regions of Lisbon and Tejo Valley (58%) and Alentejo (39%).

The most abundant agricultural residues in Spain come from cereal straw, sunflower stalks, vine shoots, cotton stalks, olive, orange and peach tree prunings as well as other horticultural and related residues – amounting to 50 million tonnes per year (Jiménez & Rodríguez, 2010).



Agro-forestry map for Spain: Forestry map (re-classified into 18 families)(top). Crop map (bottom)(Source: Gómez *et al.*, 2010)

APPENDIX B

Estimations for Logging Activities								
	Scenario	Efficiency	PFT	Reference period	C1	C2	E1	E2
combustion	BAU	0,25	T.B. evergreen tree	0,003	0,002	0,002	0,003	0,003
combustion	BAU	0,25	T.B.deciduous tree	0,043	0,043	0,044	0,053	0,054
combustion	BAU	0,25	C. evergreen tree	0,060	0,058	0,058	0,065	0,066
combustion	BAU	0,25	Rain green shrubs	0,002	0,002	0,002	0,003	0,003
combustion	BAU	0,25	Deciduous shrubs	0,000	0,000	0,000	0,000	0,000
combustion	BAU	0,25	ALL	0,109	0,106	0,106	0,124	0,124
combustion	LOW-YIELD	0,25	T.B. evergreen tree	0,005	0,005	0,005	0,005	0,005
combustion	LOW-YIELD	0,25	T.B.deciduous tree	0,086	0,087	0,087	0,106	0,107
combustion	LOW-YIELD	0,25	C. evergreen tree	0,121	0,116	0,115	0,131	0,131
combustion	LOW-YIELD	0,25	Rain green shrubs	0,005	0,004	0,004	0,005	0,005
combustion	LOW-YIELD	0,25	Deciduous shrubs	0,000	0,000	0,000	0,000	0,000
combustion	LOW-YIELD	0,25	ALL	0,217	0,213	0,212	0,247	0,249
combustion	HIGH-YIELD	0,25	T.B. evergreen tree	0,011	0,010	0,010	0,011	0,011
combustion	HIGH-YIELD	0,25	T.B.deciduous tree	0,172	0,174	0,174	0,212	0,214
combustion	HIGH-YIELD	0,25	C. evergreen tree	0,242	0,232	0,230	0,262	0,262
combustion	HIGH-YIELD	0,25	Rain green shrubs	0,010	0,009	0,009	0,010	0,010
combustion	HIGH-YIELD	0,25	Deciduous shrubs	0,000	0,000	0,000	0,000	0,000
combustion	HIGH-YIELD	0,25	ALL	0,435	0,425	0,423	0,495	0,498
	Scenario	Eff.	PFT	Reference period	C1	C2	E1	E2
gasification	BAU	0,35	T.B. evergreen tree	0,004	0,003	0,003	0,004	0,004
gasification	BAU	0,35	T.B.deciduous tree	0,060	0,061	0,061	0,074	0,075
gasification	BAU	0,35	C. evergreen tree	0,085	0,081	0,081	0,092	0,092
gasification	BAU	0,35	Rain green shrubs	0,003	0,003	0,003	0,004	0,004

gasification	BAU	0,35	Deciduous shrubs	0,000	0,000	0,000	0,000	0,000
gasification	BAU	0,35	ALL	0,152	0,149	0,148	0,173	0,174
gasification	LOW-YIELD	0,35	T.B. evergreen tree	0,007	0,007	0,007	0,008	0,008
gasification	LOW-YIELD	0,35	T.B.deciduous tree	0,121	0,122	0,122	0,148	0,150
gasification	LOW-YIELD	0,35	C. evergreen tree	0,169	0,163	0,161	0,183	0,184
gasification	LOW-YIELD	0,35	Rain green shrubs	0,007	0,006	0,006	0,007	0,007
gasification	LOW-YIELD	0,35	Deciduous shrubs	0,000	0,000	0,000	0,000	0,000
gasification	LOW-YIELD	0,35	ALL	0,304	0,298	0,296	0,346	0,348
gasification	HIGH-YIELD	0,35	T.B. evergreen tree	0,015	0,014	0,014	0,015	0,015
gasification	HIGH-YIELD	0,35	T.B.deciduous tree	0,241	0,243	0,244	0,297	0,300
gasification	HIGH-YIELD	0,35	C. evergreen tree	0,338	0,325	0,323	0,366	0,367
gasification	HIGH-YIELD	0,35	Rain green shrubs	0,014	0,013	0,012	0,014	0,014
gasification	HIGH-YIELD	0,35	Deciduous shrubs	0,000	0,000	0,000	0,000	0,000
gasification	HIGH-YIELD	0,35	ALL	0,608	0,595	0,592	0,693	0,697

Estimations for Thinning activities								
	Scenario	Eff.	PFT	Reference period	C1	C2	E1	E2
combustion	BAU	0,25	T.B. evergreen tree	0,001	0,001	0,001	0,001	0,001
combustion	BAU	0,25	T.B.deciduous tree	0,014	0,014	0,015	0,018	0,018
combustion	BAU	0,25	C. evergreen tree	0,020	0,019	0,019	0,022	0,022
combustion	BAU	0,25	Rain green shrubs	0,001	0,001	0,001	0,001	0,001
combustion	BAU	0,25	Deciduous shrubs	0,000	0,000	0,000	0,000	0,000
combustion	BAU	0,25	ALL	0,036	0,035	0,035	0,041	0,041
combustion	LOW-YIELD	0,25	T.B. evergreen tree	0,002	0,002	0,002	0,002	0,002
combustion	LOW-YIELD	0,25	T.B.deciduous tree	0,029	0,029	0,029	0,035	0,036
combustion	LOW-YIELD	0,25	C. evergreen tree	0,040	0,039	0,038	0,044	0,044
combustion	LOW-YIELD	0,25	Rain green shrubs	0,002	0,001	0,001	0,002	0,002
combustion	LOW-YIELD	0,25	Deciduous shrubs	0,000	0,000	0,000	0,000	0,000
combustion	LOW-YIELD	0,25	ALL	0,072	0,071	0,071	0,082	0,083
combustion	HIGH-YIELD	0,25	T.B. evergreen tree	0,004	0,003	0,003	0,004	0,004
combustion	HIGH-YIELD	0,25	T.B.deciduous tree	0,057	0,058	0,058	0,071	0,071
combustion	HIGH-YIELD	0,25	C. evergreen tree	0,081	0,077	0,077	0,087	0,087
combustion	HIGH-YIELD	0,25	Rain green shrubs	0,003	0,003	0,003	0,003	0,003
combustion	HIGH-YIELD	0,25	Deciduous shrubs	0,000	0,000	0,000	0,000	0,000
combustion	HIGH-YIELD	0,25	ALL	0,145	0,142	0,141	0,165	0,166
	Scenario	Eff.	PFT	Reference period	C1	C2	E1	E2
gasification	BAU	0,35	T.B. evergreen tree	0,001	0,001	0,001	0,001	0,001
gasification	BAU	0,35	T.B.deciduous tree	0,020	0,020	0,020	0,025	0,025
gasification	BAU	0,35	C. evergreen tree	0,028	0,027	0,027	0,031	0,031
gasification	BAU	0,35	Rain green shrubs	0,001	0,001	0,001	0,001	0,001
gasification	BAU	0,35	Deciduous shrubs	0,000	0,000	0,000	0,000	0,000

gasification	BAU	0,35	ALL	0,051	0,050	0,049	0,058	0,058
gasification	LOW-YIELD	0,35	T.B. evergreen tree	0,002	0,002	0,002	0,003	0,003
gasification	LOW-YIELD	0,35	T.B.deciduous tree	0,040	0,041	0,041	0,049	0,050
gasification	LOW-YIELD	0,35	C. evergreen tree	0,056	0,054	0,054	0,061	0,061
gasification	LOW-YIELD	0,35	Rain green shrubs	0,002	0,002	0,002	0,002	0,002
gasification	LOW-YIELD	0,35	Deciduous shrubs	0,000	0,000	0,000	0,000	0,000
gasification	LOW-YIELD	0,35	ALL	0,101	0,099	0,099	0,115	0,116
gasification	HIGH-YIELD	0,35	T.B. evergreen tree	0,005	0,005	0,005	0,005	0,005
gasification	HIGH-YIELD	0,35	T.B.deciduous tree	0,080	0,081	0,081	0,099	0,100
gasification	HIGH-YIELD	0,35	C. evergreen tree	0,113	0,108	0,108	0,122	0,122
gasification	HIGH-YIELD	0,35	Rain green shrubs	0,005	0,004	0,004	0,005	0,005
gasification	HIGH-YIELD	0,35	Deciduous shrubs	0,000	0,000	0,000	0,000	0,000
gasification	HIGH-YIELD	0,35	ALL	0,203	0,198	0,197	0,231	0,232

Agriculture Activities							
Scenario	Eff	PFT	Ref	C1	C2	E1	E2
BAU	0,25	C3 grass	0,020	0,015	0,015	0,021	0,021
BAU	0,25	C4 grass	0,016	0,010	0,010	0,016	0,015
BAU	0,25	C3 Crops	0,038	0,025	0,023	0,042	0,042
BAU	0,25	C4 Crops	0,007	0,005	0,005	0,008	0,008
BAU	0,25	all	0,082	0,055	0,052	0,086	0,086
LOW-YIELD	0,25	C3 grass	0,041	0,030	0,029	0,042	0,042
LOW-YIELD	0,25	C4 grass	0,031	0,021	0,019	0,031	0,031
LOW-YIELD	0,25	C3 Crops	0,076	0,049	0,047	0,083	0,083
LOW-YIELD	0,25	C4 Crops	0,015	0,010	0,009	0,016	0,016
LOW-YIELD	0,25	all	0,164	0,109	0,104	0,173	0,173
HIGH-YIELD	0,25	C3 grass	0,082	0,060	0,058	0,084	0,084
HIGH-YIELD	0,25	C4 grass	0,063	0,041	0,039	0,062	0,062
HIGH-YIELD	0,25	C3 Crops	0,153	0,098	0,093	0,167	0,167
HIGH-YIELD	0,25	C4 Crops	0,030	0,019	0,018	0,032	0,032
HIGH-YIELD	0,25	all	0,327	0,219	0,208	0,346	0,345
BAU	0,35	C3 grass	0,02867	0,020923	0,020337	0,029531	0,02947
BAU	0,35	C4 grass	0,02193	0,014378	0,013507	0,021861	0,02168
BAU	0,35	C3 Crops	0,05341	0,034433	0,032653	0,058321	0,0583
BAU	0,35	C4 Crops	0,01047	0,006771	0,006431	0,011314	0,01132
BAU	0,35	all	0,11447	0,076504	0,072927	0,121027	0,12078
LOW-YIELD	0,35	C3 grass	0,05733	0,041845	0,040673	0,059063	0,05895
LOW-YIELD	0,35	C4 grass	0,04386	0,028757	0,027013	0,043722	0,04337
LOW-YIELD	0,35	C3 Crops	0,10683	0,068866	0,065305	0,116641	0,1166
LOW-YIELD	0,35	C4 Crops	0,02093	0,013541	0,012862	0,022628	0,02264
LOW-YIELD	0,35	all	0,22895	0,153009	0,145854	0,242054	0,24156
HIGH-YIELD	0,35	C3 grass	0,11466	0,083691	0,081347	0,118125	0,1179
HIGH-YIELD	0,35	C4 grass	0,08771	0,057513	0,054026	0,087444	0,08673
HIGH-YIELD	0,35	C3 Crops	0,21366	0,137731	0,130611	0,233283	0,23321
HIGH-YIELD	0,35	C4 Crops	0,04186	0,027083	0,025725	0,045256	0,04529
HIGH-YIELD	0,35	all	0,45789	0,306018	0,291709	0,484107	0,48313